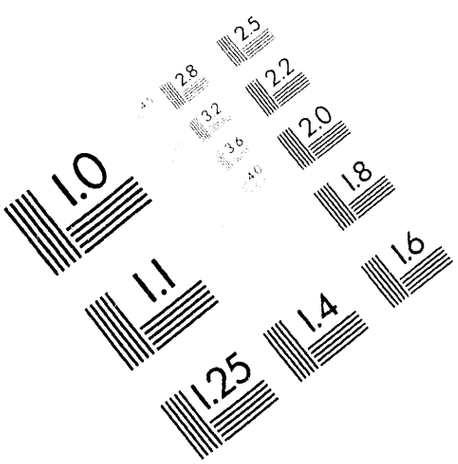

Association for Information and Image Management
1100 Wayne Avenue, Suite 1100
Silver Spring, Maryland 20910
301/587-8202

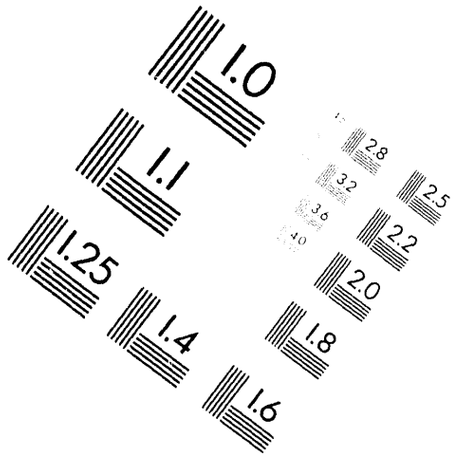

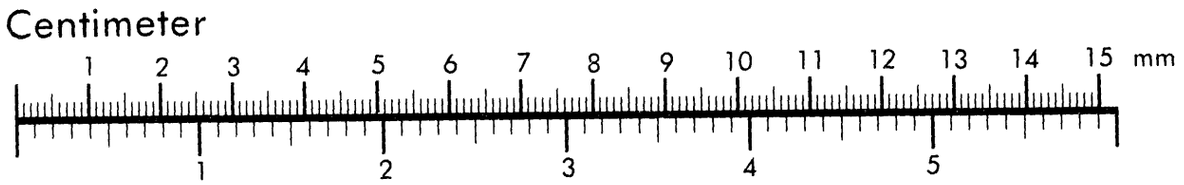

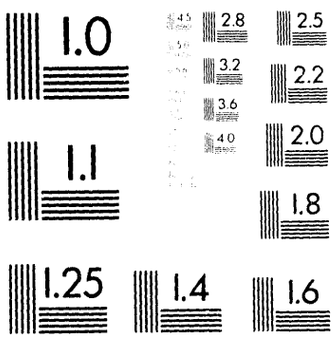

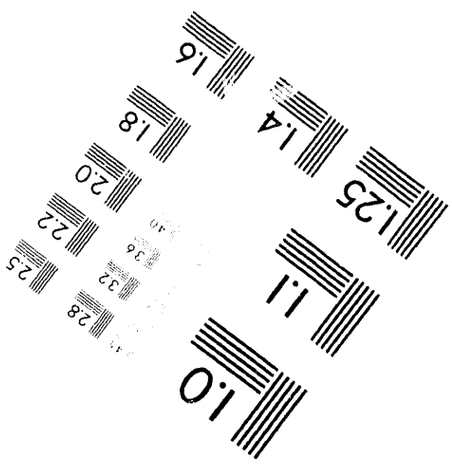

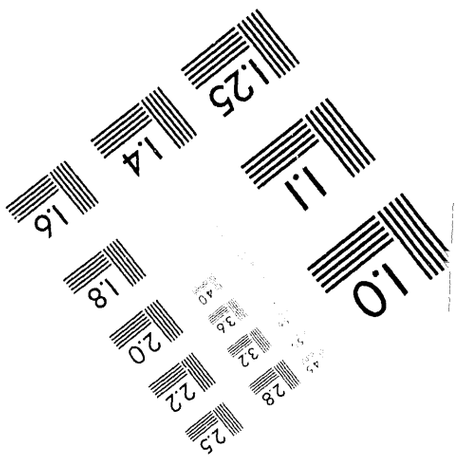

MANUFACTURED TO AIIM STANDARDS
BY APPLIED IMAGE, INC.

1 of 2

LBL-35126
UC-401

On the Role of Delocalization in Benzene: Theoretical and Experimental Investigation of the Effects of Strained Ring Fusion

Rüdiger Faust
Ph.D. Thesis

Department of Chemistry
University of California

and

Chemical Sciences Division
Lawrence Berkeley Laboratory
University of California
Berkeley, CA 94720

April 1993

This work was supported by the Director, Office of Energy Research, Office of Basic Energy Sciences, Materials Sciences Division, of the U.S. Department of Energy under Contract No. DE-AC03-76SF00098.

Table of Contents

Chapter One

Aromaticity: Criteria, Manifestations, and Structural Limitations

1.1 Introduction.

When an important compound's discovery dates back as far as 1825, one would imagine that every facet of its chemical and physical properties has been illuminated in the meantime. Benzene, however, has not ceased to challenge the chemist's notion of structure and bonding since its first isolation by Michael Faraday.[1] Mitscherlich's determination of C_6H_6 as the molecular formula,[2] along with the fact that benzene and its derivatives react by substitution rather than addition, conflicted with the already dogmatic tetravalency[3] of carbon, posing an insurmountable dilemma for 19th century chemists in their efforts to present conclusive structural proposals. Kekulé, in a lucky case of inspirational day dreaming,[4] was the first to suggest the cyclic framework of benzene[5] as an equilibrating mixture of 1,3,5-cyclohexatrienes.[6] Early attempts to explain the peculiar stability of "aromatic" compounds on electronic grounds were made by Robinson[7] and Ingold,[8] who associated the presence of an "aromatic sextet" of electrons with typical benzenoid behavior. Pauling and Wheland,[9] together with Hückel[10] eventually provided a quantum mechanical footing for the observed properties and made the resonance-based picture of benzene (**1a**, **1b**) as widely accepted as it is today.

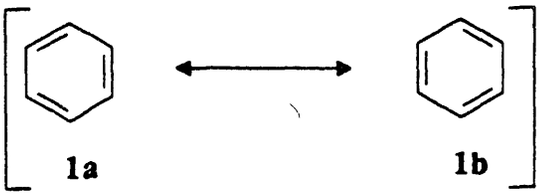

1a **1b**

Direct structural proof for its highly symmetrical D_{6h} structure was derived by Ingold from vibrational analysis of benzene and benzene-d_6[11] and was further supported by evidence gathered from diffraction experiments.[12,13] Computational geometry optimizations at high ab initio levels[14] confirm Ingold's original finding.

While the dispute over constitution and geometry of benzene appears to be settled in a satisfactory fashion, the reasons for why this compound shows D_{6h} symmetry are a matter of current debate. On the basis of valence bond principles,[15] it was generally argued that the symmetric equilibrium structure is enforced by resonance between the two dominating Kekulé forms **1a** and **1b**, pointing at the π electrons as principal contributors to the equality of CC bond lengths. Recent theoretical studies,[16] however, provide evidence that challenges this view, suggesting instead that the σ rather than the π system is responsible for the symmetric structure. This thesis will elaborate on this topic in greater detail in chapter 2.

The development of the Hückel method[10] allowed the classification of conjugated, cyclic molecules according to simple book-keeping rules. Thus, a compound containing cyclic arrays of (4n+2)π electrons are labelled "aromatic", while those with (4n)π circuits are termed "antiaromatic".[17] Cyclobutadiene (**2**),[18] the prototype of the latter class of compounds, for long eluded experimental scrutiny, but its dibenzo-derivative biphenylene (**3**), a molecule combining aromatic and antiaromatic π electronic arrangements within a single molecular framework, was extensively studied.[19] The concept of juxtaposing these two antipodal electronic features by constructing compounds with alternating four- and six-membered

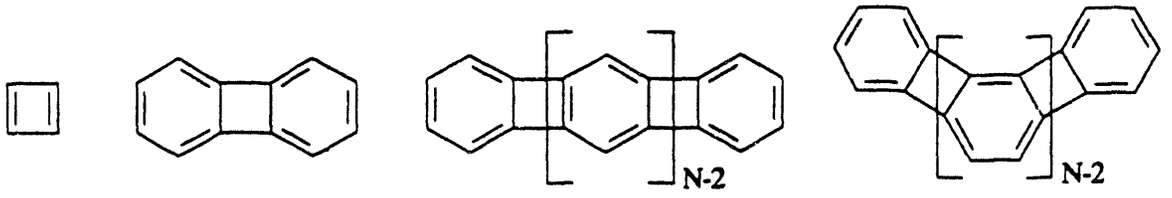

2 **3** **4** (N=3,4,5) **5** (N=3) **6** (N=4,5)

rings was further developed by Vollhardt, who synthesized linearly (**4**)[20] and angularly (**5**, **6**)[21] extended homologs of **3** and named this novel class of compounds [N]phenylenes, according to their number of benzene rings. One of the most remarkable and, in the context of the present thesis, most important characteristic of angular [3]phenylene (**5**) is

its degree of CC bond alternation around the central six-membered ring.[21a] The presence of such CC bond length variations, resembling that of an idealized 1,3,5-cyclohexatriene, was subsequently shown to prevail to an even greater extent in the benzenoid core of a hexasilylated derivative of triangular [4]phenylene (**7**).[22a]

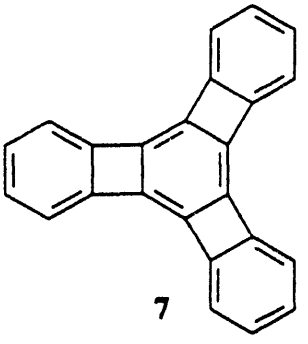

7

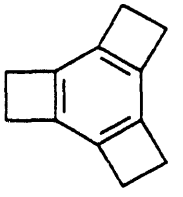

8

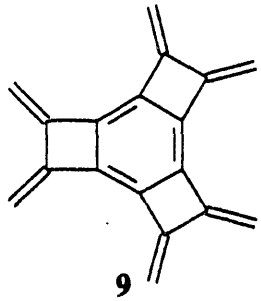

9

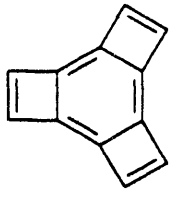

10

Both, strain and π electronic effects can be invoked to explain this phenomenon and an ab initio study of model compounds **8 - 10**, aimed at understanding the relative contribution of these factors to the observed topologies is delineated in chapter 4. Also included are the results of a computational investigation of chromiumtricarbonyl coordination to **8 - 10**, a project prompted by the observation that the barrier to rotation around the metal arene axis can be related to the degree of π delocalization in the free hydrocarbon.[23] First experimental data involving the corresponding complex of **5**[24] and those of derivatives of **7** have been reported.[25]

The striking dissimilarity in the chemical properties of **1** and **7** is borne out by the ease with which the latter can be hydrogenated,[26] whereas the aromatic behavior of the former is typified by the requirement of more drastic conditions.[27] The thermodynamic parameters of the conversion of **7** to its hexahydrogenated derivative have been determined and are discussed in the conceptual framework of "strain" and "aromaticity" in chapter 3.

The advent of buckminsterfullerene C_{60} (**11**)[28], a novel, spherical allotrope of carbon, has rekindled interest in non-planar, polycyclic, aromatic hydrocarbons, as

evidenced by two recently developed routes into the large-scale preparation of corannulene (**12**),[29] originally synthesized by Barth and Lawton.[30] The unique bowl-shaped topology[31] of this molecule motivated our own entry into this field of research and results of synthetic and computational efforts pertaining to cup-shaped hydrocarbon **13** are presented in chapter 5.

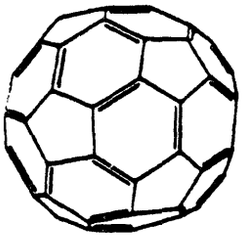

11

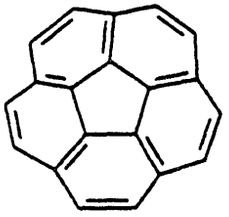

12

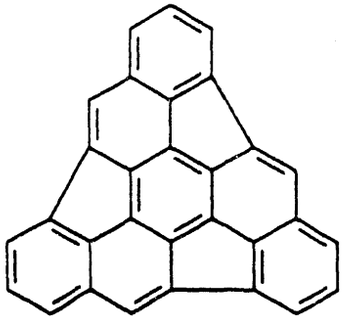

13

The remainder of chapter 1 will focus on current notions of aromaticity, approaches to the quantification of the latter, and an exploration of the effects of strain on the benzene nucleus. A brief introduction into natural bond orbital (NBO) analysis[32] and natural resonance theory (NRT),[33] crucial quantum mechanical tools employed in the course of the investigations, forms the last section of this chapter.

1.2 Aromaticity, Resonance Energy, and π Delocalization.

"In discussing any scientific problem, it is highly desirable that all the words and terms employed should be capable of precise definition. The expression "aromatic character" unfortunately does not satisfy this desideratum, for it is used in different connotations corresponding to different individual interests".[34] Although the notion of aromaticity has evolved considerably from its original conception as being related to the pleasant (aromatic) fragrance of certain compounds, little progress has been made toward a generally applicable definition or an unambiguous quantification of this term since Robinson's apt remark in 1959. Soon after the discovery of benzene, aromatic behavior was associated with enhanced chemical stability of these compounds, as evident from their reluctance to take part in reactions with reagents like cold sulfuric acid and radical initiators, and their tendency to undergo substitution rather than addition. The original tenet, to correlate the rate of reaction with the degree of aromaticity was invalidated by modern thermodynamics,[35] in which reaction rates are associated with the free energy of a transition state, hence precluding a priori conclusions about the ground state phenomenon of aromatic stabilization. Over the years, however, a few criteria have emerged that do allow, usually within narrowly defined limits, a classification of compounds into aromatic or non-aromatic (or pseudo-aromatic or antiaromatic[36]) categories.[37] It should be kept in mind that, depending on which indicator is used, a particular molecule can fall into any of those categories. Some of the more important criteria for aromaticity, particularly those with relevance to this thesis, are outlined below.

1.2.1 Resonance Energy.[38]

The term "resonance energy" (RE) was originally introduced to describe the extra energetic stability of a resonance hybrid over a non-delocalized reference state that is the main contributor to the overall structure of this molecule.[39] It thus follows that this resonance energy, referred to as "vertical resonance energy",[40] is not an observable

property, but can only be approximated invoking theoretical and/or experimental techniques. In the case of benzene, the model from which to derive this quantity is the hypothetical 1,3,5-cyclohexatriene with non-delocalized, "ethylenic" CC double bonds. Simple Hückel molecular orbital (HMO) treatments[10] of benzene result in a resonance stabilization of 2β with respect to this reference, a quantity equivalent to the energy required for the $^1B_{1u}$-$^1A_{1g}$ (lowest $\pi \rightarrow \pi^*$) electronic transition of this molecule. The corresponding UV absorption band appears at 207 nm[41a,b] or roughly 138 kcal mol^{-1}, assigning a value of -69 kcal mol^{-1} to β. Other approximations[41a] yield estimates of -16 to - 56 kcal mol^{-1} leaving wide margins for speculation.

The desire to rely on a less fictitious benzene model than 1,3,5-cyclohexatriene, along with the inadequacies of the Hückel method, led to the development of Dewar's perturbation molecular orbital (PMO) theory.[42] This approach considers the formation of extended conjugated π systems as perturbations of smaller, acyclic fragments that can be joined either intra- or intermolecularly. Even alternant hydrocarbons, for example, can be derived from union of two odd alternant radicals. In this case, the first-order change in energy δE (i.e., the energy of bond formation) is proportional to twice the sum of the products of the coefficients a_i of the non-bonding molecular orbital (NBMO) at the interacting centers (eq 1.1).

$$\delta E = 2(\sum_i a_i)\,\beta \qquad (1.1)$$

The procedure can be illustrated by the interaction of two allyl radicals, leading to either 1,3,5-hexatriene or benzene, depending on the number of unions. (Figure 1.1). Given an NBMO coefficient of $a = 1/\sqrt{2}$, a comparison of δE in the construction of these molecules reveals that benzene has a resonance energy of β with respect to the open chain polyene. PMO analysis of cyclobutadiene (2) formation from allyl and methyl radicals (●), on the other hand, predicts no change in energy (Figure 1.2). Inspection of the corresponding δE

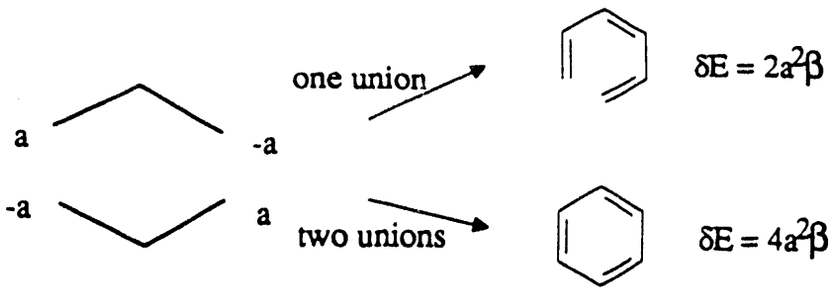

Figure 1.1 PMO Treatment of Benzene and 1,3,5-Hexatriene.

values reveals that **2** is destabilized with respect to 1,3-butadiene, a finding corroborated by the exceedingly high reactivity of the former.[18a-e] The PMO extension of HMO theory

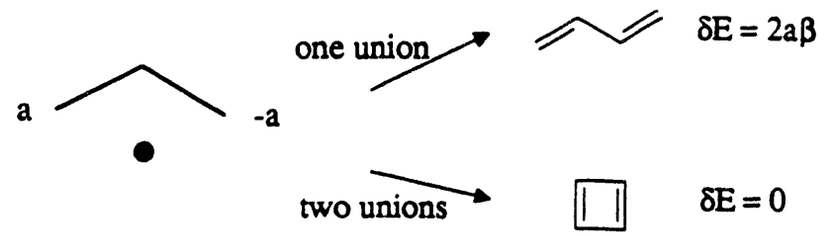

Figure 1.2 PMO Treatment of Cyclobutadiene and 1,3-Butadiene.

is able to overcome some of the problems associated with the latter, such as the failure to explain the aromatic behavior of the (4n)π system pyrene (**14**). In addition, PMO

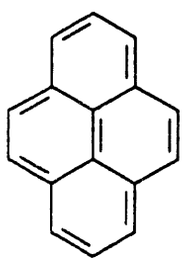

14

theory successfully validates Hückel's (4n+2) rule.[43] Within Dewar's theoretical framework, however, the original definition of resonance energy has shifted, now employing isoconjugate, acyclic polyenes as reference compounds. Although it is advantageous that these are generally synthetically accessible, the problem of assigning a

value to resonance integral β remains. It should also be noted that the outcome of energetic evaluations of large polycyclic systems critically depends on the choice of fragmentary building blocks.[25]

In attempts to further quantify aromatic stabilization, Dewar and de Llano[44] devised a semiempirical SCF-LCAO-MO (PPP) method to construct non-delocalized, "conjugated", cyclic polyenes from CC bond increments derived from their linear, acyclic counterparts. Resonance energies for delocalized molecules can then be determined as the difference between the heats of atomization (an observable quantity) of the cyclic, conjugated hydrocarbons and computed values for their non-resonating, cyclic model compounds. It could be demonstrated that sign and magnitude of the energies thus obtained can serve as criteria for aromaticity in a chemical sense with sufficient accuracy in most cases. The so-called "Dewar resonance energy" of benzene amounts to -20 kcal mol^{-1}, considerably lower than the thermochemical measure[45] of -36 kcal mol^{-1} (vide infra). This discrepancy is rationalized by the fact that the partial double bond character of CC "single" bonds in open chain polyenes is incorporated into the cyclic model compounds.

Hess and Schaad[46] applied Dewar's method of bond increments to HMO theory and, in an effort to make molecules of varying π electron count more comparable to one another, suggested the use of resonance energy per electron (REPE) as a measure for aromaticity. Assuming a value of -32.74 kcal mol^{-1} for β,[46b] these authors estimate REPE for benzene to be of the magnitude -2.22 kcal mol^{-1}, whereas cyclobutadiene is predicted to be destabilized by a REPE of 8.79 kcal mol^{-1}.

Dewar's concept of resonance energy also gave impetus to and forms the basis of Randic's graph theoretical treatment of aromaticity, the model of conjugated circuits.[47] In this theory, the various Kekulé structures of any given conjugated, cyclic hydrocarbon are decomposed into all possible (4n+2) and (4n)π cycles, which are then assigned energy values, whose sign and magnitude depends on the number of π electrons (Table 1.1).

Table 1.1 Energy Contributions of Individual π Circuits.[47d]

Circuit Type	Number of π electrons	Energy [eV]
4n + 2	6	-0.869
	10	-0.247
	14	-0.100
4n	4	0.781
	8	0.222
	12	0.090

Resonance energies are then calculated by simply adding increments of individual π circuits, followed by normalization according to the number of Kekulé structures and π electrons. This procedure is illustrated in an analysis of angularly fused benzodicyclobutadiene **15** (Figure 1.3), a compound whose structural and electronic features will be discussed in more detail in chapter 4. The five neutral resonance hybrids of **15** are depicted in Figure 1.3, together with their contributing π circuits. Employment of energy increments from Table 1.1 furnishes a resonance energy of 0.981 eV per Kekulé form, reflecting destabilization of the 10π electron system by virtue of antiaromatic, cyclobutadienoid substructures. Analogous treatment of the linear isomer **16** yields a more

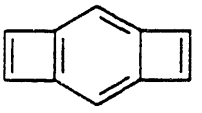

16

favorable value of 0.445 eV, clearly at odds with chemical intuition that would predict less stability for **16** if compared to **15**. This discrepancy has its origin in equally weighing contributions from all Kekulé structures, even highly unlikely ones such as **15c** or **15d**.

While delocalization energies can thus be obtained for a wide range of compounds without the need to resort to elaborate computational techniques, it is evident from the above example that the model of conjugated circuits can only be approximate.

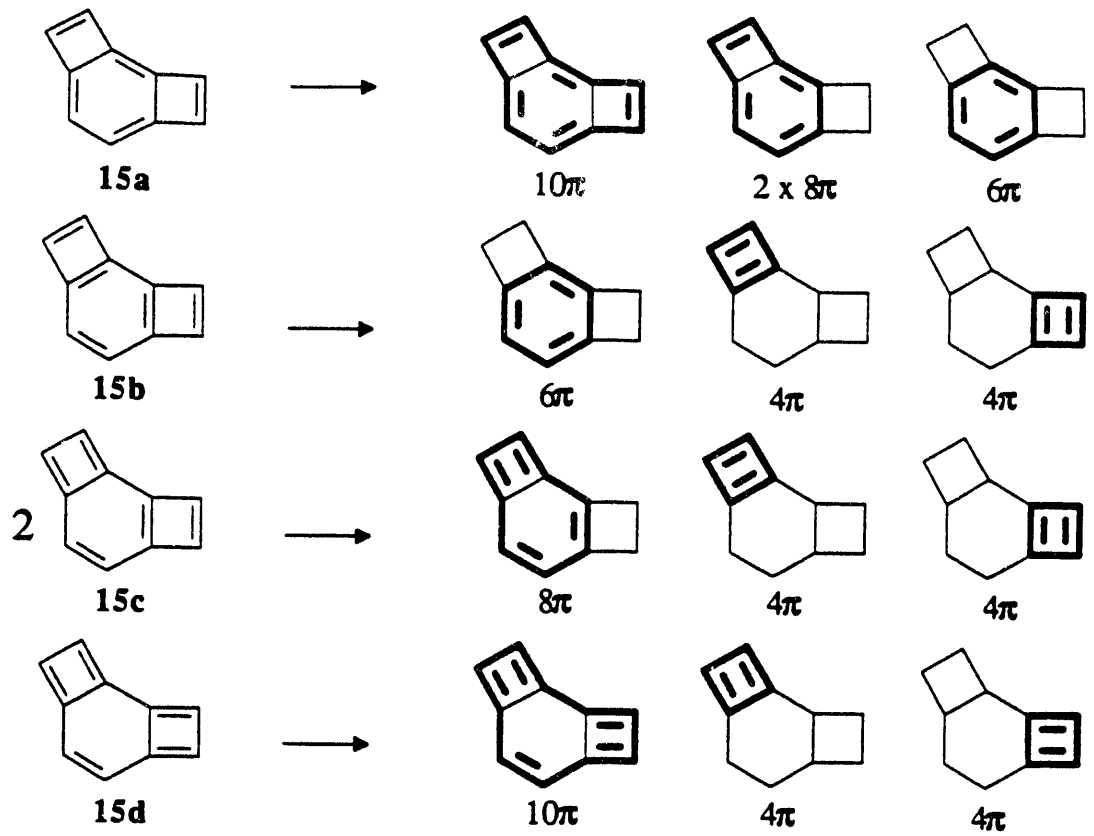

Figure 1.3 Application of the Model of Conjugated Circuits to Benzodicyclobutadiene **15**.

Advances in quantum mechanics and computational resources led to calculations of resonance energies with ab initio methods.[48] Working with localized wavefunctions from double zeta basis sets, Kollmar[49] determined the resonance stabilization of benzene to be -25.7 kcal mol^{-1}. Other approaches[14,50] employed homodesmotic equations,[51] in which bond types and atom hybridizations are balanced to account for contributions from the σ frame, thereby essentially maintaining Dewar's polyenes as reference structures (eq 1.2). Resonance energies of the annulene A_N under consideration can then be obtained by difference between the total energy of A_N and the sum of the energies of the acyclic hydrocarbons (eq 1.3). Depending on the level of theory and the exact form[50b] of the

$$n/2\ H_2C{=}CH{-}CH{=}CH_2 \longrightarrow A_N + n/2\ H_2C{=}CH_2 \qquad (1.2)$$

$$RE(A_N) = \Delta H_f^\circ(A_N) - n\,[\Delta H_f^\circ(H_2C{=}CH_2) - \Delta H_f^\circ(H_2C{=}CH{-}CH{=}CH_2)] \qquad (1.3)$$

homodesmotic equation, the calculated values for benzene range from -33.3 kcal mol^{-1} (RHF/4-31G*)[50a] to -22.6 kcal mol^{-1} (MP3/6-31G).[14] Although delocalization energies of some other benzenoid and nonbenzenoid hydrocarbons have been investigated[14,49,50] in that fashion, the computational demands of ab initio calculations are generally so high that only relatively small molecules can be studied.

Consideration of homodesmotic equations provides the opportunity to focus entirely on experimental data in the estimation of stabilization energies. Using only published values for the heats of formation of 1,3-butadiene, benzene, and ethylene for the quantities of eq 1.3, George et al.[51a] calculated what he named "homodesmotic stabilization energy" for benzene to be -21.2 kcal mol^{-1}, in excellent agreement with ab initio predictions.[14,44,50b] Applications of this approach seem to be limited only by the availability of thermochemical data[52] and the formulation of appropriately balanced homodesmotic equations.

Precomputational attempts to estimate resonance energies from experimentally derived energy contributions relied mainly on measurements of heats of combustion or heats of hydrogenation.[39b,52] Compilation of data obtained by the former method allowed the assignment of energy increments to individual types of bonds,[53] whose sum is then used for comparison with the determined ΔH_f° of the conjugated molecule and the energy content $\sum E$ of a non-resonating reference state (eq 1.4).

$$\Delta H_f^\circ = \sum E + \mathrm{RE} \qquad (1.4)$$

Differences are then attributed to what is called an "empirical resonance energy", which, in the case of benzene, amounts to a stabilization of -36 kcal mol^{-1}.[39b] Besides the deliberate choice of incremental bond energy terms, data obtained in this fashion generally suffer from the fact that relatively small values are estimated from large, experimentally derived numbers. For example, an error of 1% in the heat of combustion of benzene[39b]

(789.1 kcal mol^{-1}) translates into 7.9 kcal mol^{-1}, a substantial uncertainty compared to 36 kcal mol^{-1} quoted above.

The absolute magnitude of experimental errors is somewhat diminished if heat of hydrogenation data[39b,52,54] are used to assess the degree of resonance stabilization. The empirical resonance energy is then expressed as the difference between the ΔH_H of the cyclic conjugated molecule under consideration and that of a "suitable" model compound. As exemplified for benzene in Table 1.2, the point of reference is absolutely critical. Thus, RE values for benzene range from -48.6 kcal mol^{-1} (reference: ethylene) to -25.9 kcal mol^{-1} (reference: 1,3-butadiene), depending on the nature of the model compound employed (note that most commonly the cyclohexene-based RE value is used). Invoking ΔH_H data as a measure for the molecular property of resonance stabilization bears the problem that, in addition to the necessarily arbitrary choice of reference compounds, the

Table 1.2 ΔH_H Data for Selected Unsaturated Hydrocarbons.[a]

Compound	ΔH_H[b]	RE[c]
benzene	-49.8	-
ethylene	-32.8	-48.6
cis-2-butene	-28.6	-36.0
1,3-butadiene	-57.1	-25.9
cis-1,3,5-hexatriene	-80.5	-30.7
cyclohexene	-28.6	-36.0
1,3-cyclohexadiene	-55.4	-33.3

([a]) Values in kcal mol^{-1}. ([b]) Taken from ref 54.

([c]) RE = $[\Delta H_H(\text{model})/n]\times 3 - \Delta H_H(\text{benzene})$, where n equals the number of formal double bonds in the model.

unavoidable inclusion of changes in delocalization-independant contributions (e.g, strain, rehybridization, hyperconjugation)[38d,55] might obscure pure π electronic effects. Considerations of this kind are further alluded to in chapter 3.

1.2.2 Bond Equalization and Planarity.

The notion that delocalizing interactions between adjacent π systems have an effect on the geometries of conjugated molecules was firmly established by valence bond and molecular orbital theory[9b] in their correct prediction of the symmetric D_{6h} structure of benzene.[11-13] Hückel's classification scheme[10] provided the basis to associate aromatic character of cyclic, conjugated (4n+2)π hydrocarbons with almost equal CC bond lengths (e.g., ~ 1.40 Å in benzene), whereas antiaromatic (4n)π species were viewed to exhibit alternating CC bonds of lengths in the typical range[56] for isolated single (~1.54 Å) and double (~1.33 Å) bonds. This concept was borne out by X-ray crystallographic analyses of monocyclic π systems, such as the cyclobutadiene derivative **17**,[57] benzene (**1**),[11-13] cyclooctatetraene (**18**),[58] ar i its dianion[59] (Figure 1.4). Thus, benzene and the aromatic 10π system $\mathbf{18}^{2-}$ reveal CC bonds of equal lengths within their respective frameworks,

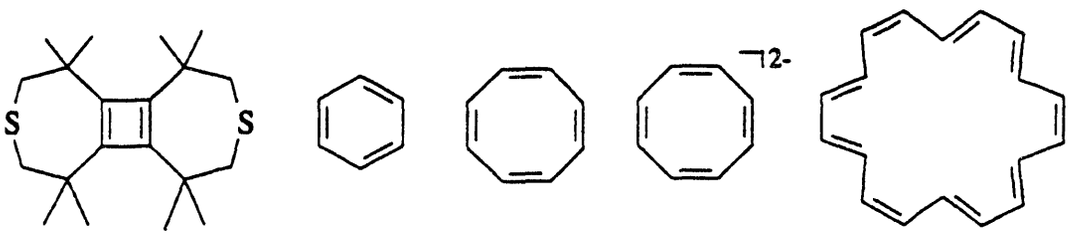

	17	**1**	**18**	$\mathbf{18}^{2-}$	**19**
R_{CC}(short)	1.344Å	1.398Å	1.362Å	1.406Å	1.382Å
R_{CC}(long)	1.588Å	1.398Å	1.465Å	1.406Å	1.419Å

Figure 1.4 CC Bond Lengths of Annulene Perimeters in Selected Conjugated Hydrocarbons in Å.

centering around 1.40 Å. Species with formally antiaromatic π electron count like **17** and **18**, on the other hand, show alternating single and double bonds with internuclear CC distances from 1.326 Å (1.344Å) to 1.465 Å (1.588 Å) in **18** (**17**). In addition, **18** adopts a tub conformation in the solid state to minimize unfavorable π interactions.

While the relation between π delocalization and bond length appears to hold for the smaller annulenes, discrepancies seem to exist between the various criteria for aromaticity when applied to [18]annulene (**19**). Structure elucidation by X-ray crystallography disclosed two distinct CC bond lengths of 1.352 Å and 1.419Å,[60] a surprising result, since **19** was initially judged to conform with Hückel's rule by spectroscopic evidence such as ^{1}H NMR data[61] (cf. section 1.2.3). The phenomenon of bond alternation in large cyclic polyenes, regardless of their π electron count, was predicted computationally by Longuett-Higgins[62] and Dewar,[63] whose work points at a threshold of n = 26 in the size of the [n]annulenes, after which π delocalization effects are supposed to break down entirely. This assumption could be confirmed in the ^{1}H NMR spectroscopic investigation of tridehydro[26]annulene and pentadehydro[30]annulene,[64] none of which are able to sustain a diamagnetic ring current (cf. section 1.2.3), thereby failing to qualify as aromatic molecules by this criterion. Structural data derived from X-ray diffraction of [n]annulenes with n>18 could not be obtained, a fact that, in light of borderline cases as **19**, reflects the impracticality and overall insufficiency of this measure of aromaticity. Furthermore, knowledge about the relative positions of the nuclei in a given molecular framework does not automatically allow conclusions regarding their electronic interactions (e.g., π delocalization). For a discussion of the geometrical dependence of π delocalization, see section 1.2.3 and chapters 2 and 4.

To overcome some of the shortcomings of bond alternation as a criterion for aromaticity, Binsch and Heilbronner[37b,65] devised the theoretical concept of "second-order bond fixation", in which they propose bond alternation to be predictable by inspection of the eigenvalues λ_i and eigenvectors d_i of the bond-bond polarizability matrix, consisting of the second partial derivatives of the π electron energy with respect to bond lengths. The most favorable bond distortion is given by those d_i belonging to the largest eigenvalue λ_{max}. Should this quantity exceed a critical value $\lambda_{crit}=1.22\ \beta_0^{-1}$, the σ compression energy can be overcome and the molecule will show second-order bond

fixation, either dynamic or static in nature. On this basis, it was suggested that conjugated π systems should be called aromatic if they show "neither strong first-order nor second-order bond fixation".[65c] This definition seems to accommodate the stabilities of simple hydrocarbons including azulene (**20**) and correctly predicts the instabilities of pentalene (**21**) and heptalene (**22**) (Figure 1.5). However, the concept fails to explain the observed bond alternation in **19**,[65b] thereby revealing a lack of generality that, in conjunction

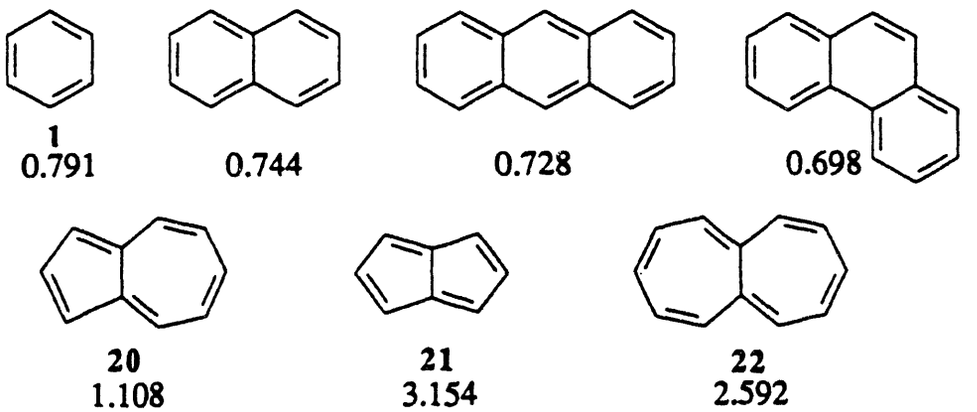

Figure 1.5 Second-Order Bond Fixation in Selected Hydrocarbons.
Values are λ_{max} in units of β_o and are taken from refs 65 b,c.

with the arbitrary choice of λ_{crit} and the speculative meaning of the expression "strong bond fixation", might have prompted Heilbronner's sarcastic excuse to have initiated such a proposal (cf. discussions in ref 37b, pp 35 and 235).

Planarity of conjugated π systems was long considered a prerequisite for effective π delocalization and hence aromaticity. But structural and spectroscopic investigation of

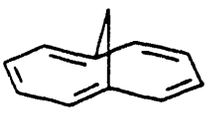

23

compounds like 1,6-methano[10]annulene (**23**),[66] [18]annulene (**19**),[60] corannulene (**12**),[30,31] and buckminsterfullerene (**11**)[67] suggest that even in cases of considerable deviation from planarity stabilizing π interactions are operational (cf. section 1.3.2),

rendering these molecules aromatic by various other criteria, among them UV and NMR spectroscopy. It thus appears that concepts that regard aromaticity as a purely structural phenomenon result in too narrowly defined terms that fail to include a large variety of compounds.

1.2.3 Magnetic Properties.

Early investigations of the magnetic properties of organic compounds[68] indicated large magnetic susceptibilities of cyclic conjugated π systems, an effect whose origin was difficult to explain in light of the behavior of other saturated or unsaturated molecules. Pauling[69] was able to rationalize the observed diamagnetic anisotropy of aromatic hydrocarbons by postulating the presence of π electronic currents induced by an external magnetic field (Figure 1.6). Although the nature of these ring currents has been an issue of debate,[70] this model forms the basis of a variety of magnetic criteria by which to judge aromatic behavior.

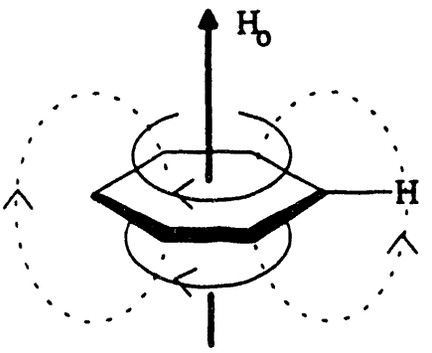

Figure 1.6 Effect of External Magnetic Field on Benzene: The Ring Current Model.

Since anisotropies are exceedingly difficult to measure directly, Dauben et al.[71] suggested the use of the more easily determined molar magnetic susceptibility χ_m. He proposed as a criterion of aromaticity the exaltation Λ, defined as the difference between

the observed χ_m and the value χ_m', estimated from bond increments[72] of a cyclic polyene of the same structure (eq 1.5).[73] Measurements have been made for a large variety of

$$\Lambda = \chi_m - \chi_m' \qquad (1.5)$$

compounds,[71c] generally resulting in sizable exaltations for molecules typically considered aromatic (e.g., benzene: Λ = 13.7; napthalene: Λ = 30.5), whereas negligibly small values are interpreted as indications of non-aromatic character (e.g., cyclooctatetraene (**18**): Λ = -0.9; fulvene: Λ = 1.1; heptalene (**22**): Λ = -6). This method proved to be successful in the classification of several distorted systems, such as **23** and the [9]paracyclophane (**24**, n=9) (see also section 1.3.2), none of which exhibit exaltations significantly different from those of the corresponding unperturbed counterparts naphthalene and

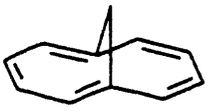

23
Λ = 36.8

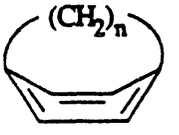

24(n=9)
Λ = 15

benzene. The problems associated with the use of bond increments derived from model compounds become apparent in the treatment of heterocycles, whose exaltations are accessible, but less reliable. Thus, no prediction can be made with certainty regarding the relative degree of aromaticity in thiophene (Λ = 13.0), pyrrole (Λ = 10.2), and furan (Λ = 8.9). Likewise, destabilizing antiaromatic effects are not readily detected, though some negative values for Λ have been observed. However, the immensely broad range of applications, and the ease with which data are obtained and interpreted, render the diamagnetic susceptibility exaltation, at least qualitatively, one of the more useful measures of aromaticity.

Perhaps the most readily observed indicator for diamagnetic ring currents is the influence they exhibit on the NMR chemical shifts of protons (but also other magnetically active nuclei) in the vicinity of cyclic, conjugated π systems.[74] Inspection of Figure 1.6 suggests that in $(4n+2)\pi$ systems the induced magnetic field outside the periphery of the ring is aligned with the applied one, whereas that inside the cycle is opposed to it. Thus, outside ring hydrogens are deshielded and experience a downfield shift relative to purely olefinic protons (cf. those of cyclohexene: δ 5.5 ppm), while those inside are shielded and resonate upfield. This concept is illustrated in the ^{1}H NMR spectra of cyclophane **25**[75] and annulene **19**[76] (Figure 1.7). The magnetic behavior of $(4n)\pi$ systems on the other hand, is dominated by paramagnetic ring currents[77] arising from low lying electronically excited states. The resulting reversal of the above correlation between chemical shift and relative location in space is illustrated in the spectral data of [16]annulene (**26**)[78]

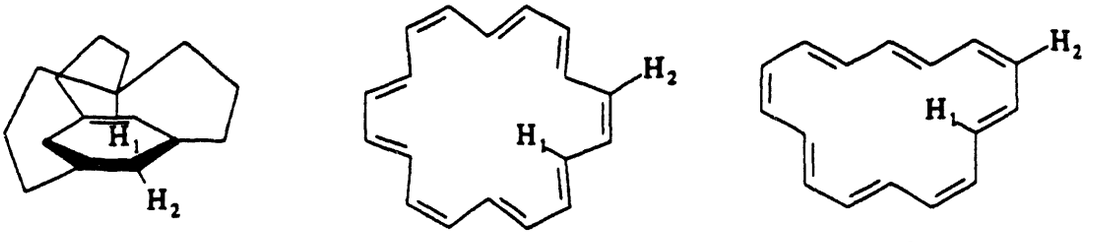

	25	**19**	**26**
$\delta(H_1)$:	-4.03 ppm	-2.99 ppm	10.56 ppm
$\delta(H_2)$:	6.86 ppm	9.28 ppm	5.33 ppm

Figure 1.7 Selected ^{1}H NMR Chemical Shifts of Some Cyclic Conjugated Molecules Demonstrating their Magnetic Anisotropy
(^{a}) $CDCl_3$, 25 C. (^{b}) THF-d_8, -60 C. (^{c}) 20% CS_2/80% THF-d_8, -130 C.

(Figure 1.7), where endocyclic protons clearly resonate downfield compared to exocyclic ones. This apparently unambiguous relation prompted Elvidge and Jackman[79] to propose ^{1}H NMR chemical shifts as a quantitative measure for aromaticity. It was soon realized, however, that structural features (e.g., strain, hybridization, bond alternation), not only para- or diamagnetic ring currents may contribute importantly to the nuclear magnetic

properties of conjugated molecules, thus in many cases prohibiting the unequivocal classification of the latter [cf., for example, the discussion[21c,25,80] surrounding the NMR spectroscopic behavior of biphenylene (**3**)].

In order to circumvent some of the caveats mentioned above, Mitchell[81] devised a system that allows to probe the relative ability of two structural subunits to sustain diamagnetic ring currents. The hydrogens of the internal methyl groups of

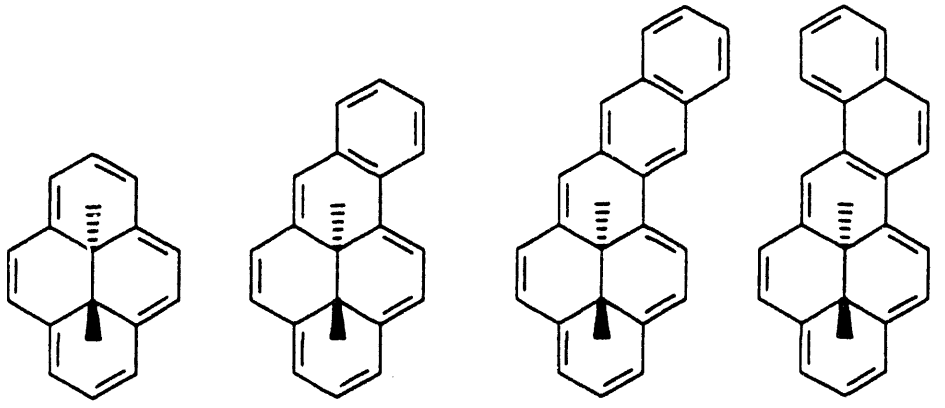

27 **28** **29** **30**

$\delta(CH_3)$: -4.25 ppm -1.62 ppm -0.44 ppm -2.78 ppm

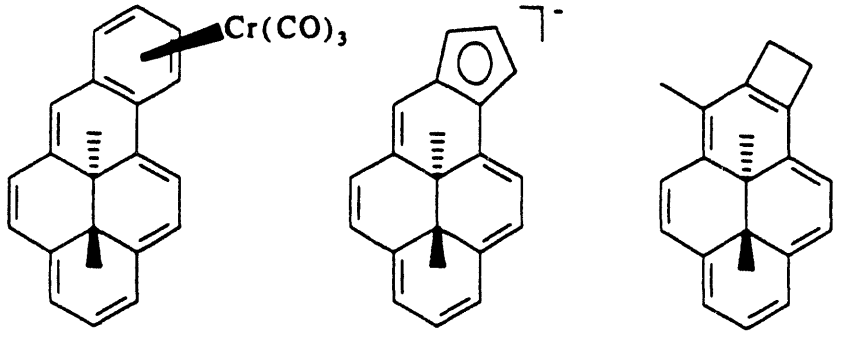

31 **32** **33**

$\delta(CH_3)$: -0.98 ppm -3.17 ppm -4.23 ppm

Figure 1.8 ^{1}H NMR Chemical Shifts of Internal Methyl Groups in Dihydrodimethylpyrene Derivatives.

dihydrodimethylpyrene **27** are strongly shielded (δ -4.25 ppm) due to effective π delocalization along the periphery of this formal [14]annulene (Figure 1.8). The chemical

shift of these protons is very sensitive to the magnitude of the ring current, which in turn is influenced by the presence of a second conjugated π system fused to the pyrene nucleus. Thus, incorporation of highly delocalized fragments, such as benzene in **28**, results in diminished π electronic fluctuation in the pyrenoid substructure, as the ring current induced in the additional aromatic sextet interferes with the one along the periphery of unperturbed **27**. Suppression of π delocalization along the pyrene core is apparent from the chemical shift of the methyl protons in **28** (δ -1.62 ppm), which appear significantly downfield form the corresponding absorption in **27** (δ -4.25 ppm). Using chemical shift changes caused by fusion of the benzene nucleus as a reference, Mitchell was able to compare what he calls the "effective aromaticity"[81g] of various conjugated systems (Figure 1.8). Annelation of a naphthalene unit to **27**, for example, furnished **29** and **30**, both of which reveal effective suppression of the diamagnetic ring current along the [14]annulene substructure. The influence of linear fusion on the chemical shift of the methyl protons is considerably larger than that exerted by angular arrangement. This is evident from the corresponding resonances of **29** (δ -0.44 ppm), which appear considerably downfield from those of **30** (δ -2.78 ppm) This result is in complete agreement with Clar's rule,[82] which predicts a maximization of aromaticity in the least annelated (i.e., the terminal) benzene rings of polybenzenoid hydrocarbons. Preferences of this type prevent extended π delocalization in **30**. An example for a metal-complexed benzannulene is compound **31**,[81f] which shows methyl proton resonances at -0.98 ppm and -0.87 ppm, downfield from those in uncoordinated **28** (δ -1.62 ppm). Since anisotropy effects of the $Cr(CO)_3$ at the location of the methyl groups were shown to be negligible over such a distance, it was concluded that benzenechromium tricarbonyl has a greater degree of aromaticity than benzene itself. It should be noted, however, that other factors such as depletion of electron density or rehybridization effects may have to be considered to explain the observed behavior. In the non-alternant cyclopentadienylanion-fused **32** the upfield resonance of the methyl protons in **32** (δ -3.17 ppm) relative to those in **28** (δ-1.62

ppm) suggests that the former is less delocalized (i.e., less aromatic) than benzene,[81g] a finding that is supported by results from various other methods. Of particular interest in the context of this thesis is the implication that angular strain imposed on cyclic conjugated π systems by small-ring fusion is not sufficient to reduce the extent of their diamagnetic ring current. Thus, the diagnostic chemical shift in the cyclobutene derivative **33**[81c] (δ -4.23 ppm) is only marginally different from that in unsubstituted **28** (δ -1.62 ppm), indicating unperturbed π delocalization despite manipulations of the σ frame. This argument will be further corroborated in the analysis of the effects of four-membered ring fusion to the benzene nucleus (chapter 4).

It is evident that the proton chemical shift provides a versatile tool to gain insight into the electronic nature of delocalized π systems, although this observable is liable to and difficult to segregate from influences originating from factors not necessarily associated with aromaticity. Alternative NMR methods[83] relying on coupling constants rather than chemical shift data to evaluate the degree of π delocalization will not be discussed here.

1.2.4 Hindered Rotation of the $Cr(CO)_3$ Tripod.

While coordination of the $Cr(CO)_3$ tripod to hydrocarbons containing the benzene nucleus has long interested scientists from bond theoretical, structural, and lately synthetic points of view,[84] the prediction that the barrier to rotation around the metal arene axis

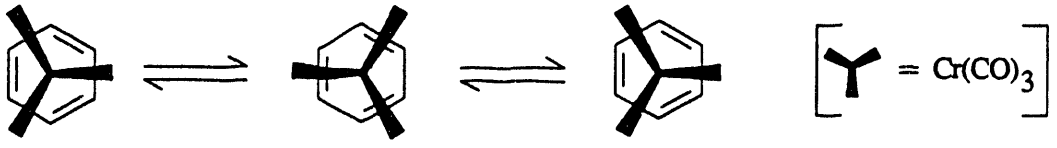

34a **34b** **34a**

could serve as a probe for the degree of π delocalization in the latter is of relatively recent origin. Experimental data[85] point at a negligibly small activation energy for degenerated tripod rotation in benzenechromium tricarbonyl (**34**), but results from extended Hückel

techniques[23a] suggest an increase of this quantity to sizable 19.4 kcal mol^{-1} in case of fully localized benzenoid π electrons.

Synthesis and structural characterization of angular [3]phenylene (**5**)[21a] and triangular [4]phenylene (**7**)[22a] provided compounds with which to test the computational prediction. If the observed decline in bond equalization along the series **1** → **3** → **5** → **7** (Figure 1.9) can be directly related to the amount of π delocalization in the annelated benzene core, one would expect increasing

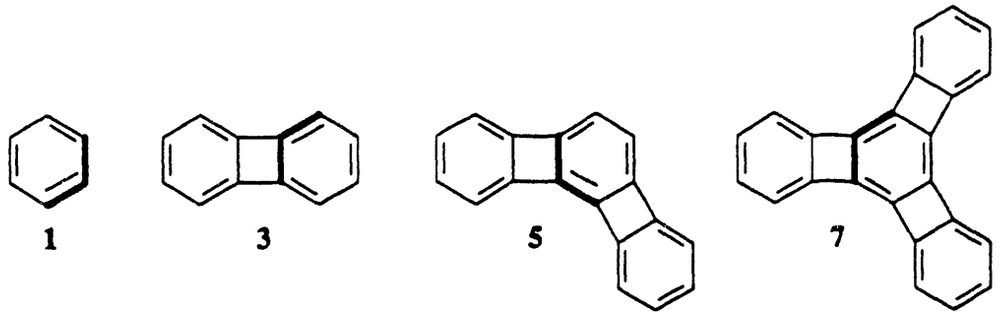

R_{CC}(short):	1.398 Å[12b]	1.372 Å[86]	1.345 Å[21a]	1.333 Å[22a]
R_{CC}(long):	1.398 Å	1.426 Å	1.449 Å	1.502 Å

Figure 1.9 CC Bond Length Variations in Benzocyclobutadienologs of Benzene. Values Shown Represent the Experimentally Determined Highlighted Longest (Shortest) Internuclear Distances in the Most Annelated Benzene Cores. Data for **7** are those of its 2,3,6,7,10,11-Hexakis(trimethylsilyl)derivative.

barriers to tripod rotation of their corresponding $Cr(CO)_3$ complexes. Whereas activation energies of $Cr(CO)_3$ rotation in **34** and **35** were calculated to be prohibitively small (0.3 kcal mol^{-1} for **34**[23a] and 0.8 kcal mol^{-1} for **35**[87] by extended Hückel methods) to permit experimental scrutiny, dynamic NMR studies on compounds **36-38**[24,25,88] (Figure 1.10) disclosed rotational barriers of 8.2 kcal mol^{-1} (**36**),[89] 11.5 kcal mol^{-1} (**37**), and 9.7 kcal mol^{-1} (**38**), thereby confirming theoretical predictions. The obtained values are relatively low compared to the calculated standard for localized **34** ($\Delta G^{\ddagger}$ 19.4 kcal mol^{-1}), suggesting that significant π delocalization is still operational in **36-38**, despite the highly

distorted geometries of their central six-membered rings. Simple bond order-bond length relationships[9e] indicate uncomplexed **38** (**36**) to be 77% (53%) localized with respect to an idealized 1,3,5-cyclohexatriene. Application of these percentages to $\Delta G^{\ddagger}$ of **34** leads to an estimated barrier of 14.9 kcal mol^{-1} (10.3 kcal mol^{-1}) for **38** (**36**), obviously larger than the observed one. The inconcistencies in the above

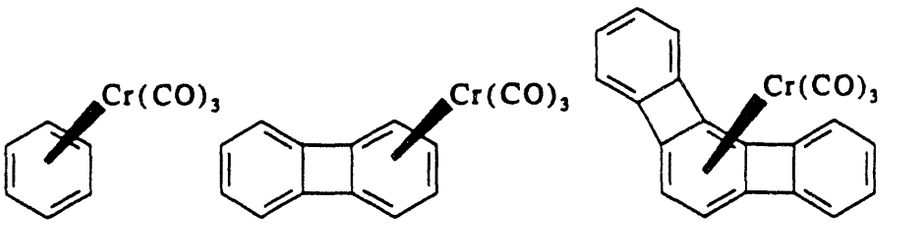

34 **35** **36**

$\Delta G^{\ddagger}$ 0.3 kcal mol^{-1} *a* 0.8 kcal mol^{-1} *b* 8.2 kcal mol^{-1} *c*

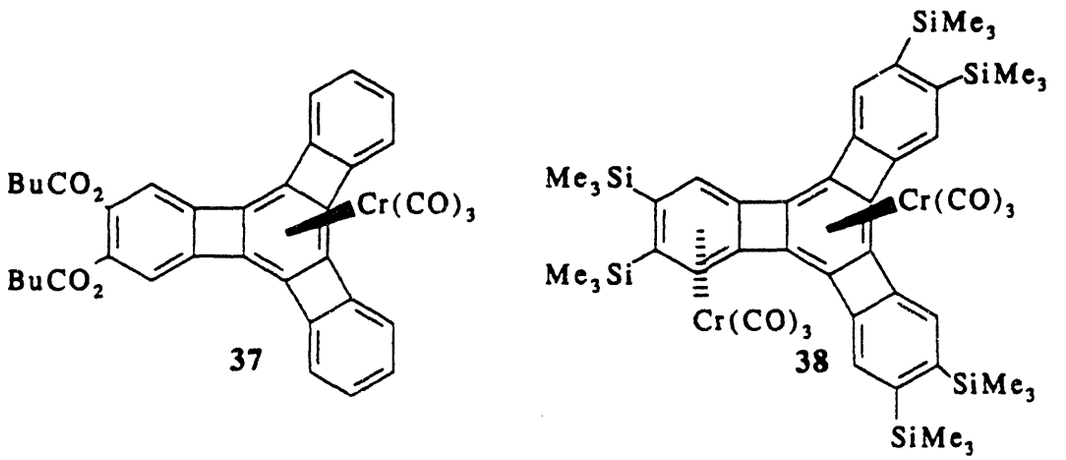

$\Delta G^{\ddagger}$ 11.5 kcal mol^{-1} *d* 9.7 kcal mol^{-1} *d,e*

Figure 1.10 Barriers to Rotation of the $Cr(CO)_3$ Tripod Complexed to Benzene and some Benzocyclobutadieno-fused Derivatives. (*a*) Results from Extended Hückel Calculations.[23a,87] (*b*) Results from Extended Hückel Calculations.[87] (*c*) See ref 89. (*d*) Ref 25. (*e*) Only the Barrier of Centrally Bound $Cr(CO)_3$ Could be Determined.

correlation are at least partly attributable to the fact that structural changes associated with localization of benzene have not been considered in the derivation of $\Delta G^{\ddagger}$ for **34**. While the fluxional behavior of $Cr(CO)_3$ in its arene complexes is sensitive to their degree

of π delocalization, the need for better model systems that more closely reflect the geometrical features of **36** to **38** is apparent. This conclusion has provided impetus for the ab initio investigation of $Cr(CO)_3$ coordination to benzenes fused to four-membered rings, the results of which are delineated in chapter 4.

1.3 Exploration of Structural Limitations of π Delocalization in Benzene.

The realization that a high degree of planarity and CC bond length equality is a prerequisite (and/or a manifestation) of effective π delocalization in conjugated systems provides the basis of extensive research aimed at exploring the structural limitations of aromatic behavior in the benzene nucleus. To this end, geometrical deformations are conceivable to occur either in-plane or out-of-plane with respect to the six-membered ring. Examples for both types of distortions will be discussed below.

1.3.1 In-Plane Distortions of the Benzene Core: Small-Ring Fusion.

Based on simple geometrical arguments, Mills and Nixon[90] explained observed differences in the product distribution obtained in electrophilic substitution experiments of indane (**39**) and tetralin with a preferential π electronic arrangement in the former in the sense of **39a**.

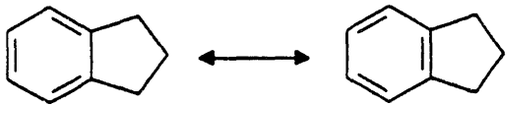

39a **39b**

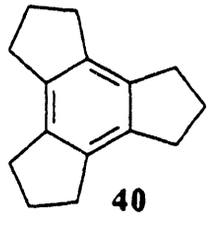

40

Although subsequent work[91] proved the conclusions drawn from the original data erroneous, the so-called "Mills-Nixon (MN) effect", now more broadly defined as strain-induced benzenoid CC bond alternation, has fueled a long-standing debate pertaining to its existence and origin, and inspired the synthesis of a variety of small-ring annelated benzenes. Initial support for the Mills-Nixon postulate was derived from theoretical

studies[92] and from NMR spectroscopic investigations[93] that suggested ring current reductions in **39** (**40**) to about 70% (40%) compared to that of benzene. These findings, however, could not be substantiated by susceptibility exaltation measurements,[71c] inspection of $^4J_{HH}$ coupling constants,[94] or by X-ray crystallographic analysis of **40**[95] that revealed no significant bond alternation of the benzene core. Consequently, synthetic efforts turned to further decreasing the size of the annlated ring, resulting in the preparation of the highly strained benzocyclobutenes **41**, **42**, and **8**.[96] Surprisingly, structural investigation of **41**[96b] showed no indication of an appreciable MN effect, thereby assigning pivotal roles to X-ray diffraction studies of **42** and in particular of **8**, for which various theoretical methods predicted substantial bond alternation.[97]

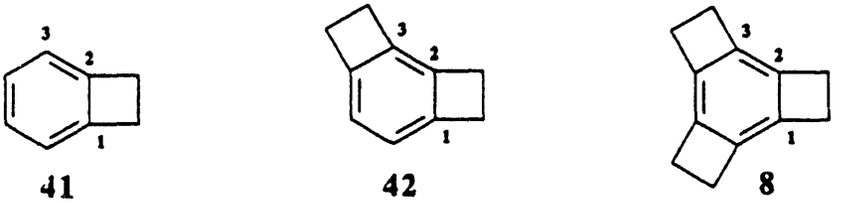

	41	**42**	**8**
$R_{1\text{-}2}$	1.391 Å[a]	1.402 Å[b]	1.415 Å[b,c]
$R_{2\text{-}3}$	1.385 Å	1.385 Å	1.391 Å

Figure 1.11 Selected Benzenoid CC Bond Lengths of Benzocyclobutenes **41**, **42**, and **8**. ([a]) Ref 96b. ([b]) Ref 25. ([c]) Values are those of one of the two Independent Molecules Present at 125 K.

Only very recently could computational and experimental results be brought to agreement (Figure 1.11). Crystallographic analysis of **42** and **8**[25,98] disclosed benzenoid CC bond alternations strongly inidicative of the presence of MN distortions. It is noteworthy that the observed structural variations originate primarily from perturbations of the σ framework and do not a priori allow conclusions regarding the π electronic distribution. The hypothesis that the σ and π systems are to a first approximation independent of each other, might explain why the observed bond alternation in **8** does not enforce olefinic reactivity patterns[25] nor is it reflected in the NMR, UV, IR, and mass

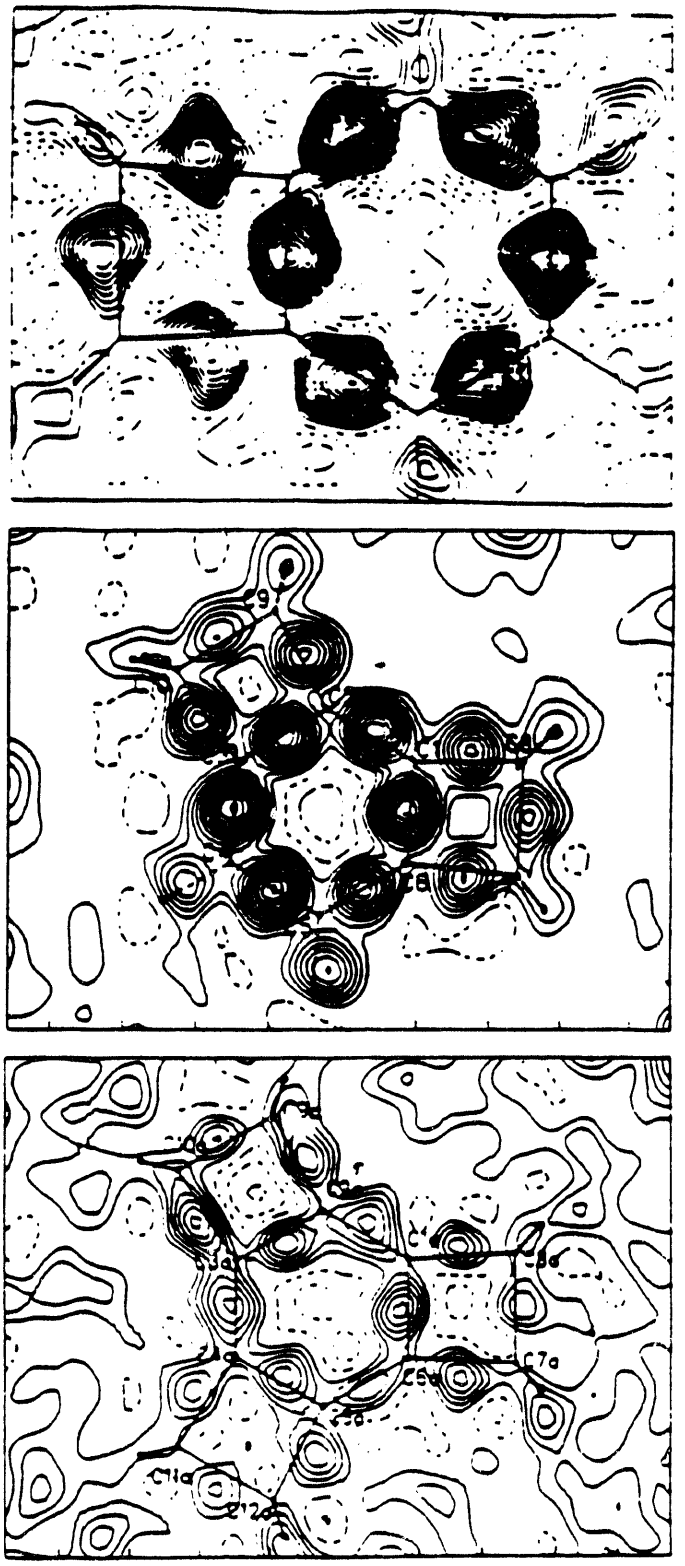

Figure 1.12 XX Deformation Electron Densities of Benzocyclobutenes 41[96b] (Top), 42[25] (Center), and 8[25] (Bottom).

spectroscopic data of **8**,[96g] all of which implying unperturbed aromatic π delocalization (cf. the discussion of angular strain effects, section 1.2.3, and chapter 4).

XX deformation electron density studies on **41**, **42**, and **8**[25,96b,98] (Figure 1.12) reveal that strain, caused by cyclobutene fusion to the benzene nucleus, manifests itself in the formation of bent bonds. To accommodate bond angle deviations from unstrained values, the maxima of electron density are shifted exocyclic in peripheral bonds involved in ring fusion, whereas those common to both substructures show endocyclic departures from their respective internuclear axes.

Both structural effects, bending and length alternation of bonds, can be explained at the atomic level with rehybridization schemes, first proposed by Finnegan and Streitwieser[99] (Figure 1.13). They suggest that in order to retain effective overlap in binding to their neighbors, the carbons at the ring junctions make use of the more directional orbitals of higher p character in bonds to atoms in the smaller ring, leaving hybrids of increased s content for bonds adjacent to the site of fusion. This rehybridization model has received support from several theoretical studies.[97a,d,e]

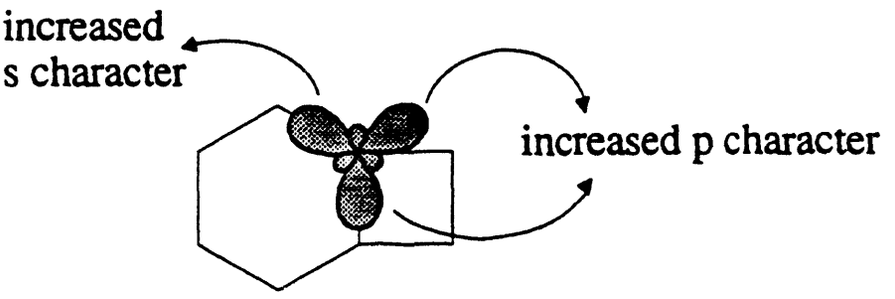

Figure 1.13 The Streitwieser-Finnegan Model of Rehybridization in Strained Aromatic Systems.

The effects of strain do have a direct bearing on the observed geometry of the phenylenes **5** and **7** (cf. Figure 1.9, section 1.2.4). In these systems, the benzene nucleus is incorporated into extensively delocalized π networks via four-membered rings, raising the

possibility of enhanced bond alternation to minimize antiaromatic, cyclobutadienoid interactions as in **7b**. The relative contribution of σ and π effects to the topology of these

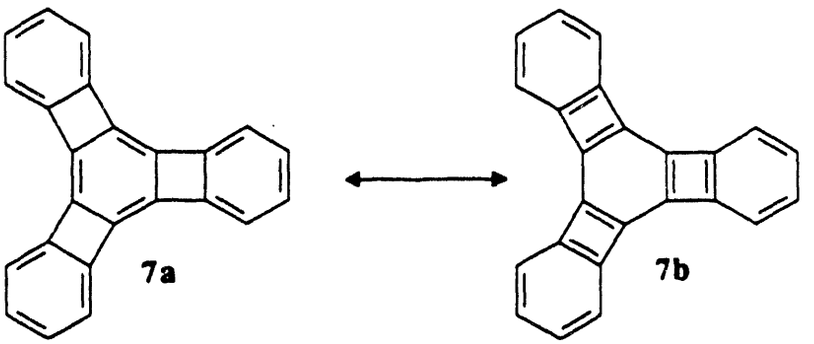

7a **7b**

compounds is subjected to computational scrutiny as outlined in chapter 4.

Among the most highly strained members of small-ring annelated benzenes are certainly those involving cyclopropene.[100] In this case, the strain energy is so high (about 68 kcal mol^{-1} in **43**[101]) that fusion of more than one three-membered ring appears to exceed the current limit of stability of these compounds. One of the record holders in this respect is presumably **44**,[102a] recently synthesized by Billups et al. Structural determination of **43**, **44**,[100b,103] and numerous other cycloproparenes[100,103b] show that without exception the bond common to three-membered rings is always shortest, thereby preventing benzenoid distortions in a MN sense. Furthermore, the bonds adjacent to the

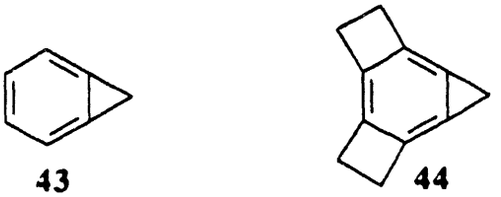

43 **44**

site of fusion in **43** are also contracted with respect to benzene, in apparent mismatch to geometries associated with either one of the two Kekulé forms. Since reactivity studies[104] and NMR data[100] show no clear indication for ring current reduction, it was concluded[105] that the concept of π electronic localization, as judged by internuclear distances, is of little value.

1.3.2 Out-of-Plane Distortions of the Benzene Core.

Three-dimensional benzene distortions are most prominently exemplified in the para-cyclophanes **24**,[106] a class of compounds where the aliphatic tether enforces a boat conformation of the six-membered ring. Since the extent to which the benzene core deviates from planarity critically depends

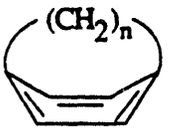

24 (n=6-14,16)

on the number of atoms in the bridge, attempts were made to explore the limits of stability by decreasing the chain length. While there are claims[107] for the intermediacy of a [5]para-cyclophane (**24**, n = 5), the next higher homolog **24**(n = 6) appears to be the smallest isolable molecule of this type.[108] X-ray diffraction studies[109] on a crystalline derivative of **24**(n = 6) revealed that the benzenoid carbon centers attached to the alkyl tether are bent 19.4° out of the plane defined by the four remaining six-membered ring atoms. The strained nature of this compound is reflected in its chemical reactivity,[109] that is dominated by typical olefinic behavior (e.g, facile hydrogentation, cis-1,2-bromination, etc.). Ground state properties of **24** (n = 6), on the other hand, such as those inferred from NMR[109] or photoelectron spectroscopic data,[106e] cannot be interpreted as being due to loss of aromaticity.

Another class of out-of-plane distorted benzenes are those that are hexasubstituted by bulky groups.[110,111] Most of these sterically congested molecules adopt boat conformations[110] in the solid state, whereas the recently prepared hexakis(trimethylgermyl)benzene[111b] and its hexakis(trimethylsilyl) analog[111c] **45** prevail as chair structures, with average benzenoid torsion angles of 9.8° in the latter. As in the para-cyclophanes, the distortional strain in **45** gives rise to increased photo- and thermochemical reactivity, the thermolytic disrupture of the benzene ring at temperatures

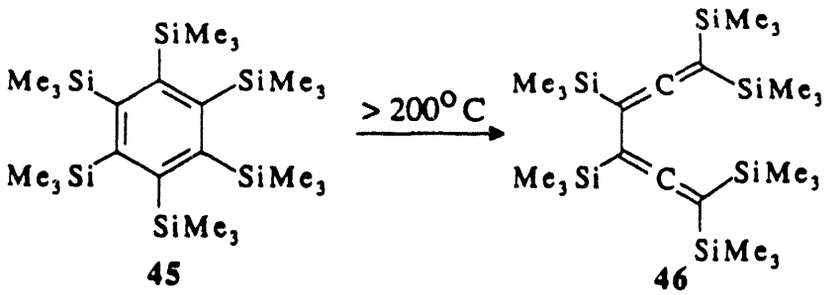

45 46

above 200°C to yield hexasilylated bisallene **46** being a remarkable example. Again, this chemistry is in apparent contrast to NMR spectroscopic evidence, which shows no indication of a breakdown in π delocalization in **45**, the chemical shifts of all magnetically active nuclei being well in the range for other planar, aromatic hydrocarbons.[74]

The fact that even polycyclic aromatic hydrocarbons are liable to non-planar deformations has been aptly demonstrated in the synthesis of the helicenes[112] (e.g., **47**), in which helical structures arise from non-bonded repulsions between layers of ortho-fused benzene rings. A computational investigation by Herndon et al.[113] led to the conclusion that deviation from planarity is indeed an abundant geometrical feature of cata-condensed polybenzenoids, of which the helicenes are a sub-group. A recent example for the breadth of structural variations is provided in the characterization of hydrocarbon **48**,[114] a molecule revealing a longitudinally twisted anthracene moiety.

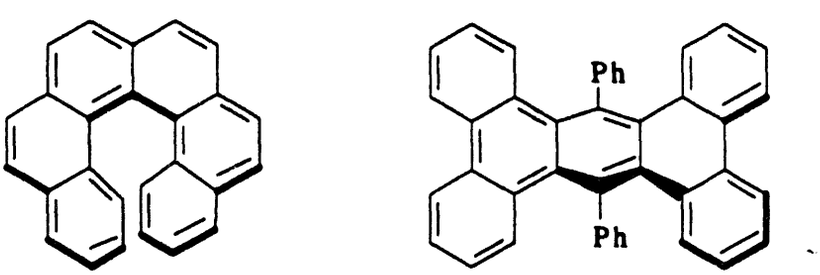

47 48

This distortion amounts to a torsional angle of 65.7° end to end with roughly equal contributions from each of the three benzenoid rings. In view of these severe deformations, the compound proved to be surprisingly stable. Lack of reactivity to air,

light, acids, or bases, in conjunction with unremarkable spectroscopic data, indicate the presence of a relatively unperturbed π system.

The same incongruity between geometry of the σ frame and π electronic properties is borne out in the chemical and physical behavior buckminsterfullerene (**11**)[115] and corannulene (**12**)[29,30] molecules currently enjoying much of the limelight. Despite their spherical (**11**) or bowl-shaped (**12**) topology, both compounds can only be classified aromatic by all applicable criteria.

11

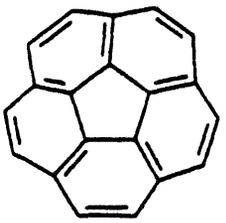

12

This brief survey of geometrical distortions of the benzene nucleus clearly documents the system's reluctance to diminish its degree of aromaticity. Thus, the contentions of Shaik and Hiberty[16] that dispute the role of π delocalization as a driving force in chemistry are of particular interest and are subject of the following chapter.

1.4 Natural Bond Orbital Analysis and Natural Resonance Theory.

The way synthetic chemists visualize (and rationalize) molecular properties differs considerably from the views employed by most quantum chemists. Whereas the latter often derive information about the electronic structure of a molecule from analysis of a calculated molecular orbital wavefunction, the former group uses valence bond based "electron-pushing" schemes to explain geometries and reactivity. Natural bond orbital (NBO) analysis[32] was designed to bridge the gap by providing a "chemist's basis set"[32b] that allows the computational description of molecules in terms of Lewis (dot) structures

of localized bonds and lone pairs. Since portions of this thesis rely strongly on the NBO method, some of its characteristic features are presented below.

The essence of NBO analysis is the occupancy-weighted symmetric orthogonalization procedure, that allows transformation of the first-order density matrix to a localized bond orbital basis, whose elements fulfill the requirement of orthonormality and maximum occupancy by electrons. This last criterion is of particular importance, since it leads to the identification of the orbitals that best reflect the components of an idealized Lewis structure. Density representations in form of the NBO basis permit the characterization of one-center elements (i.e., core orbitals and lone pairs) and two-center vectors (the bond orbitals σ). It has been demonstrated[32b] that these three computationally derived constitutive elements of Lewis structures typically describe more than 99% of the total electron density.

Bonding properties can be further evaluated by decomposing bond orbital σ_{AB} into normalized hybrid contributions h_A and h_B, the natural hybrid orbitals (NHOs).[32a]

$$\sigma_{AB} = c_A h_A + c_B h_B \qquad (1.6)$$

The hybrid h_A (h_B) reflects, for example, the exponent λ in the hybridization sp^λ of the bond orbital A (B) uses when binding to B (A). Strain-induced rehybridization can then be determined by examination of the NHOs of the corresponding atoms, and bond bending is revealed in the deviations of the hybrid vectors from the internuclear axes. This method was employed in the investigation of small-ring annelated benzenes (chapter 4).

Decomposition of NBOs according to eq 1.6 concurrently leads to orbitals of antibonding character (eq 1.7), which can be used to describe departures from covalency, i.e., delocalization. The energy content associated with these antibonds can be

$$\sigma_{AB}^* = c_B h_A - c_A h_B \qquad (1.7)$$

assessed by deleting the corresponding NBOs from the basis set and recalculating the total energy of the wavefunction. Similarly, the influence of delocalizing deviations from covalency on structural features of a molecule can be demonstrated by geometry reoptimization with respect to the energy of the truncated wavefunction. Possibilities of this sort will prove useful in the course of investigations delineated in chapters 2 and 4.

The fact that the NBO routine searches for Lewis structures that best describe the total electron density distribution, opens the opportunity to evaluate contributions of various resonance forms to the wavefunction. This concept was implemented in the development of natural resonance theory (NRT),[33] which is based on the NBO method. Density operator $\hat{\Gamma}$ is defined (eq 1.8) as the sum over the idealized density operators $\hat{\Gamma}_\alpha$ of the αth resonance structure, scaled by the resonance weights $\{\omega_\alpha\}$.

$$\hat{\Gamma} = \sum_\alpha \omega_\alpha \hat{\Gamma}_\alpha \tag{1.8}$$

While $\hat{\Gamma}_\alpha$ is obtained from quantities of the NBO analysis of the full wavefunction (vide supra), $\{\omega_\alpha\}$ are calculated within the constraints of eq 1.9 by variational optimization to best represent NBO occupancies.

$$\sum_\alpha \omega_\alpha = 1; \quad \omega_\alpha \geq 0 \tag{1.9}$$

This formalism will be used to gain insight into the π electronic distribution of distorted and small-ring annelated benzenes (chapter 2 and 4).

Chapter Two

The Role of Delocalization in Benzene

2.1 Introduction

The electronic factors leading to a symmetric D_{6h} benzene of equivalent CC bond lengths were thought to be dominated by π delocalization since the seminal work by Pauling, Wheland, and Hückel.[9,10] Based on valence bond principles,[15,39] the equilibrium structure of benzene (**1**) was viewed as being caused by resonance mixing of the two Kekulé forms **1a** and **1b**, leading to a carbon frame with internuclear distances intermediate between those of idealized single and double bonds. This traditional picture of benzene was recently challenged by Shaik, Hiberty, and coworkers,[16] who attributed

1a **1b**

the observed equality of CC bond lengths to properties of the σ rather than the π electrons. Support for this alternative viewpoint was derived from computational studies of individual σ and π contributions to the total energies on performing in-plane distortions of **1**. It was found that, in contrast to the σ component, the (yet to be defined) π energy is stabilized by imposing bond alternating geometries on **1**, implying that π delocalization is not a driving force but instead "a byproduct of the σ imposed geometric constraints".[16e] Shaik and Hiberty pointed out that their approach provides explanations for the distortive tendencies of a variety of species with π components isoelectronic to that of **1**. The findings that hexagonal H_6 (**49**) is instable with respect to 3 H_2,[116] whereas the cluster Li_6 (**50**) resists such fragmentation,[16d,116a,117] were seen to represent extremes of atomic properties, those of carbon ranging between the two. Furthermore, the elusiveness of

hexaazabenzene (**51**)[118] was interpreted as another piece of evidence for the prediction that "only atoms that form weak two-electron bonds with low-lying triplet excitation

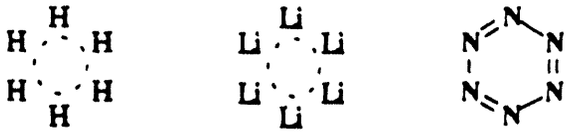

49 **50** **51**

energy can generate delocalized species that are stable toward a localizing distortion".[16e] Schleyer's remark that "there is no magic in six electrons",[119] aptly summarizes this hypothesis.

While this subject has been an issue of some debate,[120] results obtained from analysis of similar energy partitioning schemes are in qualitative agreement with the above conclusions.[62a, 121-123] Jug and Köster[121] evaluated energy components during Shaik-type deformations of **1** and several other delocalized, heterocyclic compounds, observing in each case that the behavior of the π contributions indicates the preference for alternating geometries. Stanger and Vollhardt,[122] using a different distortion, examined benzene with HCC angles increasingly bent in a pairwise fashion, ultimately resulting in a highly strained structure **52** that exhibits significant CC bond alternation in accord with

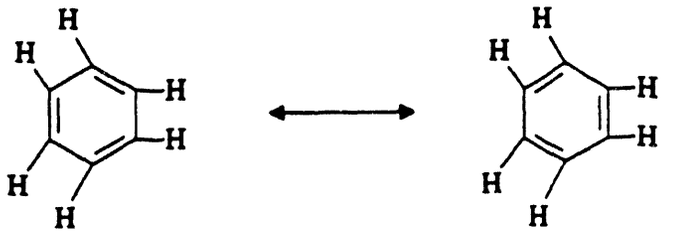

52a **52b**

52a. Again, their analysis of the π contribution to changes in the total energy indicate a π electronic stabilization relative to energies of the symmetric D_{6h} structure.

These conclusions conflict with those derived from localized orbital analysis, a method employing non-delocalized wavefunctions that are constructed, for example, by replacing benzenes' three delocalized π orbitals by a set of non-resonating, "ethylenic"

ones. Using a simple, localized π electron wavefunction, Mulliken and Parr[124] estimated that benzene favors a geometry with alternating CC bond lengths by roughly 37 kcal mol^{-1} over the more symmetric D_{6h} structure. Thus, their analysis suggests, at least qualitatively, that π delocalization is responsible for the equilibrium geometry. More recently, Kollmar[49] reexamined benzene at the ab initio level, calculating that in the absence of π delocalization, a bond alternating structure is preferred by 30 kcal mol^{-1}, thereby supporting the conclusions of Mulliken and Parr. Evidently, discrepancy exists between the findings obtained from localized wavefunctions and those derived from σ-π energy partitioning analyses. This chapter will present a comparison study of benzene applying both of these methods to two different types of distortion, in an effort to gain insight into the nature of π delocalization and its role with regard to geometry. All calculations reported here were performed by either GAUSSIAN 90[125] or GAMESS[126] at the SCF level of theory with the split-valence 6-31G* basis.[48,127]

2.2 Description of Benzene Distortions.

As outlined above, the two inherently different benzene deformations employed previously both lead to alternating CC bond lengths (R_1, R_2) around the ring. The quantity d is conveniently used as a measure for the degree of alternation, $d = 0$ thereby referring to the equilibrium geometry with equivalent bond lengths.

$$d = R_1 - R_2 \tag{2.1}$$

The first distortion, initially investigated by Shaik and Hiberty,[16e] and hence denoted d_{SH}, centers around a geometry $d_{SH} = 0$ in which $R_1 = R_2 = 1.40$ Å. Structures with $d_{SH} \neq 0$ arise from variations in R_1, R_2 within the constraint that the nuclear repulsions contribution to the total energy remains constant, equal to that of the equilibrium geometry (for an explanation of this restriction, see section 2.4). Clearly, this requirement leads to bond alternation (**53**): R_1 necessarily lengthens, for example, to

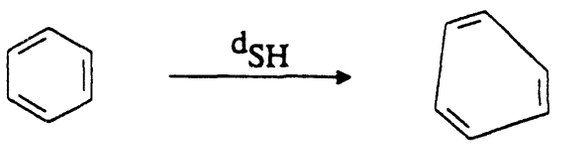

1 **53**

compensate for increased nuclear repulsions as R_2 shortens (Table 2.1). The most distorted geometry investigated along d_{SH} has alternating bond lengths of 1.240 Å and 1.579 Å (d_{SH} = 0.339 Å) with all other internal coordinates constrained to standard values (R_{CH} = 1.08 Å, ∠HCC = 120°). The nuclear repulsions energies for each point are included as reference in Table 2.1, demonstrating invariance of this quantity within 0.2 kcal mol^{-1} (0.0003 a.u.).

Table 2.1 Benzene Geometries Along the d_{SH} and d_{SV} Distortion Coordinates.[a]

d_{SH}	R_{CC}(long)	R_{CC}(short)	V^{nn} [b]
0.0000	1.4000	1.40	202.96786
0.0403	1.4203	1.38	202.96786
0.0811	1.4411	1.36	202.96783
0.1224	1.4624	1.34	202.96781
0.1644	1.4844	1.32	202.96777
0.2070	1.5070	1.30	202.96771
0.2502	1.5302	1.28	202.96796
0.2941	1.5541	1.26	202.96767
0.3388	1.5778	1.24	202.96741

d_{SV}	R_{CC}(long)	R_{CC}(short)	∠HCC
0.0000	1.3862	1.3862	120
0.0376	1.4076	1.3702	110
0.0939	1.4468	1.3529	100
0.2002	1.5290	1.3288	90

([a]) Bond lengths in Å, angles in degrees. ([b]) Nuclear repulsions energy in a.u.

The second distortion, d_{SV}, was originally examined by Stanger and Vollhardt,[122] and centers around a geometry d_{SV} = 0 corresponding to benzene optimized at the RHF/6-31G* level of theory ($R_1 = R_2$ = 1.386 Å). Variations of d_{SV} arise from decreasing the HCC bond angles in a pairwise fashion from their equilibrium value of 120° to highly strained 90° in **52**, with all other internal coordinates optimized (Table 2.1).

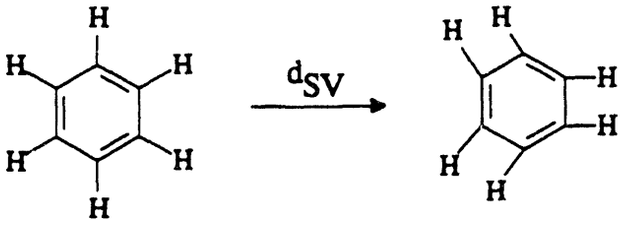

1 **52**

As demonstrated previously,[97d-f,105] this procedure induces bond alternation within the ring due to rehybridization of the carbon centers. In **52**, for example, the optimized geometry has CC bond lengths of 1.329Å and 1.529 Å (d_{SV} = 0.200 Å).

It is to these two benzene distortions that localizing orbital and σ-π energy partitioning methods will be applied.

2.3 Localized Orbital Analysis.

The effect of π delocalization in benzene can be assessed by comparing the properties of the delocalized SCF wavefunction with those of a localized Kekulé system. This is the approach previously taken by Mulliken, Parr, and Kollmar.[49,124] Computationally, localizing the benzene wavefunction is a three step procedure: (i) transformation of the π MOs to an orthogonal set of symmetry equivalent atomic hybrids, (ii) construction of the localized π orbitals from the in-phase combination of adjacent hybrids, and (iii) substitution of the localized orbitals into the SCF wavefunction. Step (i) is well-defined for minimal basis sets containing only one p_π function per carbon. But for an extended basis set with two or more such functions per carbon (such as 6-31G*), the transformation is not straightforward. NBO analysis[32] assists here by calculating the $2p_\pi$

hybrids of maximum occupancy (i.e., the set of hybrids that best reflects the π electron distribution, cf. section 1.4). It is important to realize that the localization procedure (i) - (ii) has absolutely no influence on the form of the σ orbitals, but effectively mixes part of the virtual π space into the set of occupied π orbitals. As a result, the energy of the localized system, $E^{(loc)}$, is greater than the variational SCF energy E_0, raised by an amount equivalent to the vertical resonance energy[40] (cf. section 1.2.1).

$$E_0 = E^{(loc)} + E^{(deloc)} \qquad (2.2)$$

Inspection of Table 2.2 (Table 2.3) and Figure 2.1 (Figure 2.2) reveals that benzene, at its equilibrium geometry is strongly stabilized by a π delocalization energy $E_\pi^{(deloc)}$ of -143 kcal mol^{-1} (-147 kcal mol^{-1}) These values compare favorably with that

Table 2.2 Relative Energies of Benzene Along the d_{SH} Distortion Coordinate.[a]

d_{SH}	E_0	$E^{(loc)}$ [b]	E_π (SH) [c]	E_π (JK) [d]	$E_\pi^{(SV)}$ [e]
0.0000	0.0	143.29	0.00	0.00	0.00
0.0403	0.59	125.56	-1.26	-3.64	-0.69
0.0811	2.42	111.12	-5.06	-14.46	-2.70
0.1224	5.67	100.04	-11.32	-32.00	-6.09
0.1644	10.56	92.39	-19.88	-55.46	-10.73
0.2070	17.36	88.26	-30.54	-83.95	-16.19
0.2502	26.38	87.76	-43.11	-116.57	-22.78
0.2941	37.94	91.02	-57.38	-152.56	-30.06
0.3388	52.36	98.19	-73.18	-191.25	-38.09

([a]) Distortions in Ångstroms, energies in kcal mol^{-1}. For a definition of individual energy contributions, see text.(1 a.u. = 627.5 kcal mol^{-1}). ([b]) Relative to E_0 = -230.70188 a.u. ([c]) Relative to $E_\pi^{(SH)}$ = -6.35865 a.u. ([d]) Relative to $E_\pi^{(JK)}$ = -9.30336 a.u. ([e]) Relative to $E_\pi^{(SV)}$ = -1.14870 a.u.

obtained from HMO analysis of UV absorption bands of benzene ($E_\pi^{(deloc)}$ = -138 kcal mol^{-1}; cf. section 1.2.1) and also, to a lesser extent, to the vertical delocalization energies

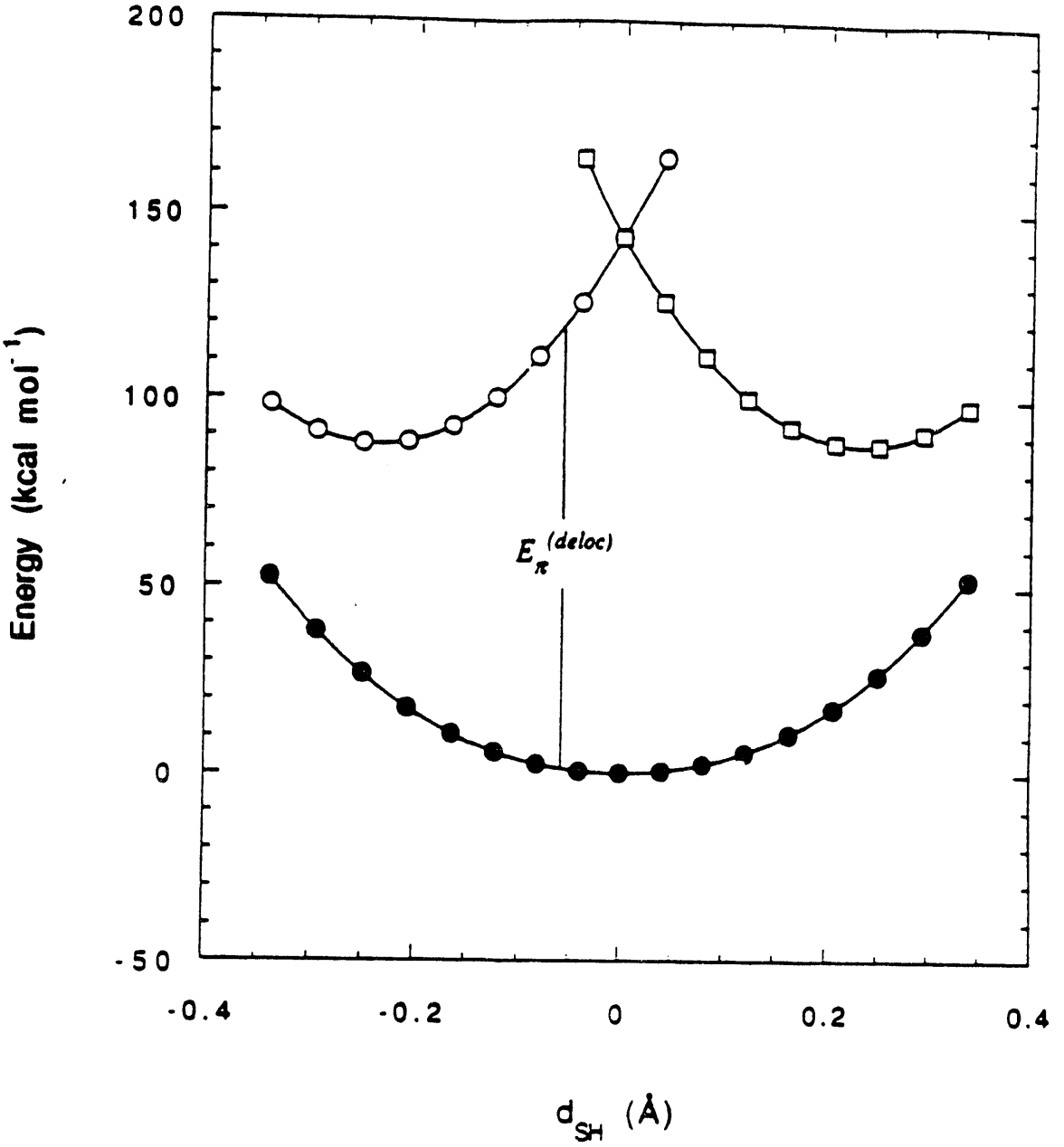

Figure 2.1 Behavior of the Total Energy E_0 (filled circles) and the Energies $E^{(loc)}$ of the Kekulé Structures **1a** (Circles) and **1b** (Squares) Along the d_{SH} Distortion Coordinate.

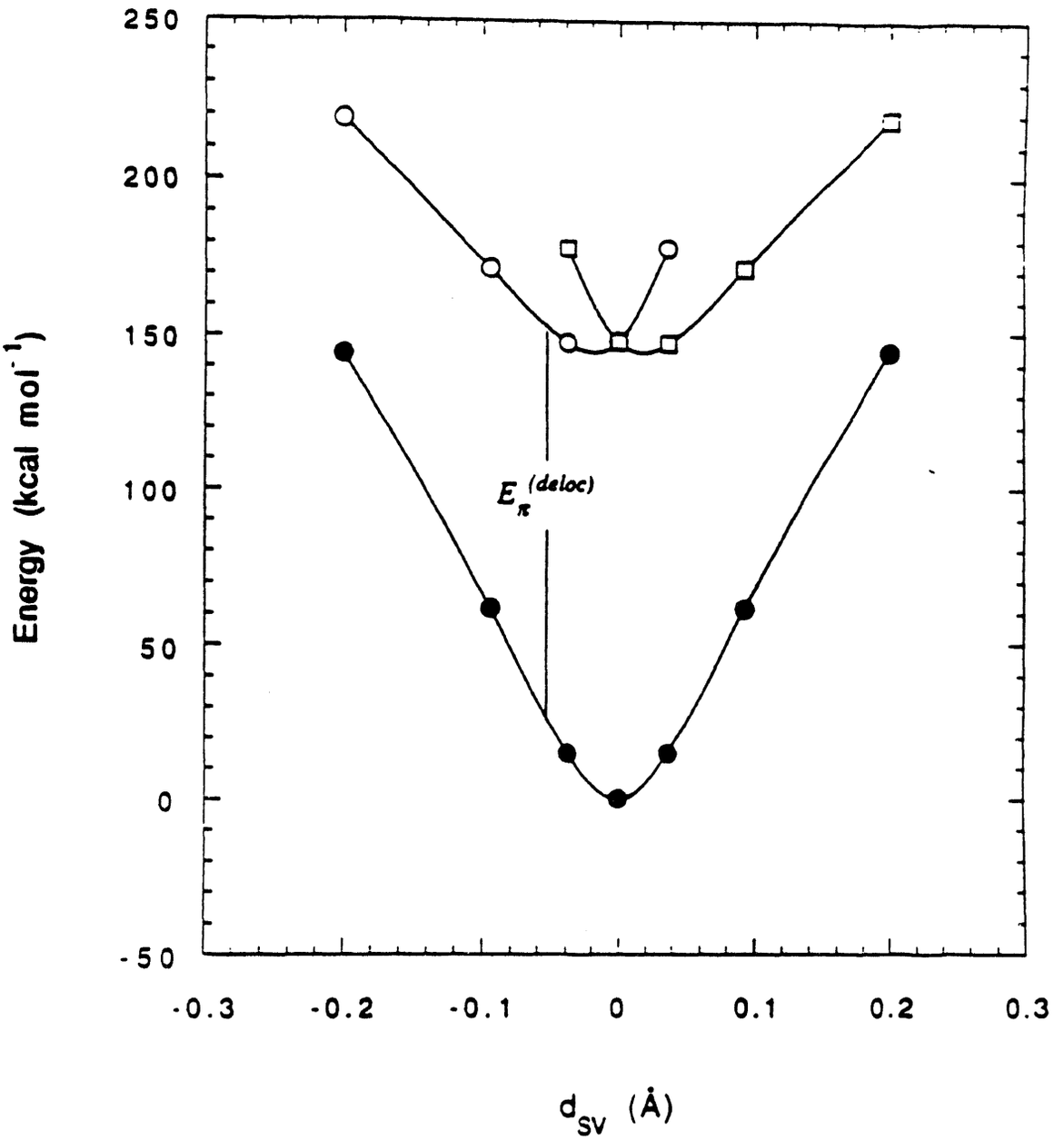

Figure 2.2 Behavior of the Total Energy E_0 (filled Circles) and the Energies $E^{(loc)}$ of the Kekulé Structures **1a** (Circles) and **1b** (Squares) Along the d_{SV} Distortion Coordinate.

computed by Kollmar[49] ($E_\pi^{(deloc)}$ = -96.4 kcal mol^{-1}) and Mulliken and Parr[124] ($E_\pi^{(deloc)}$ = -73 kcal mol^{-1}). Results from localized orbital analysis for benzene geometries along the d_{SH} distortion coordinate (Table 2.2) are graphically depicted in Figure 2.1. The lower curve shows energy E_0 of the delocalized SCF wavefunction, whereas the two upper ones represent $E^{(loc)}$ of the two localized Kekulé structures that are degenerate at d_{SH} = 0. For a specified geometry, the delocalization energy $E_\pi^{(deloc)}$ corresponds to the difference between the E_0 and $E^{(loc)}$ curves. As anticipated, $E_\pi^{(deloc)}$ is most stabilizing at the symmetric geometry and monotonically weakens as the carbon framework is increasingly distorted. However, it is particular noteworthy that delocalization is effective in all geometries, even highly deformed ones. For instance, at d_{SH} = 0.207 Å [R_{CC}(short) = 1.300 Å; R_{CC}(long) = 1.507 Å; Table 2.1], a geometry that topologically resembles an idealized 1,3,5-cyclohexatriene, $E_\pi^{(deloc)}$ still amounts to -71 kcal mol^{-1}, a reduction by only a factor of 2 over $E_\pi^{(deloc)}$ in unperturbed benzene. It thus appears misleading to judge resonance effects based on geometric grounds, a conclusion that is consistent with results from NRT analysis (cf. section 1.4) of distorted **53**. The resonance weights to the

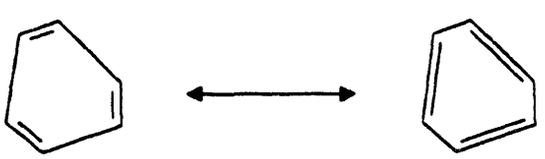

53a **53b**

overall π electronic distribution in benzene shift from 50:50 at the equilibrium geometry d_{SH} = 0 to 76:20 at d_{SH} = 0.21 Å in favor of **53a**, thereby revealing that the contribution of the less important Kekulé form remains sizable even in deformed frameworks (cf. discussion in sections 1.3 and 4.1.3).

Also apparent from Figure 2.1 is the fact that $E^{(loc)}$ is minimized near d_{SH} = ± 0.23 Å [R_{CC}(short) ~ 1.29 Å; E_{CC}(long) ~ 1.52 Å], an indication that benzene favors bond alternation in the absence of π delocalization.

Similar conclusions can be derived from localized orbital analysis along the d_{SV} distortion coordinate (Table 2.3; Figure 2.2). In this case, bending of HCC angles leads to a more rapid increase in E_0 as compared to the analogous behavior of this quantity along d_{SH}. Again, $E_\pi^{(deloc)}$ is demonstrated to have a stabilizing influence throughout the range of deformation, showing a declining trend in magnitude as the degree of distortion increases. Similar to observations described for d_{SH}, one finds a reduction of $E_\pi^{(deloc)}$ at a

Table 2.3 Relative Energies of Benzene Along the d_{SV} Distortion Coordinate.[a]

d_{SV}	E_0	$E^{(loc)}$ [b]	$E_\pi^{(SH)}$ [c]	$E_\pi^{(JK)}$ [d]	$E_\pi^{(SV)}$ [e]
0.0000	0.00	147.13	0.00	0.00	0.00
0.0376	14.82	146.67	2.36	-4.50	-0.63
0.0939	61.34	170.77	12.65	-23.46	-2.26
0.2002	143.95	218.48	41.21	-82.85	-5.71

([a]) Energies in kcal mol^{-1}. For a definition of individual energy contributions, see text. (1 a.u. = 627.5 kcal mol^{-1}) ([b]) Relative to E_0 = -230.70314 a.u. ([c]) Relative to $E_\pi^{(SH)}$ = -6.40980 a.u. ([d]) Relative to $E_\pi^{(JK)}$ = -9.29506 a.u. ([e]) Relative to $E_\pi^{(SV)}$ = -1.15920 a.u.

cyclohexatrienoid topology [d_{SV} = 0.200 Å; R_{CC}(short) = 1.329 Å; R_{CC}(long) = 1.529 Å; Table 2.1) by a factor of 2 relative to the value of the equilibrium structure at d_{SV} = 0. This seems to indicate that the degree of π delocalization at this particular geometry of the carbon frame is independent from the type of distortion. The minimum in the localized wavefunction for d_{SV} is less pronounced than that found for d_{SH}, the former pointing at a geometry near d_{SV} = ±0.02 Å [R_{CC}(short) ~1.38 Å; R_{CC}(long) ~ 1.40 Å; ∠ HCC ~ 115°].

To investigate the effect of π delocalization further, a full geometry reoptimization of benzene (D_{3h} symmetry constraints imposed) with respect to $E^{(loc)}$ was performed. The resulting structure exhibits significant bond alternation [R_{CC}(short) = 1.307 Å; R_{CC}(long) = 1.565 Å] with slightly distorted HCC bond angles (∠HCC = 114.9°). The energy of the

localized wavefunction at this geometry is 63 kcal mol^{-1} less than at $d_{SV} = 0$, a large energy difference that must be overcome by delocalization to stabilize the latter geometry.

Thus, in contrast to the contentions of Shaik and Hiberty,[16] localized orbital analysis suggests that π delocalization is an important symmetrizing force in benzene and is at least in part responsible for its D_{6h} equilibrium structure.

2.4 Energy Partitioning Analysis.

An alternative approach for analyzing benzene is based on the energy partitioning schemes of Shaik and Hiberty,[16] Jug and Köster,[121] and Stanger and Vollhardt.[122] These methods decompose the total energy, E_0, into separate σ and π electronic components and a nuclear repulsions term V^{nn} (eq 2.3). Although in-plane (σ) and out-of-plane (π)

$$E_0 = E_\sigma + E_\pi + V^{nn} \tag{2.3}$$

character of canonical benzene MOs are easily identified, the Coulomb and exchange interactions of electrons occupying orbitals of differing symmetry prevent the unique separation of these energies into σ and π contributions. Despite this complication, several partitioning schemes have been proposed.

Approaches of this type have generally been limited to the analysis of single configuration, restricted Hartree-Fock (RHF) wavefunctions.[128] (Extensions that include configuration interaction have been made,[16e] but will not be considered here.) At this level of theory, the total energy is given by eq 2.4, where h_{ii} is the

$$E_0 = \sum_i (h_{ii} + \varepsilon_i) + V^{nn} \tag{2.4}$$

core Hamiltonian (i.e., electronic kinetic energy and nuclear attraction terms) and ε_i is the orbital energy of the ith MO, often expressed in terms of Coulomb and exchange integrals J_{ij} and K_{ij}, respectively (eq 2.5).

$$\varepsilon_i = h_{ii} + \sum_{ij}(2J_{ij} - K_{ij}) \qquad (2.5)$$

The partitioning scheme developed by Shaik and Hiberty assigns all σ, π interaction terms (i.e., Coulomb and exchange integrals of the form $J_{\sigma\pi}$ and $K_{\sigma\pi}$) to the π component. Thus, these authors define σ and π energies as shown in eq 2.6, where the summations are restricted to MOs of the specified symmetry type. The energy associated

$$E_{\sigma}^{(SH)} = \sum_{i}^{\sigma}(h_{ii} + \varepsilon_i) - \sum_{i}^{\sigma}\sum_{j}^{\pi}(2J_{ij} - K_{ij}) \qquad (2.6a)$$

$$E_{\pi}^{(SH)} = \sum_{i}^{\pi}(h_{ii} + \varepsilon_i) + \sum_{i}^{\sigma}\sum_{j}^{\pi}(2J_{ij} - K_{ij}) \qquad (2.6b)$$

with nuclear repulsions, V^{nn}, (eq 2.3) is not incorporated into the electronic contributions (eq 2.6), necessitating separate consideration of the former quantity when analyzing energetic changes. To circumvent this problem, Shaik and Hiberty chose to investigate the d_{SH} distortion, along which V^{nn} remains constant.

Jug and Köster[121] proposed an alternative way to decompose the total energy E_{σ}. They evenly distribute the interaction terms J_{ij}, K_{ij} between E_{σ} and E_{π} and partition V^{nn} according to the formal number of σ and π electrons, (n_{σ}, n_{π}) on each atomic center A,B, separated by a distance R_{AB} (eq 2.7).

$$E_{\sigma}^{(JK)} = \sum_{A}\sum_{A>B}\left(\frac{n_A^{\sigma}\, n_B^{\sigma}}{R_{AB}} + \frac{1}{2}\,\frac{n_A^{\sigma}\, n_B^{\pi} + n_A^{\pi}\, n_B^{\sigma}}{R_{AB}}\right) \qquad (2.7a)$$

$$E_{\pi}^{(JK)} = \sum_{A}\sum_{A>B}\left(\frac{n_A^{\pi}\, n_B^{\pi}}{R_{AB}} + \frac{1}{2}\,\frac{n_A^{\sigma}\, n_B^{\pi} + n_A^{\pi}\, n_B^{\sigma}}{R_{AB}}\right) \qquad (2.7b)$$

The resulting energy components can be written in the simple form of eq 2.8.

$$E_\sigma^{(JK)} = \sum_i (h_{ii} + \varepsilon_i) + V_\sigma^{nn} \tag{2.8a}$$

$$E_\pi^{(JK)} = \sum_i (h_{ii} + \varepsilon_i) + V_\pi^{nn} \tag{2.8b}$$

This procedure allows a more consistent treatment of electrons and nuclei and, in addition, removes the need for geometrical restrictions in the assessment of energetic changes on distortion. However, an important point of criticism is that the phenomenon of delocalization, which this partitioning scheme is meant to investigate, is a purely electronic effect that may potentially be obscured by nuclear repulsions.

A third way to decompose the total energy is that employed by Stanger and Vollhardt,[122] who calculated $E_\pi^{(SV)}$ as the sum of orbital energies, in direct analogy to a

$$E_\pi^{(SV)} = \sum_i \varepsilon_i \tag{2.9}$$

Walsh-type analysis.[123] All other energy contributions, including the π-type core Hamiltonian terms of eqs 2.6b and 2.8b are assigned to the σ system. As a result, this method can be judged inferior to those described above, but has its merit in its simplicity and is considered here for comparison with earlier work. The numerical values of E_π obtained from application of these partitioning schemes to the total energy along the d_{SH} and d_{SV} distortion coordinates are listed in Tables 2.2 and 2.3, respectively, with graphic representations in Figures 2.3 and 2.4

Energy analysis of benzene deformations according to Shaik and Hiberty, d_{SH}, unambiguously show that E_π is maximized at the symmetric geometry for each of the partitioning methods considered (Figure 2.3). Thus, distorting benzene to increasingly bond alternating geometries results in a monotonic decrease of the total π energy. This behavior led to the suggestion[16e] that the π system favors cyclohexatrienoid structures, and hence to cast doubt on the role of delocalization. The magnitude of the variation in E_π depends critically on its underlying definition. For example, this component is diminished

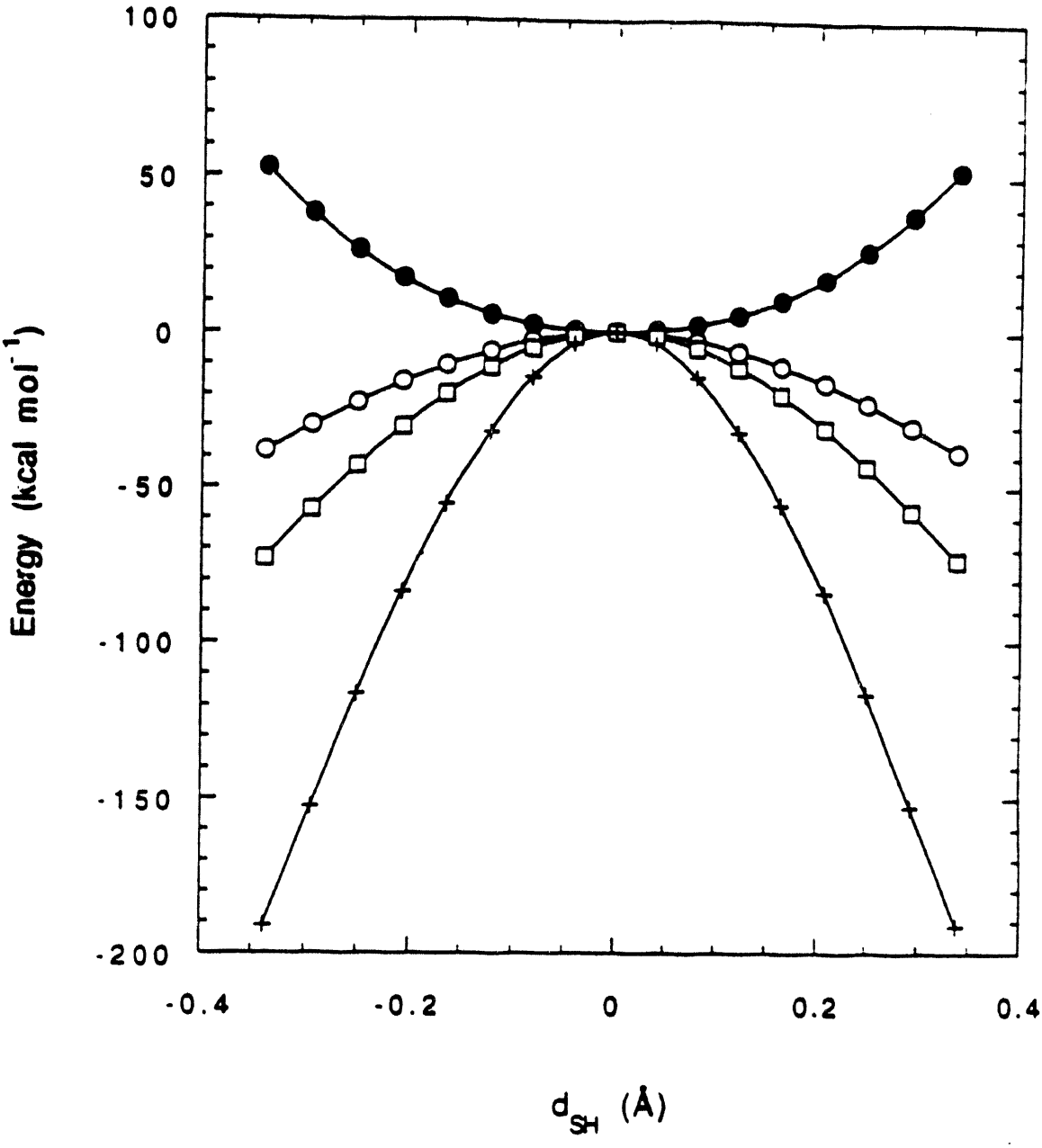

Figure 2.3 Geometry Dependence of the Total Energy E_0 (filled Circles) and the π Energy Components $E\pi^{(SV)}$ (Circles), $E\pi^{(SH)}$ (Squares), and $E\pi^{(JK)}$ (Pluses) Along the d_{SH} Distortion Coordinate.

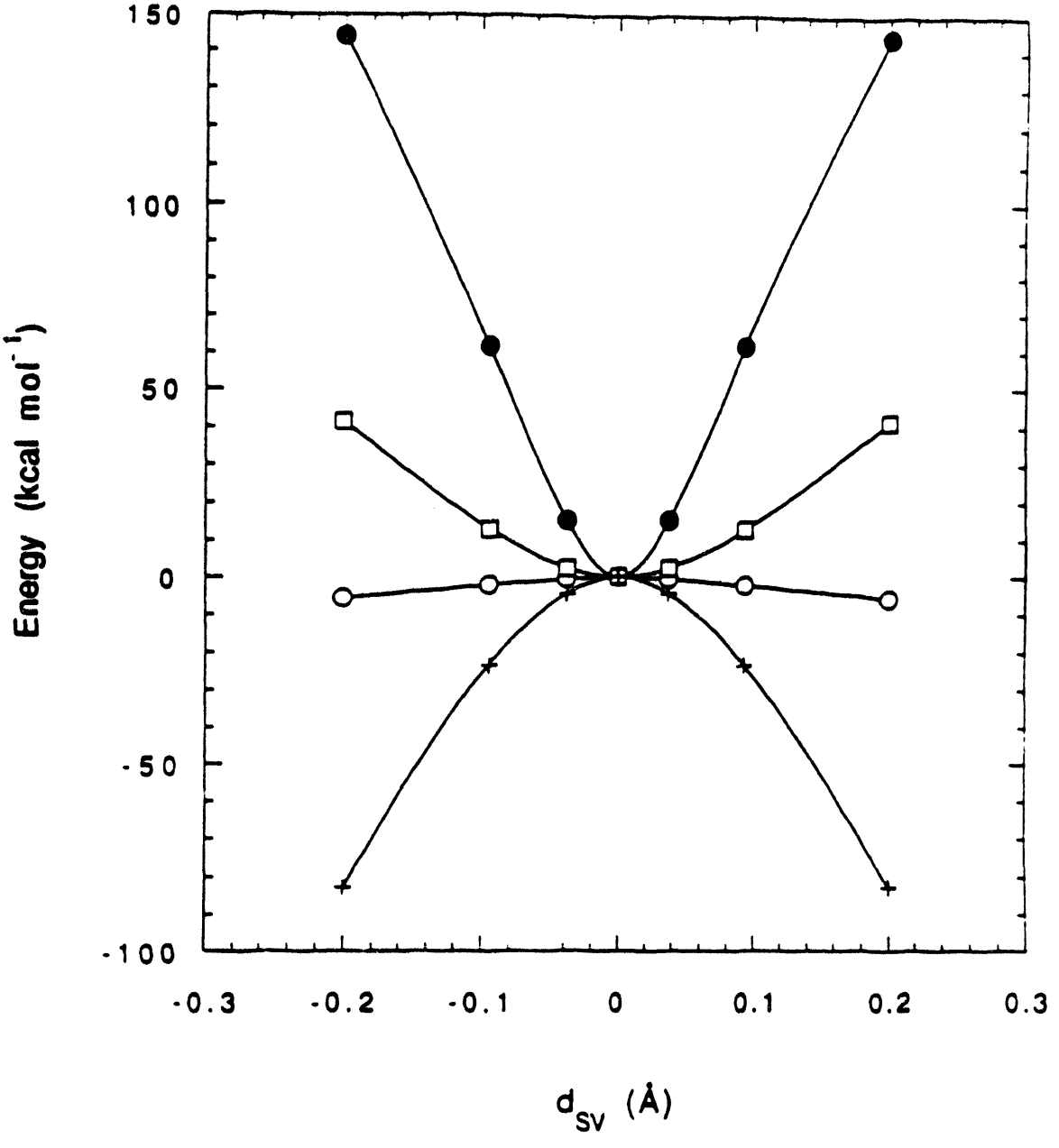

Figure 2.4 Geometry Dependence of the Total Energy E_0 (filled Circles) and the π Energy Components $E_\pi^{(SV)}$ (Circles), $E_\pi^{(SH)}$ (Squares), and $E_\pi^{(JK)}$ (Pluses) Along the d_{SV} Distortion Coordinate.

by 38 ($E_\pi^{(SV)}$), 73 ($E_\pi^{(SH)}$), and 191 ($E_\pi^{(JK)}$) kcal mol^{-1} at the most distorted geometry (d_{SH} = 0.3388 Å) relative to D_{6h} benzene.

Differences in the behavior of E_π are even more dramatic along the d_{SV} distortion coordinate (Figure 2.4). While $E_\pi^{(JK)}$ and $E_\pi^{(SV)}$ again possess maxima at the unperturbed benzene geometry d_{SV} = 0, $E_\pi^{(SH)}$ is minimized at this point! Based on their analysis of d_{SV} deformations, Stanger and Vollhardt[122] supported the views of Shaik and Hiberty,[16] who limited their investigation to d_{SH}. Although the trend in $E_\pi^{(SV)}$ along d_{SV} and that of $E_\pi^{(SH)}$ along d_{SH} are in qualitative agreement with one another, the more direct comparison of these two components in Figure 2.4 reveals opposite behavior.

Clearly, conclusions derived from energy partitioning analyses depend critically on the method selected to decompose the total energy and on the details of the geometry distortion. It is intriguing, however, that with only one exception, the π energy favors bond alternating geometries. However, the quantity E_π should not be confused with π delocalization, which was conclusively shown to stabilize benzene's D_{6h} symmetric structure. Interpretations that judge the influence of π delocalization based on such energy partitioning schemes can therefore be misleading. To further corroborate this view, the relationship between orbital localization and energy decomposition analyses will be examined below.

2.5. Comparison of Localized Orbital and Energy Partitioning Methods.

Direct comparison of the two procedures employed to investigate the role of delocalization in benzene is provided by applying a partitioning scheme to the energy of the localized wavefunction, $E^{(loc)}$. The preferred scheme of those presented in section 2.4 is the one devised by Shaik and Hiberty, since it affords a simplification from the assignment of all σ-π interactions to the π component. Thus, $E^{(loc)}$ can be decomposed

$$E^{(loc)} = E_\sigma^{(loc)} + E_\pi^{(loc)} + V^{nn} \qquad (2.10)$$

into σ and π contributions according eq 2.10. Because the localization procedure has no influence on the form of the σ orbitals (vide supra), $E_\sigma^{(loc)}$ is equivalent to $E_\sigma^{(SH)}$ in eq 2.6a. Using this equivalence and substituting eq 2.10 into eq 2.2 results in eq 2.11.

$$E_0 = E_\sigma^{(SH)} + E_\pi^{(loc)} + E_\pi^{(deloc)} + V^{nn} \qquad (2.11)$$

Comparison of the latter with eq 2.3 reveals that the π component of the Shaik and Hiberty method has a contribution from the localized part of the SCF wavefunction in addition to the entire delocalization component.

$$E_\pi^{(SH)} = E_\pi^{(loc)} + E_\pi^{(deloc)} \qquad (2.12)$$

A priori, there is no reason to anticipate that the geometry dependence of $E_\pi^{(SH)}$ should be fully associated with the energy term of π delocalization, $E_\pi^{(deloc)}$ and indeed, an important contribution of $E_\pi^{(loc)}$ to the former is calculated (Table 2.4; Figure 2.5).

Table 2.4 Shaik Hiberty Analysis of Localized Benzene Wavefunctions.[a]

d_{SH}	$E_\pi^{(SH)}$ [b]	$E_\pi^{(deloc)}$ [c]	$E_\pi^{(loc)}$ [d]
0.0000	0.00	-143.29	143.29
0.0403	-1.26	-124.97	123.71
0.0811	-5.06	-108.70	103.64
0.1224	-11.32	-94.37	83.05
0.1644	-19.88	-81.83	61.95
0.2070	-30.54	-70.90	40.36
0.2502	-43.11	-61.38	18.27
0.2941	-57.38	-53.08	-4.30
0.3388	-73.18	-45.83	-27.35

([a]) Distances in Å, energies in kcal mol^{-1}. ([b]) Values taken from Table 2.2.
([c]) Calculated as $E_\pi^{(deloc)} = E_0 - E^{(loc)}$ with values from Table 2.2.
([d]) Calculated as $E_\pi^{(loc)} = E_\pi^{(SH)} - E_\pi^{(deloc)}$.

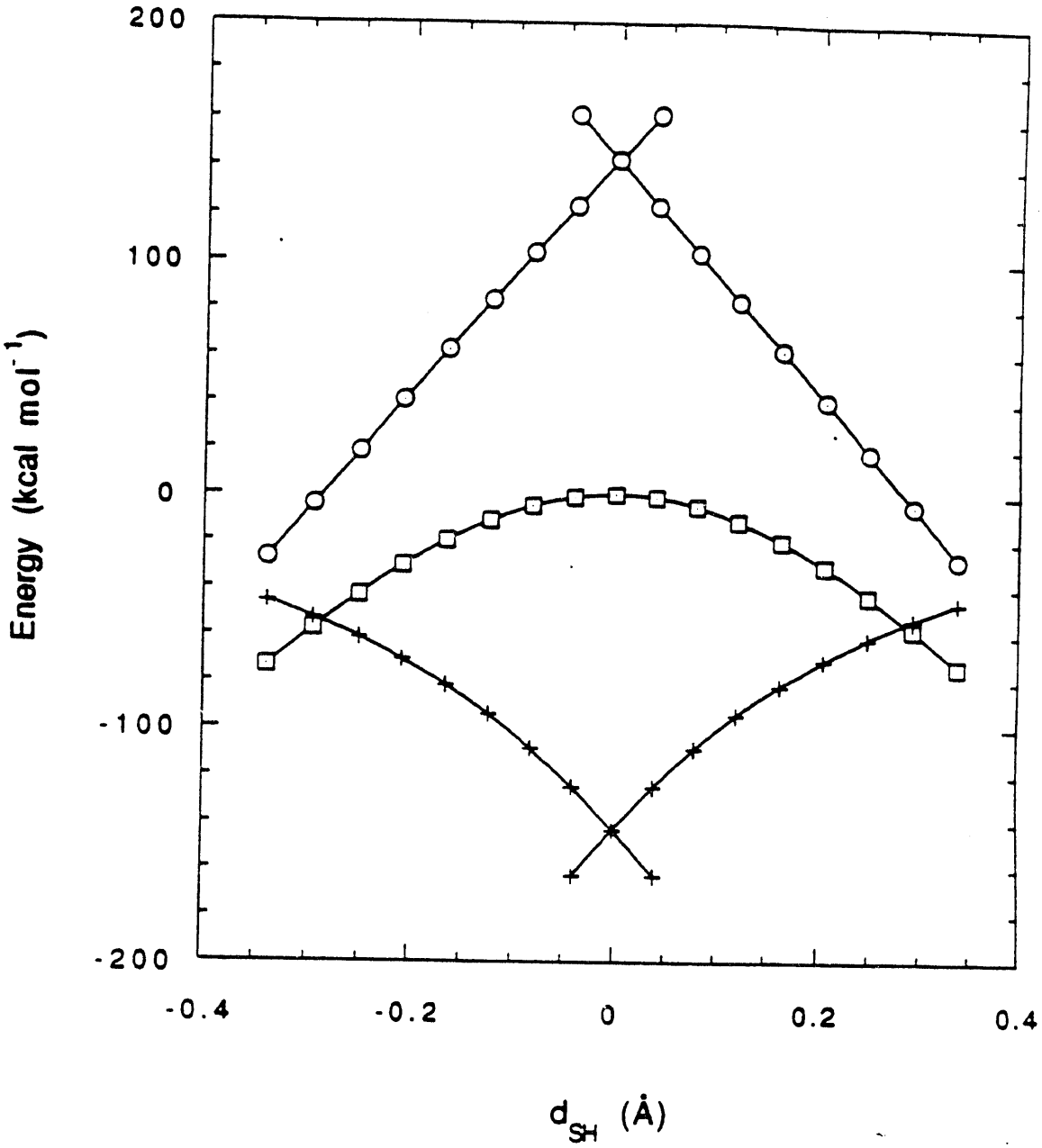

Figure 2.5 Shaik-Hiberty Analysis of the Localized Benzene Wavefunctions Showing $E_\pi^{(SH)}$ (Squares), $E_\pi^{(loc)}$ (Circles), and $E_\pi^{(deloc)}$ (Pluses).

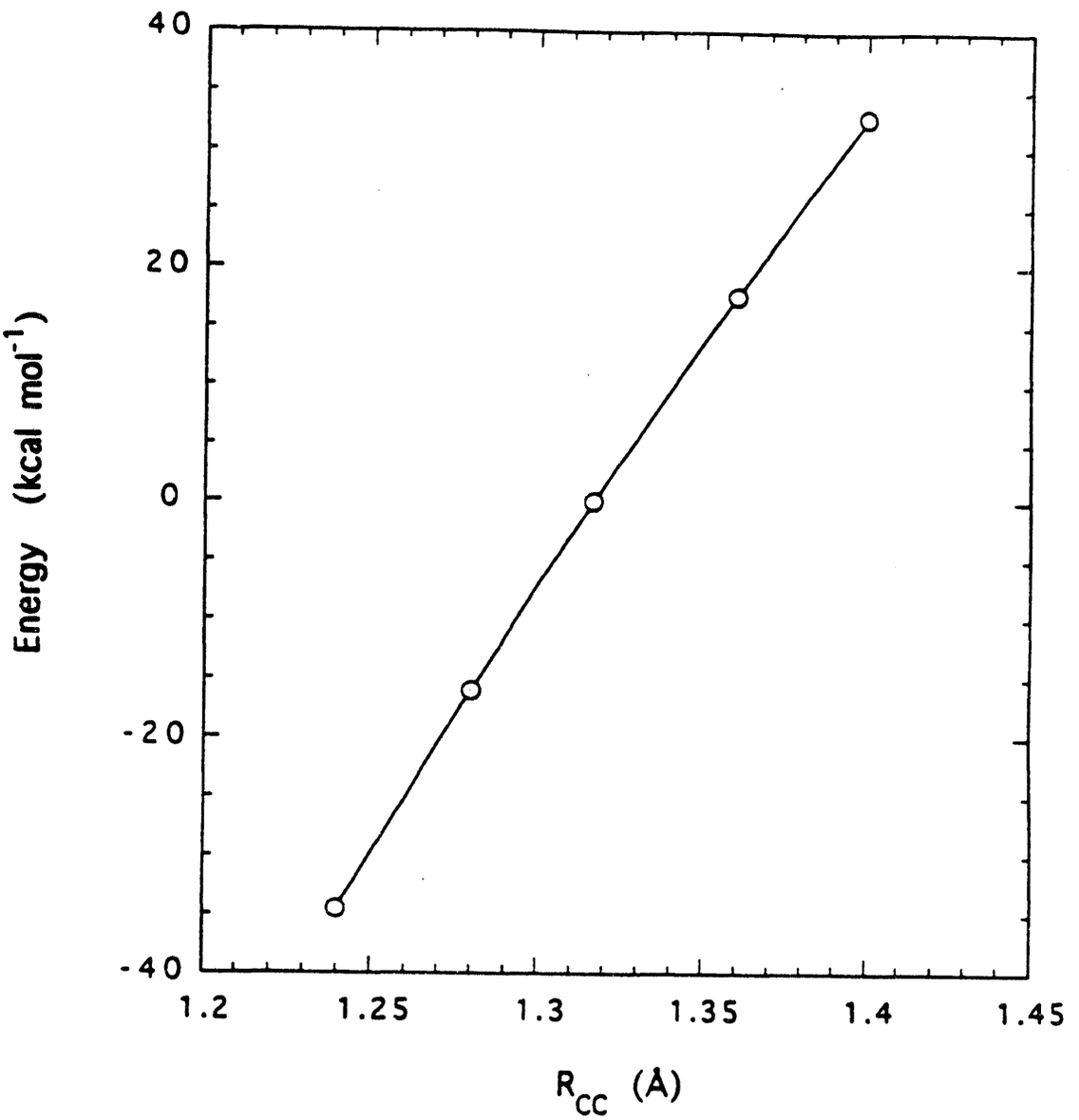

Figure 2.6 Bond Length Dependence of $E_\pi^{(SH)}$ for Ethylene. Values Given are Relative to the Optimized CC Bond Length (1.317 Å), with all other Coordinates Fixed at their RHF/6-31G* Optimized Values.

The localized π electronic energy rapidly decreases with increasing distortion of the benzene ring, a trend that is not entirely unexpected. This energy corresponds to that of the three ethylenic π orbitals of the localized Kekulé structure, decreasing as the carbon centers of these orbitals approach each other. For comparison, the CC bond length dependence of $E_\pi^{(SH)}$ for ethylene is shown in Figure 2.6. Because the π system of this molecule is localized ($E_\pi^{(deloc)} = 0$), the plotted values represent $E_\pi^{(loc)}$. It follows that even in the absence of delocalization, decreasing the CC bond length results in a stabilization of the π component. The tendency for $E_\pi^{(SH)}$ to favor short bond lengths is similar to the behavior of the electronic energy of the H_2 molecule, showing asymptotically decreasing values as the internuclear distance approaches the united atom limit (cf., for example, the portion of the Morse potential of H_2 dominated by the Coulomb attraction term).

This analysis demonstrates that the π energy as defined by Shaik and Hiberty cannot serve as a meaningful criterion by which to judge the role of π delocalization. The behavior of $E_\pi^{(SH)}$ on benzene deformations along d_{SH} is dominated by contributions from portions of the localized wavefunctions, which in themselves are geometry dependent and potentially obscure delocalization effects.. The importance of the latter was shown by investigating energetic and geometric changes of benzene on complete localization. The results suggest that π delocalization is an important symmetrizing force, a view in accord with classical resonance theory.

Chapter Three

The Thermochemical Properties of Benzocyclobutadienologs

3.1 Introduction.

In discussing the dynamic behavior of chromium arene complexes (section 1.2.4), it was pointed out that successive fusion of benzocyclobutene moieties on the benzene nucleus leads to structures with increasing degrees of bond alternation in the σ frame (Figure 1.9). The culmination of this trend is revealed in the X-ray crystallographic analysis[22a] of 2,3,6,7,10,11-hexakis(trimethylsilyl)triangular [4]phenylene (**54**), showing bond lengths around the central six-membered ring typically associated with CC single and double bonds.[130]

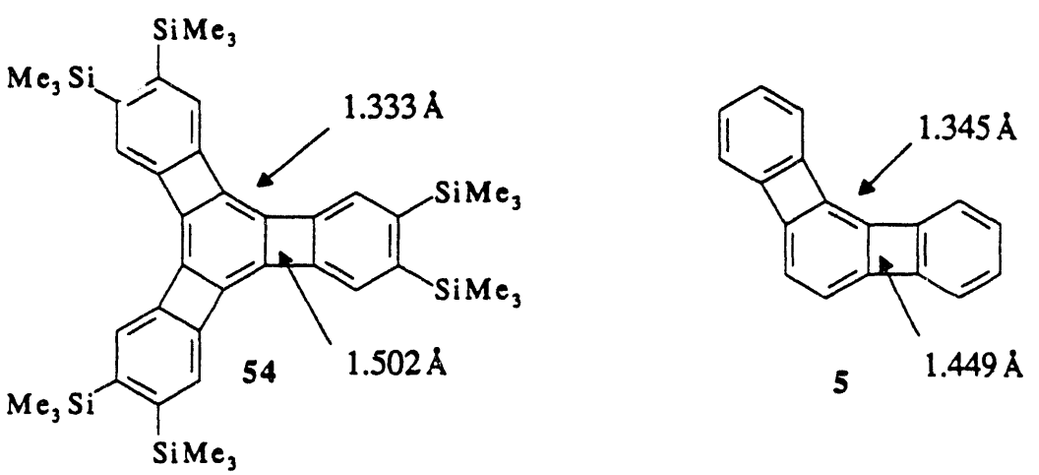

Figure 3.1 Illustration of the Degree of Bond Alternation Observed in Angular Phenylenes.

Topologically, this renders **54** and hence its unsubstituted parent **7** derivatives of the hitherto elusive 1,3,5-cyclohexatriene, the classical reference model for non-delocalized benzene. The olefinic nature of the central double bonds in **7** and **54** also becomes apparent from the ease with which they take part in addition reactions.[25,26] Thus, **7** readily undergoes stereoselective cyclopropanation,[25] epoxidation,[25] and hydrogenation[26]

to furnish the corresponding all-cis-cyclohexane derivatives **55** - **57**, whose stereochemistry was ascertained by X-ray diffraction studies.

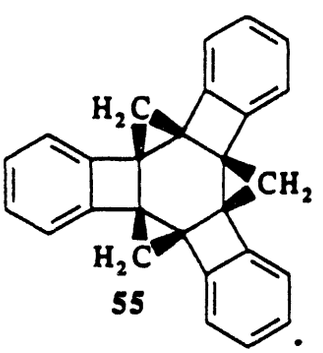

55

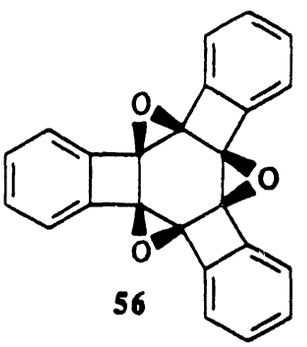

56

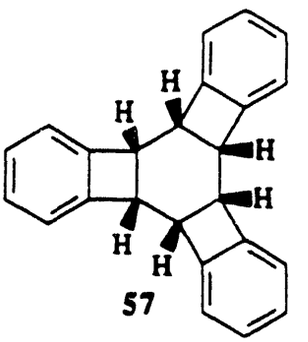

57

Common structural features of these compounds are their cup-shaped topologies and the planarity of the central six-membered rings, both imparted by fusion of strained benzocyclobutene moieties (Figure 3.2).

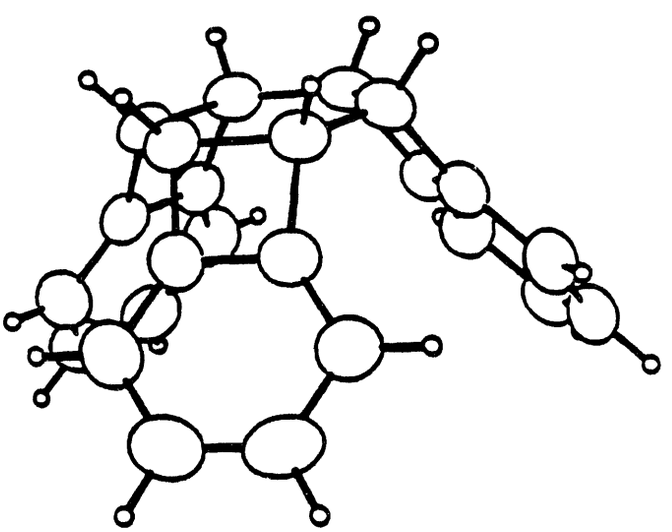

Figure 3.2 X-Ray Structure of all-*cis*-Tris(benzocyclobuta)cyclohexane.

While planar cyclohexane structures have been observed previously,[132] the superior amount of ring strain in **57** is highlighted by an unprecedented degree of bond alternation around the central six-membered ring (1.599 Å along, 1.511 Å adjacent to the four-membered rings) and by the fact that unraveling the cyclohexane unit

thermochemically is a facile, stereospecific, disrotatory process.[26] This behavior is in stark contrast to the thermal stability of its debenzo relative, *cis*-tris[2.2.2]-σ-homobenzene.[133a] Furthermore, in a disubstituted derivative of this latter molecule the four-membered rings are twisted in the solid state to allow a chair conformation of the six-membered ring,[133b] whereas in **57**, the benzofusion enforces four- and therefore six-ring planarity.

The crystal structure of angular [3]phenylene (**5**) shows similar, but less pronounced cyclohexatrienoid character in the central six-membered ring[21a] (Figure 3.1). Although the chemistry of **5** has been less thoroughly explored than that of its higher homologue **7**, the former could likewise be smoothly converted into its hexahydrogenated derivative, which was assigned the all-cis stereochemistry based on NMR spectroscopic evidence.[21a]

The bond alternating 1,3,5-cyclohexatriene moieties of **5** and **7** are unique structural features that have associated with them electronic properties of fundamental interest in relation to the resonance stabilization of benzene (cf. section 1.2.1). Therefore, the heats of hydrogenation (ΔH_H) of these compounds have been determined in collaboration with Prof. Donald Rogers, Long Island University, New York. In addition, relevant heats of formation (ΔH_f°) data of **5** and **7** were obtained by combustion analysis in cooperation with Prof. Christoph Rüchardt, University of Freiburg, Germany. The synthesis of the material necessary for these studies has been previously described[22a,25] and is summarized in Scheme 3.1.

3.2 ΔH_H and ΔH_f° Data of Angular [3]- and Triangular [4]Phenylene.

From the outset of this work, it was expected that the strain imposed on the central six-membered ring in **5** and **7** in conjunction with π electronic effects would sufficiently diminish the degree of delocalization (i.e., aromaticity), resulting in a ΔH_H significantly more exothermic than the value of -49.8 kcal mol^{-1} obtained for benzene.[54] This notion was indeed confirmed calorimetrically. The experimental ΔH_H values[136] of -66.8 ± 1.2

kcal mol^{-1} and -71.6 ± 2.1 kcal mol^{-1} for **5** and **7**, respectively, seem to suggest that neither molecule benefits to a large extent from aromatic stabilization. However, in light of the thermochemical outcome of hydrogenation

Scheme 3.1[a]

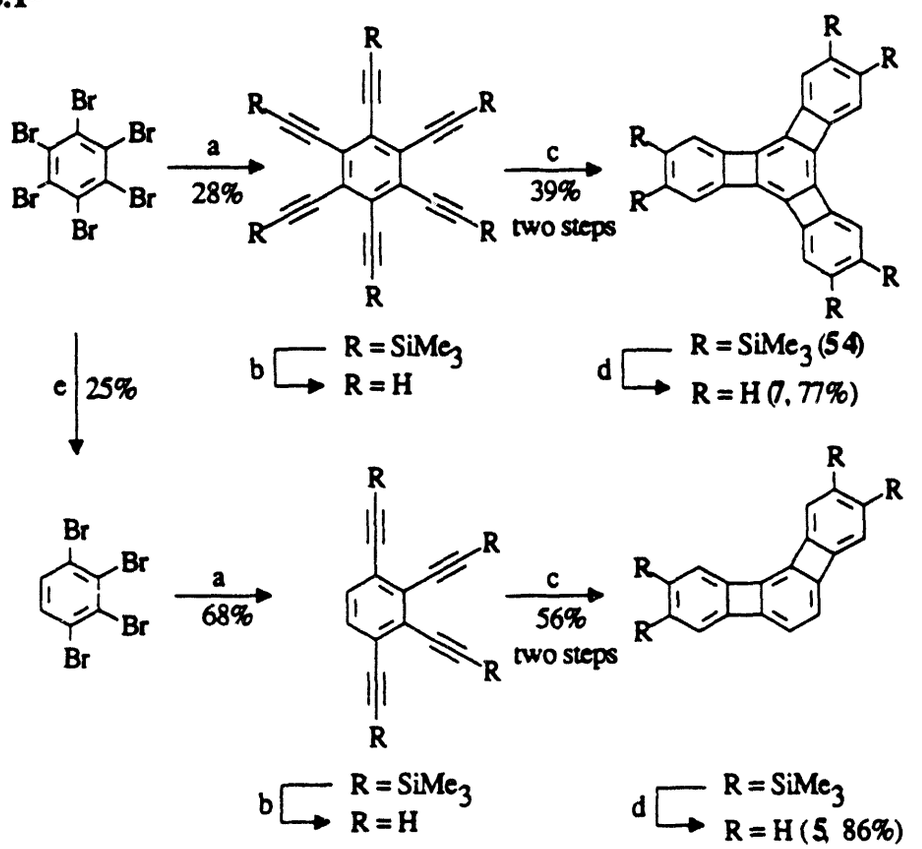

[a] (a) Me_3SiCCH; CuI; $Pd(PPh_3)_2Cl_2$; Et_3N; 110°C; 18h. (b) $KF{\cdot}2H_2O$; DME; 18-crown-6; r.t.; 15 min. (c) BTMSE; $CpCo(CO)_2$; hν; Δ; 18h. (d) CF_3COOH; $CHCl_3$; r.t.; 18 h. (e) NH_2NH_2 (80% in H_2O); EtOH; Δ; 3d (ref 135a).

experiments involving trienes like *cis*-1,3,5-hexatriene (**58**)[54] or tricyclo[4.4.2.$0^{1,6}$]-dodeca-2,4,8-triene (**59**)[137] (Figure 3.3), one would anticipate ΔH_H for an apparently non-delocalized cyclohexatriene such as **7** to exceed 80 kcal mol^{-1}. Furthermore, the difference in the measured reaction enthalpies for the hydrogenation of **5** and **7** is surprisingly small, indicating an increase of this quantity in irregular increments along the series **1**→**3**→**5**→**7**.

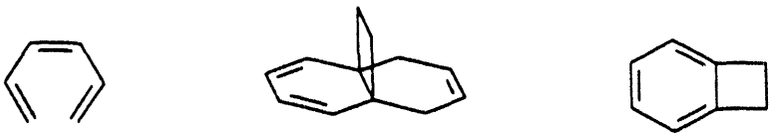

	58	59	41
ΔH_H	-80.5[54]	-81.8[137]	-54.0[139]

Figure 3.3 Experimental Heats of Hydrogenation of Selected Trienes in kcal mol^{-1}.

Unfortunately, ΔH_H data for biphenylene (3), necessary to support this assumption, could not be obtained, because attempts to devise a catalytic system that would selectively hydrogenate one six-membered ring of 3 were unsuccessful,[25] contrary to literature claims.[138]

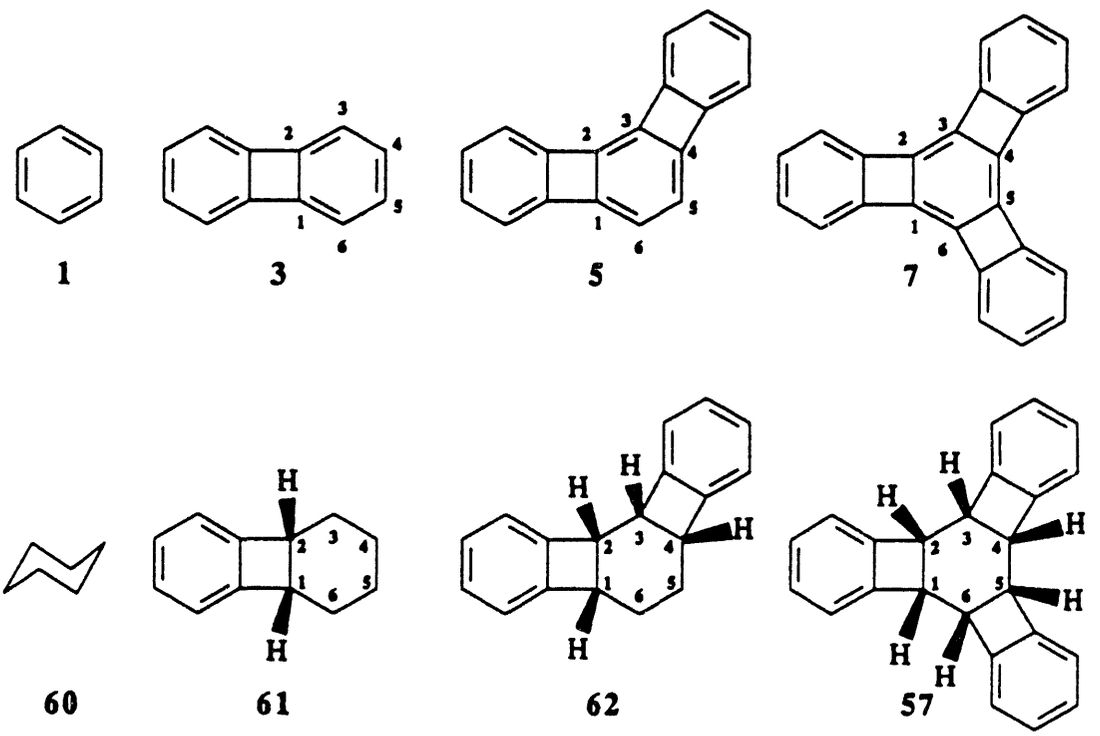

Figure 3.4 Benzocyclobutadienologs and their Hexahydrogenated Derivatives.

Satisfactory explanations of the observed enthalpies have to address the degree of π delocalization and the amount of ring strain in both reactants and hydrogenation products. The latter effect on calorimetric ΔH_H determinations is evident from comparison

of pertinent data for benzene[54] (**1**, ΔH_H = -49.8 kcal mol^{-1}) and benzocyclobutene[139] (**41**, ΔH_H = -54.0 kcal mol^{-1}), for which there are no clear crystallographic[96b] or spectroscopic[96a] indications of perturbations in the π system (cf. section 1.3.1). Hence, the more exothermic value for **41** can be solely attributed to strain induced by small-ring fusion. In an attempt to shed further light on these matters, the cyclohexatriene derivatives **1**, **3**, **5**, and **7** as well as their hexahydrogenated counterparts **60** - **62**, and **57** have been subjected to computational scrutiny (Figure 3.4, Tables 3.1, 3.2, and 3.3).

Comparison of the computed geometries with available experimental data shows that the molecules under investigation are satisfactorily reproduced by both, empirical and semiempirical methods (Tables 3.1 and 3.2). The force field as well as the PM3 parameter set confirm the observed bond alternation in the phenylenes, albeit to varying degrees of accuracy. Whereas the latter tends to overestimate the distance between juncture carbon atoms (e.g, $R_{1\text{-}2}$), the former has difficulties in replicating the contracted bonds adjacent to

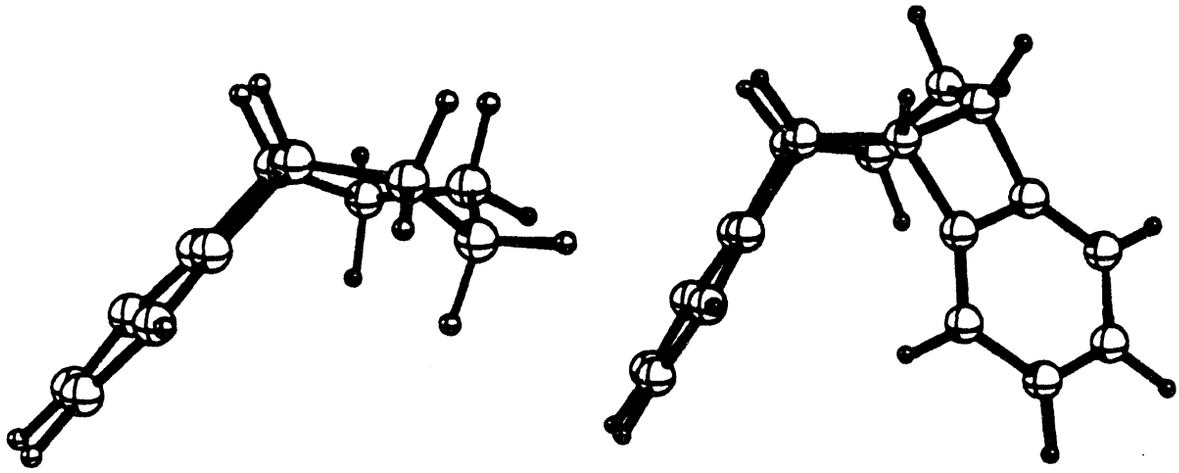

Figure 3.5 PM3 Optimized Geometries of Hexahydrogenated Biphenylene (**61**) and Angular [3]Phenylene (**62**).

the site of fusion (e.g., $R_{1\text{-}6}$). Both computational techniques locate the strongly cup-shaped structure of **57**, with extreme CC length variations in the planar cyclohexane unit, as minima on the potential energy surfaces, almost matching X-ray crystallographic results. This finding lends credibility to the predicted twist-boat conformations of **61** and **62** (Figure 3.5), which have not been structurally characterized.

Table 3.1 CC Bond Lengths of Most Annelated Six-membered Rings in Cyclohexatriene Derivatives **1**, **3**, **5**, and **7**.[a]

		1[b]	**3**[c]	**5**[d]	**7**[e]
	exp	1.398	1.426	1.449	1.495
$R_{1\text{-}2}$	MMX	1.40	1.42	1.45	1.47
	PM3	1.391	1.452	1.486	1.525
	exp	1.398	1.372	1.348	1.333
$R_{1\text{-}6}$	MMX	1.40	1.37	1.37	1.35
	PM3	1.391	1.357	1.349	1.325
	exp	1.398	1.372	1.345	1.338
$R_{2\text{-}3}$	MMX	1.40	1.37	1.35	1.35
	PM3	1.391	1.357	1.331	1.325
	exp	1.398	1.423	1.449	1.486
$R_{3\text{-}4}$	MMX	1.40	1.43	1.44	1.47
	PM3	1.391	1.423	1.486	1.525
	exp	1.398	1.385	1.348	1.335
$R_{4\text{-}5}$	MMX	1.40	1.40	1.37	1.36
	PM3	1.391	1.377	1.349	1.325
	exp	1.398	1.423	1.446	1.502
$R_{5\text{-}6}$	MMX	1.40	1.43	1.45	1.47
	PM3	1.391	1.423	1.449	1.525

([a]) Values in Ångstroms. For numbering scheme, see Figure 3.4. ([b]) Experimental values from ref 12b. ([c]) Experimental values from ref 86. ([d]) Experimental values from ref 21a. ([e]) Experimental values are those of **54** taken from ref 22a.

Table 3.2 CC Bond Lengths of Most Annelated Six-membered Rings in Cyclohexane Derivatives **60** - **62**, and **57**.[a]

		60[b]	61	62	57[c]
	exp	1.528	-	-	1.599
R_{1-2}	MMX	1.54	1.60	1.60	1.59
	PM3	1.521	1.602	1.600	1.599
	exp	1.528	-	-	1.511
R_{1-6}	MMX	1.54	1.53	1.53	1.52
	PM3	1.521	1.518	1.511	1.502
	exp	1.528	-	-	1.511
R_{2-3}	MMX	1.54	1.53	1.52	1.52
	PM3	1.521	1.521	1.506	1.502
	exp	1.528	-	-	1.599
R_{3-4}	MMX	1.54	1.54	1.60	1.60
	PM3	1.521	1.518	1.603	1.600
	exp	1.528	-	-	1.511
R_{4-5}	MMX	1.54	1.54	1.52	1.52
	PM3	1.521	1.518	1.512	1.503
	exp	1.528	-	-	1.599
R_{5-6}	MMX	1.54	1.54	1.54	1.60
	PM3	1.521	1.518	1.520	1.600

([a]) Values in Ångstroms. For numbering scheme, see Figure 3.4. ([b]) Experimental values from ref 142. ([c]) Experimental values from ref 26.

The discrepancy between MMX and PM3 is much more dramatic in their description of the molecules' energy contents (Table 3.3). Generally, force field derived heats of formation are lower than the corresponding PM3 data for the unsaturated molecules **1**, **3**, **5**, and **7**, while the opposite is observed in case of the hexahydrogenated compounds. The assumption that MMX values are of higher accuracy is supported by comparison of enthalpies stemming from PM3 calculations with those obtained experimentally.[141a,b] It is found that the semiempirical MO treatment tends to overestimate energies of unsaturated molecules, but arrives at values too low in the cases

of saturated atomic assemblies. The fact that ΔH_f° data derived from MMX optimization of **1**, **3**, **5**, and **60** are in excellent agreement with combustion results is not surprising, since these compounds have most certainly been used to parametrize the force field.[140]

Table 3.3 Heats of Formation and Hydrogenation of Cyclohexatrienes **1**, **3**, **5**, and **7**.[a]

	ΔH_f°, calc.		ΔH_f°, exp.	ΔH_H, calc.[b]		ΔH_H, exp.
	MMX[c]	PM3[d]		MMX[c]	PM3[d]	
1	19.7	23.5	19.8±0.1[e]	-49.2	-54.5	-49.8[f]
3	99.7	109.8	99.9±0.8[e]	-56.1	-73.1	-
5	181.2	193.0	173.7±1.0[g]	-67.0	-90.5	-66.8±1.2
7	263.2	274.3		-61.2	-98.4	-71.6±2.1

([a]) Values in kcal mol^{-1}. ([b]) Obtained by difference between ΔH_f°, calc. (products) and ΔH_f°, calc. (reactants). ΔH_f° values for **60** - **62**, and **57** are -29.5 (-31.0), 43.6 (36.7), 114.2 (102.5), and 202.1 (175.9) kcal mol^{-1} as calculated by MMX (PM3). ([c]) Ref 140. ([d]) Ref 141. ([e]) Ref 52b. ([f]) Ref 54. ([g]) This work.

However, the notion that these parameters can be unreservedly applied to the higher phenylenes and their hydrogenation products is rather tenuous in light of the notoriously difficult computational treatment of strained rings and the structural (and electronic) novelty of the systems investigated here. Therefore, the theoretical predictions were further calibrated by determining the ΔH_f° of **5** from combustion analysis and measurement of its heats of sublimation. As inspection of Table 3.3 reveals, none of the employed computational methods is able to correctly reproduce this datum, the MMX value exceeding the experimentally determined one by 7.5 kcal mol^{-1}, while the PM3 calculations overestimate ΔH_f° of **5** by almost 20 kcal mol^{-1}. Nevertheless, both theoretical tools are useful to investigate trends along the series **1** → **3** → **5** → **7** and their corresponding hydrogenation products.

Heats of hydrogenation can be estimated by taking the difference between the corresponding ΔH_f° data of products and reactants. A priori, there is no reason to expect

complete congruity of experimental and calculated ΔH_H values, because the former are usually determined in solution, while the latter refer to an ideal gas phase, free of intermolecular interactions. Solvation effects typically range in the order of several kcal mol^{-1}. For example, the solvation energy of methane in cyclohexane[144] amounts to 3.4 kcal mol^{-1}, and the heat of hydrogenation of benzocyclobutene (**41**) was found to be 3.7 kcal mol^{-1} more exothermic[139,145] than the initially reported value,[146] when solvation effects were taking into account. In light of these considerations, the accurate reproduction of calorimetric ΔH_H data for **1** and **5** by MMX is gratifying, but appears to be rather serendipitous (Table 3.3). Indeed, there is absolutely no agreement in the case of the ΔH_H of triangular [4]phenylene (**7**), for which the force field arrives at a value roughly 10 kcal mol^{-1} lower than that obtained experimentally. On the other hand, the divergent trends in the heats of formation of reactants and products calculated by PM3 (vide supra) leads to large overestimates in the hydrogenation enthalpies of the phenylenes. Yet, both computational techniques correctly predict declining increments in ΔH_H along the series **3** $\rightarrow$ **5** $\rightarrow$ **7** without, however, providing ad hoc explanations for such behavior.

In order to gain insight into the effects of sequential benzocyclobutene fusion to **1**, changes in ΔH_f° along the series **1**, **3**, **5**, **7** and **60** - **62**, **57** were examined (Scheme 3.2). It was found that along the phenylene series, the MMX calculated ΔH_f° values increase by almost constant increments (ca. 81 kcal mol^{-1}), whereas the corresponding data of the cyclohexane derivatives exhibit a sharp rise upon fusion of the third benzocyclobutene moiety (87.9 kcal mol^{-1} from **62** to **57**, compared to ca. 72 kcal mol^{-1} each step from **60** to **62**). PM3 evaluation of successive small-ring annelation, on the other hand, reveals declining increments along the phenylene series, from 86.3 kcal mol^{-1} on fusion of the first, to 81.3 kcal mol^{-1} on attachment of the third benzocyclobutene unit. Although less pronounced than implied by force field results, the PM3 derived values of the cyclohexane derivatives parallel those obtained by MMX, also pointing at the severe energetic requirements of locking **57** into a planar, bond alternating conformation. It thus appears

Scheme 3.2[a]

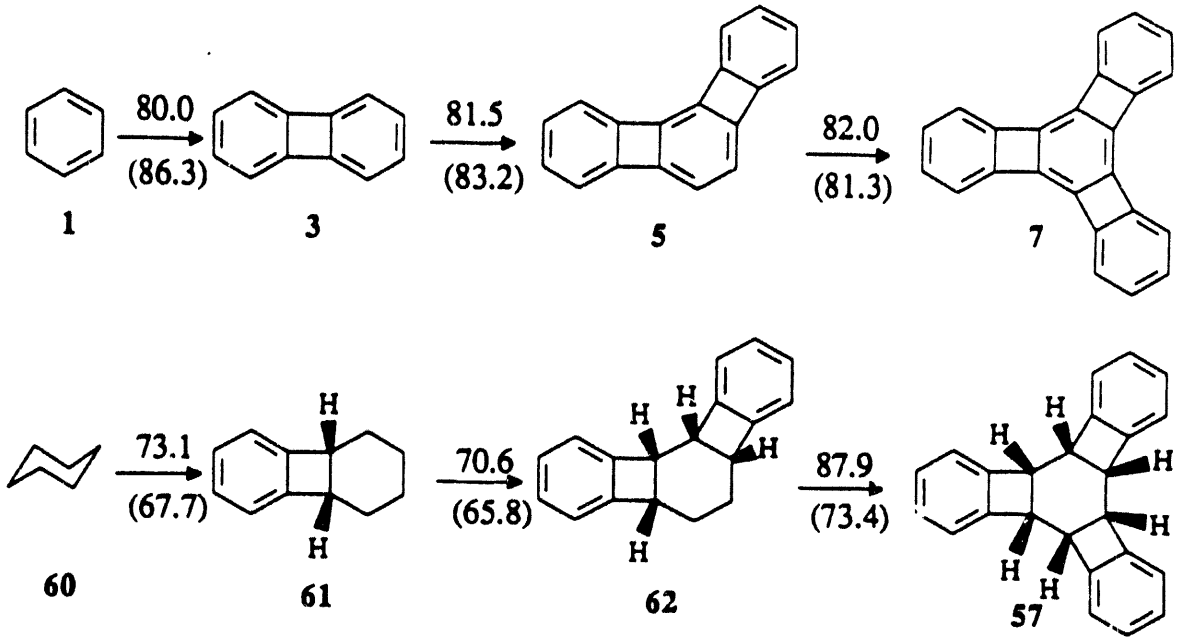

([a]) Changes in ΔH_f° with successive benzocyclobutene fusion. Values shown are in kcal mol^{-1} computed by MMX (PM3) and taken from Table 3.3.

that the cyclohexane nucleus retains to some extent its conformational flexibility throughout the first two annelations, but that fusion of the third small-ring fragment leads to a rigid framework of high energy. This interpretation is supported by the geometries of **61**, **62**, and **57** (Figures 3.2 and 3.5), suggesting significant strain contributions from **57** to the unexpectedly low ΔH_H of **7**.

The importance of strain on the thermochemical outcome of hydrogenation experiments of the phenylenes can be further demonstrated by investigating model compounds that are void of potentially interfering π electronic effects. Pairwise distortion of benzene's HCC angles to 90° has been used previously[122] to induce bond alternation similar to that observed in **7** (chapter 2). Employing the PM3 parameter set, this approach was extended to mimic one- and twofold four-membered ring fusion as in **3** and **5** and also to include structural deformations of the cyclohexane nuclei in **61**, **62**, and **57** (Table 3.4, Figure 3.6). Comparison between the geometries of the model compounds and those of

the fully annelated systems (Tables 3.1 and 3.2) reveals good agreement, the less pronounced bond alternation of the former being attributable to restriction of the distortion angle to 90°, whereas 85° are observed in the parent molecules.[21a,22a,26]

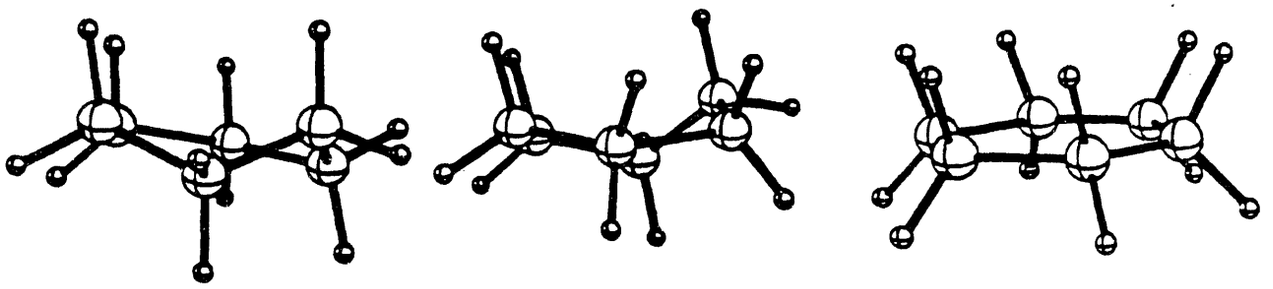

Figure 3.6 PM3 Optimized Geometries of Distorted Cyclohexanes **65** - **67** (Left to Right).

Table 3.4 Energies and CC Bond Lengths of Distorted Benzenes and Cyclohexanes.[a]

	1	**63**	**64**	**52**
ΔH_f°	23.5	58.3	91.2	122.8
$R_{1\text{-}2}$	1.391	1.456	1.418	1.501
$R_{1\text{-}6}$	1.391	1.359	1.352	1.329
$R_{2\text{-}3}$	1.391	1.359	1.333	1.329
$R_{3\text{-}4}$	1.391	1.415	1.418	1.501
$R_{4\text{-}5}$	1.391	1.380	1.352	1.329
$R_{5\text{-}6}$	1.391	1.415	1.435	1.501
	60	**65**	**66**	**67**
ΔH_f°	-31.0	-13.5	-0.6	18.1
$R_{1\text{-}2}$	1.521	1.576	1.576	1.570
$R_{1\text{-}6}$	1.521	1.513	1.507	1.494
$R_{2\text{-}3}$	1.521	1.508	1.498	1.494
$R_{3\text{-}4}$	1.521	1.517	1.577	1.570
$R_{4\text{-}5}$	1.521	1.518	1.507	1.494
$R_{5\text{-}6}$	1.521	1.518	1.520	1.570

([a]) PM3 values. Energies in kcal mol^{-1}, bond lengths in Ångstroms. For numbering scheme, see Scheme 3.3.

The bent cyclohexanes show twist-boat conformations (**65**, **66**) and a planar D_{3h} structure (**67**) consistent with the geometries of the benzocyclobutene-fused compounds.

Of particular interest are the energy changes associated with stepwise distortion of HCC bond angles in the models (Scheme 3.3). Along the benzene series, it is evident that ΔH_f° is raised by slightly decreasing increments, from 34.8 kcal mol^{-1} on bending of the first pair of HCC angles to 31.6 kcal mol^{-1} for the third. The greater ability of the cyclohexanes to accommodate angular strain is reflected in the smaller magnitude of Δ ΔH_f° upon distortion, increasing by only 17.5 kcal mol^{-1} on going from **60** to **65**. Introduction of a second set of bent bonds is energetically even less demanding,

Scheme 3.3[a]

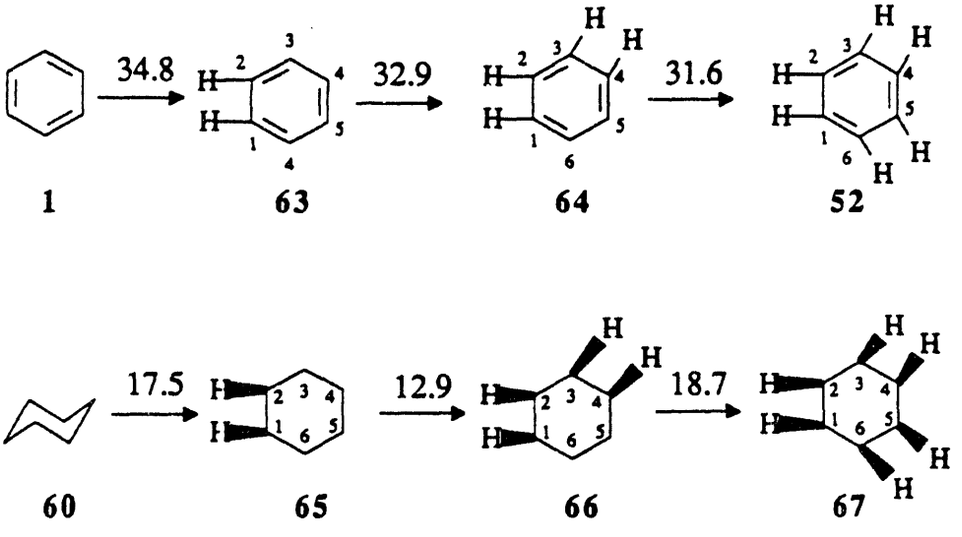

([a]) Energetic changes in benzene and cyclohexane upon pairwise restricting HCC angles to 90°. Values shown are $\Delta\Delta H_f^\circ$ in kcal mol^{-1} obtained from PM3 calculations.

(12.9 kcal mol^{-1}), while distortion of the third pair of HCC angles (**66** → **67**) requires an additional energy of 18.7 kcal mol^{-1}, indicative of the increasing rigidity of the six-membered ring. Hence, the last two steps in the cyclohexane series show a trend in $\Delta\Delta H_f^\circ$ that is opposed to that found in the benzenes.

From the above analysis, it is apparent that the energetic behavior of benzene and cyclohexane on distortion coincides with that of the fully annelated systems, irrespective of the presence of π electronic effects in the latter. While lacking accuracy in reproducing the heats of hydrogenation of the phenylenes, the employed computational tools thus allow to confidently conclude that the ΔH_H data are greatly influenced by (if not dominated) strain in the products of the reaction. Exact quantification of such steric constraints imposed on the respective σ frames presents a formidable challenge, but a general idea about the magnitudes involved can be obtained from the following considerations.

Numerous studies have addressed the dynamics of the various cyclohexane conformers,[147] but none of them discusses distorted geometries as those observed (or predicted) for **61**, **62**, and **57**. Variable temperature IR spectroscopy on solid cyclohexane established the twist-boat conformation to be 5.5 kcal mol^{-1} higher in energy than the chair ground state.[148] Optimizations of the former geometry at high ab initio levels[147] (DZP basis set on carbon, D_2 symmetry imposed) predict differences in CC bond lengths of only 0.007 Å, a value easily surpassed in the structure of **65** ($R_{1\text{-}2}$ - $R_{1\text{-}6}$ = 0.063 Å). Accordingly, PM3 calculations arrive at energy increases of 17.5 kcal mol^{-1} on distortion of **60** to **65**, and 30.4 kcal mol^{-1} on deformation to **66**. Since planar (D_{6h}) cyclohexane is a saddle point of higher order on the potential energy surface, this geometry has received less attention.[149] Employing semiempirical MINDO/2 calculations,[149a] differences in the enthalpy of the D_{3d} (chair) and D_{6h} structures of **60** were computed to amount to 15.5 kcal mol^{-1}. The authors note, however, that this parameter set is notorious in underestimating bending-force constants and strain energies. Ab initio studies with minimal basis sets[149b] indicate an energy increase of 40.2 kcal mol^{-1} on going from D_{3d} to D_{6h}. Considerations of the severe geometric restrictions in **67** (wiht its bond alternating D_{3h} structure) leads to strain energies of 49 kcal mol^{-1} with PM3, and 76.8 kcal mol^{-1} at the SCF/6-31G* level of theory.[150]

Dearth of experimental data also exists along the benzene (phenylene) series. Biphenylene (**3**) was shown to be endowed with ring strain amounting to 64.3 kcal mol^{-1} relative to biphenyl.[151] Based on the corresponding model compound, **63**, PM3 predicts about half of that, the energy increasing by only 34.8 kcal mol^{-1} from **1** to **63**. Similarly, the semiempirical MO method seems to underestimate the strain inherent in **52** (99.3 kcal mol^{-1}), for which SCF/6-31G* calculations yield a value of 144.0 kcal mol^{-1} (chapter 2, Table 2.3).

Considering only data derived at the latter level of theory, one obtains a release in strain energy of 67.2 kcal mol^{-1} when **52** is transformed into **67**, a result on the same order of magnitude as ΔH_H for **7**. It thus appears that antiaromatic (cyclobutadienoid) interactions across the four-membered rings in the phenylenes are only minor contributors to the observed heats of formation, the major ones being ring strain effects. Certainly, conclusions with respect to π electronic interactions (e.g., aromaticity, resonance stabilization) cannot be drawn from the calorimetric results without reservation, rendering interpretations of ΔH_H data in terms of "empirical resonance energy" speculative. The relative contributions of σ (strain) and π (delocalization) effects on the geometries of models compounds of **5** and **7** are subject of the investigation outlined in the following chapter.

Chapter Four

Ab Initio Study of Benzenes Fused to Four-Membered Rings

4.1 Rehybridization, Delocalization, and Antiaromaticity.

4.1.1 Introduction.

The long-standing dispute regarding the presence of CC bond length variations along the perimeter of benzene nuclei fused to small rings has recently been settled by X-ray crystallographic analysis[25,98] of tricyclobutabenzene (**8**, section 1.3.1, Figure 1.11), disclosing small, but significant distortions in the sense originally proposed by Mills and Nixon.[90] More pronounced 1,3,5-cyclohexatriene moieties have been observed in the benzocyclobutadieno-fused benzenes biphenylene (**3**),[86] angular [3]phenylene (**5**),[21a] and triangular [4]phenylene (**7**),[22a] the degree of CC bond length alternation increasing along the series. In these systems, the benzene nuclei are incorporated into extensively delocalized π networks via four-membered rings, raising the possibility of enhanced differences in bond length to minimize antiaromatic, cyclobutadienoid interactions.

Strain is certainly one of several contributors to the observed bond alternation in annelated benzenes. Depending on the nature of the fused carbocycle, conjugative or hyperconjugative interactions between the substituents and the benzenoid π system may simultaneously enforce structural variations in the σ frame. The notion that σ strain alone would suffice to reduce the D_{6h} symmetry of benzene to D_{3h} has been supported by model

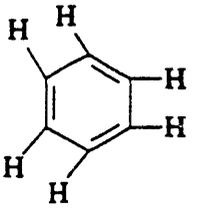

52

studies[97f,122] involving pairwise bending of HCC angles from an optimal value of 120° to highly strained 90°, (**52**), thereby mimicking fusion to four-membered rings. As delineated

in chapter 2, π delocalization in **52** remains substantial, even at this distorted geometry. Thus, formation of the cyclohexatrienoid topology may be attributed mainly to σ rehybridization effects induced by the strained carbon framework.[97f] Rehybridization has been invoked previously[99] to explain reactivity patterns in fused benzenes, and recently was the subject of a computational investigation aimed at understanding the origin of the Mills-Nixon effect.[97d] These interpretations, however, are either based on empirical reasoning or on the application of maximum overlap methodology[153] and do not take into account π resonance and hyperconjugative interactions. It was further suggested[97f] that the "flexibility" of the electronic distribution at the benzene substituents is responsible for the degree of bond alternation and that the formation of bent bonds[154] prevents certain systems from adopting a cyclohexatrienoid geometry.

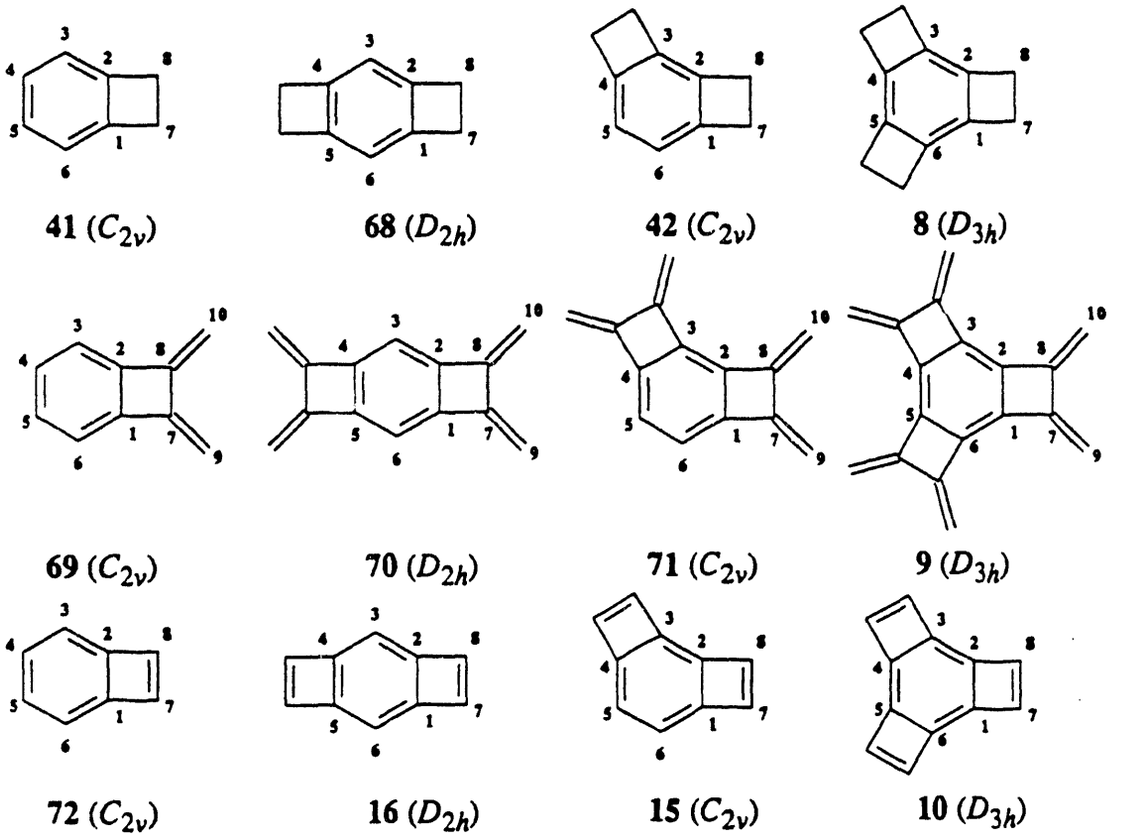

Figure 4.1 Numbering Scheme and Symmetries of Benzocyclobutenes Considered in this study.

In order to elucidate the effects of four-membered ring fusion on the structural and electronic characteristics of the benzene nucleus, a comprehensive ab initio study was conducted on appropriately functionalized benzocyclobutenes, whose geometries reflect the salient features of **3**, **5**, and **7** (Figure 4.1). Inspection of the optimized structures of these model compounds provides insight into the effect of various degrees of strain and π conjugation (or hyperconjugation) on the geometry of the benzene frame. Applying natural bond orbital (NBO)[32] analysis (cf. section 1.2.4) to the computed wavefunctions of the benzocyclobutenes allows discrimination between such σ and π electronic effects. All calculations reported in this chapter were performed by either GAUSSIAN 90[125] or GAMESS[126] at the SCF level of theory, with the split valence 3-21G[155] basis, unless otherwise stated. Geometries are optimized within designated symmetry constraints (Figure 4.1).

4.1.2 Geometries and Rehybridization in Benzocyclobutenes.

In light of the great interest the Mills-Nixon effect has received over the years, the amount of experimental data on the molecules depicted in Figure 4.1 is surprisingly small. Several of the unsubstituted compounds are known,[96,156] but crystallographic data are available only for the cyclobutabenzene series **41**, **68**, **42**, and **8**.[25,96b,157] Comparison with ab initio optimized structures (Table 4.1) reveals good agreement. In the 3-21G calculated geometries, the CC bond lengths within the six-membered rings are slightly smaller by an average of 0.012 Å. The discrepancy is somewhat larger in the cyclobutene substructure (overestimation by 0.016 Å on average), a region in which highly extended basis sets are necessary to account for the "strained" electronic distribution.[48]

The effect of fusion to four-membered rings is apparent in the structural variation of the benzene frame (Table 4.1). Generally, the common bond (C1-C2) is elongated, whereas the adjacent benzenoid bond is contracted with respect to unsubstituted benzene. Hence, the quantity ΔR, defined as the difference between these two bond lengths (eq 4.1),

$$\Delta R = R_{1\text{-}2} - R_{1\text{-}6} \qquad (4.1)$$

is a useful measure of the degree of bond alternation and is considered throughout the following discussion.

The geometry of the benzene nucleus along the series **41**, **68**, **42**, and **8** is only weakly perturbed by four-membered ring fusion. Thus, ΔR increases from 0.004 Å in **41** to only 0.047 Å in **8**, a finding that reproduces reasonably well the observed Mills-Nixon effect. This interpretation is further corroborated in the hybridizations of the benzenoid carbons (Table 4.2). It is evident from the hybrids at the center of annelation in the cyclobutabenzenes that small-ring fusion leads to some redistribution of p-character along the carbon-carbon bonds, the longer bonds showing higher percentage p-character than the shorter ones [cf. h(1-2) = $sp^{2.21}$ with h(1-6) = $sp^{1.58}$ in **41**]. However, the unsubstituted carbons in **41**, **68**, and **42** use hybrids [h(6-1) and h(6-5) ranging from $sp^{1.85}$ to $sp^{1.92}$] essentially identical to those of benzene ($sp^{1.88}$), suggesting that the amount of ring strain transmitted along the σ framework is negligible. The usefulness of the hybridization concept in explaining the geometrical changes associated with fusion of cyclobutene to the benzene nucleus has recently been demonstrated by Maksic et al.[97d] Comparison of the carbon hybrids derived from the maximum overlap method[97d] with those obtained from NBO analysis reveals excellent agreement between these two inherently different approaches and allows correlation of molecular properties with computed hybridizations with a reasonable degree of certainty.[158]

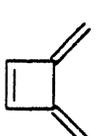

73

The benzene isomer 3,4-dimethylenecyclobutene (**73**)[159] has attracted a great deal of attention due to its intriguing electronic properties that have been borne out by both theory and experiment.[160] Based on HMO resonance energies, this compound was

Table 4.1. Energies and CC Bond Lengths of Annelated Benzenes.[a]

	41[b]	**68**[b]	**42**[c]	**8**[c]
energy	-305.846455	-382.276199	-382.2732244	-458.699833
R(1-2)	1.386 (1.391)	1.390 (1.399)	1.397 (1.402)	1.408 (1.408)
R(1-6)	1.370 (1.385)	1.382 (1.394)	1.372 (1.392)	1.361 (1.390)
R(1-7)	1.538 (1.518)	1.538 (1.521)	1.540 (1.518)	1.538 (1.528)
R(2-3)	1.370 (1.385)	1.382 (1.394)	1.361 (1.385)	1.361 (1.391)
R(2-8)	1.538 (1.518)	1.538 (1.521)	1.536 (1.518)	1.538 (1.525)
R(3-4)	1.396 (1.400)	1.382 (1.394)	1.397 (1.402)	1.408 (1.415)
R(4-5)	1.386 (1.399)	1.390 (1.399)	1.372 (1.392)	1.361 (1.391)
R(5-6)	1.396 (1.400)	1.382 (1.394)	1.408 (1.413)	1.408 (1.412)
R(7-8)	1.600 (1.576)	1.596 (1.575)	1.599 (1.582)	1.598 (1.579)
	69	**70**	**71**	**9**
energy	-381.111513	-532.807635	-532.803494	-684.495982
R(1-2)	1.398	1.405	1.410	1.424
R(1-6)	1.370	1.381	1.372	1.359
R(1-7)	1.504	1.502	1.504	1.498
R(2-3)	1.370	1.381	1.359	1.359
R(2-8)	1.504	1.504	1.501	1.498
R(3-4)	1.396	1.381	1.410	1.424
R(4-5)	1.389	1.405	1.472	1.359
R(5-6)	1.396	1.381	1.408	1.424
R(7-8)	1.530	1.528	1.530	1.531
R(7-9)	1.312	1.312	1.312	1.309
R(8-10)	1.312	1.312	1.312	1.309
	72	**16**	**15**	**10**
energy	-304.611533	-379.791546	-379.819669	-455.039433
R(1-2)	1.426	1.392	1.484	1.524
R(1-6)	1.399	1.381	1.326	1.309
R(1-7)	1.546	1.568	1.519	1.503
R(2-3)	1.339	1.381	1.313	1.309
R(2-8)	1.546	1.568	1.519	1.503
R(3-4)	1.438	1.381	1.484	1.533
R(4-5)	1.358	1.392	1.326	1.309
R(5-6)	1.438	1.381	1.487	1.524
R(7-8)	1.337	1.331	1.343	1.341

([a]) SCF/3-21G values. Energies are given in Hartrees, bond lengths in Ångstroms. Cf. CC bond length of benzene (3-21G): 1.385 Å. For numbering scheme, see Figure 4.1.

([b]) Experimental values (in parentheses) from ref 96b. ([c]) Experimental values in parentheses from ref 25. Those for **8** correspond to one of two independent molecules present in the unit cell at 125 K. For details, see refs 25 and 98.

Table 4.2. NHO Character of Selected Carbon Centers.[a]

	41	**68**	**42**	**8**
h(1-2)	2.21 (2.28)	2.16 (2.19)	2.21	2.28 (2.19)
h(1-6)	1.58 (1.61)	1.60 (1.61)	1.56	1.55 (1.66)
h(1-7)	2.34(2.21)	2.36 (2.28)	2.37	2.31 (2.22)
h(2-1)	2.21 (2.28)	2.16 (2.19)	2.27	2.28 (2.19)
h(2-3)	1.58 (1.61)	1.60 (1.61)	1.57	1.55 (1.66)
h(2-8)	2.34 (2.21)	2.36 (2.28)	2.28	2.31 (2.22)
h(6-1)	1.88 (1.80)	1.91 (1.94)	1.85	1.55 (1.66)
h(6-5)	1.91 (2.00)	1.91 (1.94)	1.92	2.28 (2.19)
	69	**70**	**71**	**9**
h(1-2)	2.33	2.30	2.35	2.45
h(1-6)	1.55	1.51	1.54	1.54
h(1-7)	2.26	2.25	2.27	2.17
h(2-1)	2.33	2.30	2.42	2.45
h(2-3)	1.55	1.51	1.56	1.54
h(2-8)	2.26	2.25	2.17	2.17
h(6-1)	1.91	1.94	1.87	1.54
h(6-5)	1.91	1.94	1.92	2.45
	72	**16**	**15**	**10**
h(1-2)	2.44	2.15	2.35	3.01
h(1-6)	1.40	1.51	1.54	1.33
h(1-7)	2.34	2.53	2.27	2.12
h(2-1)	2.44	2.15	2.82	3.01
h(2-3)	1.40	1.51	1.37	1.33
h(2-8)	2.43	2.53	2.19	2.12
h(6-1)	1.80	1.93	1.69	1.33
h(6-5)	2.04	1.93	2.17	2.12

([a]) Values listed (SCF/3-21G) are the exponents λ of the sp^{λ} hybrids. Hybrid *h*(A-B) is centered on A, directed toward B. For comparison, λ = 1.88 in benzene. Values in parentheses are taken from ref 97d and converted from %s character to sp^{λ} hybridization using $\lambda = (\%s)^{-1} - 1$. For numbering scheme, see Figure 4.1.

classified to maintain some aromatic character,[160b] opening the opportunity to juxtapose aromatic and antiaromatic substructures within one molecular framework by fusing **73** onto benzene. This design found its realization in the synthesis of **69** by Cava and Mitchell,[156e] but high reactivity prevented rigorous structural characterization and presumably discouraged attempts to synthesize the higher homologs **70**, **71**, and **9**.

Comparison of the calculated geometries of **69-71** and **9** with those of the cyclobutabenzene series (Table 4.1) reveals that the effect of annelating 3,4-dimethylenecyclobutene is similarly small. Thus, ΔR increases from 0.028 Å in **69** to only 0.065 Å in **9**, a trend not significantly different from that found along **41**, **68**, **42**, and **8**. One possible explanation for the slightly higher degree of bond alternation in the former group of molecules relies on the greater extent of rehybridization at the centers of annelation. The bond connecting the two ortho substituents ($R_{7,8}$) is somewhat shorter in the dimethylenecyclobutenofused series (cf. $R_{7,8}$ = 1.600 Å in **41** and $R_{7,8}$ = 1.530 Å in **69**), resulting in increased ring strain imposed on the benzene frame. This strain in turn manifests itself in greater rehybridization at the carbon centers, as evident from inspection of Table 4.2. Hence, to maximize overlap with neighboring carbons, the annelated centers of dimethylenecyclobuteno-fused benzenes consistently use hybrids of higher percentage p-character along C1-C2 and of higher percentage s-character along C1-C6 relative to the hybrids of **41**, **68**, **42**, and **8**. An alternative explanation for the enhanced bond alternation in **69-71**, and **9** is based on antiaromatic interactions across the four-membered rings, a possibility that will be further explored below. However, analysis of the geometries suggests that 3,4-dimethylenecyclobutene (**73**) possesses only weak antiaromatic character.

The small incremental increase of ring strain resulting from stepwise dimethylenecyclobutene fusion to benzene along the series is reflected in the changes of rehybridization. Thus, the hybrid of center 1 directed along the site of annelation [h(1-2)] ranges from $sp^{2.33}$ in **69** to $sp^{2.45}$ in **9**, whereas a hybrid of nearly fixed $sp^{1.54}$ character is used to form the shorter benzenoid bond C1-C6. Again, the unsubstituted carbons in **69-72** remain largely unaffected by annelation [cf. h(6-1) and h(6-5)], indicating that fusion of up to two dimethylenecyclobutene units does not cause serious distortions of the σ skeleton.

A completely different picture arises when benzene is fused to cyclobutadiene (**2**), the antiaromatic species par excellence. Here, bond alternation is already evident with

annelation of the first ring (ΔR = 0.087 Å in **72**) and reaches a maximum in tricyclobutadienobenzene (ΔR = 0.215 Å in **10**) with benzenoid bond lengths of 1.524 Å and 1.309 Å, respectively. Although it is tempting to attribute the cyclohexatrienoid geometry entirely to interactions between the ethylenic part of the molecule and the π system of the six-membered ring, one should also recognize that the dramatically short cyclobutadiene bond C7-C8 ($R_{7\text{-}8}$ = 1.337 Å in **72**) severely perturbs the σ framework. Shortening of $R_{7\text{-}8}$ induces a compression of bond angle C2-C1-C7 (88.4° in **72** as opposed to 94.0° in **41**), resulting in increased rehybridization at the centers of annelation. Accordingly, fusion of one cyclobutadiene moiety causes redistribution of p-character from $sp^{1.88}$ in unsubstituted benzene to $sp^{2.44}$ [h(1-2)] and $sp^{1.40}$ [h(1-6)] in **72**. The extent of rehybridization is even greater in angularly fused **15** ($sp^{2.82}$ and $sp^{1.37}$ at center 2) and reaches extreme values of $sp^{3.01}$ and $sp^{1.23}$ in trisannelated **10**. In contrast to the cyclobuteno- and dimethylenecyclobuteno-fused series, the effect of ring strain is also apparent in the hybrids of unsubstituted carbon centers. Thus, h(6-1) and h(6-5) in **72** ($sp^{1.80}$ and $sp^{2.04}$, respectively) show an appreciable deviation from the carbon hybrids in benzene, the strain-induced rehybridization being even more pronounced in **15** [h(6-1) = $sp^{1.69}$, h(6-5) = $sp^{2.17}$]. In linearly fused **16**, on the other hand, the symmetry equivalent bonds C1-C6 and C5-C6 are equally strained, leading to hybrids ($sp^{1.93}$) at center 6 that are only marginally different from those of benzene. Note that NBO analysis of rehybridization effects in annelated benzenes is in full accord with, and thereby provides a quantum mechanical basis for, earlier hybridization models.[99]

Comparison of the calculated geometries of **72**, **15**, and **10** with those of **3**,[86] **5**,[21a] and **7**[22a] clearly shows less pronounced bond alternation in the latter series of molecules as one might anticipate in light of the different extents to which σ and π effects are operational. In the cyclobutadieno-fused systems, bonds between carbons 7 and 8 (Table 4.1) are significantly shorter than the analogous bonds in **3**, **5**, and **7** (cf. 1.426 Å, 1.413 Å, and ca. 1.405 Å, respectively), resulting in reduced strain imposed on the central ring

of the phenylenes. In addition, antiaromatic interactions are largely attenuated by strong delocalization in the terminal benzene rings (vide infra). It is clear, on the other hand, that dimethylenecyclobuteno-fused benzenes (**69**, **71**, and **9**) do not serve as good model compounds for **3**, **5**, and **7**, the former systems showing nearly unperturbed benzene nuclei.

Stanger has attributed the remarkable difference of bond alternation in **8** and **10** in part to the increased "flexibility" of sp^3 hybridized substituent carbons of the former, which enables the system to effectively evade angular strain inherent in the four-membered rings by forming bent bonds to the benzene nucleus.[97f] Indeed, such electron density shifts have been observed in XX deformation studies of benzocyclobutenes **41**, **42**, and **8** (section 1.3.1, Figure 1.12). Stanger's conclusion, although intuitively appealing because of the more diffuse electronic distribution around sp^3 carbons cannot be substantiated by the present quantum mechanical calculations. Inspection of bonding properties of trisannelated benzenes reveals nearly identical degrees of bond bending, clearly independent from the extent of bond alternation (Table 4.3). For example, the deviation of

Table 4.3 Deviations of the Electron Density Maxima between C1 and C7 from the Internuclear Axes.[a]

	8	**9**	**10**
NHO[b]	19.4	19.4	19.4
EC[c]	9.4	10.6	11.6
BCP[d]	2.5	2.7	3.1

([a]) SCF/3-21G values in degrees. ([b]) Natural hybrid orbital *h*(1-7). ([c]) Electronic centroid formed from hybrids *h*(1-7) and *h*(7-1). ([d]) Bond critical points, see ref 161.

h(1-7) from the internuclear axes is almost invariant along the series **8** (19.4°), **9** (19.4°), and **10** (21.5°). While differing in absolute magnitude, evaluation of the locations of electronic centroids and bond critical points[161] likewise point at the irrelevance of bond bending to length variations in the benzene core. Furthermore, Stanger tacitly implies that

all benzenes annelated by sp^2 carbons should exhibit pronounced bond alternation, a conclusion obviously at odds with the calculated geometry of **9**. Instead, the above analysis suggests that the C7-C8 distance in the four-membered ring is largely responsible for rehybridization at the centers of annelation and thereby contribute importantly to the degree of bond alternation in the benzene nucleus, particularly in cyclobutadieno-fused **10**. In addition to these strain arguments, **10** has to accommodate π electronic effects that should reinforce the cyclohexatrienoid structure in accord with the original Mills-Nixon postulate. Both of these contributions are sufficiently diminished in **8**, leading to nearly equal CC bond lengths in the six-membered ring. The importance of π delocalization for the benzene geometry will be addressed below.

4.1.3 Natural Resonance Theory Analysis of Benzocyclobutenes.

In order to evaluate resonance contributions to the wavefunctions of the various benzocyclobutenes, the natural resonance theory (NRT)[33] formalism was employed, which is based on the NBO method (cf. section 1.4). The discussion will be restricted to the two dominant Kekulé forms A and B in the annelated benzenes with C_{2v} and D_{3h} symmetries (Table 4.4). Compounds **68**, **70**, and **16** are of D_{2h} symmetry, for which the two resonance structures are identical.

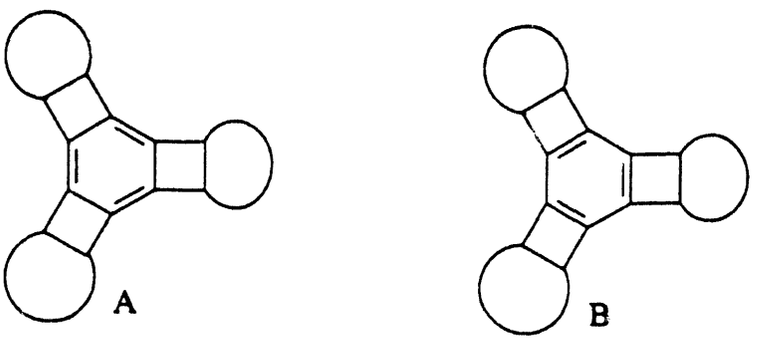

From the data presented, it is apparent that the π electronic distribution generally favors structure A with benzenoid double bonds adjacent to the site of fusion, thus supporting the

original prediction made by Mills and Nixon. This preference, however, is rather small in **41**, **42**, **8**, and **69** with the ratio of the weights of resonance forms A and B barely exceeding unity. Introducing antiaromatic, cyclobutadienoid substructures into the atomic assembly, such as in **72**, **15**, and **10** suppresses the resonance contributions of B, the ratios

Table 4.4 NRT Analysis of Annelated Benzenes.[a]

	41	**42**	**8**
ω_A	51.1	53.5	56.5
ω_B	46.2	44.3	43.3
ω_A/ω_B	1.1	1.2	1.3
	69	**71**	**9**
ω_A	47.3	44.4	43.2
ω_B	42.4	35.1	29.0
ω_A/ω_B	1.1	1.3	1.5
	72	**15**	**10**
ω_A	59.5	71.3	64.5
ω_B	22.3	11.6	4.4
ω_A/ω_B	2.7	6.1	14.7

([a]) Values given are percentage weights ω_A and ω_B for the dominant resonance forms A and B (see text). Dipolar structures account for the residual resonance weights.

ranging from 2.7 in the monoannelated case to a dramatic 14.7 in trisannelated **10**. Obviously, the relative resonance weights of the two Kekulé forms reflect the degree of bond alternation in these molecules, although it has been noted that the relationship between bond length and order can be misleading if strained ring systems are involved.[101,105,162] Further support for the predominance of A in cyclobutadieno-fused benzenes is obtained by comparing the energies of linear and angular isomers of bisannelated benzenes (Scheme 4.1). Whereas angular **42** and **71** are destabilized with respect to their corresponding linear analogs by 1.9 kcal mol^{-1} and 2.6 kcal mol^{-1},

Scheme 4.1[a]

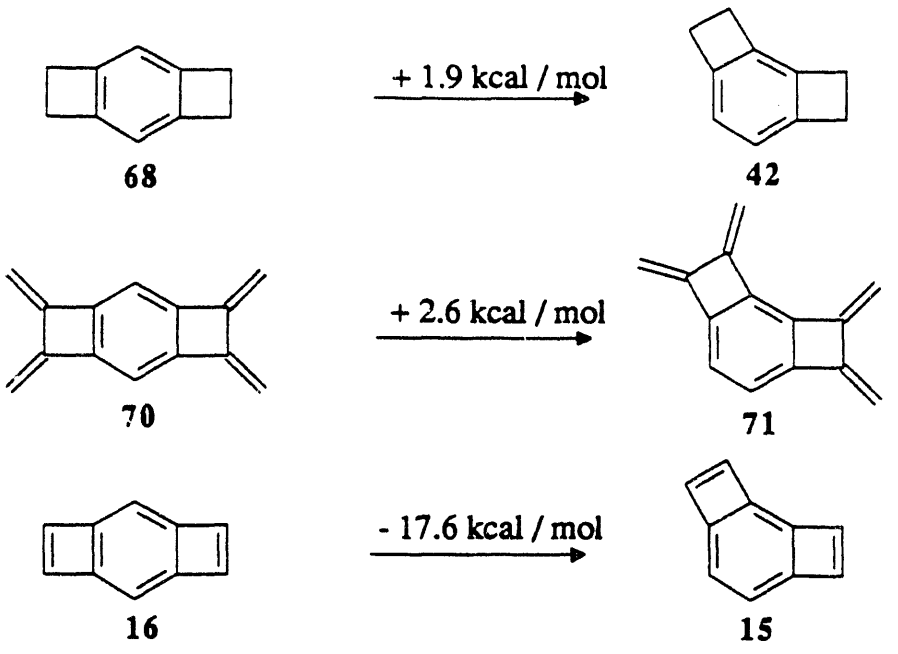

68 **42** **70** **71** **16** **15**

[a] Energies are calculated from data given in Table 4.1 (1 a.u. = 627.5 kcal mol^{-1}).

respectively, cyclobutadieno-fused **15** is stabilized by 17.6 kcal mol^{-1} relative to its linear isomer. The lower energy content of **15** clearly arises from its ability to avoid cyclobutadienoid resonance forms, the slight destabilization of **42** and **71** presumably originates from increased strain caused by angular fusion. In light of these findings, it is surprising that **74**[163], the only tricyclic benzodicyclobutadiene derivative known, is linearly fused.

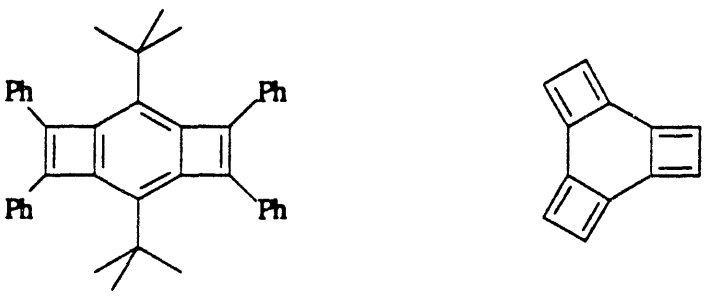

74 **10a**

It is noteworthy that NRT analysis of the cyclobutadieno-fused benzenes shows no evidence for contributions by resonance forms with a radialenic arrangement of double

bonds, as depicted in **10a**, lending support to conclusions derived from X-ray data of derivatives of **72**.[157] The ease with which metal fragments like CpCo and $Fe(CO)_3$ coordinate in an η^4 fashion to the cyclobutadiene moiety of **72** and **16**[164] therefore seems to derive from a π electronic distribution in accord with resonance structures A and/or B.

4.1.4 Delocalization and Hyperconjugation in Trisannelated Benzenes.

The above discussion geometries and hybridizations developed the concept that the σ skeleton of the benzene frame responds to imposed strain in a bond alternating fashion. In addition to such σ effects, four-membered ring fusion to the benzene nucleus also gives rise to hyperconjugative (**41**, **68**, **42**, and **8**) and conjugative (**69-72**, **9**, **10**, **15**, and **16**) interactions. The presence of hyperconjugation between the benzenoid π system and methylene group orbitals[165] (Figure 4.2) of appropriate symmetry (π_{CH}, π^*_{CH}) has been established by photoelectron spectroscopy.[96g,166]

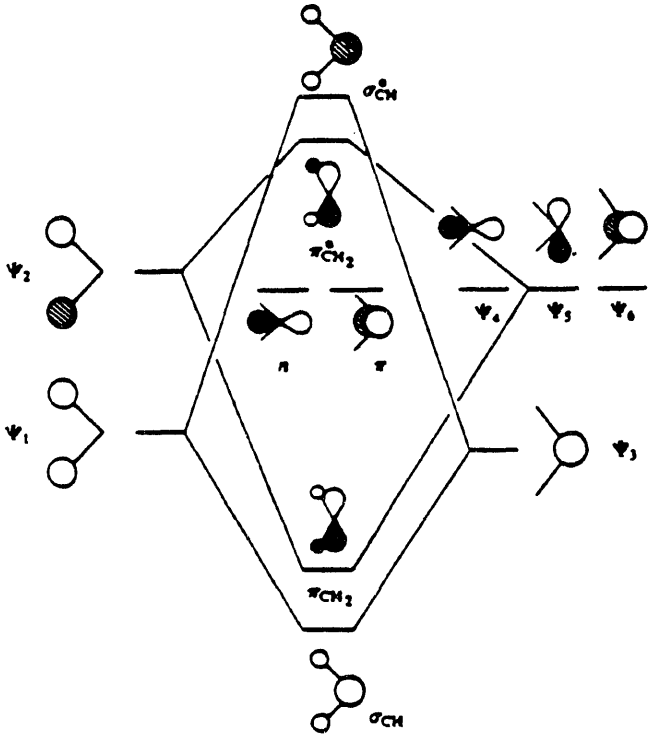

Figure 4.2 Construction of Group Orbitals of Methylene.[165b]

Similarly, in dimethylenecyclobuteno- and cyclobutadieno-fused benzenes, resonance form B is susceptible to antiaromatic interactions within the four-membered ring, thereby favoring the double bond arrangement of A. It thus appears that hyperconjugation, π delocalization, and σ effects do have an important influence on the geometry of the benzene nucleus, but quantification of each of these contributions remains speculative. The NBO method lends itself to an assessment of such conjugative effects by geometry reoptimization with suppression of selected interactions (cf. section 1.4). Because perturbation of the benzene nucleus by external groups is of main concern, all π type interactions between those and the benzenoid substructures were deleted, while maintaining "aromatic" π delocalization in the latter. For reasons of computational economy and because bond alternation is most pronounced in trisannelated benzenes, attention will be focused on **8**, **9**, and **10** (Table 4.5).

Table 4.5 Bond Lengths of Trisannelated Benzenes Reoptimized with Selected NBO Deletions.[a]

	8	**9**	**10**
NBO deletion[b]	π_{CH}-π^*; π-π^*_{CH}	π - π^*	π - π^*
R(1-2)	1.381 (-0.027)	1.377 (-0.047)	1.448 (-0.076)
R(1-6)	1.380 (+0.019)	1.385 (+0.026)	1.329 (+0.020)
R(1-7)	1.590 (+0.052)	1.570 (+0.072)	1.627 (+0.124)
R(7-8)	1.595 (-0.003)	1.514 (-0.017)	1.319 (-0.022)
R(7-9)		1.309 (±0)	
R(7-H)	1.077 (-0.004)		1.066 (±0)
Δ*R*	0.001 (-0.046)	0.007 (-0.058)	0.119 (-0.096)

([a]) SCF/3-21G values in Ångstroms. Bond length changes with respect to the fully optimized structures of Table 4.1 are listed in parentheses. For numbering scheme, see Figure 4.1. ([b]) For details regarding the type of deletion, see text.

Geometry reoptimization with deletion of pertinent π type interactions between the cyclobutene and the benzene moieties generally results in significantly reduced bond

alternation in the six-membered ring. In the absence of π_{CH}-π^*_{CC} and π_{CC}-π^*_{CH} interactions between the methylene groups and the benzene frame, **8** reoptimizes to a structure with essentially equal benzenoid carbon bond lengths, indicating that bond alternation in delocalized **8** is caused by hyperconjugation rather than angular strain. Likewise, when **9** is reoptimized with deletion of π delocalization between the exocyclic double bonds (i.e., C7-C9) and those of the benzene frame, ΔR diminishes to from 0.065 Å in the fully delocalized system to only 0.007 Å, demonstrating that π-π^* interaction is responsible for bond alternation in **9**. The residual ΔR (after reoptimization) is only marginally larger than that of **8**, suggesting that the increase of ring strain, going from the cyclobuteno-fused benzenes to the dimethylenecyclobuteno-annelated series, is minimal.

The importance of antiaromatic interactions in cyclobutadieno-fused **10** becomes apparent when π conjugation between the ethylenic double bonds and the central ring is deleted. In this case, reoptimization leads to a ΔR of 0.119 Å that is greatly diminished from that of the fully delocalized system (ΔR =0.215 Å). Therefore, the π delocalization of **10** (or its propensity to minimize antiaromaticity) contributes roughly half (56%) of the calculated bond alternation, the remainder being attributable to strain (rehybridization) effects.

In conclusion, NBO analysis of annelated benzenes reveals that perturbations of the σ frame (i.e., strain effects) are less severe than usually anticipated. The main sources of benzenoid bond alternation appear to be hyperconjugation and π delocalization within the fused ring systems, although strain induced changes in the hybridization are important in determining the geometry of highly strained **10**.

4.2. Chromium Tricarbonyl Complexation to Trisannelated Benzenes.

Extended Hückel calculations by Hoffmann et al.[23a] suggest increasing rotational barriers of the chromium tricarbonyl tripod complexed in an η^6 fashion to arenes with decreasing degrees of π delocalization. This expectation was experimentally fulfilled by

dynamic NMR studies of $Cr(CO)_3$ coordination to the central six-membered rings of angular [3]phenylene (**5**)[24] and derivatives of triangular [4]phenylene (**7**)[25,88] (cf. section 1.2.4). However, the measured barriers to rotation around the metal arene axes (8.2 kcal mol^{-1} for coordinated **5**, 11.5 kcal mol^{-1} for 2,3-bis(butoxycarbonyl)-substituted, coordinated **7**) are far lower than Hoffmann predicted for $Cr(CO)_3$ attached to localized benzene (19.4 kcal mol^{-1}).[23a]

Explanations for the incongruity between theory and experiment either point at substantial residual π delocalization in the phenylenes [a feature supported by ab initio investigations of distorted benzenes (chapter 2) and benzocyclobutenes (vide supra)] or at the inadequacy of the reference system in describing the observed dynamic behavior. Clearly, using benzenechromium tricarbonyl (**34**) as a model compound for $Cr(CO)_3$-coordinated phenylenes leaves unaddressed the geometric distortions of the benzene core arising from four-membered ring fusion.

To rectify this situation, calculations were performed at the ab initio level on complexes **34**, and **75-77**. A compromise between computational economy and accommodation of the complex bonding pattern of transition metal coordination compounds was achieved by using MIDI basis sets[167] on C, H, and O, and a chromium

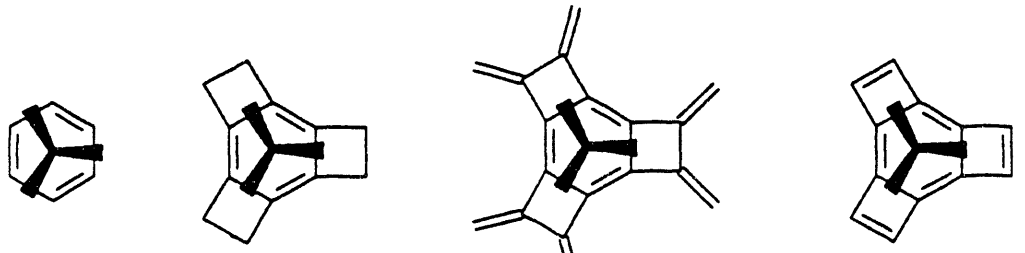

34 **75** **76** **77**

basis set [equal to [11s7p4d]/(5s3p2d)] developed by Williamson and Hall.[168] All geometries are fully optimized within C_{3v} symmetry constraints at the SCF level. Limited computational resources for these formidable calculations prohibited examinations of harmonic vibrational frequencies. Two conformations, referred to as "endo" and "exo",

are considered for each of the systems **75-77** (Figure 4.3). The one in which the carbonyls reside directly above the four-membered rings is labeled "endo", whereas the conformation with COs bisecting the non-annelated benzenoid bonds is denoted "exo".

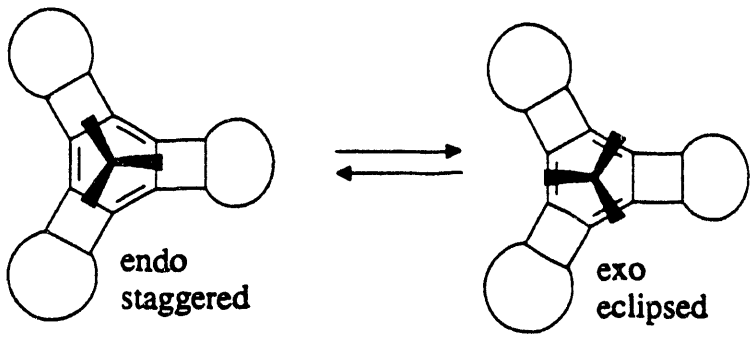

Figure 4.3 Conformations in Chromium Arene Complexes.

The terms "staggered" and "eclipsed" refer to the relative orientation of the $Cr(CO)_3$ tripod and the formal double bonds in the benzene substructure as depicted in Figure 4.3. Energetic differences between the endo/exo conformations correspond to rotational barriers around the metal arene axis. In addition, their sensitivity to the degree of delocalization can be assessed by NBO analysis of the computed wavefunctions.

4.2.1 Geometries of Chromium Arene Complexes.

In light of the large number of electrons, the multitude of electronic states, and the various modes of bonding available to late transition metals, computational treatment of systems involving chromium is notoriously difficult.[169] Due to the size of the calculations at ab initio levels, they have to be confined to moderately extended basis sets[168] that less accurately reproduce the geometries usually encountered in, for example, SCF/6-31G* optimizations of hydrocarbons.[48] However, structures of the chromium complexes agree reasonably well with available data[170] as can be seen from the corresponding values listed in Table 4.6.

Table 4.6 Energies and Selected Geometrical Parameters of Arenechromium Tricarbonyl Complexes.[a]

	34	75		76		77	
		endo	exo	endo	exo	endo	exo
energy	-1607.4011	-1836.5829	-1836.5800	-2062.3112	-2062.3112	-1832.9382	-1832.9174
R(1-2)	1.409	1.428	1.408	1.447	1.426	1.512	1.522
R(1-6)	1.389	1.368	1.368	1.364	1.383	1.326	1.318
R(1-7)		1.532	1.532	1.497	1.498	1.506	1.503
R(7-8)		1.600	1.600	1.519	1.521	1.344	1.346
R(7-9)				1.313	1.313		
$R_{(Cr\text{-}Bz)}$[b]	1.824	1.860	1.828	1.867	1.817	1.988	2.374
$R_{(Cr\text{-}CO)}$	1.871	1.850	1.856	1.871	1.879	1.859	1.842
R(C-O)	1.148	1.152	1.151	1.148	1.147	1.150	1.153

([a]) SCF values using MIDI on C, H, O, and a Williamson/Hall[168] basis set on Cr. Energies in a.u., bond lengths in Ångstroms. For numbering scheme, see Figure 4.1. ([b]) Distance of chromium to the center of the benzenoid six-membered ring.

The controversy over whether or not attachment of $Cr(CO)_3$ to benzene reduces the local symmetry of the latter from D_{6h} to D_{3h}[171,172] has been brought to an end by the low temperature X-ray study of **34**,[173] revealing regular bond alternation between 1.402 Å and 1.418 Å. This experimental finding is well reproduced by the present ab initio calculations that predict two distinct CC bond lengths of 1.389 Å and 1.409 Å. Applying bond length-bond order relationships[9c] to this (preferred) conformation allows its denomination as staggered.[174] Larger deviations from the crystal structure of **34** are found in the ligand-metal distances, particularly in that between chromium and the center of the benzene ring ($R_{Cr\text{-}Bz}$), whose value is overestimated by 0.1 Å in the calculations. The computed bond lengths involving the carbonyl groups are, with $R_{Cr\text{-}CO}$ = 1.871 Å and $R_{C\text{-}O}$ = 1.148 Å, in better agreement with data observed in the solid state ($R_{Cr\text{-}CO}$ = 1.842 Å; $R_{C\text{-}O}$ = 1.157 Å). Geometry optimizations of chromium attached to trisannelated benzenes (**75-77**) generally find endo orientations between tripod and arene to be the most

stable conformations, completely in line with results from structure determinations of **35**[87] and **36**[175] (Figure 4.4). NRT analysis of the uncomplexed hydrocarbons (section 4.1.3)

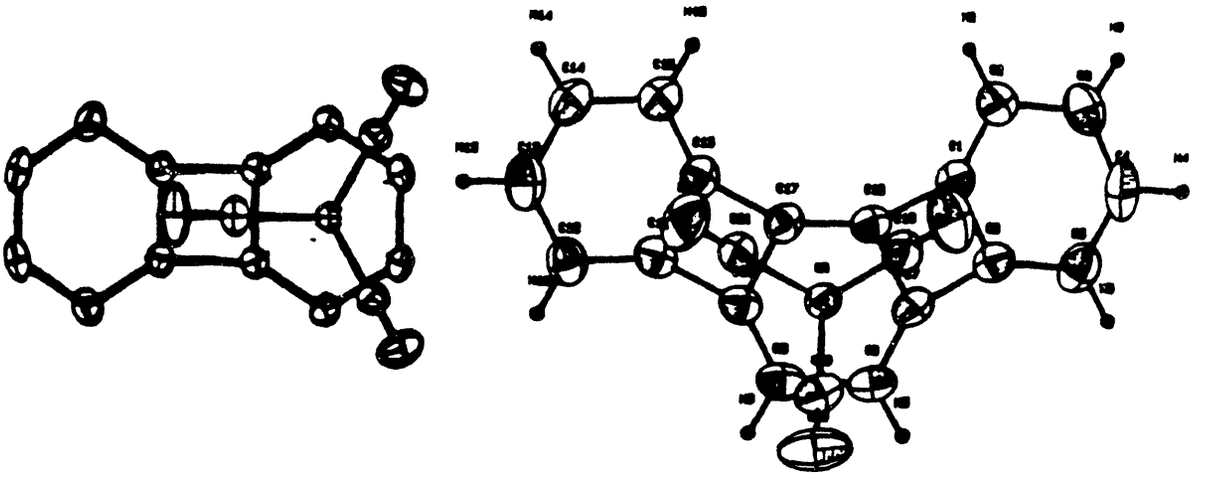

Figure 4.4 X-Ray Structures of Biphenylenechromium Tricarbonyl (**35**)[87] and Angular [3]Phenylenechromium Tricarbonyl (**36**).[175]

predicts dominant π electronic arrangements of benzenoid double bonds exocyclic with respect to the annelated four-membered rings. By analogy, molecular orbital considerations of **35**[87] rationalize the predicted endo-staggered conformation, revealing that the strongest binding interactions occur between regions of high electron density of the biphenylene ligand ($1\pi_a$, $2\pi_a$, $2\pi_s$) and empty 2e orbitals on $Cr(CO)_3$ that are staggered relative to the three carbonyls.

Comparison of chromium-arene distances in **75-77** with available experimental data[170] again shows the former values to be largely overestimated by the present ab initio calculations. Whereas X-ray derived values rarely exceed 1.76 Å, those computed for **75-77** range from 1.817 Å (exo **76**) to 2.374 Å (exo **77**). Interestingly, in the exo conformations of **75** and **76** the chromium nuclei lie closer to the hydrocarbon than in the endo orientations, despite the lower energy of the latter. Since short bonds are commonly

associated with strong binding interactions, the calculated equilibrium geometries of **75** and **76** suggest contributions from interfering factors, e.g. steric or electrostatic repulsions emanating from the four-membered rings. In case of cyclobutadieno-fused **77**, the metal center is extremely remote from the benzene core ($R_{Cr\text{-}Bz}$ of 1.988 Å and 2.374 Å for endo and exo conformers), implying only weak bonding between chromium and the more localized hydrocarbon. Apparently, the distance is large enough to override repulsive interactions, leading to a larger $R_{Cr\text{-}Bz}$ value than expected for the less stable exo form.

Inspection of Tables 4.6 and 4.7 reveals that the arenes generally experience elongation of benzenoid CC bond lengths upon complexation with $Cr(CO)_3$, a trend also observed for **35**[87] and **36**[175] with respect to **3**[86] and **5**,[21a] indicative of the depletion of electron density from the coordinated hydrocarbon. Geometric changes are more pronounced in the transformations of the uncomplexed benzenoids to the endo conformer, reflecting stronger interactions between metal center and organic ligand. Comparison of the geometries of uncomplexed arene and endo orientations of **75** and **76** shows that lengths of the long bonds ($R_{1\text{-}2}$) are increased by larger amounts (0.028 Å) than those of the short ones (e.g., 0.005 Å in **75**).

Table 4.7. CC Bond Lengths of Uncomplexed Arene Ligands.[a]

	34	**75**	**76**	**77**
R(1-2)	1.384 (+0.025)	1.400 (+0.028)	1.419(+0.028)	1.518 (-0.006)
R(1-6)	1.384 (+0.005)	1.363 (+0.005)	1.361 (+0.003)	1.311 (+0.015)
R(1-7)		1.533 (-0.001)	1.495 (+0.002)	1.500 (+0.006)
R(7-8)		1.602 (-0.002)	1.523 (-0.004)	1.348 (-0.004)
R(7-9)			1.314 (+0.001)	

([a]) SCF/MIDI values in Ångstroms. For numbering scheme, see Figure 4.1. Changes upon $Cr(CO)_3$ coordination with respect to the more stable endo conformers are given in parentheses.

The peculiar electronic properties of **77** are highlighted by the reversal of the trend delineated above for **75** and **76**. Thus, $R_{1\text{-}2}$ of the uncoordinated hydrocarbon suffers contraction by 0.006 Å, while bond distance $R_{1\text{-}6}$ is increased by 0.015 Å. As borne out by ab initio investigations of tricyclobutadienobenzene (**10**) in section 4.1, the molecule's features differ considerably from those of related benzocyclobutenes (e.g., **8** and **9**), foreshadowing the dissimilarities of the computed geometries of **75** , **76**, and **77**.

4.2.2 Barriers to Rotation Around the Metal Arene Axis.

Rotational barriers ΔE in compounds **75-77** are defined as energy differences between their respective exo and the more stable endo conformations (eq 4.2).

$$\Delta E = E_{exo} - E_{endo} \qquad (4.2)$$

To judge the sensitivity of this measure to delocalization in the π ligand, the barriers were reevaluated with all or some orbital interactions deleted from the SCF wavefunctions (cf. section 1.4).

Two types of delocalizations, referred to as internal (i) and external (e), contribute importantly in trisannelated benzenes. The former concerns π-π* interactions within the six-membered rings, while the latter focuses on departures from covalency between the benzenoid π system and orbitals of appropriate symmetry in the annelated rings. There are two ways to delete internal delocalization (i and i'), each corresponding to one of the Kekulé forms A and B (section 4.1.3), leading to staggered or eclipsed orientations between double bonds and carbonyls. Energy differences between localized and delocalized wavefunctions resulting from the former type of NBO deletions are labeled ΔE^{deloc}(i), while those of the latter are designated ΔE^{deloc}(i') (Table 4.8). The analysis of rotational barriers in **34**, and **75-77** is summarized in Table 4.9, whose values are related to the delocalization energies through eq 4.3, where ΔE is the rotation barrier for the fully

delocalized molecule and ΔE(x) that for the (x)-localized systems, with (x) corresponding to the type of NBO deletion.

$$\Delta E(x) = \Delta E^{deloc}_{exo}\ (x) - \Delta E^{deloc}_{endo}\ (x) + \Delta E \qquad (4.3)$$

Inspection of Table 4.8. shows that the energetic changes upon localizing the wavefunctions of **34**, and **75-77** are in full agreement with results from NRT analysis of the uncoordinated hydrocarbons (section 4.1.3). Generally, ΔE^{deloc}(i') is larger than ΔE^{deloc}(i), suggesting that localization of benzenoid π orbitals along CC bonds exocyclic with respect to the fused four-membered rings is energetically more favorable than in the opposite direction. The differences are larger in the endo conformations of **75** and **76** where (i) deletions create a staggered orientation of double bonds and carbonyls with stronger bonding interactions. Accordingly, energetic changes between (i) and (i') localizations are somewhat attenuated along the exo series, because orbital overlap between metal and arene is greater with ethylenic π systems along the site of fusion. Quite remarkable are the enormous energetic changes of **77** with respect to localization pattern (i'), reflecting the destabilizing, antiaromatic effect of cyclobutadienoid interactions. NBO deletions according to (i) result in far lower delocalization energies, regardless of $Cr(CO)_3$ orientation.

The fact that interactions between the benzenoid π system and the four-membered rings are sizable is demonstrated by the large ΔE^{deloc}(e) values, ranging from 62.9 kcal mol^{-1} in endo-**75** to 103.9 kcal mol^{-1} in exo-**77**. Not surprisingly, their magnitude suggests that hyperconjugation (in **75**) is less stabilizing than π-π* delocalization (as in **76**, **77**). Since "aromatic" conjugation within the benzene frame remains unaffected, ΔE^{deloc}(e) is essentially independent from conformations of the chromium tripod. Stereochemical aspects become more important when combinations of external and internal deletions (ei and ei') are applied. In analogy to (i, i') localizations, it is found that the value of

ΔE^{deloc}(ei) is smaller in the endo than in the exo forms, whereas that of ΔE^{deloc}(ei') suggests greater stabilization of the exo conformers of **75** and **76**.

Table 4.8 Delocalization Energies of Chromium Arene Complexes.[a]

	34	**75**		**76**		**77**	
		endo	exo	endo	exo	endo	exo
ΔE^{deloc}(i)	102.8	95.5	121.7	81.6	103.7	35.4	35.9
ΔE^{deloc}(i')	135.9	153.6	119.1	153.5	118.0	215.1	257.5
ΔE^{deloc}(e)		62.9	63.9	102.9	103.1	93.2	103.9
ΔE^{deloc}(ei)		158.46	186.7	190.6	216.8	155.2	172.0
ΔE^{deloc}(ei')		227.6	191.8	277.5	237.0	331.7	343.0

([a]) SCF values in kcal mol^{-1} using MIDI on C, H, O and a Williamson/Hall[168] basis set on Cr. Delocalization energies ΔE^{deloc} are calculated as E(x) - E for the respective conformations (x refering to the type of NBO deletion, see text).

Although by definition cyclobutadienoid interactions are not operational in **77**, its exo orientation still has a delocalization energy ΔE^{deloc}(ei') more than 10 kcal mol^{-1} larger than the alternative rotamer, indicative of unfavorable π orbital arrangement along the long ($R_{1\text{-}2}$ = 1.522 Å) annelated bonds.

The stereochemical preferences outlined above are borne out in the corresponding rotational barriers of **34**, and **75-77** listed in Table 4.9. Despite overestimating chromium-arene distances, the present ab initio calculations predict a negligibly small ΔE value of 0.3 kcal mol^{-1} for **34**, completely in line with extended Hückel and, more importantly, experimental results,[85] thereby lending support for the outcome of the energy evaluations. Similar to **34**, the rotational barriers of **75** and **76** are estimated to be below the threshold of detectability by dynamic NMR spectroscopy,[176] a finding that compares well with the corresponding value of 3.5 kcal mol^{-1} computed for benzocyclobutene (**41**).[87] Only the dynamic processes of **77** appear to be amenable to experimental scrutiny with a predicted ΔE of 13.0 kcal mol^{-1}. This result meets expectations derived from comparison with

coordinated phenylenes[24,25,88] which conveys that **77** should have a slightly larger rotational barrier because of enhanced σ strain and π delocalization effects (cf. section 4.1.2).

Table 4.9 Rotational Barriers in Chromium Arene Complexes.[a]

	34[b]	**75**	**76**	**77**
ΔE	0.3	1.6	0.0	13.0
ΔE(i)	33.1	27.8	22.1	13.6
ΔE(i')		-32.9	-35.5	55.5
ΔE(e)		2.6	0.2	23.7
ΔE(ei)		29.8	26.3	29.8
ΔE(ei')		-34.5	-40.5	24.3

([a]) SCF values in kcal mol^{-1} using MIDI on C, H, O, and a Williamson/Hall[168] basis set on Cr. Rotational barriers ΔE are calculated as E_{exo} - E_{endo} (except for **34**). For details regarding the type of localization (e, i, or i'), see text. ([b]) ΔE calculated as the energy difference between the staggered conformation and that in which the COs eclipse the benzene carbons.[174] ΔE(i) = E(i') - E(i).

Deletion of aromatic interactions in the benzene units leads to greatly increased rotational barriers. In case of **34**, ΔE(i) amounts to 33.1 kcal mol^{-1}, clearly larger than Hoffmann's value[23a] of 19.4 kcal mol^{-1}. Along the series **75-77**, ΔE (i) declines from 27.8 kcal mol^{-1} in **75** to 13.6 kcal mol^{-1} in **77**, the latter value seemingly unaffected by the localization procedure. Imposing a benzenoid double bond arrangement in the opposite sense leads to "antibarriers" in **75** [ΔE(i') = -32.9 kcal mol^{-1}] and **76** [ΔE(i') = -35.5 kcal mol^{-1}], reflecting the greater stabilities of their respective exo conformers. Antiaromatic substructures in the corresponding Kekulé forms of **77** result in a huge ΔE(i') of 55.5 kcal mol^{-1}, because of the molecule's pronounced endo preference.

Marginal increases of the ΔE(e) values for **75** and **76** (and a relatively moderate one in case of **77**) with respect to ΔE suggest that suppression of delocalization between cyclobutene and benzenoid parts of the molecules leaves the rotational barriers essentially

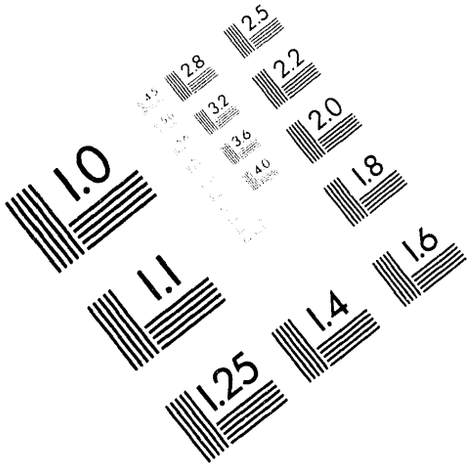

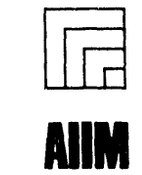

Association for Information and Image Management

1100 Wayne Avenue, Suite 1100
Silver Spring, Maryland 20910

301/587-8202

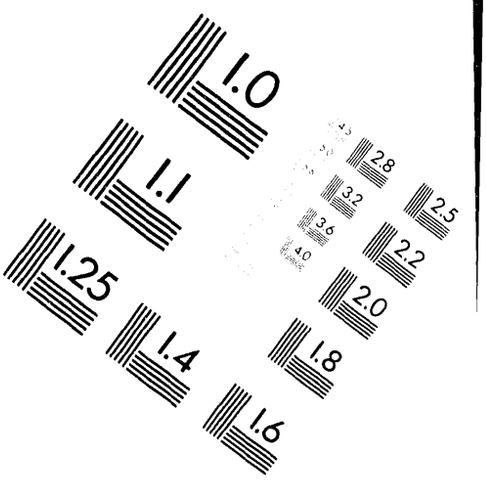

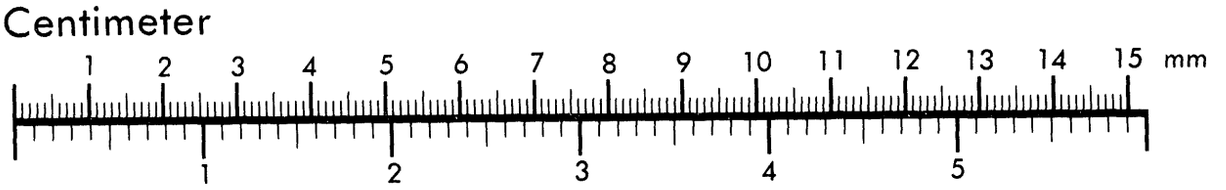

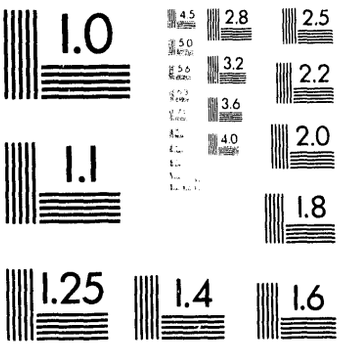

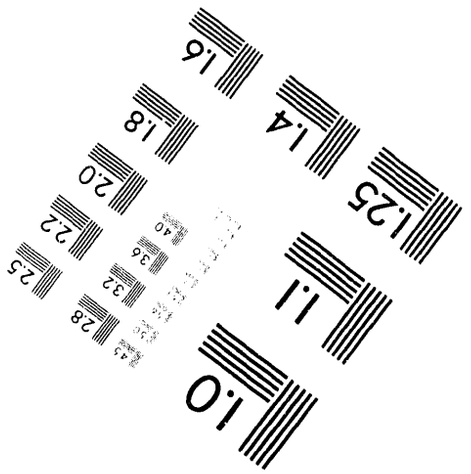

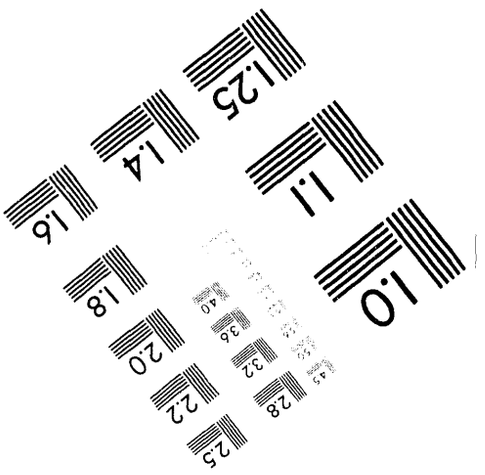

2 of 2

unaffected. When the systems are localized externally as well as internally, differences between the π ligands vanish almost entirely, leading to ΔE(ei) values between 26.3 kcal mol^{-1} (**76**) and 29.8 kcal mol^{-1} (**75**, **77**). These data deviate only slightly from ΔE(i) of **34** (33.1 kcal mol^{-1}), suggesting that structural deformations of the benzene nucleus play only a minor role in the dynamic behavior of the $Cr(CO)_3$ tripod. Comparing the numbers of ΔE(ei) with the experimentally determined ones for the triangular [4]phenylene derivatives (e.g., 11.5 kcal mol^{-1} for **37**) clearly establishes the presence of extensive delocalization in the latter, despite their topologically cyclohexatrienoid benzene frames. Again, imposing alternative double bond arrangements in the arenes (ei') leads to "antibarriers" in **75** (ΔE(ei') = -34.5 kcal mol^{-1}) and **76** (ΔE(ei') = -40.5 kcal mol^{-1}), and to a (positive) rotational barrier in **77** (ΔE(ei') = 24.3 kcal mol^{-1}).

Ab initio evaluations of the energies associated with the dynamic properties of **34** and **75-77** nicely reproduce the experimental observations made on the phenylene systems. Rotational barriers in the latter appear to be dominated by sizable delocalization effects rather than by geometric deformations within their respective benzene nuclei.

Chapter Five

Non-Planar Polycyclic Aromatic Hydrocarbons

5.1 Introduction.

The excitement generated by the investigation of the now readily available buckminsterfullerene (11)[28,177] has sparked interest in the construction of non-planar, polycyclic, aromatic hydrocarbons that constitute cross-sections of soccerball C_{60}. These bowl-shaped molecules could serve as a reference with which to model some of the fullerene's physical and chemical properties, such as aromatic behavior, strain effects, and endohedral[178] complexation.

11

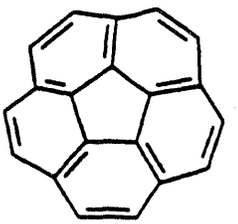

12

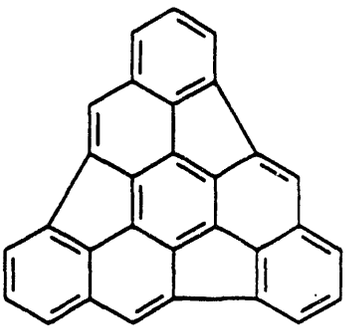

13

Deviation from planarity in spherical carbon clusters is achieved by the introduction of pentagons into the atomic assembly. Fusion of each five-membered ring to only benzene nuclei rather than to a second cyclopentadienyl provides for maximum thermodynamic stability in the fullerenes. The structural prototype for this connectivity pattern is corannulene (12),[29,30] whose cup-shaped topology was confirmed X-ray crystallographically.[31] Another example of cyclopentadienyl-induced departure from planarity can be envisaged in the molecular framework of triindeno-[4,3,3a,2,1-*cdef*:4',3',3a',2',1'-*ijkl*:4'',3'',3a'',2'',1''-*opqr*]triphenylene (13), whose bowl-shape should be enforced by virtue of the three five-membered rings. McKee and Herndon[179]

proposed the carbon skeleton of **13** as a suitable precursor for a rational synthesis of C_{60}, since dimerization of appropriately oriented molecules of **13** (molecular formula $C_{30}H_{12}$) would result in a compound with the correct number and arrangement of carbon atoms. Because of the anticipated unusual structural (and hence electronic) features and its promise as a building block for the fullerenes, the properties of **13** were investigated by means of semiempirical MO calculations, and synthetic entries to its carbon framework were sought. The results of both of these efforts are described in the following sections.

5.2 Semiempirical Calculations.

Geometry optimization of **13** (C_3-symmetry constraint imposed) using the MNDO parameter set[141] clearly predicts the cup-shaped topology to be a minimum on the $C_{30}H_{12}$ potential energy surface (Figure 5.1), with deviation from planarity of 39°. This clearly surmounts the degree of non-planarity in corannulene (26.8°)[31] and is close to the value found for C_{60} (31°)[67a]. The planar C_{3h} structure of **13** is estimated to be 77.3 kcal mol^{-1}

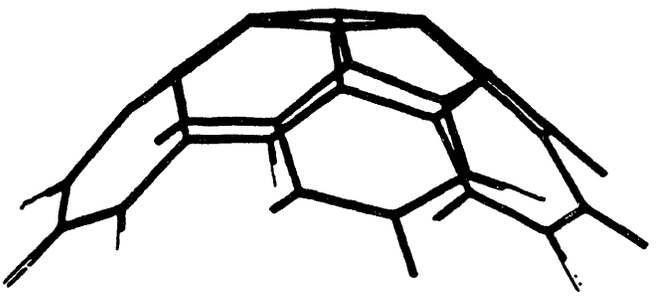

Figure 5.1 MNDO Optimized Geometry of **13**.

higher in energy than the equilibrium C_3 geometry (Table 5.1), thereby essentially excluding bowl-inversion along this pathway. In fact, frequency analysis of the C_{3h} conformation disclosed three negative eigenvalues, characteristic for a saddle point of higher order. Interestingly, the corresponding process for corannulene was experimentally

determined[180] to have an activation energy of only 10.2 kcal mol^{-1} and is believed to proceed through a planar transition state.[29b] This finding, well reproduced computationally at various levels of theory,[29b,181] suggests that it is the larger degree of pyramidalization[182] of central ring carbons in **13** that enforces its superior rigidity relative to **12**.

Table 5.1 Energies and Selected Bond Lengths of Hydrocarbons **13** and **78**.[a]

	13 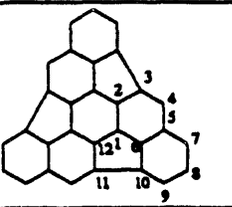	**78**[b]
ΔH_f°	252.5[c]	344.6[d]
R(1-2)	1.385 [-0.027/0.001]	1.411 [-0.043/-0.015]
R(1-6)	1.430 [-0.027/-0.004]	1.432 [-0.043/-0.027]
R(1-12)	1.452 [-0.027/0.001]	1.478 [-0.043/-0.015]
R(2-3)	1.470 [0.001/-0.003]	1.470 [-0.015/-0.021]
R(3-4)	1.395 [-0.003/0.021]	1.400 [-0.021/0.060]
R(4-5)	1.467 [0.021/-0.040]	1.462 [0.060/-0.027]
R(5-6)	1.414 [-0.040/-0.004]	1.417 [-0.027/-0.027]
R(5-7)	1.442 [-0.040/-0.022]	1.443 [-0.027/-0.010]
R(6-10)	1.466 [-0.004/-0.024]	1.464 [-0.027/-0.044]
R(7-8)	1.392 [-0.022/-0.078]	1.392 [-0.010/-0.052]
R(8-9)	1.442 [-0.078/-0.009]	1.443 [-0.0052/0.029]
R(9-10)	1.383 [-0.009/-0.024]	1.385 [0.029/-0.044]
R(10-11)	1.505 [-0.024/-0.003]	1.502 [-0.044/-0.021]
R(Li-Bz)[e]		1.827[f] [0.507]

([a]) MNDO values (C_3-symmetry constraint imposed. Heats of formation in kcal mol^{-1}, bond lengths *R*(A-B) in Ångstroms, atomic charges [A/B] in electron-units. Cf. CC bond length in D_{6h}-benzene (MNDO): 1.407 Å [-0.059 e]. For reasons of clarity, the numbering scheme deviates from IUPAC recommendations. ([b]) Convex coordination of Li^+ to **13**. ([c]) ΔH_f° of C_{3h} conformation: 329.8 kcal mol^{-1}. ([d]) ΔH_f° of concave isomer: 389.3 kcal mol^{-1}. ([e]) Distance between Li and midpoint of the central benzene ring. ([f]) Corresponding value of concave isomer: 2.048 Å.

Inspection of CC bond lengths of **13** (Table 5.1) reveals that its strained carbon framework can be expected to exhibit bond alternation in the central benzenoid ring, with bonds calculated to be elongated along the side of five-membered ring fusion and contracted adjacent to it. Thus, $R_{1\text{-}2}$ (1.385 Å) is computed to be 0.067 Å shorter than $R_{1\text{-}12}$ (1.452 Å), which compares to a MNDO value for unperturbed benzene of 1.407 Å, intermediate between the former two. Similar patterns have been observed in (or are predicted for) other small-ring annelated benzenes (cf. sections 1.3.1 and 4.1.2), and are also present in the polybenzenoid hydrocarbons triphenylene[183] (bond lengths of 1.411 Å and 1.470 Å in the central benzene ring), C_{60}[67b] (1.388 Å and 1.432 Å), and corannulene[31] (CC distance along six-six juncture: 1.391 Å; along six-five juncture: 1.413 Å). Thus, the extent to which bond alternation is predicted to occur in **13** significantly exceeds the values observed in related compounds, and although MNDO calculations tend to slightly overestimate aromatic internuclear distances, they are a potential source for novel, strain-driven chemistry (cf. chapter 3 and ref 67).

The longest bonding internuclear distance is that between carbon centers 10 and 11 (and symmetry-equivalent positions), whose computed value of 1.505 Å implies mainly single bond character and hence only marginal transmission of π electron density along this path. Whereas the relatively long value for $R_{2\text{-}3}$ (1.470 Å) renders neutral Kekulé structures with a radialenic double bond arrangement as in *B* (Figure 5.2) unlikely,

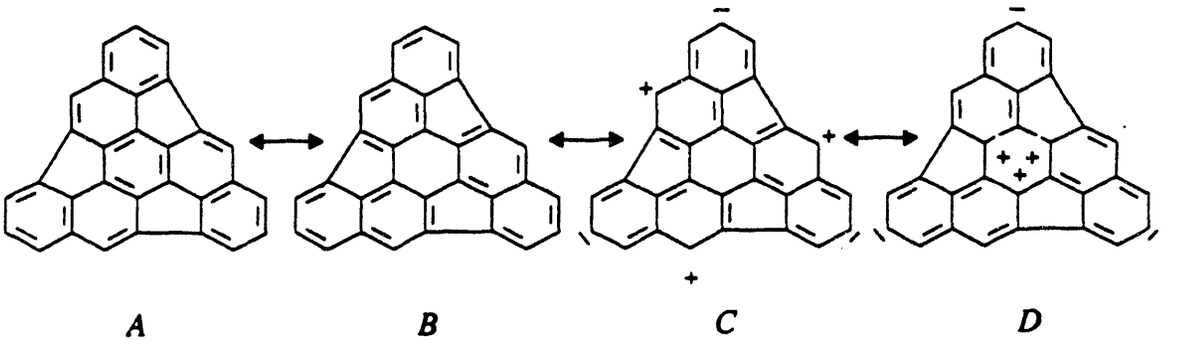

A *B* *C* *D*

Figure 5.2 Selected Resonance Structures of **13**.

examination of the atomic charge distribution of the carbon skeleton of **13** (Table 5.1) indicates that multipolar resonance forms like *C* and *D* might contribute importantly to its overall electronic description. For example, the large negative charge on C8 (-0.078 e) in conjunction with positive carbon center 4 (0.021 e) clearly point at a π electronic distribution in accord with resonance structure *C*. Alternatively, tripolar forms like *D* are less likely because of charge concentration in the central benzene ring, a conclusion supported by the value of $R_{2\text{-}3}$ (vide supra) and an almost electroneutral carbon center 2.

The hemispherical geometry of **13** offers two topologically different coordination sites and thereby provides the opportunity to mimic exo-[67] and endohedral[184] metal complexes of C_{60}. Of the possible symmetry-unique locations for ligand attachment, only those along the molecule's C_3 axis were examined computationally by coordinating Li^+ to **13** (Table 5.1). Surprisingly, it was found that complexation from the outside of the bowl as in **78** (Figure 5.3) is favored by 44.7 kcal mol^{-1} over the alternative concave arrangement,

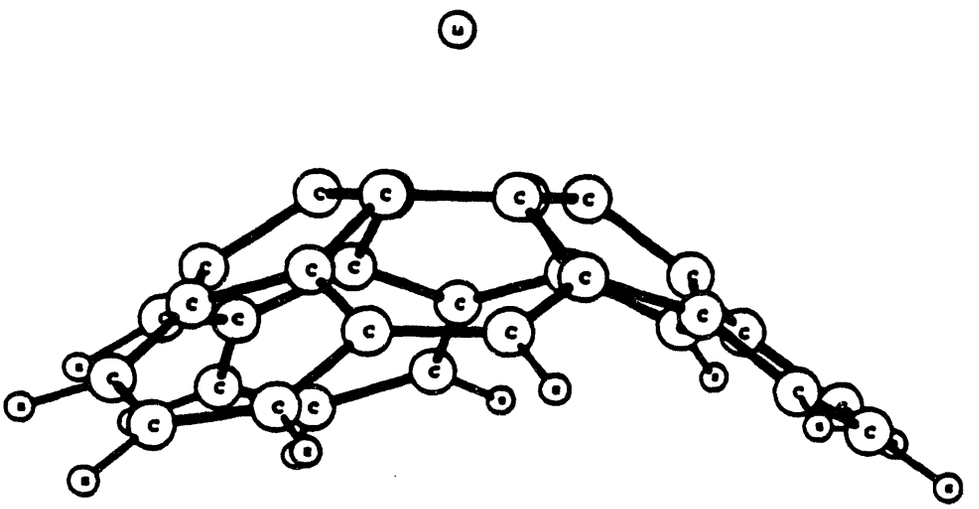

Figure 5.3 Convex Isomer of **78**.

in which the metal resides inside the hemisphere. Since the interaction between Li^+ and **13** is purely electrostatic, this result implies that the electron density is greater on the outside

of the bowl than on the inside. Preferential convex coordination can thus be explained by pyramidalization (or rehybridization) of central ring carbons in a fashion that increases the spatial extensions of the p-type atomic orbitals on the outside of the bowl. This phenomenon has its aliphatic analogon in alkenes of facial differentiality such as norbornene, where exo attack by electrophiles is favored over endo addition.[185] Along these lines, weak bonding between Li^+ and **13** in the concave configuration is revealed by the long distance between the metal and the midpoint of the central benzene ring ($R_{Li\text{-}Bz}$: 2.048 Å). In the more stable convex coordination of **78** Li^+ is located only 1.827 Å away from the arene, indicative of stronger binding interactions. Under the imposed symmetry constraints, the geometric changes upon metal complexation are largest for carbon centers 1,2, and 12, where depletion of electron density causes an increase in their respective bond lengths. Concurrently, the atoms accumulate more negative charge relative to **13** to counterbalance the cationic character of the metal, which retains the equivalent of half an electron in the complex. Structural effects at locations more remote from the coordination site are only minor.

Interestingly, a similar preferred lithium complexation pattern has been observed in tetralithiated corannulene,[186] in which case calculations support spectroscopic evidence for four Li cations attached to the convex side of the bowl. Thus, synthesis of a metal fragment coordinated to cup-shaped hydrocarbons in a concave fashion appears to be a formidable task.

5.3 Synthetic Approaches to Triindenotriphenylene.

It is evident from the discussion above that **13** holds great promise for a fascinating chemistry, and hence its synthetic accessibility was explored. Retrosynthetic analysis readily points at tribenzo[*c,i,o*]triphenylene (**79**)[187] as a suitable starting point, since threefold oxidative CC bond formation[188] along its periphery would directly provide **13**. Alternatively, the target molecule can be envisaged to be derived from 1,3,5-tris(2'-

ethynylphenyl)benzene (**80**), where triple [4+2] cycloaddition between alkyne moieties and biphenyl substructures should generate the required carbon connectivities of the framework of **13**. Results obtained from pursuing both pathways are presented below.

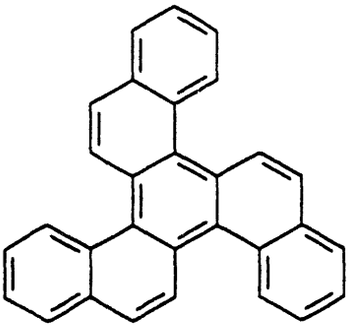

79

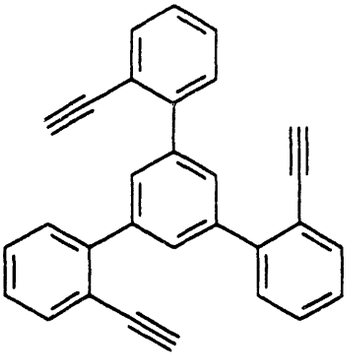

80

5.3.1 Tribenzo[*c,i,o*]triphenylene Route to Triindenotriphenylene.

Synthesis of tribenzo[*c,i,o*]triphenylene, as outlined in Scheme 5.1, followed a modification of the original procedure by Laarhoven and van Broekhoven.[189] Thus, methyl ester **81** was generated in moderate yield by Perkin-condensation[190] of 1-naphthyl-acetic acid with 2-naphthaldehyde followed by esterification with methanol. Photo-cyclization of **81** furnished benzochrysene-derivative **82**, which was subsequently transformed to aldehyde **83** via a $LiAlH_4$-reduction, Swern-oxidation[191] sequence. Attempts to reduce **82** directly to **83** with diisobutylaluminum hydride[192] at low temperatures were unsuccessful, resulting in a mixture of the corresponding benzylic alcohol and starting material. Employing Wittig methodology,[193] **83** was converted to stilbene **84** which then was photocyclized according to Katz et al.[194] to furnish **79** in 40%. This relatively low yield in the last step is caused by competing photoreactions of **84** to form a side product, which Laarhoven[187] assumed to be 12-phenylnaphtho[2,1-*b*]pyrene (**85**). This impurity was present to variable amounts (typically between 20% and 50% of the converted material) and had to be separated from **79** by multiple column

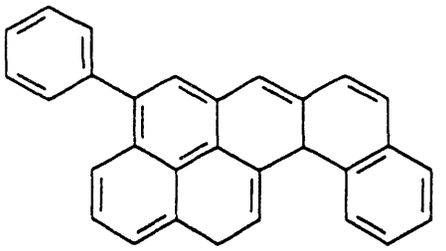

85

chromatography and HPLC. The identity of **79** was established by comparison of its spectral data with those reported.[187] Most notable are the characteristic chemical shifts of

Scheme 5.1[a]

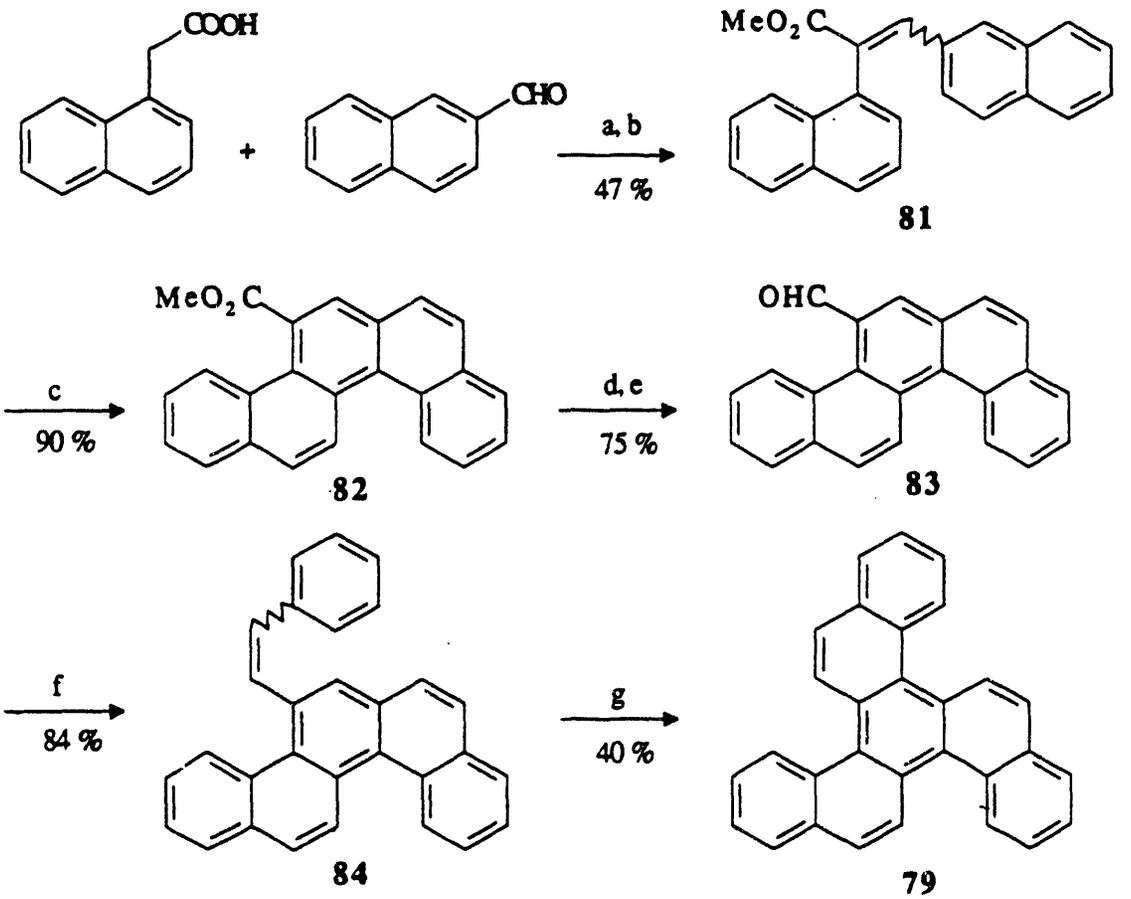

[a] (a) Acetic anhydride, Et_3N; 150° C; 12h. (b) MeOH, toluene, H_2SO_4, cat.; Δ; 24h. (c) h ν (300 nm), C_6H_{12}, I_2, cat.; r.t.; 70h. (d) $LiAlH_4$, THF; 0° C; 60 min. (e) $(COCl)_2$, Me_2SO, CH_2Cl_2; -78° C; 30 min. (f) $[PhCH_2PPh_3]^+Br^-$, BuLi, THF; Δ; 60 min. (g) hν (350 nm), C_6H_6, propylene oxide, I_2; 10° C; 10h.

hydrogens connected to C4 and C5 (and symmetry-equivalent positions), which are projected toward the bay regions of the molecule and hence exhibit low field absorptions of δ 8.96 ppm and δ 8.93 ppm that are split into sets of doublets (or pseudo-doublets).

With tribenzo[*c*,*i*,*o*]triphenylene at hand, its reactivity under various cyclodehydrogenation conditions was investigated (Table 5.2). Initial attempts aimed at introducing three five-membered rings into the carbon framework of **79** were encouraged by findings of Studt and Win,[188e] who transformed benzo[*c*]phenanthrene (**86**) to benzo[*g*,*h*,*i*]fluoranthene (**87**) by simply pyrolysing the former in the presence of a platinum-catalyst on carbon support (Scheme 5.2).

Scheme 5.2

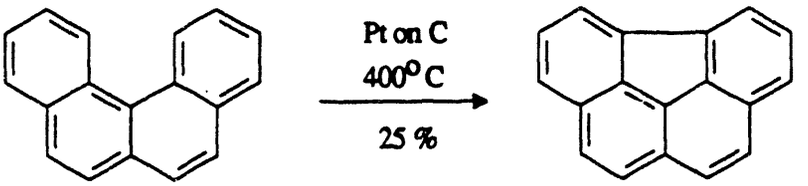

86 **87**

It was hoped that analogous treatment of **79** would generate desired hydrocarbon **13**, possibly in a stepwise process as delineated in Scheme 5.3. However, exposure of **79** to

Scheme 5.3

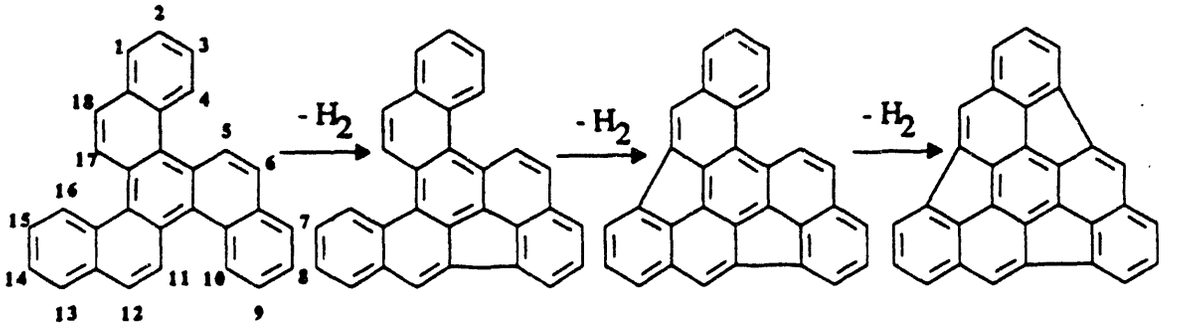

79 **88** **89** **13**

reaction conditions employed by Studt and Win resulted only in the isolation of doubly dehydrogenated product **88** in 25% yield, while some evidence for tetradehydrogenated **89** indicate its presence in only trace amounts. None of hexadehydrogenated **13** was detectable in the reaction mixture. Similar product distributions were obtained in attempts to convert **79** to **13** by means of Lewis acid mediated, intramolecular Scholl-coupling reactions[188a] involving $AlCl_3$ and $CuCl_2$ in refluxing CS_2. In the absence of oxidizing copper salts, no conversion of **79** to tractable cyclodehydrogenation products was observed. Likewise, flash vacuum pyrolysis of **79** (up to 800 °C) led to essentially quantitative recovery of starting material, thereby demonstrating its thermal stability.

Table 5.2 Results of Cyclodehydrogenation Experiments of **79**.[a]

	79[b]	**88**	**89**	**13**
Pt on C 400° C; 60 min sealed tube	13%	25%	trace	-
FVP[c] 800° C; 0.05 torr	95%	-	-	-
$AlCl_3$/NaCl eutectic mix 110° C; 2h	72%	-	-	-
$AlCl_3/CuCl_2$ CS_2; Δ; 10h	35%	28%	trace	-

([a]) Percentages are isolated yields. ([b]) Recovered starting material. ([c]) Flash vacuum pyrolysis.

Symmetry reduction from C_3 (**79**) to C_1 (**88**, **89**) in the course of the cyclodehydrogenation, together with only minute amounts of the material obtained,

prevented rigorous structural characterization of the latter two compounds. The assumption of a single five-membered ring in **88** is backed by its ^{1}H NMR spectrum, most notably by a prominent singlet at δ 8.49 ppm that can be attributed to an isolated hydrogen adjacent to the newly formed ring juncture. ^{1}H NMR data for **89** revealed only two complex multiplets of equal integration centered around 7.72 and 7.55 ppm. Further spectroscopic support for the structural assignments of **89** and **89** was assembled as follows: (i) High resolution mass spectroscopy established $C_{30}H_{16}$ (**88**) and $C_{30}H_{14}$ (**89**) as the molecular formulae; (ii) the low resolution mass spectra of **88** and **89** (Figure 5.4) reveal no appreciable fragmentation under the ionization conditions, a behavior in accord with other polycyclic aromatic hydrocarbons;[195] (iii) UV spectra of compounds **79**, **88**, and **89** (Figure 5.5) exhibit a bathochromic trend of λ_{max} from 404 nm (log ε: 3.19) in **79**, over 414 nm (log ε: 3.24) in **88**, to 462 nm (log ε: 1.84) in **89**, a trend consistent with increasing ring strain along the series.[96g,196] Furthermore, the dramatic decline in the logarithms of the extinction coefficients from **88** to **89** can be interpreted as evidence for a significant deviation from planarity[197] in the latter, a conclusion strongly supported by computational geometry optimizations of the two molecules (vide infra, Figure 5.6).

Although single and double cyclodehydrogenation of **79** can be confidently postulated in light of the arguments presented above, it should be noted that skeletal rearrangements in the course of Lewis acid catalyzed reactions of this type are known.[198]

To provide a rationalization for the unexpected difficulties in achieving the third and crucial ring closure, **79** and its dehydrogenation products were subjected to computational scrutiny employing the MNDO parameter set (Figure 5.6, Table 5.3). Geometry optimization of **79** leads to a propeller-like (chiral) conformation in the gas phase at 0 K. At room temperature, however, the molecule's equilibrating mobility is large, as evidenced by its simple ^{1}H NMR spectrum and as further corroborated by dynamic NMR studies of its smaller relative, benzo[*c*]phenanthrene (**86**).[199] Incorporation

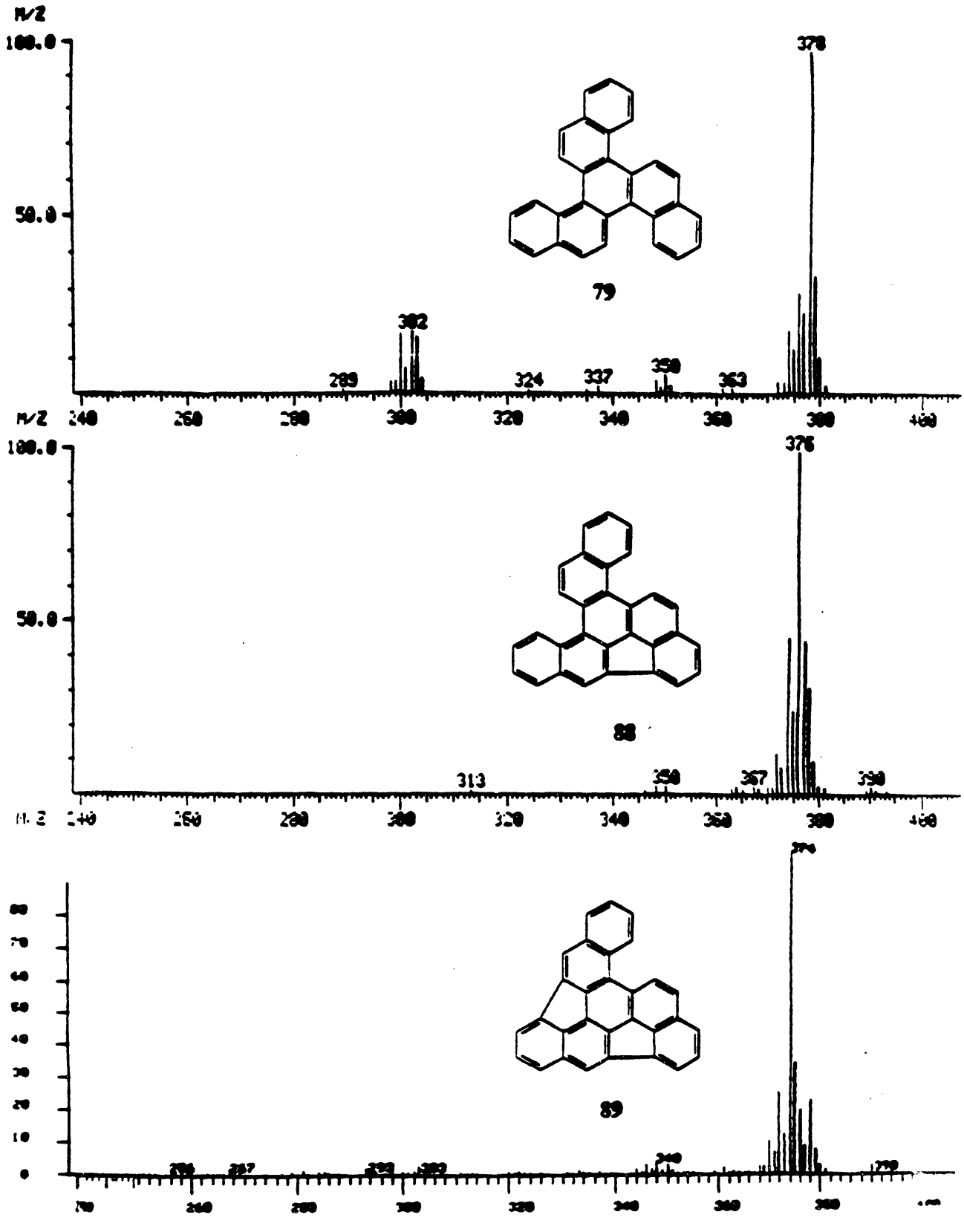

Figure 5.4 Mass Spectra of 79 and its Cyclodehydrogenation Products.

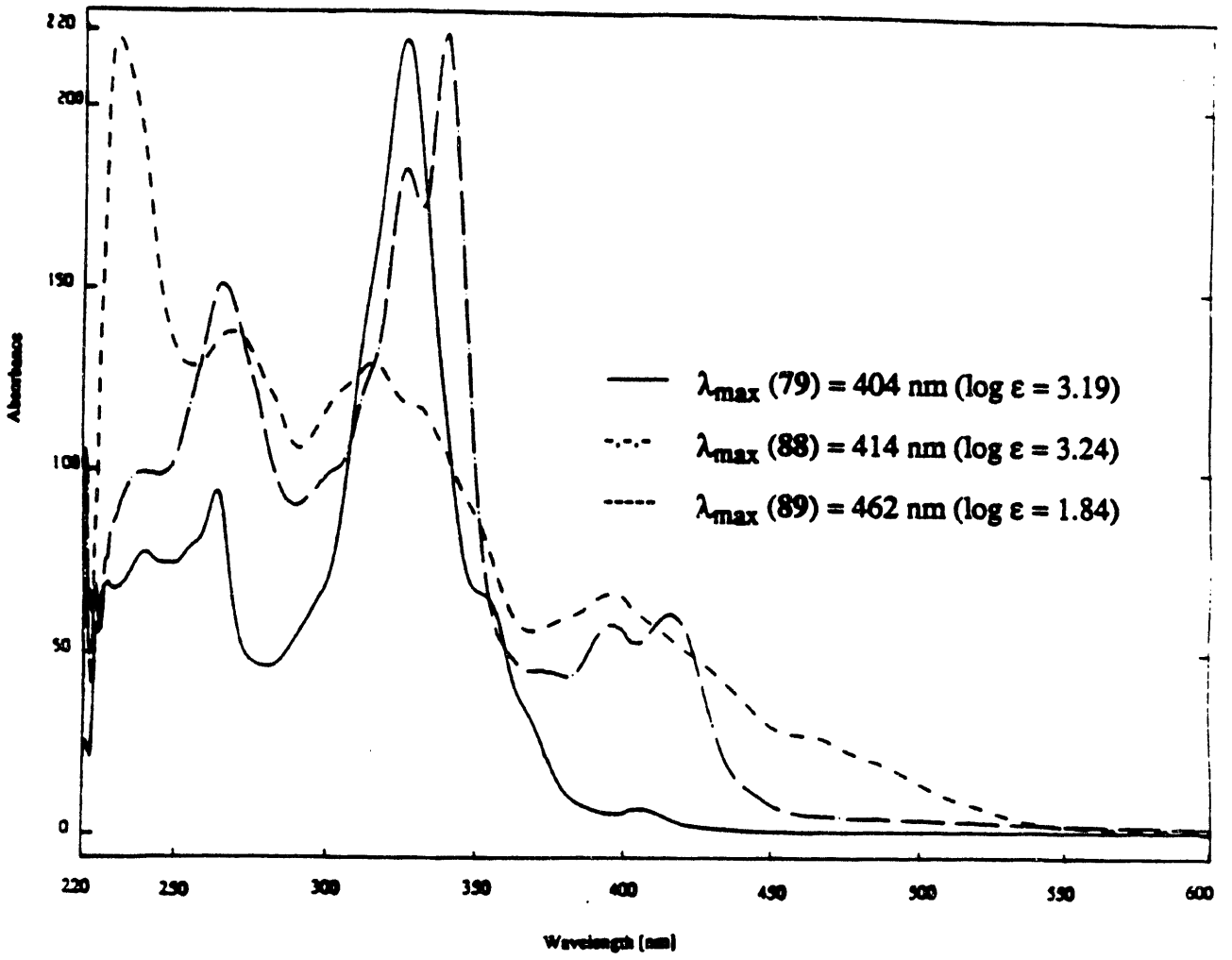

Figure 5.5 UV Absorption Spectra of **79** (——), **88** (-·-·-), and **89** (---) in Hexanes.

of one five-membered ring into the framework of **79** forces large regions of the carbon skeleton of **88** to adopt a planar orientation. Only with the second cyclodehydrogenation step, leading to **89**, the molecule is locked into a non-planar conformation. These theoretically predicted geometric changes on successive ring closure are paralleled in the respective UV spectra of **79**, **88**, and **89** (vide supra, Figure 5.5).

Table 5.3 Energies and Selected Internuclear Distances of **79** and its Cyclodehydrogenation Products.[a]

	79[b]	**88**	**89**	**13**[b]
ΔH_f°	155.1	155.5	194.1	252.5
R(4-5)	3.060	1.491	1.501	1.502
R(10-11)	3.060	3.257	1.506	1.502
R(16-17)	3.060	3.252	3.470	1.502

([a]) MNDO values. Energies in kcal mol^{-1}, internuclear distances in Ångstroms. For numbering scheme, based on **79**, see Scheme 5.3. ([b]) C_3-symmetry constraint imposed.

Thermodynamically, the reaction sequence leading from **79** to **13** is feasible, the driving force being the stepwise release of dihydrogen. Not unexpectedly, the third ring closure from **89** to **13**, which brings the out-of-plane distortion of the carbon framework to completion, is energetically the most demanding. Of major significance for the outcome of the cyclodehydrogenation experiments with **79** are changes in the non-bonding distances of remaining bay region carbon centers while connecting a pair in a different region of the molecule. Thus, ring closure of **79** along C4 and C5 leads to **88**, where carbons 10, 11, and 16, 17 are spread by more than 3.25 Å, an increase of almost 0.2 Å with respect to **79**. This effect becomes even more dramatic with introduction of the second five-membered ring, which enforces a non-bonded distance between the remaining unconnected carbon centers 16 and 17 of 3.470 Å, thereby presumably preventing the third CC bond formation.

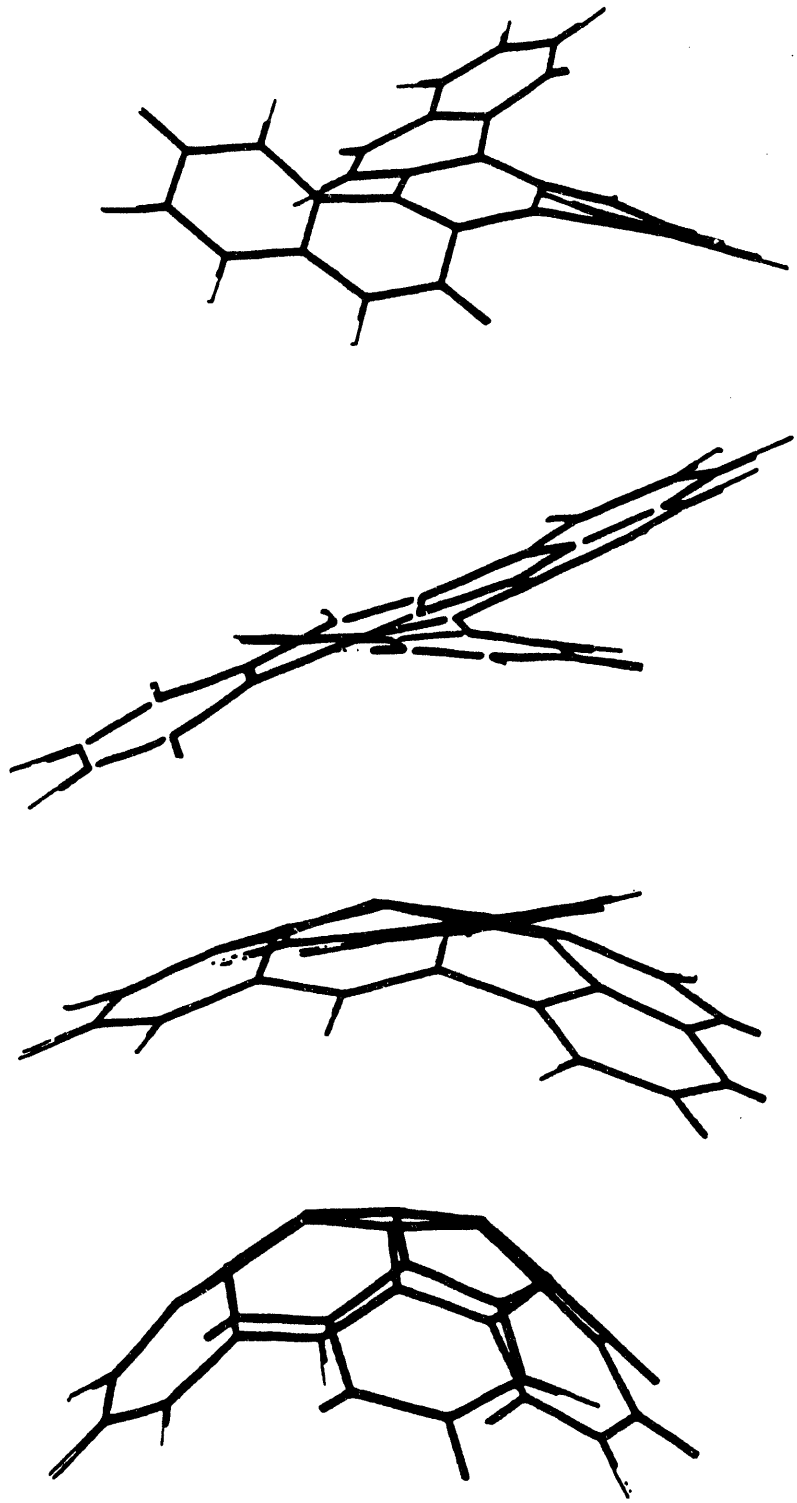

Figure 5.6 MNDO Optimized Geometries of **79**, **88**, **89**, and **13** (Top to Bottom).

Clearly, either functionalization of the bay regions of **79** or a precursor with greater structural flexibility is warranted for the successful synthesis of **13**. An example for the latter type of approach is described in the following.

5.3.2 1,3,5-Tris(2'-ethynylphenyl)benzene Route to Triindenotriphenylene.

Threefold intramolecular [4+2] cycloaddition between the alkyne and biphenylene moieties of **80** provides a conceptual alternative in the construction of the carbon framework of **13**. Given the reluctance of both, unactivated CC triple bonds to serve as dienophiles and biphenylenes to react as dienes in thermally induced Diels-Alder reactions, attempts to materialize Scheme 5.4 constitute a rather daring effort, although some conversions of this type are known.[189,200]

Scheme 5.4

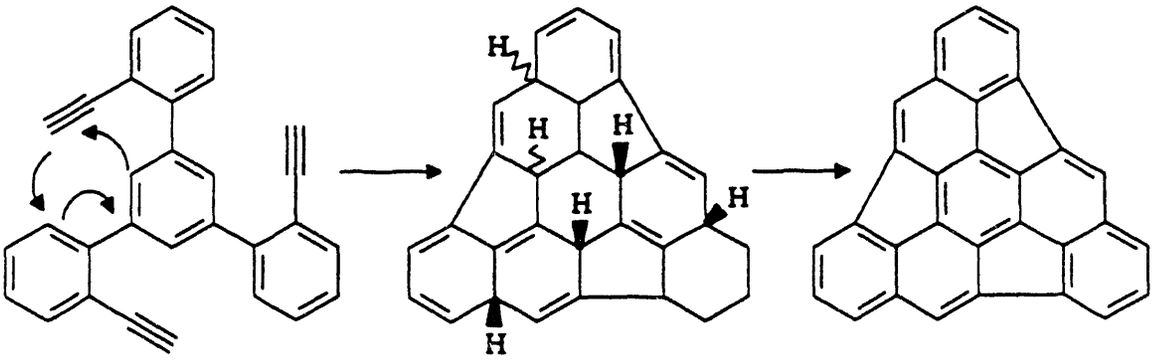

80 **13**

Initially, synthetic approaches to **80** were based on the fortuitous discovery that the dianion of phenylacetylene (**90**), generated by deprotonation with Schlosser's base,[201] can be regioselectively monostannylated to furnish **91** in moderate yield (Scheme 5.5). Although all starting material was consumed in the course of the Palladium-catalyzed[202] coupling reaction between tin-arene **91** and 1,3,5-tribromobenzene (**92**), the product defied all efforts to its isolation, polymerizing on the SiO_2 surface of the chromatography

Scheme 5.5[a]

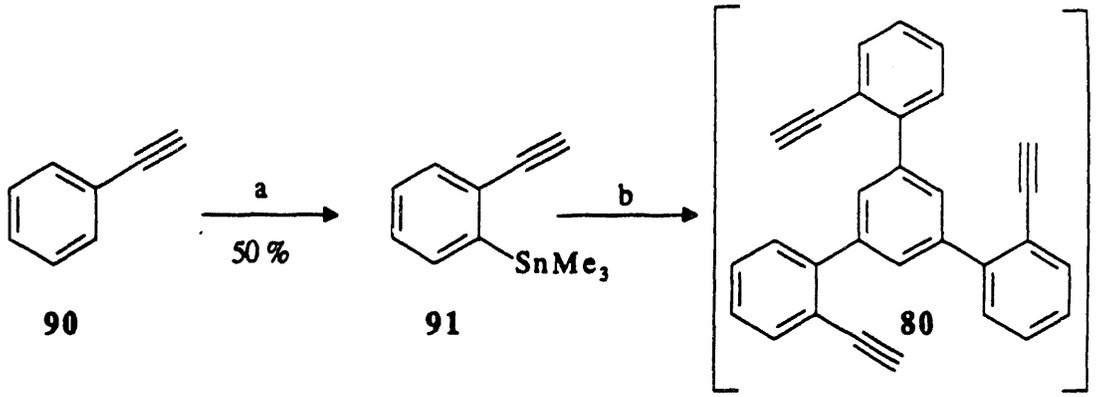

[a] (a) 2 eq. BuLi, 2 eq. tBuOK, Me_3SnCl; -78° C; 60 min. (b) 1,3,5-tribromobenzene (**92**), $Pd(PPh_3)_4$, dioxane; Δ; 5d.

column. Attempts to trisilylate the trianion resulting from deprotonation of (postulated) **80** with trimethylsilyl chloride prior to the reaction work-up were met with no success.

Since protection of the reactive alkynes units with silyl groups promised a less cumbersome product separation from the reaction mixture, **95** was prepared with methodology previously developed by Diercks and Vollhardt[21a] (Scheme 5.6). Thus, *ortho*-bromoiodobenzene (**93**) was alkynylated to give **94**, which, upon lithium-halide exchange and treatment with Me_3SnCl furnished **95** in a yield of 87%.

Scheme 5.6[a]

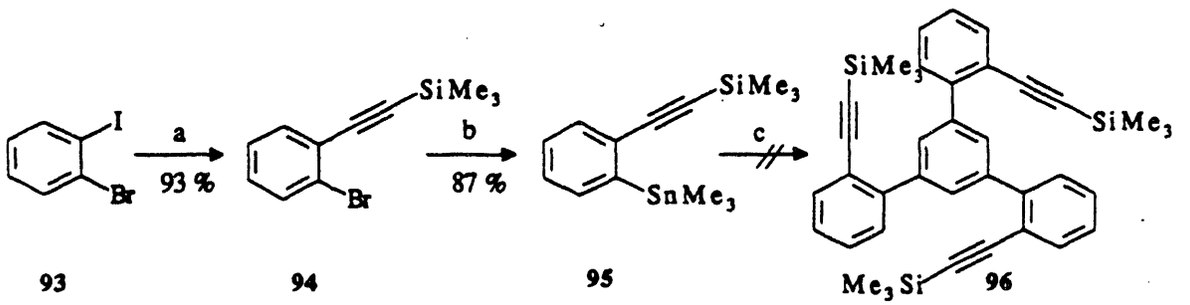

[a] (a) Me_3SiCCH, $PdCl_2(PPh_3)_2$, Et_3N, CuI; r.t.; 2.5d. (b) 1. BuLi, THF 2. Me_3SnCl, THF; -78° C; 15 min. (c) **92**, $Pd(PPh_3)_4$, dioxane; Δ; 5d.

Unfortunately, subjection of **95** and **92** to Stille-type coupling conditions did not generate the desired product **96**, resulting only in catalyst decomposition after 5d at reflux.

Synthesis of **96** was ultimately achieved in 28% yield by palladium-catalyzed threefold stannylation of **92** with hexamethylditin,[203] followed by reaction of thus obtained 1,3,5-tris(trimethylstannyl)benzene (**97**) with **94** (Scheme 5.7). With material appropriately functionalized for intramolecular Diels-Alder reactions at hand, the behavior of **96** on exposure to elevated temperatures was investigated. Disappointingly, neither heating of a $CDCl_3$ solution of **96** to 180° C in a sealed tube, nor flash vacuum pyrolysis

Scheme 5.7[a]

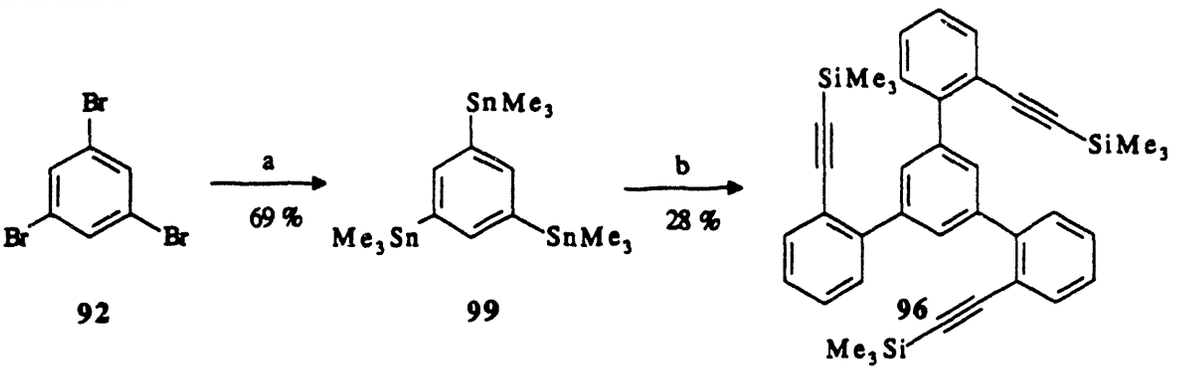

92 **99** **96**

[a] (a) Me_6Sn_2, $Pd(PPh_3)_4$, toluene; Δ; 60 min. (b) **94**, $Pd(PPh_3)_4$, dioxane; Δ; 5d.

(800° C, 0.05 torr) resulted in any detectable conversion of starting material. Attempts to remove the trimethylsilyl protecting groups led to polymerization of the free trialkyne, similar to observations made while performing the reaction sequence delineated in Scheme 5.5.

Clearly, a successful strategy for the construction of **13** along this route critically depends on the possibility to obtain **80** in pure form. Even more promising, however, appears to be an activation of its alkyne units by electron-withdrawing substituents such as alkoxycarbonyl groups which are known to facilitate thermally initiated [4+2] cyclo-additions.

Chapter Six

Experimental Details and Input Decks

General.

Unless otherwise noted, all materials were obtained from commercial suppliers and used without further purification. Tetrahydrofuran (THF), diethyl ether (Et_2O), 1,4-dioxane, 1,2-dimethoxyethane (DME), benzene, and toluene were distilled from sodium benzophenone ketyl immediately prior to use. Dimethylsulfoxide (DMSO) was dried over molecular sieves (4 Å), distilled in vacuo and stored under nitrogen. Carbon disulfide was pressed through a short column of neutral alumina, and triethylamine (NEt_3), methylene chloride (CH_2Cl_2), and chloroform ($CHCl_3$) were refluxed over CaH_2. Acetic anhydride was distilled from sodium acetate and stored under nitrogen. Butyllithium solutions were titrated with diphenyl acetic acid. The compounds trimethylsilylethyne,[204] bis(trimethylsilyl)ethyne,[205] 1,2,3,4-tetrabromobenzene,[135a] *ortho*-bromoiodobenzene (**93**),[206] tetrakis(triphenylphosphine)palladium [$Pd(PPh_3)_4$],[207] bis(triphenylphosphine)-palladium dichloride [$Pd(PPh_3)_2Cl_2$],[208] cyclopentadienylcobalt dicarbonyl [$CpCo(CO)_2$],[209] and 1-bromo-2-(trimethylsilylethynyl)benzene (**94**)[21a] were synthesized according to literature procedures. Triangular [4]phenylene (**7**), used in the course of the calorimetric studies described in chapter 3, was generously provided by Debbie Mohler. All reactions involving oxygen-sensitive reagents employed degassed solvents. Transfer of these materials was carried out in a glovebox, via syringe, or using standard Schlenk techniques, and the reaction mixtures were maintained under nitrogen until workup.

Photocyclizations were performed in quartz or Vycor glass tubes previously rinsed with hexamethyldisilazane in a Rayonet photoreactor RPR 100 equipped with lamps of the appropriate wavelength range and a cryostat as an external cooling device. Irradiation in the course of cobalt-mediated cyclizations was effected by a Sylvania ELH 300W slide projector lamp, powered by a variable transformer at an applied potential of 40-60 V.

Thin-layer chromatography was done on EM Reagents Kieselgel 60 F_{254} or EM Reagents neutral aluminum oxide 60 F_{254} sheets (0.2 mm coating). Flash chromatography refers to the method of Still et al.[210] and was conducted on EM Scientific SiO_2 (230-240 mesh). Column chromatography used Baker SiO_2 (60-200 mesh) or Alpha Al_2O_3 (60 mesh). High pressure liquid chromatography (HPLC) employed an IBM LC/9533 instrument equipped with and LC/9522 fixed wavelength (254 nm) detector. For semi-preparative separations, two sequentially connected columns were used, each 25 cm × 10 mm ID and packed with Microsorb 5 μm silica. Gas-liquid chromatography (GLC) was performed with a Hewlett-Packard 5880 instrument on a 6 ft × 2 mm ID glass column containing 3% OV-101 on Chromosorb W-HP (80/ mesh).

Melting points were determined in open capillaries with a Thomas-Hoover Uni-melt apparatus and are uncorrected. A Hewlett-Packard 8450 diode array spectrometer was used for the recording of UV-Vis spectra, a Perkin-Elmer model 681 instrument for analysis in the IR range. ^1H NMR and $^{13}C\{^1H\}$ NMR spectra were collected on the UCB-300 instrument, consisting of Cryomagnet System magnet, Nicolet 293A pulse programmer, and Nicolet Model 1280 data collecteion system. Data are reported as follows: chemical shifts in parts per million (ppm) relative to internal tetramethylsilane or residual solvent peaks (multiplicity, coupling constant in Hertz, number of hydrogens). The multiplicities observed are indicated as s (singlet), d (doublet), m (multiplet), and td (triplet of doublets).

Mass spectra and elemental analyses were provided by the Microanalytical Laboratory, operated by the College of Chemistry, University of California at Berkeley.

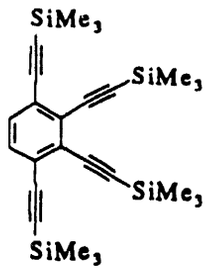

1,2,3,4-Tetrakis(trimethylsilylethynyl)benzene.[25] Trimethylsilylethyne (7.89 g, 11.3 mL, 80.28 mmol) and 1,2,3,4-tetrabromobenzene (2.74 g, 6.96 mmol) together with catalytic amounts of $Pd(PPh_3)_4$ (0.56 g, 0.80 mmol) and CuI (0.05 g, 0.30 mmol) were dispersed in triethylamine (100 mL) in a Fisher-Porter bottle equipped with a Teflon stopcock. The closed reaction vessel was heated in a sand bath to 100 °C for 36 h, after which it was cooled to room temperature. Volatiles were distilled at ambient under reduced pressure and the residual material chromatographed on SiO_2 (ca. 120 g) using 5% CH_2Cl_2 in hexanes. The last eluting band furnished the product as pale yellow flakes (1.23 g, 38%) after crystallization from ethanol: mp 124 - 125 °C; ^1H NMR (300 MHz, $CDCl_3$) δ 7.26 (s, 2H), 0.25 (s, 18H), 0.22 (s, 18H). Lit.[25] mp 128 °C; UV-Vis (hexanes) λ_{max} (log ε) 217 (3.82), 227 (3.83), 258 (4.68), 273 (4.86), 287 (4.69), 296 (4.47), 307 (4.74) nm; IR ($CHCl_3$) 3004, 2957, 2891, 2141, 1461, 1387, 1251, 1013, 945, 873, 833, 695, 641 cm^{-1}; MS (70 eV) *m/z* (rel. intensity) 462 (M^+, 5), 428 (6), 355 (9), 327 (9), 239 (20), 73 (100); ^1H NMR (300 MHz, $CDCl_3$) δ 7.29 (s, 2H), 0.27 (s, 18H), 0.24 (s, 18H); $^{13}C\{^1H\}$ NMR (75.5 MHz, $CDCl_3$) δ 131.31, 128.44, 125.85, 103.55, 102.57, 101.14, 100.61, 0.09, -0.03. HRMS Calcd for $C_{26}H_{38}Si_4$: 462.20507. Found: 462.20400.

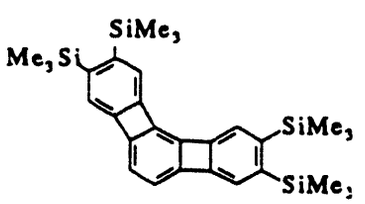

2,3,8,9-Tetrakis(trimethylsilyl) Angular [3]Phenylene.[25] A solution of 1,2,3,4-tetrakis(trimethylsilylethynyl)benzene (0.51 g, 1.11 mmol), $KF{\cdot}2H_2O$ (6.87 g, 79.7 mmol),

and 18-crown-6 (0.178g, 0.67 mmol) in DME (120 mL) was stirred at room temperature for 15 min. The liquid was decanted into a 100 mL pear-shaped flask sealed with a rubber septum and then degassed by flushing the system with argon. To this solution, $CpCo(CO)_2$ (250 μl, 1.96 mmol) was added via syringe. After completion, the resulting deep red mixture was injected by means of a syringe pump over a period of 8 h into degassed, refluxing bis(trimethylsilyl)ethyne (100 mL) contained in a 500 mL round-bottom flask equipped with condenser under argon. During the addition and for 10 h thereafter, the vessel content was irradiated by an external slide projector lamp, while maintaining reflux. After cooling to room temperature, the DME was distilled by rotary evaporation and excess bis(trimethylsilyl)ethyne revovered by vacuum transfer. The resulting brown residue was subjected to flash chromatography on SiO_2 (ca. 50 g), eluting with 2% CH_2Cl_2 in hexanes. The first colored band furnished the product as bright yellow crystals (0.39 g, 68%): mp 188 - 190 °C; ^1H NMR (300 MHz, $CDCl_3$) δ 7.24 (s, 2H), 7.17 (s, 2H), 6.18 (s, 2H), 0.40 (s, 18H), 0.35 (s, 18H). Lit.[25] mp 190 °C; UV-Vis (hexanes) λ_{max} (log ε) 206 (4.49), 228 (4.61), 245 (4.52), 277 (4.33), 287 (4.67), 292 (4.65), 301 (4.88), 310 (4.54), 316 (4.54), 326 (4.90), 366 (3.84), 388 (3.82), 410 (3.73) nm; IR ($CHCl_3$) 2949, 1402, 1253, 1054, 851, 823, 684, 636 cm^{-1}; MS (70 eV) *m/z* (rel. intensity) 517 (8), 516 (29), 515 (55), 514 (M^+, 100), 499 (7), 483 (9), 442 (6), 411 (7), 74 (8), 73 (97); ^1H NMR (300 MHz, $CDCl_3$) δ 7.25 (s, 2H), 7.18 (s, 2H), 6.16 (s, 2H), 0.37 (s, 18H), 0.35 (s, 18H); $^{13}C\{^1H\}$ (75.5 MHz, $CDCl_3$) δ 150.19, 149.76, 148.62, 148.49, 147.87, 137.26, 125.05, 123.97, 114.58, 2.64, 2.58. HRMS Calcd for $C_{30}H_{42}Si_4$: 514.23637. Found: 514.23530.

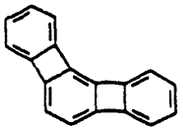

Angular [3]Phenylene (5).[12,25] Trifluoroacetic acid (20 mL) was added to a solution of 2,3,8,9-tetrakis(trimethylsilyl)angular [3]phenylene (1.34 g, 2.60 mmol) in $CHCl_3$ (100 mL). The reaction mixture was allowed to stir at room temperature for 18 h, then successively washed with water (2 × 100 mL), saturated aqueous sodium bicarbonate solution (2 × 100 mL), and again with water (2 × 50 mL). The organic layer was dried over $MgSO_4$. Filtration and rotary evaporation of solvent was followed by column chromatography on silica (ca. 70 g), eluting with 20% CH_2Cl_2 and left **5** (0.50 g, 85%) as yellow needles: mp 184 - 185 °C; ^1H NMR (300 MHz, $CDCl_3$) δ 6.83 - 6.95 (m, 8H), 6.12 (s, 2H). Lit.[21a] mp 185 °C; ^1H NMR (300 MHz, $CDCl_3$) δ 6.92 (m, 8H), 613 (s, 2H).

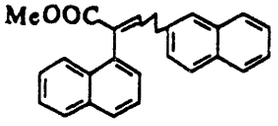

1-Mehtoxycarbonyl-1-(α-naphthyl)-2-(β-naphthyl) ethylene (81). A solution of 2-naphthaldehyde (10.00 g, 64.03 mmol) and 1-naphthylacetic acid (11.92 g, 64.03 mmol) in acetic anhydride (20 mL) and triethylamine (10 mL) was heated to reflux in a nitrogen atmosphere for 12 h. The reaction mixture was cooled to room temperature and hydrolyzed with concentrated hydrochloric acid (20 mL). The resulting precipitate was filtered, washed with water (3 × 150 mL), dried in vacuo, and crystallized from glacial acetic acid to yield 11.90 g of light yellow crystals. The material was dissolved in toluene (100 mL) and heated to reflux together with methanol (80 mL) and concentrated sulfuric acid (5 mL) for 8 h. After cooling to room temperature, the layers were separated, the organic phase was successively washed with water (20 mL), aqueous sodium bicarbonate solution (5%, 20 mL), and again water (20 mL), then dried over $MgSO_4$. Filtration and

evaporation of solvent left 10.08 g of crude material that was crystallized from ethanol to yield **81** as pale yellow crystals (9.56 g, 47%): mp 116 - 117 °C; UV-Vis (cyclohexane) λ_{max} (log ε) 223 (4.89), 262 (4.57), 270 (4.56), 308 (4.37) nm; IR (CH_2Cl_2) 2953, 1714, 1641, 1437, 1361, 1313, 1293, 1280, 1243, 1194, 1172, 1157, 1127, 983, 854, 818 cm^{-1}; MS (70 eV) *m/z* (rel. intensity) 338 (M^+, 29), 307 (8), 279 (69), 212 (99), 181 (100), 152 (84); ^1H NMR (300 MHz, $CDCl_3$) δ 8.29 (s, 1H), 7.87 (d, J = 5.9 Hz, 2H), 7.83 (d, J = 5.9 Hz, 2H), 7.60 - 7.25 (m, 7H), 6.77 (d, J = 1.3 Hz, 1H), 6.73 (d, J = 1.3 Hz, 1H), 3.75 (s, 6H); $^{13}C\{^1H\}$ (75.5 MHz, $CDCl_3$) δ 168.49, 142.14, 133.83, 133.61, 133.19, 132.71, 131.91, 131.86, 131.79, 130.53, 128.39, 128.36, 127.58, 127.27, 127.23, 126.94, 126.40, 126.27, 126.09, 126.01, 125.70, 124.92, 52.36. Anal. Calcd for $C_{24}H_{18}O_2$: C, 85.18; H, 5.36. Found: C, 85.03; H, 5.37.

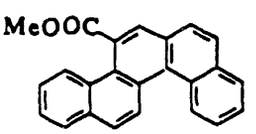

13-Methoxycarbonyl-benzo[*c*]chrysene (82). A solution of **81** (4.00 g, 11.82 mmol) and iodine (150 mg, 0.59 mmol) in cyclohexane (800 mL) was irradiated at a frequency range centered around 300 nm at room temperature. The reaction was monitored by thin-layer chromatography, which, after 70 h, indicated that all starting material had been converted. Rotary evaporation of the solvent left 4.45 g of a brown material that was crystallized from ethanol to afford **82** as yellow crystals (3.58 g, 90%): mp 156 - 157 °C; UV-Vis (hexanes) λ_{max} (log ε) 205 (4.68), 233 (4.32), 298 (4.73), 321 (4.31) nm; IR (CH_2Cl_2) 2954, 1724, 1223, 1214, 1164, 1102 cm^{-1}; MS (70 eV) *m/z* (rel. intensity) 336 (M^+, 100), 305 (77), 277 (82); ^1H NMR (300 MHz, $CDCl_3$) δ 8.91 (d, J = 8.9 Hz, 1H), 8.25 (m, 1H), 8.15 (s, 1H), 7.89 - 7.78 (m, 4H), 7.65 - 7.59 (m, 6H), 3.98 (s, 3H); $^{13}C\{^1H\}$ (75.5 MHz, $CDCl_3$) δ 172.29, 134.11, 132.17, 129.78, 129.56, 129.16, 129.03, 128.70, 128.69, 128.66, 128.63, 128.54, 128.27, 127.88, 126.87, 126.78, 126.71, 126.60, 126.23, 125.64, 52.76. Anal. Calcd for $C_{24}H_{16}O_2$: C, 85.69; H, 4.79. Found: C, 85.72; H, 4.76.

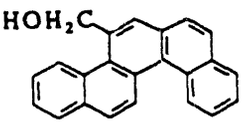

13-Hydroxymethylbenzo[*c*]chrysene. To a solution of **82** (1.51 g, 4.49 mmol) in THF (30 mL) was added dropwise via syringe a solution of $LiAlH_4$ in Et_2O (2.5 mL, 1M, 2.5 mmol) under nitrogen while cooling from the outside with an ice bath. Stirring was continued at 0 °C for 30 min. The bright orange reaction mixture was hydrolyzed with water (5 mL), transferred into a separatory funnel and extracted with Et_2O (2 × 50 mL). The combined organic phases were dried over $MgSO_4$. Filtration and removal of solvent left 1.38 g of crude material, which was flash chromatographed on silica (ca. 75 g) eluting with CH_2Cl_2. Crystallization of the resulting pale yellow oil from hexanes/2-propanol furnished the product as fine white needles (1.13 g, 81%): mp 130 - 131 °C; UV-Vis (acetonitrile) λ_{max} (log ε) 235 (4.28), 298 (4.52), 317 (4.19), 338 (3.21) nm; IR (KBr) 3379, 1033, 828, 806, 746, 712 cm^{-1}; MS (70 eV) *m/z* (rel. intensity) 308 (M^+H, 100), 289 (36), 276 (41); ^1H NMR (300 MHz, $CDCl_3$) δ 8.6 (m, 2H), 7.8 - 7.7 (m, 5H), 5.04 (s, 2H); $^{13}C\{^1H\}$ NMR (75.5 MHz, $CDCl_3$) δ 135.42, 133.29, 132.22, 129.91, 129.85, 129.78, 129.38, 128.62, 128.39, 128.33, 128.25, 127.92, 127.41, 127.36, 127.08, 126.72, 126.02, 125.89, 125.84, 125.77, 125.64, 125.31, 65.81. Anal. Calcd for $C_{23}H_{16}O$: C, 89.58; H, 5.23. Found: C, 89.47; H, 5.10.

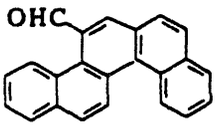

13-Benzo[*c*]chrysenecarbaldehyde (83). To a solution of oxalyl chloride (0.32 mL, 3.63 mmol) in CH_2Cl_2 (5 mL), cooled to -78 °C, was added dropwise DMSO (0.56 mL, 7.27 mmol) diluted with CH_2Cl_2 (5 mL). After 2 min, 13-hydroxymethylbenzo[*c*]chrysene dissolved in CH_2Cl_2 (10 mL) was slowly introduced via syringe. Stirring was continued for 30 min at that temperature, before triethylamine (3 mL) was canulated into the reaction mixture. The solution was allowed to warm to room temperature. After

hydrolysis with water (50 mL), the mixture was transferred into a separatory funnel and extracted with CH_2Cl_2 (2 × 50 mL). The combined organic phases were successively washed with water (20 mL), dilute hydrochloric acid (5%, 10 mL), water (20 mL), aqueous sodium bicarbonate solution (5%, 10 mL), and again with water (20 mL) then dried over $MgSO_4$. Filtration and rotary evaporation of the solvent left 1.05 g of a solid material which was crystallized from ethyl acetate to yield bright yellow needles of **83** (0.90 g, 93%): mp 155 - 156 °C; UV-Vis (THF) λ_{max} (log ε) 221 (4.40), 236 (4.31), 292 (4.59), 301 (4.63), 352 (3.89), 410 (3.18) nm; IR (KBr) 3173, 1686, 828, 814, 789, 746, 712 cm^{-1}; MS (70 eV) *m/z* (rel. intensity) 306 (M^+, 100), 277 (59), 153 (6), 138 (34); ^1H NMR (300 MHz, $CDCl_3$) δ 10.64 (s, 1H), 8.94 (d, J = 9.2 Hz, 1H), 8.44 (s, 1H), 7.7 - 7.9 (m, 5H); $^{13}C\{^1H\}$ NMR (75.5 MHz, $CDCl_3$) δ 182.81, 134.45, 133.22, 132.46, 130.23, 129.97, 129.88, 129.44, 129.21, 129.07, 128.98, 128.63, 128.38, 128.22, 127.79, 127.25, 127.17, 127.05, 126.44, 126.42, 126.37, 126.26. Anal. Calcd for $C_{23}H_{14}O$: C, 90.17; H, 4.61. Found: C, 90.08; H, 4.58.

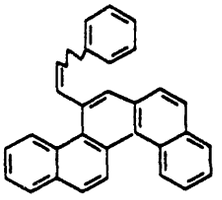

13-(2-Phenylethylene)benzo[*c*]chrysene (84). Butyllithium (1.87 mL, 2.01M in heptane, 3.75 mmol) was slowly added via syringe to a cooled (0 °C) solution of benzyltriphenylphosphonium bromide (1.63 g, 3.75 mmol) in THF (20 mL) under nitrogen. After the deep red solution had been stirred for 10 min at that temperature, a solution of **83** (1.00g, 3.26 mmol) in THF (20 mL) was added dropwise. The reaction mixture was refluxed for 60 min, cooled to room temperature, and hydrolyzed with water (50 mL). The layers were separated and the aqueous phase was extracted with Et_2O (2 × 50 mL). The combined organic phases were washed with water (3 × 20 mL) and dried over $MgSO_4$.

Filtration and rotary evaporation of the solvent left 2.29 g of an orange, viscous oil which was flash-chromatographed on silica (ca. 77 g), eluting with 50% CH_2Cl_2 in hexanes to afford yellow crystals of **84** (1.17 g, 94%) as a 1:1 mixture of cis/trans isomers (as determined by ^1H NMR): UV-Vis (hexanes) λ_{max} (log ε) 208 (4.69), 233 (4.56), 254 (4.32), 307 (4.79), 343 (4.24) nm; IR (CH_2Cl_2) 3029, 1422, 1269, 1258, 895, 834, 814, 758, 719, 701 cm^{-1}; MS (70 eV) *m/z* (rel. intensity) 380 (M^+, 100), 303 (84), 190 (7), 151 (15); ^1H NMR (300 MHz, $CDCl_3$) δ 9.37 (d, J = 9.02 Hz, 1H), 9.00 - 8.85 (m, 4H), 8.78 (d, J = 8.19 Hz, 1H), 8.04 - 7.04 (m, 33H), 6.88 (d, J = 11.92 Hz, 1H); $^{13}C\{^1H\}$ NMR (75.5 MHz, $CDCl_3$) mixture of cis/trans isomers showed 40 partly overlapping absorptions between 137.74 and 125.18 ppm. Anal. Calcd for $C_{30}H_{20}$: C, 94.70; H, 5.30. Found: C, 94.59; H, 5.04.

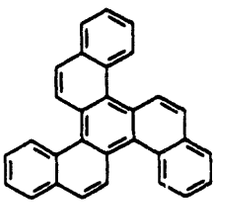

Tribenzo[*c,i,o*]triphenylene (79).[187] A solution of **84** (0.65 g, 1.71 mmol) and iodine (0.43 g, 1.71 mmol) in benzene (1000 mL) was degassed by flushing the system with argon for 30 min at 10 °C. Propylene oxide (32 mL, 0.45 mmol) was added and the purple mixture irradiated at a wavelength range centered around 350 nm at 10 °C for 15 h, after which the color had turned yellow. Rotary evaporation of the solvent left 1.26 g of yellow material that was chromatographed on a column of neutral alumina (ca. 80 g), eluting with 20% CH_2Cl_2 in hexanes, to afford 380 mg of a mixture of **79** and a second compound, tentatively identified as **85**.[187] Further purification was achieved by HPLC (serial assembly of SiO_2 and Al_2O_3 columns, 20% CH_2Cl_2 in hexanes as the eluent system, flow rate 6 ml min^{-1}) to furnish **79** (250 mg, 40%) as a pale yellow amorphous solid: mp 232 - 233 °C;

UV-Vis (CH_2Cl_2) λ_{max} (log ε) 228 (4.20), 240 (4.25), 264 (4.34), 326 (4.70), 404 (3.19) nm; MS (70 eV) *m/z* (rel. intensity) 378 (M^+, 100), 302 (18), 189 (22); ^1H NMR (300 MHz, $CDCl_3$) δ 8.96 (d, J = 4.39 Hz, 3H), 8.93 (d, J = 8.91 Hz, 3H), 8.06 (m, 3H), 7.96 (d, J = 9.01 Hz, 3H), 7.68 (m, 6H); $^{13}C\{^1H\}$ NMR (75.5 MHz, $CDCl_3$) δ 133.04, 129.88, 129.09, 128.04, 127.97, 127.74, 126.46, 126.14, 125.88, 125.71. Lit.[187] mp 233 - 234 °C; UV-Vis (MeOH) and ^1H NMR (100 MHz, CS_2) spectra presented in ref. 187 are in satisfactory agreement with the data obtained.

Cyclodehydrogenation of 79 on Pt/C. Tribenzo[*c,i,o*]triphenylene (**79**) (80 mg, 0.21 mmol) was thoroughly mixed with Pt on carbon (40 mg, 10%) in an agate mortar and transferred into a Pyrex glass tube that was sealed under reduced pressure. Its lower part, containing the reaction material, was immersed into a sand bath that was gradually heated to 400 °C and kept at this temperature for 60 min. After cooling to room temperature, the glass tube was crushed into a round-bottom flask and the soluble material extracted with $CHCl_3$ (50 mL). Filtration and evaporation of solvent left 70 mg of orange material which was subjected to column chromatography on alumina (ca. 20 g). The first fraction was eluted with 5% CH_2Cl_2 in hexanes and afforded starting material (10 mg, 13%), as ascertained by ^1H NMR spectroscopy. Increasing the polarity of the solvent system to 30% CH_2Cl_2 in hexanes furnished a second, red-orange solid (20 mg, 25%) that was tentatively identified as **88** and showed the following physical properties: UV-Vis (CH_2Cl_2) λ_{max} (log ε) 228 (3.50), 265 (3.63), 327 (3.72), 340 (3.78), 395 (3.21), 414 (3.24) nm; MS (70 eV) *m/z* (rel. intensity) 376 (M^+, 100), 187 (29), 149 (19), 111 (15), 97 (20), 71 (48); ^1H NMR (300 MHz, $CDCl_3$) δ 9.37 (d, J = 8.1 Hz, 1H), 9.33 (d, J = 9.1 Hz, 1H), 9.22 (d, J = 7.5 Hz, 1H), 9.06 (d, J = 9.0 Hz, 1H), 8.49 (s, 1H), 8.24 - 8.03 (m, 6H), 7.87 - 7.60 (m, 5H). HRMS Calcd for $C_{30}H_{16}$: 376.1262. Found: 376.1246.

A third fraction could be eluted with 50% CH_2Cl_2 in hexanes and afforded minute amounts (less than 5 mg) of a red compound which was tentatively assigned structure **89**

based on the following physical properties: UV-Vis (CH_2Cl_2) λ_{max} (log ε) 231 (2.74), 268 (2.54), 315 (2.52), 329 (2.47), 395 (2.22), 462 (sh, 1.84); MS (70 eV) *m/z* (rel. intensity) 374 (M^+, 100), 187 (41), 149 (36), 112 (24), 97 (33), 85 (32); ^1H NMR (300 MHz, $CDCl_3$) δ 7.72 (m), 7.55 (m). HRMS Calcd for $C_{30}H_{14}$: 374.1093. Found: 374.1097.

Attempted Cyclodehydrogenation of 79 by Flash Vacuum Pyrolysis. Tribenzo[*c,i,o*]-triphenylene (79) (80 mg, 0.21 mmol) was placed in a quartz tube whose opposite end was connected to an oil pump via a Schlenk line vacuum system and whose central part was surrounded by a pyrolysis furnace. The tube was evacuated to 0.05 torr and the furnace gradually heated to 800 °C. Sublimation of the organic material was accelerated by wrapping the outside end of the tube with heating tape and slowly increasing its temperature to ca. 60 °C. After several minutes, condensation of yellow material at the cooler end of the quartz tube behind the furnace was observed. After all starting material had disappeared from its original location, the system was cooled to room temperature, then vented with nitrogen. The material that had passed through the heated part of the tube was directly washed from the quartz walls into an NMR tube with $CDCl_3$ while maintaining a continuous flow of nitrogen throughout the system. Recording of ^1H NMR spectral data revealed that only starting material had been collected. The recovery was 75 mg (95%).

Attempted Cyclodehydrogenation of 79 using a Eutectic Mix of $AlCl_3$ and NaCl. An equimolar mixture (3g) of anhydrous $AlCl_3$ and NaCl was thoroughly mixed with 79 (50 mg, 0.13 mmol). The resulting powder was placed in a round-bottom flask under nitrogen that was gradually heated to 100 °C and kept at this temperature for 2 h. After cooling to room temperature, the black solid was quenched with water (30 mL) and the solution extracted with Et_2O (2 × 10 mL). The combined organic layers were dried over $MgSO_4$.

Filtration and evaporation of solvent left a yellow material (36 mg) whose identity was established to be **79** by ^{1}H NMR spectroscopy. The recovery was 72%.

Cyclodehydrogenation of 79 using $AlCl_3$ and $CuCl_2$ in CS_2. Anhydrous aluminum trichloride (0.40 g, 2.60 mmol) and copper dichloride (tip of a spatula) were added to a solution of **79** (50 mg, 0.13 mmol) in CS_2 (5 mL). The solution, which had turned deep blue immediately after addition, was heated to reflux for a period of 10 h. After cooling to room temperature, the solution was hydrolyzed with dilute hydrochloric acid (5%, 20 mL) and extracted with CH_2Cl_2 (2 × 20 mL). The combined organic layers were washed with water (2 × 20 mL) and dried over $MgSO_4$. Filtration and evaporation of solvent left a dark red material that was subjected to column chromatography on neutral alumina (ca. 50 g), eluting initially with 20% CH_2Cl_2 in hexanes. The first fraction contained a yellow solid which was identified as starting material based on its ^{1}H NMR spectrum (18 mg, 35% recovery). The second band furnished a red orange compound (14 mg, 28%) of identical physical properties as those described for **88**. A third, bright yellow fraction eluted with 50% CH_2Cl_2 in hexanes, affording minute amounts (ca. 2 mg) of a red material which showed the same spectral data as those reported for **89**.

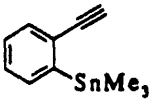

1-Ethynyl-2-trimethylstannylbenzene (91). A solution of potassium *t*-butoxide (12.34 g, 0.11 mol) in THF (60 mL) was cooled to -78 °C before butyllithium (69 mL, 1.6 M in heptane) diluted with THF (50 mL) was added dropwise via syringe. Ethynylbenzene (5.11 g, 0.05 mol) was slowly introduced and stirring of the resulting green slurry continued for 1h at -78 °C, before a solution of trimethyltin chloride (21.92 g, 0.11 mol) in THF (50 mL) was injected into the mixture by syringe. The white suspension was allowed to warm to room temperature, then hydrolyzed with water (100 mL). The aqueous phase

was extracted with Et_2O (2 × 50 mL) and the combined organic layers were washed with water (3 × 100 mL) and dried over $MgSO_4$. Filtration and evaporation of solvent left a yellow oil (7.48 g) which was subjected to column chromatography on SiO_2 (ca. 50 g), eluting with hexanes, to furnish **91** as a colorless oil (6.66g, 50%): UV-Vis (hexanes) λ_{max} (log ε) 208 (4.51), 241 (4.02), 252 (3.97), 274 (2.46), 280 (2.42) nm; IR (CH_2Cl_2) 3308, 2921, 1459, 1436, 1194, 1114, 782 cm^{-1}; MS (70 eV) *m/z* (rel. intensity) 251 (M^+-CH_3, 100), 221 (51); ^1H NMR (300 MHz, $CDCl_3$) δ 7.47 - 7.39 (m, 2H), 7.24 - 7.19 (m, 2H), 3.03 (s, 1H), 0.31 (s, J_{Sn-H} = 56.0 Hz, 9H); $^{13}C\{^1H\}$ NMR (75.5 MHz, $CDCl_3$) δ 146.29 (J_{Sn-C} = 447.0 Hz), 135.52 (J_{Sn-C} = 32.7 Hz), 132.12 (J_{Sn-C} = 30.9 Hz), 129.32 (J_{Sn-C} = 25.2 Hz), 128.16 (J_{Sn-C} = 9.0 Hz), 127.98 (J_{Sn-C} = 41.5 Hz), 85.85, 77.72, -8.89. Anal. Calcd for $C_{11}H_{14}Sn$: C, 49.87; H, 5.33. Found: C, 49.95; H, 5.28.

1-Ethynyl-2-tributylstannylbenzene could be synthesized in a similar fashion to give a colorless oil (55%): ^1H NMR (300 MHz, $CDCl_3$) δ 7.56 (m, 2H), 7.30 (m, 3H), 3.12 (s, 1H), 1.60 (m, 6H), 1.41 (m, 6H), 1.35 (m, 6H), 0.97 (t, J = 7.25 Hz, 9H);$^{13}C\{^1H\}$ NMR (75.5 MHz, $CDCl_3$) δ 146.70, 136.17 (J_{Sn-C} = 26.5 Hz), 132.31, 129.63 (J_{Sn-C} = 514.7 Hz), 127.87, 127.83, 86.29, 77.11, 29.19 (J_{Sn-C} = 17.7 Hz), 27.41 (J_{Sn-C} = 59.4 Hz), 13.70, 10.08 (J_{Sn-C} = 345.1 Hz).

Palladium-Mediated Coupling of 91 with 1,3,5-Tribromobenzene. A solution of **91** (4.60 g, 17.36 mmol), 1,3,5-tribromobenzene (0.91 g, 2.89 mmol) and $Pd(PPh_3)_4$ (1.00g, 0.87 mmol) in 1,4-dioxane (30 mL) was heated to reflux under argon. After 5 d, GLC analysis indicted that all starting material had been consumed. The dark reaction mixture was cooled to room temperature and filtered through a ceramic fritte covered with a pad of celite. Dilution with hexanes (50 mL) precipitated a pale yellow solid (Ph_3PO) that was separated by vacuum filtration. Evaporation of solvents left a dark brown oil that was subjected to column chromatography on SiO_2 (ca. 30 g), using hexanes as the eluent.

Upon elution, the column material adopted a bright yellow color. Changing the solvent system successively from hexanes to benzene, to chloroform, to acetone, and finally extracting the column content with a mixture of MeOH and CH_2Cl_2 (1:1) did not produce any identifiable compound.

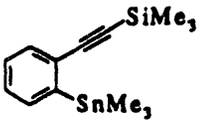

1-Trimethylsilylethynyl-2-trimethylstannylbenzene (95). 1-Bromo-2-trimethylsilylethynylbenzene (**94**) (1.00 g, 3.95 mmol) dissolved in THF (5 mL) was added to a cooled solution (-78 °C) of butyllithium (2.7 mL, 1.6 M in heptane, 4.34 mmol) in THF (5 mL) via syringe. Stirring of the deep yellow reaction mixture was continued for 15 min, before trimethyltin chloride (0.86 g, 4.34 mmol) in THF (5 mL) was injected. The system was allowed to warm to room temperature, diluted with Et_2O (20 mL), and hydrolyzed with aqueous ammonium chloride (10%, 50 mL). The organic layer was washed with water (2 × 50 mL) and dried over $MgSO_4$. Filtration and removal of solvents left a yellow oil (1.36 g) which was subjected to column chromatography on SiO_2 (ca. 30 g), eluting with hexanes, to furnish **95** as a colorless oil (1.18 g, 87%): bp (0.2 torr) 141 °C; UV-Vis (hexanes) λ_{max} (log ε) 253 (4.2), 265 (4.15) nm; IR ($CHCl_3$) 2964, 2157, 1457, 1434, 1255, 872, 848 cm^{-1}; MS (70 eV) *m/z* (rel. intensity) 323 (M^+ - Me, 100), 293 (29), 173 (64), 73 (52); ^1H NMR (300 MHz, $CDCl_3$) δ 7.50 (m, 2H), 7.30 (m, 2H), 0.32 (s, J_{Sn-H} = 55.8 Hz, 9H), 0.22 (s, J_{Si-H} = 6.9 Hz); $^{13}C\{^1H\}$ NMR (75.5 MHz, $CDCl_3$) δ 145.90 (J_{Sn-C} = 454.2 Hz), 135.41 (J_{Sn-C} = 36.4 Hz), 131.91 (J_{Sn-C} = 34.0 Hz), 130.41 (J_{Sn-C} = 24.6 Hz), 128.14, 127.72 (J_{Sn-C} = 44.0 Hz), 107.36, 94.24, -0.04, -8.92 (J_{Sn-C} = 717.2 Hz). Anal. Calcd for $C_{14}H_{22}SiSn$: C, 49.88; H, 6.58. Found: C, 50.35; H, 6.64.

Attempted Palladium-Mediated Coupling of 95 with 1,3,5-Tribromobenzene. A solution of **95** (2.24 g, 6.64 mmol), 1,3,5-tribromobenzene (0.35 g, 1.11 mmol), and

$Pd(PPh_3)_4$ (0.13 g, 0.11 mmol) in degassed 1,4-dioxane (30 mL) was heated to reflux under argon. The reaction was monitored by GLC analysis which, even after five days, did not show any appreciable consumption of starting material. After an additional period of 2 weeks, the solution had turned dark brown and none of the starting materials could be detected. The mixture was cooled to room temperature, and filtered through celite. Rotary evaporation of the solvent left a dark brown oil (2.95 g) which was subjected to column chromatography on SiO_2 (ca. 200 g), eluting with 5% ethyl acetate in hexanes. In the collected fractions, only the decomposition products triphenylphosphine oxide and trimethyltin bromide could be identified.

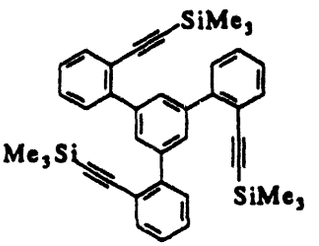

1,3,5-Tris(2'-trimethylsilylethynylphenyl)benzene (96). A solution of 1,3,5-tris-(trimethylstannyl)benzene (99) (0.48 g, 0.85 mmol), 1-bromo-2-(trimethylsilylethynyl)-benzene (94) (1.29 g, 5.10 mmol) and $Pd(PPh_3)_4$ (0.15 g, 0.13 mmol) in degassed 1,4-dioxane (10 mL) was heated to reflux under argon. The reaction was monitored by GLC analysis which, after 5 d, indicated that all starting material had been consumed. The reaction mixture was allowed to cool to room temperature, and filtered through a pad of celite. Evaporation of the volatiles was first performed on a rotary evaporator, then in an oil pump vacuum at room temperature over night. The remaining dark oil (1.55 g) was subjected to column chromatography on SiO_2 (ca. 80 g). The first two fractions, containing excess aryl halide and an unidentified, but non-silylated product, were eluted with hexanes. The solvent was gradually changed to 10% ethyl acetate in hexanes to collect a third fraction that furnished a brown-yellow oil (0.22 g) which was shown by GLC to consist of two compounds. Column chromatography of this material on neutral

alumina (ca. 30 g), eluting with 5% CH_2Cl_2 in hexanes, afforded **96** as yellow crystals (140 mg, 28%) that could be obtained in analytically pure form by sublimation (50 °C, 0.05 torr): mp 155 - 156 °C; UV-Vis (hexanes) λ_{max} (log ε) 232 (5.21), 258 (4.87), 303 (4.23), 326 (3.77) nm; MS (70 eV) *m/z* (rel. intensity) 594 (M^+, 12), 521 (M^+ - $SiMe_3$, 41), 506 (19), 491 (17), 475 (9), 447 (25), 433 (63), 417 (33), 351 (10), 73 (100); ^1H NMR (400 MHz, CD_2Cl_2) δ 8.03 (s, 3H), 7.59 (dd, J = 6.5 Hz, J = 1.2 Hz, 3H), 7.57 (dd, J = 6.7 Hz, J = 1.1 Hz, 3H), 7.42 (td, J = 7.5, 1.4 Hz, 3H), 7.31 (td, J = 7.6, 1.3 Hz, 3H), -0.03 (s, 27H); $^{13}C\{^1H\}$ NMR (100 MHz, CD_2Cl_2) δ 143.89, 139.69, 133.99, 129.96, 129.71, 129.18, 127.38, 121.70, 105.09, 98.15, -0.39. Anal. Calcd for $C_{39}H_{42}Si_3$: C, 78.73; H, 7.11. Found: C, 78.79; H, 7.16.

Attempted Cyclization of 96 under Flash Vacuum Pyrolysis Conditions. Tris(trimethylsilylethynylphenyl)benzene **96** (30 mg, 0.05 mmol) was placed in a quartz tube whose opposite end was connected to an oil pump via a Schlenk line vacuum system and whose central part was surrounded by a pyrolysis furnace. The tube was evacuated to 0.05 torr and the furnace gradually heated to 800 °C. Sublimation of the organic material was accelerated by wrapping the outside end of the tube with heating tape and slowly increasing its temperature to ca. 60 °C. After 1.5 h, condensation of pale yellow material at the cooler end of the quartz tube behind the furnace was observed. After all starting material had disappeared from its original location, the system was cooled to room temperature, then vented with nitrogen. The material that had passed through the heated part of the tube was directly washed from the quartz walls into an NMR tube with $CDCl_3$ while maintaining a continuous flow of nitrogen throughout the system. Recording of ^1H NMR spectral data revealed that only starting material had been collected. The recovery was 28 mg (95%).

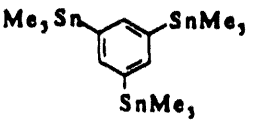

1,3,5-Tris(trimethylstannyl)benzene (99). A solution of 1,3,5-tribromobenzene (1.00 g, 3.18 mmol), hexamethylditin (11.09 g, 11.44 mmol), and $Pd(PPh_3)_4$ (0.20 g, 0.17 mmol) in degassed toluene was heated to reflux for 60 min under argon. The reaction mixture was allowed to cool to room temperature, then filtered through a pad of celite. Evaporation of the volatiles was first performed in the vacuum of a rotary evaporator, therafter in an oil pump vacuum to yield a colorless oil (1.56 g) that was subjected to column chromatography on SiO_2 (ca. 60 g), using hexanes as eluent. Collection of the first fraction furnished, after removal of the solvent, **99** as a colorless oil (1.24 g, 69%): MS (70 eV) *m/z* (rel. intensity) 551 (M^+ - Me, 100), 521 (13), 491 (12), 389 (41), 268 (17), 165 (23); ^1H NMR (300 MHz, $CDCl_3$) δ 7.66 (s, 3H), 0.40 (s, J_{Sn-H} = 54.7 Hz, 27H); $^{13}C\{^1H\}$ NMR (75.5 MHz, $CDCl_3$) δ 143.12 (J_{Sn-C} = 30.7 Hz), 141.97 (J_{Sn-C} = 151.0 Hz, J_{Sn-C} = 31.5 Hz), -9.42 (J_{Sn-C} = 321.8 Hz). Anal. Calcd for $C_{15}H_{30}Sn_4$: C, 31.80; H, 5.34. Found: C, 32.29; H, 5.17.

1

```
PM3 BONDS PRECISE T=2400M SYMMETRY
benzene
d6h
C     0.000000  0     0.000000  0     0.000000  0    0  0  0
C     1.391083  1     0.000000  0     0.000000  0    1  0  0
C     1.391083  0   120.000000  0     0.000000  0    2  1  0
C     1.391083  0   120.000000  0     0.000000  0    3  2  1
C     1.391083  0   120.000000  0     0.000000  0    4  3  2
C     1.391083  0   120.000000  0     0.000000  0    5  4  3
H     1.094729  1   120.000000  0   180.000000  0    1  6  5
H     1.094729  0   120.000000  0   180.000000  0    2  1  6
H     1.094729  0   120.000000  0   180.000000  0    3  2  1
H     1.094729  0   120.000000  0   180.000000  0    4  3  2
H     1.094729  0   120.000000  0   180.000000  0    5  4  3
H     1.094729  0   120.000000  0   180.000000  0    6  5  4
0     0.000000  0     0.000000  0     0.000000  0    0  0  0
2,    1,    3,
2,    1,    4,
2,    1,    5,
2,    1,    6,
7,    1,    8,
7,    1,    9,
7,    1,   10,
7,    1,   11,
7,    1,   12,
```

1

```
 $CONTRL  MEMORY=50000  SCFTYP=RHF  RUNTYP=ENERGY  COORD=ZMT
 $BASIS  GBASIS=N21  NGAUSS=3  $END
 $NBO  RESONANCE  $END
 $DATA
Benzene...rhf/3-21g//rhf/3-21g
Dnh 6

C
C       1   1.3848245
C       2   1.3848245  1   120.0000000
C       3   1.3848245  2   120.0000000  1     0.0000000  0
C       4   1.3848245  3   120.0000000  2     0.0000000  0
C       5   1.3848245  4   120.0000000  3     0.0000000  0
H       1   1.0724699  2   120.0000000  3   180.0000000  0
H       2   1.0724699  1   120.0000000  6  -180.0000000  0
H       3   1.0724699  4   120.0000000  5   180.0000000  0
H       4   1.0724699  3   120.0000000  2  -180.0000000  0
H       5   1.0724699  6   120.0000000  1   180.0000000  0
H       6   1.0724699  5   120.0000000  4  -180.0000000  0
 $END
```

3

```
PM3 PRECISE LOCALISE BONDS T=2400M
biphenylene
d2h
 C    0.000000  0    0.000000  0    0.000000  0   0   0   0
 C    1.422894  1    0.000000  0    0.000000  0   1   0   0
 C    1.376627  1  122.274819  1    0.000000  0   2   1   0
 C    1.422874  1  122.281588  1   -0.388258  1   3   2   1
 C    1.356631  1  115.561331  1    0.313395  1   4   3   2
 C    1.451995  1  122.157007  1   -0.075457  1   5   4   3
 C    1.486237  1   89.987370  1  179.974443  1   6   5   4
 C    1.451747  1   90.011441  1    0.025757  1   7   6   5
 C    1.356694  1  122.177809  1  179.930044  1   8   7   6
 C    1.422805  1  115.546298  1    0.054891  1   9   8   7
 C    1.376738  1  122.282472  1   -0.014582  1  10   9   8
 C    1.422836  1  122.277092  1   -0.039840  1  11  10   9
 H    1.092737  1  123.466875  1 -179.898432  1   1   6   5
 H    1.095274  1  118.123733  1  180.022859  1   2   1   6
 H    1.095275  1  119.605475  1  179.791231  1   3   2   1
 H    1.092735  1  120.959395  1 -179.748746  1   4   3   2
 H    1.092730  1  123.481902  1  180.026775  1   9   8   7
 H    1.095280  1  118.114253  1  179.959637  1  10   9   8
 H    1.095271  1  119.605659  1  179.975315  1  11  10   9
 H    1.092733  1  120.991345  1  180.039879  1  12  11  10
 0    0.000000  0    0.000000  0    0.000000  0   0   0   0
```

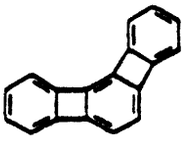

5

```
PM3 PRECISE LOCALISE BONDS T=2400M
angular[3]
c2v
C    0.000000  0    0.000000  0    0.000000  0   0   0   0
C    1.418744  1    0.000000  0    0.000000  0   1   0   0
C    1.379607  1  122.329439  1    0.000000  0   2   1   0
C    1.419067  1  122.184017  1    0.113765  1   3   2   1
C    1.359952  1  115.641086  1   -0.105913  1   4   3   2
C    1.449394  1  122.179323  1    0.047829  1   5   4   3
C    1.482415  1   90.876876  1  179.968860  1   6   5   4
C    1.486479  1   88.912337  1   -0.024279  1   7   6   5
C    1.331165  1  117.397641  1  179.974238  1   8   7   6
C    1.486305  1  117.602065  1    0.051900  1   9   8   7
C    1.348895  1  124.717078  1   -0.092182  1  10   9   8
C    1.448562  1  117.726477  1    0.058876  1  11  10   9
C    1.482262  1   88.923790  1  180.012751  1  10   9   8
C    1.449508  1   90.879630  1    0.003974  1  13  10   9
C    1.359934  1  122.156317  1  179.979234  1  14  13  10
C    1.419157  1  115.644894  1   -0.025927  1  15  14  13
C    1.379631  1  122.184986  1    0.031042  1  16  15  14
C    1.418733  1  122.337124  1   -0.027531  1  17  16  15
H    1.092832  1  123.269176  1  179.979861  1   1   6   5
H    1.095394  1  118.211176  1  179.979801  1   2   1   6
H    1.095287  1  119.539623  1  180.055084  1   3   2   1
H    1.092859  1  121.085470  1  179.904045  1   4   3   2
H    1.093069  1  122.825708  1  180.033094  1  11  10   9
H    1.093038  1  119.406405  1  179.998461  1  12  11  10
H    1.092859  1  123.285181  1  179.987264  1  13  14  13
H    1.095280  1  118.308246  1 -179.954334  1  16  15  14
H    1.095394  1  119.449782  1  180.002130  1  17  16  15
H    1.092810  1  121.046705  1  180.007269  1  18  17  16
0    0.000000  0    0.000000  0    0.000000  0   0   0   0
```

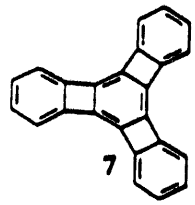


```
AM1 T=2400M PRECISE
triangulene
d3h
C     0.000000  0     0.000000  0     0.000000  0    0    0    0
C     1.419349  1     0.000000  0     0.000000  0    1    0    0
C     1.383730  1   122.039078  1     0.000000  0    2    1    0
C     1.419315  1   122.144352  1    -0.056414  1    3    2    1
C     1.363897  1   116.285155  1    -0.005668  1    4    3    2
C     1.462169  1   121.588300  1     0.054305  1    5    4    3
C     1.469190  1    91.218944  1   180.006081  1    6    5    4
C     1.525159  1    88.774916  1     0.001354  1    7    6    5
C     1.325354  1   119.996867  1   179.970949  1    8    7    6
C     1.525239  1   119.999509  1    -0.007870  1    9    8    7
C     1.325376  1   120.001111  1     0.027242  1   10    9    8
C     1.525091  1   119.996816  1    -0.031112  1   11   10    9
C     1.469180  1    88.777208  1   180.030621  1   10    9    8
C     1.462144  1    91.217570  1    -0.018066  1   13   10    9
C     1.363963  1   121.589016  1   180.000482  1   14   13   10
C     1.419187  1   116.299161  1     0.002891  1   15   14   13
C     1.383873  1   122.133963  1    -0.013060  1   16   15   14
C     1.419411  1   122.032577  1     0.007483  1   17   16   15
C     1.469163  1    88.775960  1   180.034287  1   12   11   10
C     1.462158  1    91.221245  1    -0.002667  1   19   12   11
C     1.363958  1   121.591456  1   180.004513  1   20   19   12
C     1.419324  1   116.282375  1     0.012620  1   21   20   19
C     1.383737  1   122.143045  1     0.000512  1   22   21   20
C     1.419402  1   122.042540  1    -0.009894  1   23   22   21
H     1.097675  1   123.296472  1   180.010774  1    1    6    5
H     1.100617  1   118.240676  1   180.031600  1    2    1    6
H     1.100724  1   119.673149  1   179.969969  1    3    2    1
H     1.097656  1   120.408623  1   180.037747  1    4    3    2
H     1.097671  1   123.285381  1   179.996452  1   15   14   13
H     1.100712  1   118.205170  1   179.981185  1   16   15   14
H     1.100595  1   119.718313  1   180.009434  1   17   16   15
H     1.097677  1   120.396476  1   180.014255  1   18   17   16
H     1.097647  1   123.298174  1   180.008427  1   21   20   19
H     1.100721  1   118.184243  1   180.003354  1   22   21   20
H     1.100614  1   119.714592  1   179.996241  1   23   22   21
H     1.097659  1   120.409108  1   180.011363  1   24   23   22
0     0.000000  0     0.000000  0     0.000000  0    0    0    0
```

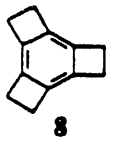

8

```
 $CONTRL  SCFTYP=RHF  TIMLIM=100000 RUNTYP=OPTIMIZE COORD=ZMT  $END
 $BASIS  GBASIS=N21 NGAUS=3 $END
 D$NBO  ARCHIVE  RESONANCE  $END
 $DEL  NOSTAR  $END
 $DATA
triscyclobutanobenzene  ...  rhf/3-21G//rhf/3-21G
Dnh 3

 C
 C       1    1.4074808
 C       2    1.3611968  1    120.0000000
 C       3    1.4074808  2    120.0000000  1      0.0000000  0
 C       4    1.3611968  3    120.0000000  2      0.0000000  0
 C       5    1.4074808  4    120.0000000  3      0.0000000  0
 C       1    1.5375586  2     93.5540334  3    180.0000000  0
 C       2    1.5375586  1     93.5540334  6   -180.0000000  0
 C       3    1.5375586  4     93.5540334  5   -180.0000000  0
 C       4    1.5375586  3     93.5540334  2   -180.0000000  0
 C       5    1.5375586  6     93.5540334  1   -180.0000000  0
 C       6    1.5375586  5     93.5540334  4   -180.0000000  0
 H       7    1.0808324  1    114.9320705  6    -65.0022023  0
 H       7    1.0808324  1    114.9320705  6     65.0022023  0
 H       8    1.0808324  2    114.9320705  3    -65.0022023  0
 H       8    1.0808324  2    114.9320705  3     65.0022023  0
 H       9    1.0808324  3    114.9320705  2    -65.0022023  0
 H       9    1.0808324  3    114.9320705  2     65.0022023  0
 H      10    1.0808324  4    114.9320705  5    -65.0022023  0
 H      10    1.0808324  4    114.9320705  5     65.0022023  0
 H      11    1.0808324  5    114.9320705  4    -65.0022023  0
 H      11    1.0808324  5    114.9320705  4     65.0022023  0
 H      12    1.0808324  6    114.9320705  1    -65.0022023  0
 H      12    1.0808324  6    114.9320705  1     65.0022023  0
 $END
```

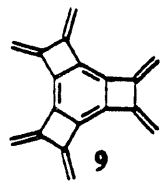

9

```
 $CONTRL  SCFTYP=RHF  RUNTYP=ENERGY  COORD=ZMT  $END
 $BASIS  GBASIS=N21  NGAUSS=3  $END
 $NBO  RESONANCE  $END
 $DATA
tris(methylenecyclobuta)benzene  ...  rhf/3-21g//rhf/3-21g
Dnh 3

 C
 C       1   1.4244306
 C       2   1.3582869  1   120.0000000
 C       3   1.4244306  2   120.0000000  1       .0000000  0
 C       4   1.3582869  3   120.0000000  2       .0000000  0
 C       5   1.4244306  4   120.0000000  3       .0000000  0
 C       1   1.5005680  2    92.0042357  3   -180.0000000  0
 C       7   1.3123326  1   136.4629382  6       .0000000  0
 C       2   1.5005680  1    92.0042357  6    180.0000000  0
 C       9   1.3123326  2   136.4629382  3       .0000000  0
 C       3   1.5005680  4    92.0042357  5   -180.0000000  0
 C      11   1.3123326  3   136.4629382  2       .0000000  0
 C       4   1.5005680  3    92.0042357  2   -180.0000000  0
 C      13   1.3123326  4   136.4629382  5       .0000000  0
 C       5   1.5005680  6    92.0042357  1    180.0000000  0
 C      15   1.3123326  5   136.4629382  4       .0000000  0
 C       6   1.5005680  5    92.0042357  4   -180.0000000  0
 C      17   1.3123326  6   136.4629382  1       .0000000  0
 H       8   1.0725027  7   121.5231289  1       .0000000  0
 H       8   1.0728805  7   121.4304519  1   -180.0000000  0
 H      10   1.0725027  9   121.5231289  2       .0000000  0
 H      10   1.0728805  9   121.4304519  2    180.0000000  0
 H      12   1.0725027 11   121.5231289  3       .0000000  0
 H      12   1.0728805 11   121.4304519  3    180.0000000  0
 H      14   1.0725027 13   121.5231289  4       .0000000  0
 H      14   1.0728805 13   121.4304519  4    180.0000000  0
 H      16   1.0725027 15   121.5231289  5       .0000000  0
 H      16   1.0728805 15   121.4304519  5    180.0000000  0
 H      18   1.0725027 17   121.5231289  6       .0000000  0
 H      18   1.0728805 17   121.4304519  6    180.0000000  0
 $end
```

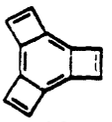

10

```
 $CONTRL  SCFTYP=RHF  RUNTYP=ENERGY  COORD=ZMT  $END
 $BASIS  GBASIS=N21  NGAUSS=3  $END
 $NBO  ARCHIVE  RESONANCE  $END
 $DATA
Triscyclobutenobenzene  ...  rhf/3-21g//rhf/3-21g
Dnh 3

 C
 C       1    1.5237931
 C       2    1.3092120  1   120.0000000
 C       3    1.5237931  2   120.0000000  1     0.0000000  0
 C       4    1.3092120  3   120.0000000  2     0.0000000  0
 C       5    1.5237931  4   120.0000000  3     0.0000000  0
 C       1    1.5031042  2    86.6472091  3  -180.0000000  0
 C       2    1.5031042  1    86.6472091  6   180.0000000  0
 C       3    1.5031042  4    86.6472091  5   180.0000000  0
 C       4    1.5031042  3    86.6472091  2   180.0000000  0
 C       5    1.5031042  6    86.6472091  1   180.0000000  0
 C       6    1.5031042  5    86.6472091  4   180.0000000  0
 H       7    1.0654868  1   133.1714078  6     0.0000000  0
 H       8    1.0654868  2   133.1714078  3     0.0000000  0
 H       9    1.0654868  3   133.1714078  2     0.0000000  0
 H      10    1.0654868  4   133.1714078  5     0.0000000  0
 H      11    1.0654868  5   133.1714078  4     0.0000000  0
 H      12    1.0654868  6   133.1714078  1     0.0000000  0
 $END
```

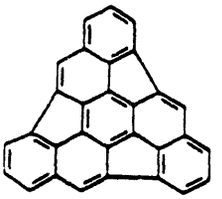

13

```
PM3 PRECISE SYMMETRY T=2400M

c3
XX    0.000000  0    0.000000  0    0.000000  0   0   0   0
 C    1.391492  1    0.000000  0    0.000000  0   1   0   0
XX    1.000000  0   90.000000  0    0.000000  0   1   2   0
 C    1.391492  0   90.000000  0  120.000000  0   1   3   2
 C    1.391492  0   90.000000  0 -120.000000  0   1   3   2
 C    1.421164  1   90.000000  0  -58.404819  1   1   3   2
 C    1.421164  0   90.000000  0  120.000000  0   1   3   6
 C    1.421164  0   90.000000  0 -120.000000  0   1   3   6
 C    1.420482  1  119.529888  1  139.869845  1   2   6   5
 C    1.420482  0  119.529888  0  139.869845  0   5   8   4
 C    1.420482  0  119.529888  0  139.869845  0   4   7   2
 C    1.442959  1  109.738835  1 -150.049281  1   9   2   6
 C    1.442959  0  109.738835  0 -150.049281  0  10   5   8
 C    1.442959  0  109.738835  0 -150.049281  0  11   4   7
 C    1.394910  1  120.840026  1    8.205119  1   9   2   6
 C    1.394910  0  120.840026  0    8.205119  0  10   5   8
 C    1.394910  0  120.840026  0    8.205119  0  11   4   7
 C    1.453801  1  109.682887  1  143.311765  1   7   2   6
 C    1.453801  0  109.682887  0  143.311765  0   6   5   8
 C    1.453801  0  109.682887  0  143.311765  0   8   4   7
 C    1.376642  1  118.703444  1 -151.818324  1  18   7   2
 C    1.376642  0  118.703444  0 -151.818324  0  19   6   5
 C    1.376642  0  118.703444  0 -151.818324  0  20   8   4
 C    1.369901  1  116.188000  1  174.606629  1  12   9   2
 C    1.369901  0  116.188000  0  174.606629  0  13  10   5
 C    1.369901  0  116.188000  0  174.606629  0  14  11   4
 C    1.424373  1  118.361804  1   -2.979608  1  24  12   9
 C    1.424373  0  118.361804  0   -2.979608  0  25  13  10
 C    1.424373  0  118.361804  0   -2.979608  0  26  14  11
 C    1.424015  1  113.846179  1 -174.503212  1  15   9   2
 C    1.424015  0  113.846179  0 -174.503212  0  16  10   5
 C    1.424015  0  113.846179  0 -174.503212  0  17  11   4
 H    1.095610  1  120.809724  1  179.488165  1  21  18   7
 H    1.095610  0  120.809724  0  179.488165  0  22  19   6
 H    1.095610  0  120.809724  0  179.488165  0  23  20   8
 H    1.094251  1  121.877219  1  179.858821  1  24  12   9
 H    1.094251  0  121.877219  0  179.858821  0  25  13  10
 H    1.094251  0  121.877219  0  179.858821  0  26  14  11
 H    1.095936  1  117.523521  1  176.311452  1  27  24  12
 H    1.095936  0  117.523521  0  176.311452  0  28  25  13
 H    1.095936  0  117.523521  0  176.311452  0  29  26  14
 H    1.095132  1  119.313087  1 -173.603292  1  30  15   9
 H    1.095132  0  119.313087  0 -173.603292  0  31  16  10
 H    1.095132  0  119.313087  0 -173.603292  0  32  17  11
 0    0.000000  0    0.000000  1    3.000000  0   0   0  0
```

15

```
 $CONTRL  TIMLIM=30000  SCFTYP=RHF  RUNTYP=ENERGY   COORD=ZMT
 $BASIS  GBASIS=N21  NGAUSS=3  $END
 $NBO  ARCHIVE RESONANCE  $END
 $DEL  NOSTAR  $END
 $DATA
meta-biscyclobutenobenzene...rhf/3-21g//rhf/3-21g
Cnv 2

C
C       1    1.4870512
C       1    1.3255418   2   117.3205485
C       2    1.3255418   1   117.3205485   3     0.0000000   0
C       3    1.4840753   1   124.7323014   2     0.0000000   0
C       4    1.4840753   2   124.7323014   1     0.0000000   0
C       3    1.5186796   5    87.1761236   1  -180.0000000   0
C       4    1.5186796   6    87.1761236   2   180.0000000   0
C       5    1.5187556   3    87.5140098   1   180.0000000   0
C       6    1.5187556   4    87.5140098   2  -180.0000000   0
H       1    1.0713715   2   119.0940298   4  -180.0000000   0
H       2    1.0713715   1   119.0940298   3   180.0000000   0
H       7    1.0655037   3   133.5693549   5  -180.0000000   0
H       8    1.0655037   4   133.5693549   6   180.0000000   0
H       9    1.0652996   5   133.5962967   3   180.0000000   0
H      10    1.0652996   6   133.5962967   4   180.0000000   0
 $END
```

16

```
# rhf/3-21g nosymm

para-biscyclobutenobenzene...rhf/3-21g//rhf/3-21g

0       1
C
C       1    1.3924154
C       2    1.3804965   1   123.9228279
C       3    1.3804965   2   112.1543441   1     0.0000000   0
C       4    1.3924154   3   123.9228279   2     0.0000000   0
C       5    1.3804965   4   123.9228279   3     0.0000000   0
C       1    1.5677499   2    88.8725997   3  -180.0000000   0
C       2    1.5677499   1    88.8725997   6  -180.0000000   0
C       4    1.5677499   5    88.8725997   6   180.0000000   0
C       5    1.5677499   4    88.8725997   3  -180.0000000   0
H       3    1.0703106   2   123.9228279   1  -180.0000000   0
H       6    1.0703106   5   123.9228279   4   180.0000000   0
H       7    1.0652360   1   134.1478238   2  -180.0000000   0
H       8    1.0652360   2   134.1478238   1  -180.0000000   0
H       9    1.0652360   4   134.1478238   5  -180.0000000   0
H      10    1.0652360   5   134.1478238   4   180.0000000   0
```

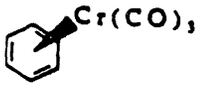

34

```
 $CONTRL  SCFTYP=RHF  RUNTYP=ENERGY  $END
 $SCF  ETHRSH=0.05  DAMP=.TRUE.  $END
 $GUESS  GUESS=MOREAD  $END
 $DATA
Benzene chromium tricarbonyl...rhf/wh-midi (staggered)
Cnv      3

 CR          24.0     .0000000000     .0000000000   -.1342012447
     S     4     1.00
     1 8177.5259       0.0175418
     2 1232.1457       0.1228663
     3  279.03868      0.4428574
     4   74.9971539    0.5508633
     S     3     1.00
     1  112.48983     -0.1050867
     2   12.095476     0.6289352
     3    5.0748415    0.4407752
     S     2     1.00
     1    9.8410604    0.2125861
     2    0.99637093 -1.074982
     P     4     1.00
     1  319.61171      0.0295675
     2   74.341057     0.1874726
     3   22.609200     0.5097071
     4    7.5085800    0.4507294
     P     2     1.00
     1    2.5272179    0.5017207
     2    0.75067260   0.5991726
     P     1     1.00
     1    0.10700000   1.0000000
     D     3     1.00
     1    8.5924219    0.1648948
     2    2.0666439    0.4996142
     3    0.46640362   0.6203377
     D     1     1.00
     1    0.15000000   1.0000000

 C            6.0    1.5676094333     .0000000000  -1.1563916540
   MIDI

 O            8.0    2.5659436621     .0000000000  -1.7233750739
   MIDI

 C            6.0    1.2086226177    -.7047061631   1.6907107088
   MIDI

 H            1.0    2.1392303699   -1.2397574762   1.6925433788
   MIDI

 $END
```

41

```
 $CONTRL  SCFTYP=RHF  RUNTYP=ENERGY  COORD=ZMT  $END
 $BASIS  GBASIS=N21  NGAUSS=3  $END
 $NBO  RESONANCE  $END
 $DEL  NOSTAR  $END
 $DATA
Benzocyclobutene...rhf/3-21g//rhf/3-21g
Cnv 2

C
C       1    1.5997199
C       1    1.5376867  2    86.0181598
C       2    1.5376867  1    86.0181598  3     0.0000000  0
C       3    1.3704115  4   122.2226762  2   180.0000000  0
C       4    1.3704115  3   122.2226762  1  -180.0000000  0
C       5    1.3964047  3   116.2289496  4     0.0000000  0
C       6    1.3964047  4   116.2289496  3     0.0000000  0
H       1    1.0807870  3   115.0017716  4   114.8141281  0
H       1    1.0807870  3   115.0017716  4  -114.8141281  0
H       2    1.0807870  4   115.0017716  3   114.8141281  0
H       2    1.0807870  4   115.0017716  3  -114.8141281  0
H       5    1.0718693  3   123.0271442  4  -180.0000000  0
H       6    1.0718693  4   123.0271442  3   180.0000000  0
H       7    1.0720611  5   119.3767394  3   180.0000000  0
H       8    1.0720611  6   119.3767394  4  -180.0000000  0
 $END
```

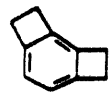

42

```
#N rhf/3-21g

meta-biscyclobutabenzene...rhf/3-21g//rhf/3-21g

0     1
C
C     1     CCa
C     1     CCb     2     alfa
C     2     CCb     1     alfa     3       0. 0
C     3     CCc     1     beta     2       0. 0
C     4     CCc     2     beta     1       0. 0
C     3     CCd     5     gama     6     180. 0
C     4     CCd     6     gama     5     180. 0
C     5     CCe     3     dlta     1     180. 0
C     6     CCe     4     dlta     2     180. 0
H     1     CHa     2     epsn     4     180. 0
H     2     CHa     1     epsn     3     180. 0
H     7     CHb     3     zeta     5      eta  0
H     7     CHb     3     zeta     5     -eta  0
H     8     CHb     4     zeta     6      eta  0
H     8     CHb     4     zeta     6     -eta  0
H     9     CHc     5     thta     3      kapa 0
H     9     CHc     5     thta     3     -kapa 0
H    10     CHc     6     thta     4      kapa 0
H    10     CHc     6     thta     4     -kapa 0

CCa           1.408
CCb           1.3717
CCc           1.397
CCd           1.5395
CCe           1.5364
CHa           1.0723
CHb           1.0809
CHc           1.0809
alfa        117.753
beta        123.9452
gama         93.56
dlta         93.9593
epsn        120.2782
zeta        115.018
eta         114.8831
thta        114.932
kapa        114.9381
```

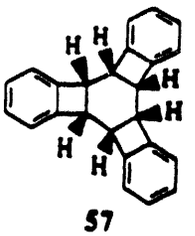

57

PM3 T=2400M PRECISE
triangulene - hexahydro, planar

C	0.000000	0	0.000000	0	0.000000	0	0	0	0	
C	1.407900	1	0.000000	0	0.000000	0	1	0	0	
C	1.386958	1	121.825804	1	0.000000	0	2	1	0	
C	1.408092	1	121.847444	1	0.023742	1	3	2	1	
C	1.369387	1	116.027346	1	-0.582744	1	4	3	2	
C	1.416075	1	122.136454	1	0.593544	1	5	4	3	
C	1.514521	1	93.471804	1	177.068259	1	6	5	4	
C	1.599143	1	86.556257	1	0.079829	1	7	6	5	
C	1.501912	1	120.030502	1	121.818547	1	8	7	6	
C	1.600256	1	120.073833	1	1.679084	1	9	8	7	
C	1.503018	1	119.822125	1	-1.932222	1	10	9	8	
C	1.599615	1	120.076743	1	0.852525	1	11	10	9	
C	1.514821	1	86.454480	1	-123.494280	1	10	9	8	
C	1.416378	1	93.519546	1	0.679371	1	13	10	9	
C	1.369495	1	122.138992	1	-177.671648	1	14	13	10	
C	1.407900	1	115.988124	1	-0.432752	1	15	14	13	
C	1.386737	1	121.886537	1	0.630073	1	16	15	14	
C	1.407633	1	121.827186	1	-0.176806	1	17	16	15	
C	1.514552	1	86.562950	1	-121.803141	1	12	11	10	
C	1.416363	1	93.436595	1	-0.215054	1	19	12	11	
C	1.369341	1	122.088962	1	-176.970130	1	20	19	12	
C	1.407696	1	116.030939	1	-0.702967	1	21	20	19	
C	1.386793	1	121.898775	1	0.599344	1	22	21	20	
C	1.408023	1	121.780698	1	0.082352	1	23	22	21	
H	1.093737	1	122.689321	1	179.812178	1	1	6	5	
H	1.095091	1	118.759557	1	-179.506948	1	2	1	6	
H	1.095058	1	119.402653	1	179.953917	1	3	2	1	
H	1.093697	1	121.285388	1	179.717131	1	4	3	2	
H	1.113034	1	124.389177	1	113.720370	1	7	11	10	
H	1.112909	1	110.260123	1	126.284874	1	8	7	11	
H	1.113296	1	109.169591	1	129.084133	1	9	8	7	
H	1.112659	1	110.368554	1	125.199321	1	10	9	8	
H	1.112998	1	108.366310	1	128.709852	1	11	10	9	
H	1.113064	1	110.222634	1	127.341130	1	12	11	10	
H	1.093724	1	122.681543	1	179.948812	1	15	14	13	
H	1.095124	1	118.718173	1	-179.445345	1	16	15	14	
H	1.095087	1	119.391812	1	179.866400	1	17	16	15	
H	1.093727	1	121.284393	1	179.817407	1	18	17	16	
H	1.093766	1	122.699292	1	179.811517	1	21	20	19	
H	1.095154	1	118.739041	1	-179.429301	1	22	21	20	
H	1.095055	1	119.399281	1	180.009856	1	23	22	21	
H	1.093744	1	121.293494	1	179.938537	1	24	23	22	
0	0.000000	0	0.000000	1	0.000000	0	0	0	0	0

60

```
PM3 PRECISE T=2400M
chair cyclohexane
d3d
C     0.000000  0    0.000000  0    0.000000  0   0   0   0
C     1.521036  1    1.000000  0    0.000000  0   1   0   0
C     1.521001  1  110.969640  1    0.000000  0   2   1   0
C     1.520682  1  111.069254  1  -55.940612  1   3   2   1
C     1.520836  1  111.059230  1   55.911631  1   4   3   2
C     1.521032  1  110.982616  1  -55.936324  1   5   4   3
H     1.108305  1  109.843033  1   65.540212  1   1   6   5
H     1.106935  1  110.072197  1 -178.258293  1   1   6   5
H     1.106799  1  110.080600  1  178.164982  1   2   1   6
H     1.108244  1  109.851846  1  -65.618384  1   2   1   6
H     1.108275  1  109.816076  1   65.741524  1   3   2   1
H     1.106843  1  110.066500  1 -178.098753  1   3   2   1
H     1.106841  1  110.046401  1  178.050897  1   4   3   2
H     1.108278  1  109.835462  1  -65.783981  1   4   3   2
H     1.108202  1  109.858977  1   65.730018  1   5   4   3
H     1.106782  1  110.074995  1 -178.054397  1   5   4   3
H     1.106897  1  110.069736  1  178.183925  1   6   5   4
H     1.108072  1  109.856150  1  -65.641990  1   6   5   4
0     0.000000  0    0.000000  0    0.000000  0   0   0   0
```

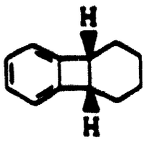

61

```
PM3 PRECISE T=2400M
biphenylene_h6
C     0.000000  0    0.000000  0    0.000000  0   0   0   0
C     1.601733  1    1.000000  0    0.000000  0   1   0   0
C     1.511524  1  118.728506  1    0.000000  0   2   1   0
C     1.517939  1  113.607468  1  -19.752349  1   3   2   1
C     1.518183  1  110.572996  1   50.609534  1   4   3   2
C     1.518044  1  110.816822  1  -68.730259  1   5   4   3
C     1.516447  1   86.384908  1  120.975403  1   1   2   3
C     1.416571  1   93.512627  1   -1.576968  1   7   1   2
C     1.368564  1  122.208477  1 -179.176440  1   8   7   1
C     1.408542  1  115.901076  1   -0.256385  1   9   8   7
C     1.386942  1  121.908760  1    0.035165  1  10   9   8
C     1.408785  1  121.874712  1    0.161161  1  11  10   9
H     1.109337  1  110.929062  1  109.743577  1   1   6   5
H     1.111381  1  111.359295  1  134.009058  1   2   1   6
H     1.108941  1  108.907377  1  101.900702  1   3   2   1
H     1.107601  1  109.149095  1 -143.086806  1   3   2   1
H     1.107195  1  109.623102  1  172.393330  1   4   3   2
H     1.108032  1  110.456476  1  -71.383978  1   4   3   2
H     1.108110  1  110.007447  1   53.692560  1   5   4   3
H     1.107293  1  110.182344  1  169.894732  1   5   4   3
H     1.107470  1  109.586933  1  174.948622  1   6   5   4
H     1.109163  1  109.323648  1  -70.088575  1   6   5   4
H     1.092994  1  122.701072  1  179.648569  1   9   8   7
H     1.095139  1  118.738121  1  180.024423  1  10   9   8
H     1.095109  1  119.377557  1 -179.915779  1  11  10   9
H     1.092928  1  121.336317  1  179.672787  1  12  11  10
0     0.000000  0    0.000000  0    0.000000  0   0   0   0
```

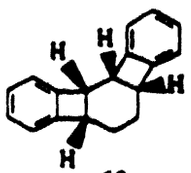

62

```
PM3 PRECISE FORCE T=2400M
hexahydro angular[3]
twist-boat
C     0.000000  0    0.000000  0    0.000000  0   0   0   0
C     1.408755  1    0.000000  0    0.000000  0   1   0   0
C     1.386782  1  121.911192  1    0.000000  0   2   1   0
C     1.408757  1  121.894015  1    0.023003  1   3   2   1
C     1.368807  1  115.933971  1    0.075139  1   4   3   2
C     1.418237  1  122.147773  1   -0.151478  1   5   4   3
C     1.513444  1   93.438274  1  179.708352  1   6   5   4
C     1.600395  1   86.585401  1   -0.435573  1   7   6   5
C     1.506299  1  117.621951  1  120.708381  1   8   7   6
C     1.602505  1  116.554989  1   22.826083  1   9   8   7
C     1.511786  1  116.321316  1   -5.350442  1  10   9   8
C     1.519930  1  112.215921  1  -38.288777  1  11  10   9
C     1.514959  1   86.515540  1 -122.414618  1  10   9   8
C     1.416922  1   93.475400  1    1.101494  1  13  10   9
C     1.368949  1  122.133111  1 -179.725899  1  14  13  10
C     1.408325  1  115.951547  1    0.113019  1  15  14  13
C     1.387062  1  121.893831  1    0.037491  1  16  15  14
C     1.408563  1  121.882275  1   -0.132681  1  17  16  15
H     1.092911  1  122.767465  1 -179.907963  1   1   6   5
H     1.095148  1  118.734632  1  180.060665  1   2   1   6
H     1.095119  1  119.374309  1 -179.898386  1   3   2   1
H     1.093235  1  121.324652  1 -179.506070  1   4   3   2
H     1.108013  1  109.502291  1   83.982059  1  11  10   9
H     1.106921  1  110.362551  1 -173.578006  1  12  11  10
H     1.094081  1  122.404169  1 -179.034092  1  15  14  13
H     1.095121  1  118.736165  1 -179.851309  1  16  15  14
H     1.095109  1  119.382446  1  179.971669  1  17  16  15
H     1.092935  1  121.369065  1 -179.789365  1  18  17  16
H     1.109975  1  111.039459  1   82.679107  1   7  12  11
H     1.111300  1  111.253312  1  130.467676  1   8   7  12
H     1.111200  1  109.548713  1  151.177040  1   9   8   7
H     1.109545  1  112.646868  1  123.922703  1  10   9   8
H     1.107400  1  109.043896  1 -160.325840  1  11  10   9
H     1.108634  1  109.821791  1  -57.247571  1  12  11  10
0     0.000000  0    0.000000  0    0.000000  0   0   0   0
```

65

PM3 PRECISE T=2400M
c6h12 mimic: biphe_h6

C	0.000000	0	0.000000	0	0.000000	0	0	0	0
C	1.576361	1	1.000000	0	0.000000	0	1	0	0
C	1.507642	1	118.731058	1	2.000000	0	2	1	0
C	1.517292	1	113.196135	1	-21.797791	1	3	2	1
C	1.517879	1	110.090181	1	53.014748	1	4	3	2
C	1.517536	1	110.639582	1	-68.274494	1	5	4	3
H	1.107913	1	90.000000	0	120.967523	1	1	2	3
H	1.100250	1	111.567286	1	113.189446	1	1	6	5
H	1.108102	1	90.000000	0	0.000000	0	2	1	7
H	1.102557	1	110.934770	1	133.747161	1	2	1	6
H	1.109040	1	109.344786	1	99.880833	1	3	2	1
H	1.107290	1	109.384675	1	-145.006491	1	3	2	1
H	1.107105	1	109.811778	1	174.694999	1	4	3	2
H	1.107870	1	110.569035	1	-68.905123	1	4	3	2
H	1.108086	1	109.934168	1	53.987815	1	5	4	3
H	1.107268	1	110.306765	1	170.188577	1	5	4	3
H	1.107547	1	109.444625	1	172.569757	1	6	5	4
H	1.108867	1	109.016430	1	-72.874518	1	6	5	4
0	0.000000	0	0.000000	0	0.000000	0	0	0	0

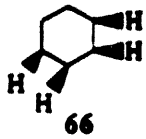

66

PM3 PRECISE T=2400M
cyclohexane:mimic ang3_h6

C	0.000000	0	0.000000	0	0.000000	0	0	0	0
C	1.576186	1	1.000000	0	0.000000	0	1	0	0
C	1.497951	1	117.234142	1	2.000000	0	2	1	0
C	1.577197	1	117.323707	1	24.397231	1	3	2	1
C	1.506939	1	115.578056	1	-0.827751	1	4	3	2
C	1.519722	1	110.326195	1	-43.722256	1	5	4	3
H	1.108537	1	90.000000	0	-119.666229	1	1	2	3
H	1.099667	1	112.577555	1	127.704517	1	1	2	3
H	1.108003	1	90.000000	0	0.000000	0	2	1	7
H	1.101284	1	111.735375	1	-132.284792	1	2	1	6
H	1.107420	1	90.000000	0	-119.302450	1	3	4	5
H	1.100927	1	111.291121	1	129.017210	1	3	4	5
H	1.106760	1	90.000000	0	0.000000	0	4	3	11
H	1.100972	1	111.568447	1	-129.705637	1	4	3	2
H	1.108148	1	109.824027	1	-56.297119	1	5	6	1
H	1.106955	1	110.378217	1	-172.329344	1	5	6	1
H	1.107085	1	110.232983	1	65.077756	1	6	5	15
H	1.107655	1	109.966216	1	-56.203893	1	6	5	4
0	0.000000	0	0.000000	0	0.000000	0	0	0	0

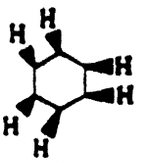

67

PM3 PRECISE T=2400M GEO-OK
cyclohexane:mimic triang_h6

C	0.000000	0	0.000000	0	0.000000	0	0	0	0	
C	1.569759	1	1.000000	0	0.000000	0	1	0	0	
C	1.493546	1	119.996851	1	2.000000	0	2	1	0	
C	1.570294	1	120.075073	1	-0.185265	1	3	2	1	
C	1.494319	1	119.889557	1	0.316457	1	4	3	2	
C	1.569605	1	120.038590	1	-0.260426	1	5	4	3	
H	1.108674	1	90.000000	0	-119.112062	1	1	2	3	
H	1.102262	1	110.508902	1	130.385827	1	1	2	3	
H	1.108573	1	90.000000	0	0.000000	0	2	1	7	
H	1.102294	1	110.482339	1	-130.392925	1	2	1	6	
H	1.108549	1	90.000000	0	-118.942561	1	3	4	5	
H	1.102370	1	110.425852	1	130.657559	1	3	4	5	
H	1.108509	1	90.000000	0	0.000000	0	4	3	11	
H	1.102125	1	110.540485	1	-130.130871	1	4	3	2	
H	1.108613	1	90.000000	0	-119.063117	1	5	6	1	
H	1.102325	1	110.481669	1	130.451754	1	5	6	1	
H	1.108616	1	90.000000	0	0.000000	0	6	5	15	
H	1.101996	1	110.475958	1	-130.346526	1	6	5	4	
O	0.000000	0	0.000000	0	0.000000	0	0	0	0	

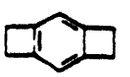

68

rhf/3-21g nosymm

para-biscyclobutenobenzene...rhf/3-21g//rhf/3-21g

O	1						
C							
C	1	1.3924154					
C	2	1.3804965	1	123.9228279			
C	3	1.3804965	2	112.1543441	1	0.0000000	0
C	4	1.3924154	3	123.9228279	2	0.0000000	0
C	5	1.3804965	4	123.9228279	3	0.0000000	0
C	1	1.5677499	2	88.8725997	3	-180.0000000	0
C	2	1.5677499	1	88.8725997	6	-180.0000000	0
C	4	1.5677499	5	88.8725997	6	180.0000000	0
C	5	1.5677499	4	88.8725997	3	-180.0000000	0
H	3	1.0703106	2	123.9228279	1	-180.0000000	0
H	6	1.0703106	5	123.9228279	4	180.0000000	0
H	7	1.0652360	1	134.1478238	2	-180.0000000	0
H	8	1.0652360	2	134.1478238	1	-180.0000000	0
H	9	1.0652360	4	134.1478238	5	-180.0000000	0
H	10	1.0652360	5	134.1478238	4	180.0000000	0

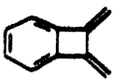

69

```
 $CONTRL  SCFTYP=RHF  RUNTYP=ENERGY  COORD=ZMT  $END
 $BASIS  GBASIS=N21  NGAUSS=3  $END
 $NBO  RESONANCE  $END
 $DEL  NOSTAR  $END
 $DATA
C10H8...methylenebenzocyclobutabenzene ...rhf/3-21g//rhf/3-21g
Cnv 2

C
C       1    1.5301849
C       1    1.5039284  2     87.4727396
C       2    1.5039284  1     87.4727396  3      0.0000000  0
C       3    1.3703146  4    122.2129670  2    180.0000000  0
C       4    1.3703146  3    122.2129670  1   -180.0000000  0
C       5    1.3962757  3    116.0234137  4      0.0000000  0
C       6    1.3962757  4    116.0234137  3      0.0000000  0
C       1    1.3118818  2    135.3568137  4   -180.0000000  0
C       2    1.3118818  1    135.3568137  3    180.0000000  0
H       5    1.0711092  3    123.0018692  4   -180.0000000  0
H       6    1.0711092  4    123.0018692  3    180.0000000  0
H       7    1.0721683  5    119.3294317  3   -180.0000000  0
H       8    1.0721683  6    119.3294317  4    180.0000000  0
H       9    1.0731620  1    121.3033652  2      0.0000000  0
H       9    1.0726213  1    121.6890203  2    180.0000000  0
H      10    1.0731620  2    121.3033652  1      0.0000000  0
H      10    1.0726213  2    121.6890203  1   -180.0000000  0
 $END
```

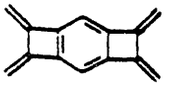

70

```
#n  rhf/3-21g

para-bis(dimethylenecyclobuta)benzene

0  1
x
x  1  1.0
c  1  cx   2  90.0
c  1  cx   2  90.0  3  180.0 0
c  3  cca  1  alfa  2   90.0 0
c  3  cca  1  alfa  2  270.0 0
c  4  cca  1  alfa  2   90.0 0
c  4  cca  1  alfa  2  270.0 0
c  5  ccb  3  beta  6  180.0 0
c  6  ccb  3  beta  5  180.0 0
c  7  ccb  4  beta  8  180.0 0
c  8  ccb  4  beta  7  180.0 0
c  9  ccd  5  gama  3    0.0 0
c 10  ccd  6  gama  3    0.0 0
c 11  ccd  7  gama  4    0.0 0
c 12  ccd  8  gama  4    0.0 0
h  1  cha  2  90.0  3    0.0 0
h  1  cha  2  90.0  4    0.0 0
h 13  chb  9  epsi  5    0.0 0
h 13  chc  9  zeta  5  180.0 0
h 14  chb 10  epsi  6    0.0 0
h 14  chc 10  zeta  6  180.0 0
h 15  chb 11  epsi  7    0.0 0
h 15  chc 11  zeta  7  180.0 0
h 16  chb 12  epsi  8    0.0 0
h 16  chc 12  zeta  8  180.0 0

cx          1.4708
cca         1.3814
ccb         1.5017
ccd         1.3122
cha         2.5411
chb         1.0729
chc         1.073
alfa       56.2143
beta      143.8665
gama      136.7817
epsi      121.6372
zeta      121.3788

 $nbo resonance $end
```

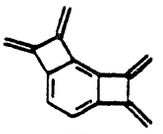

71

```
#n  rhf/3-21g

meta-bis(dimethylenecyclobuta)benzene

0   1
c
c   1  ca
c   1  cb   2  alfa
c   2  cb   1  alfa   3    0.0
c   3  cc   1  beta   2  180.0
c   4  cc   2  beta   1  180.0
c   5  cd   3  gama   1    0.0
c   6  cd   4  gama   2    0.0
c   3  ce   1  delta  2    0.0
c   4  ce   2  delta  1    0.0
c   9  cf   3  epsi   1  180.0
c  10  cf   4  epsi   2  180.0
c  11  cg   9  zeta   3  180.0
c  12  cg  10  zeta   4  180.0
h   1  ch   2  teta   4  180.0
h   2  ch   1  teta   3  180.0
h   7  cha  5  kapa   3    0.0
h   7  chb  5  theta  3  180.0
h   8  cha  6  kapa   4    0.0
h   8  chb  6  theta  4  180.0
h  13  chc 11  omega  9  180.0
h  13  chd 11  sigma  9    0.0
h  14  chc 12  omega 10  180.0
h  14  chd 12  sigma 10    0.0

ca          1.4084
cb          1.3717
cc          1.5038
cd          1.3122
ce          1.4103
cf          1.501
cg          1.3121
ch          1.0714
cha         1.0728
chb         1.073
chc         1.0729
chd         1.0726
alfa      117.7798
beta      143.7606
gama      136.8203
delta     124.1398
epsi       92.4724
zeta      136.6121
teta      120.2721
kapa      121.6005
theta     121.4204
omega     121.3897
sigma     121.5647
```

72

```
 $CONTRL  SCFTYP=RHF  RUNTYP=ENERGY  COORD=ZMT  $END
 $BASIS  GBASIS=N21  NGAUSS=3  $END
 $NBO  RESONANCE  $END
 $DEL  NOSTAR  $END
 $DATA
Benzocyclobutadiene...rhf/3-21g//rhf/3-21g
Cnv 2

C
C       1   1.3366400
C       1   1.5457380  2    91.6503960
C       2   1.5457380  1    91.6503960  3     0.0000000  0
C       3   1.3392387  4   122.6283277  2   180.0000000  0
C       4   1.3392387  3   122.6283277  1  -180.0000000  0
C       5   1.4376416  3   115.6561309  4     0.0000000  0
C       6   1.4376416  4   115.6561309  3     0.0000000  0
H       1   1.0653921  3   133.8832975  4   180.0000000  0
H       2   1.0653921  4   133.8832975  3  -180.0000000  0
H       5   1.0711256  3   123.8680886  4  -180.0000000  0
H       6   1.0711256  4   123.8680886  3   180.0000000  0
H       7   1.0718648  5   118.5506162  3   180.0000000  0
H       8   1.0718648  6   118.5506162  4   180.0000000  0
 $END
```

75

```
 $CONTRL  SCFTYP=RHF  RUNTYP=ENERGY  $END
 $SCF  DIRSCF=.FALSE.  ETHRSH=0.01  DAMP=.TRUE.  $END
 $GUESS  GUESS=MOREAD  $END
 $DATA
Triscyclobutabenzene chromium tricarbonyl (staggered)
Cnv      3

 CR          24.0     .0000000000     .0000000000   -.6785369289
      S     4     1.00
      1 8177.5259        0.0175418
      2 1232.1457        0.1228663
      3  279.03868       0.4428574
      4   74.9971539     0.5508633
      S     3     1.00
      1  112.48983      -0.1050867
      2   12.095476      0.6289352
      3    5.0748415     0.4407752
      S     2     1.00
      1    9.8410604     0.2125861
      2    0.99637093 -1.074982
      P     4     1.00
      1  319.61171       0.0295675
      2   74.341057      0.1874726
      3   22.609200      0.5097071
      4    7.5085800     0.4507294
      P     2     1.00
      1    2.5272179     0.5017207
      2    0.75067260    0.5991726
      P     1     1.00
      1    0.10700000    1.0000000
      D     3     1.00
      1    8.5924219     0.1648948
      2    2.0666439     0.4996142
      3    0.46640362    0.6203377
      D     1     1.00
      1    0.15000000    1.0000000

 C            6.0    1.5631152321     .0000000000  -1.6672441285
   MIDI

 O            8.0    2.5955381443     .0000000000  -2.1787817732
   MIDI

 C            6.0    1.2018631005    -.7139511858   1.1818498838
   MIDI

 C            6.0    2.7301105893    -.7999999170   1.2557277634
   MIDI

 H            1.0    3.1080015005   -1.2416408650   2.1704336404
   MIDI

 H            1.0    3.2193674064   -1.2498997324    .4014362351
   MIDI

 $END
```

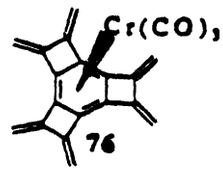

76

```
 $CONTRL  SCFTYP=RHF  RUNTYP=ENERGY  $END
 $SYSTEM  MEMORY=1500000  $END
 $SCF  DIRSCF=.FALSE.  ETHRSH=0.01  DAMP=.TRUE.  $END
 $GUESS  GUESS=MOREAD  $END
 $DATA
Tris(dimethylene)cyclobutabenzene chromium tricarbonyl (staggered)
CNV      3

 CR          24.0   0.0000000000   0.0000000000  -0.9260990379
     S    4    1.00
     1 8177.5259       0.0175418
     2 1232.1457       0.1228663
     3  279.03868      0.4428574
     4   74.9971539    0.5508633
     S    3    1.00
     1  112.48983     -0.1050867
     2   12.095476     0.6289352
     3    5.0748415    0.4407752
     S    2    1.00
     1    9.8410604    0.2125861
     2    0.99637093  -1.074982
     P    4    1.00
     1  319.61171      0.0295675
     2   74.341057     0.1874726
     3   22.609200     0.5097071
     4    7.5085800    0.4507294
     P    2    1.00
     1    2.5272179    0.5017207
     2    0.75067260   0.5991726
     P    1    1.00
     1    0.10700000   1.0000000
     D    3    1.00
     1    8.5924219    0.1648948
     2    2.0666439    0.4996142
     3    0.46640362   0.6203377
     D    1    1.00
     1    0.15000000   1.0000000

 C            6.0   1.5630684692   0.0000000000  -1.9541776036
   MIDI

 O            8.0   2.5500543857   0.0000000000  -2.5399340315
   MIDI

 C            6.0   1.2052473387  -0.7234416438   0.9412240624
   MIDI

 C            6.0   2.7006582445  -0.7596772583   0.9970947790
   MIDI

 C            6.0   3.6172052987  -1.6987364549   1.0431602866
   MIDI

 H            1.0   3.3564400738  -2.7421798141   1.0338738038
   MIDI

 H            1.0   4.6650482288  -1.4588111270   1.0857677943
   MIDI

 $END
```

77

```
 $CONTRL  SCFTYP=RHF  RUNTYP=ENERGY  $END
 $SCF  DIRSCF=.FALSE.  ETHRSH=0.01  DAMP=.TRUE.  $END
 $GUESS  GUESS=MOREAD  $END
 $DATA
Triscyclobutenobenzene chromium tricarbonyl (eclipsed)
Cnv 3

 CHROMIUM   24.0     .0000000000     .0000000000     .7639421185
     S    4    1.00
     1 8177.5259       0.0175418
     2 1232.1457       0.1228663
     3  279.03868      0.4428574
     4   74.9971539    0.5508633
     S    3    1.00
     1  112.48983     -0.1050867
     2   12.095476     0.6289352
     3    5.0748415    0.4407752
     S    2    1.00
     1    9.8410604    0.2125861
     2    0.99637093 -1.074982
     P    4    1.00
     1  319.61171      0.0295675
     2   74.341057     0.1874726
     3   22.609200     0.5097071
     4    7.5085800    0.4507294
     P    2    1.00
     1    2.5272179    0.5017207
     2    0.75067260   0.5991726
     P    1    1.00
     1    0.10700000   1.0000000
     D    3    1.00
     1    8.5924219    0.1648948
     2    2.0666439    0.4996142
     3    0.46640362   0.6203377
     D    1    1.00
     1    0.15000000   1.0000000

 CARBON      6.0  -1.5581361086     .0000000000    1.7779921325
     MIDI

 OXYGEN      8.0  -2.5372622725     .0000000000    2.3812091817
     MIDI

 CARBON      6.0   1.2555767017     .6627275458   -1.2243117748
     MIDI

 CARBON      6.0   1.9334971344    2.0045154329   -1.3194023241
     MIDI

 HYDROGEN    1.0   2.9618974979    2.2993641075   -1.3599641683
     MIDI

 $END
```

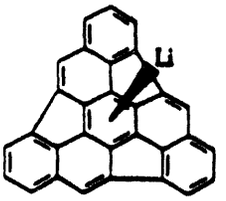

78

MNDO CHARGE=1 PRECISE SYMMETRY T=2400M
semibuckminsterfullerene - c30h12
c3

XX	0.000000	0	0.000000	0	0.000000	0	0	0	0
C	1.414241	1	0.000000	0	0.000000	0	1	0	0
XX	1.000000	0	90.000000	0	0.000000	0	1	2	0
C	1.414241	0	90.000000	0	120.000000	0	1	3	2
C	1.414241	0	90.000000	0	-120.000000	0	1	3	2
C	1.450307	1	90.000000	0	-58.415886	1	1	3	2
C	1.450307	0	90.000000	0	120.000000	0	1	3	6
C	1.450307	0	90.000000	0	-120.000000	0	1	3	6
C	1.437143	1	119.556067	1	139.506609	1	2	6	5
C	1.437143	0	119.556067	0	139.506609	0	5	8	4
C	1.437143	0	119.556067	0	139.506609	0	4	7	2
C	1.467993	1	109.907015	1	-151.663265	1	9	2	6
C	1.467993	0	109.907015	0	-151.663265	0	10	5	8
C	1.467993	0	109.907015	0	-151.663265	0	11	4	7
C	1.418685	1	120.786090	1	11.726069	1	9	2	6
C	1.418685	0	120.786090	0	11.726069	0	10	5	8
C	1.418685	0	120.786090	0	11.726069	0	11	4	7
C	1.477721	1	109.908840	1	143.291125	1	7	2	6
C	1.477721	0	109.908840	0	143.291125	0	6	5	8
C	1.477721	0	109.908840	0	143.291125	0	8	4	7
C	1.401518	1	117.452681	1	-154.312693	1	18	7	2
C	1.401518	0	117.452681	0	-154.312693	0	19	6	5
C	1.401518	0	117.452681	0	-154.312693	0	20	8	4
C	1.385955	1	114.691118	1	-177.821107	1	12	9	2
C	1.385955	0	114.691118	0	-177.821107	0	13	10	5
C	1.385955	0	114.691118	0	-177.821107	0	14	11	4
C	1.444070	1	118.647099	1	-5.229299	1	24	12	9
C	1.444070	0	118.647099	0	-5.229299	0	25	13	10
C	1.444070	0	118.647099	0	-5.229299	0	26	14	11
C	1.443747	1	112.360399	1	178.416768	1	15	9	2
C	1.443747	0	112.360399	0	178.416768	0	16	10	5
C	1.443747	0	112.360399	0	178.416768	0	17	11	4
H	1.091636	1	120.493685	1	-174.541386	1	21	18	7
H	1.091636	0	120.493685	0	-174.541386	0	22	19	6
H	1.091636	0	120.493685	0	-174.541386	0	23	20	8
H	1.090127	1	122.456590	1	176.483292	1	24	12	9
H	1.090127	0	122.456590	0	176.483292	0	25	13	10
H	1.090127	0	122.456590	0	176.483292	0	26	14	11
H	1.092750	1	117.100503	1	176.848823	1	27	24	12
H	1.092750	0	117.100503	0	176.848823	0	28	25	13
H	1.092750	0	117.100503	0	176.848823	0	29	26	14
H	1.090808	1	119.673302	1	-172.282491	1	30	15	9
H	1.090808	0	119.673302	0	-172.282491	0	31	16	10
H	1.090808	0	119.673302	0	-172.282491	0	32	17	11
Li	2.047561	1	90.000000	0	-90.000000	0	1	2	4
0	0.000000	0	0.000000	0	0.000000	0	0	0	0

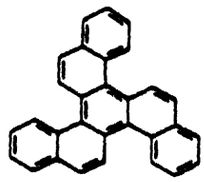

79

```
    PM3 PRECISE SYMMETRY T=2400M
    c30h18
    c3
XX    0.000000  0    0.000000  0    0.000000  0   0   0   0
 C    1.428563  1    0.000000  0    0.000000  0   1   0   0
XX    1.000000  0   90.000000  0    0.000000  0   1   2   0
 C    1.428563  0   90.000000  0  120.000000  0   1   3   2
 C    1.428563  0   90.000000  0 -120.000000  0   1   3   2
 C    1.414577  1   90.000000  0  -59.057871  1   1   3   2
 C    1.414577  0   90.000000  0  120.000000  0   1   3   6
 C    1.414577  0   90.000000  0 -120.000000  0   1   3   6
 C    1.455448  1  117.741302  1 -173.005865  1   2   6   5
 C    1.455448  0  117.741302  0 -173.005865  0   5   8   4
 C    1.455448  0  117.741302  0 -173.005865  0   4   7   2
 C    1.416686  1  123.780822  1  153.977900  1   9   2   6
 C    1.416686  0  123.780822  0  153.977900  0  10   5   8
 C    1.416686  0  123.780822  0  153.977900  0  11   4   7
 C    1.408559  1  119.380589  1  -21.063293  1   9   2   6
 C    1.408559  0  119.380589  0  -21.063293  0  10   5   8
 C    1.408559  0  119.380589  0  -21.063293  0  11   4   7
 C    1.437667  1  119.683399  1  164.950303  1   7   2   6
 C    1.437667  0  119.683399  0  164.950303  0   6   5   8
 C    1.437667  0  119.683399  0  164.950303  0   8   4   7
 C    1.353648  1  122.414564  1 -173.924404  1  18   7   2
 C    1.353648  0  122.414564  0 -173.924404  0  19   6   5
 C    1.353648  0  122.414564  0 -173.924404  0  20   8   4
 C    1.374789  1  121.652976  1  179.096380  1  12   9   2
 C    1.374789  0  121.652976  0  179.096380  0  13  10   5
 C    1.374789  0  121.652976  0  179.096380  0  14  11   4
 C    1.404918  1  120.591222  1    0.306724  1  24  12   9
 C    1.404918  0  120.591222  0    0.306724  0  25  13  10
 C    1.404918  0  120.591222  0    0.306724  0  26  14  11
 C    1.413497  1  121.035912  1 -176.916661  1  15   9   2
 C    1.413497  0  121.035912  0 -176.916661  0  16  10   5
 C    1.413497  0  121.035912  0 -176.916661  0  17  11   4
 H    1.098330  1  119.602427  1   -1.988812  1  12   9   2
 H    1.098330  0  119.602427  0   -1.988812  0  13  10   5
 H    1.098330  0  119.602427  0   -1.988812  0  14  11   4
 H    1.098620  1  118.868054  1    2.596655  1  18   7   2
 H    1.098620  0  118.868054  0    2.596655  0  19   6   5
 H    1.098620  0  118.868054  0    2.596655  0  20   8   4
 H    1.095842  1  121.232882  1  175.801124  1  21  18   7
 H    1.095842  0  121.232882  0  175.801124  0  22  19   6
 H    1.095842  0  121.232882  0  175.801124  0  23  20   8
 H    1.095158  1  120.051429  1  179.918006  1  24  12   9
 H    1.095158  0  120.051429  0  179.918006  0  25  13  10
 H    1.095158  0  120.051429  0  179.918006  0  26  14  11
 H    1.094657  1  120.817161  1  179.994598  1  27  30  15
 H    1.094657  0  120.817161  0  179.994598  0  28  31  16
 H    1.094657  0  120.817161  0  179.994598  0  29  32  17
 H    1.096185  1  119.049844  1  176.763918  1  30  15   9
 H    1.096185  0  119.049844  0  176.763918  0  31  16  10
 H    1.096185  0  119.049844  0  176.763918  0  32  17  11
 0    0.000000  0    0.000000  0    0.000000  0   0   0   0
```

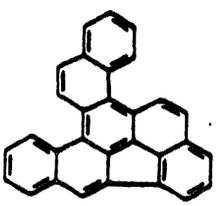

88

```
PM3 PRECISE T=2400M
c30h16
c1
C     0.000000  0    0.000000  0    0.000000  0   0   0   0
C     1.446701  1    1.000000  0    0.000000  0   1   0   0
C     1.423536  1  123.662768  1    2.000000  0   2   1   0
C     1.453584  1  118.743265  1   -3.313591  1   3   2   1
C     1.353662  1  118.179895  1   -1.975109  1   1   2   3
C     1.371786  1  113.260198  1    7.035272  1   4   3   2
C     1.460630  1  132.444363  1 -173.302317  1   4   3   2
C     1.422364  1  123.084242  1 -168.952776  1   7   4   3
C     1.415994  1  121.387030  1  176.330377  1   6   4   3
C     1.373083  1  126.783237  1   -2.007503  1   9   6   4
C     1.428933  1  118.825173  1   15.841919  1   7   4   3
C     1.357036  1  122.319222  1 -177.391452  1  11   7   4
C     1.424518  1  120.246286  1    3.858543  1  12  11   7
C     1.409378  1  119.277727  1   -5.719664  1  13  12  11
C     1.415635  1  119.978734  1  173.030458  1  13  12  11
C     1.371382  1  120.445267  1 -176.217643  1  15  13  12
C     1.418060  1  117.067380  1  173.983801  1  14  13  12
C     1.407389  1  119.418721  1    1.028922  1  16  15  13
C     1.415627  1  107.656521  1  176.680169  1   9   6   4
C     1.381773  1  121.459569  1 -177.984073  1  19   9   6
C     1.437514  1  114.717947  1    0.413368  1  20  19   9
C     1.374690  1  122.593497  1   -0.494057  1  21  20  19
C     1.431026  1  110.738769  1    0.649578  1  19   9   6
C     1.369854  1  115.971033  1 -179.523665  1  23  19   9
C     1.424829  1  118.237378  1    0.175685  1  24  23  19
C     1.420249  1  114.308527  1  179.488203  1  20  19   9
H     1.095247  1  119.333205  1  178.965110  1   1   2   3
C     1.411361  1  117.740526  1  173.779871  1   3   2   1
C     1.375566  1  121.679670  1    3.581463  1  28   3   2
C     1.402423  1  120.325584  1   -0.412901  1  29  28   3
C     1.374485  1  119.567819  1   -1.906106  1  30  29  28
H     1.098507  1  118.716491  1    5.181991  1  11   7   4
H     1.098276  1  119.565838  1 -175.366552  1  28   3   2
H     1.095118  1  120.160503  1  179.838173  1  29  28   3
H     1.094721  1  119.820553  1  178.914070  1  30  29  28
H     1.096750  1  119.853644  1 -178.510672  1  31  30  29
H     1.096248  1  120.934015  1 -177.392605  1  12  11   7
H     1.096097  1  118.906905  1    3.219024  1  15  13  12
H     1.094560  1  120.351733  1 -179.909324  1  16  15  13
H     1.098155  1  119.657848  1 -174.709861  1  17  14  13
H     1.095106  1  119.237613  1  177.404863  1  18  16  15
H     1.095788  1  117.717052  1  178.869937  1  21  20  19
H     1.098591  1  118.358736  1  178.504023  1  22  21  20
H     1.093978  1  122.063917  1  180.011463  1  24  23  19
H     1.096042  1  117.187441  1 -179.812668  1  25  24  23
H     1.094710  1  119.638009  1  179.699227  1  26  20  19
0     0.000000  0    0.000000  0    0.000000  0   0   0   0
```

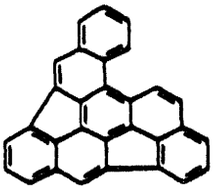

89

```
MNDO 1SCF BONDS PRECISE T=2400M
 c30h14
 c1
C     0.000000  0     0.000000  0     0.000000  0    0    0    0
C     1.477375  1     1.000000  0     0.000000  0    1    0    0
C     1.412338  1   118.329527  1     2.000000  0    2    1    0
C     1.422663  1   120.065605  1     3.212219  1    3    2    1
C     1.392418  1   121.670279  1     1.939948  1    1    2    3
C     1.358228  1   119.915459  1    -4.290076  1    4    3    2
C     1.433041  1   111.931161  1  -157.516273  1    4    3    2
C     1.408823  1   123.095901  1   158.096188  1    7    4    3
C     1.431273  1   115.529654  1  -152.384261  1    6    4    3
C     1.409443  1   126.313851  1     0.024258  1    9    6    4
C     1.474828  1   105.762366  1    -7.104508  1    7    4    3
C     1.368063  1   114.992773  1   176.422551  1   11    7    4
C     1.465076  1   119.616573  1     1.161638  1   12   11    7
C     1.467781  1   112.016256  1   179.392812  1    8    7    4
C     1.430823  1   118.543457  1   174.250643  1   13   12   11
C     1.389492  1   121.730418  1  -177.836132  1   15   13   12
C     1.428229  1   123.094369  1  -164.863047  1   14    8    7
C     1.416167  1   119.618678  1     0.802574  1   16   15   13
C     1.434759  1   103.238689  1   162.027971  1    9    6    4
C     1.400588  1   120.010166  1  -172.738971  1   19    9    6
C     1.454518  1   114.102071  1     1.778632  1   20   19    9
C     1.457551  1   109.988975  1   169.776183  1   10    9    6
C     1.468812  1   111.571865  1    -1.752832  1   19    9    6
C     1.381872  1   114.929827  1  -178.069763  1   23   19    9
C     1.442352  1   119.074197  1     1.767535  1   24   23   19
C     1.438950  1   113.886051  1   178.066272  1   20   19    9
H     1.090108  1   117.327413  1   176.496416  1    1    2    3
C     1.453125  1   129.941789  1  -157.107111  1    3    2    1
C     1.385334  1   114.040725  1   -13.260518  1   28    3    2
C     1.441199  1   118.414305  1     2.833253  1   29   28    3
C     1.439442  1   129.711290  1  -169.694324  1    2    1    3
H     1.089104  1   122.632334  1  -178.886500  1   29   28    3
H     1.092474  1   116.948207  1  -178.048204  1   30   29   28
H     1.090410  1   119.865263  1   -14.349234  1   31    2    1
H     1.090372  1   121.754960  1  -173.121731  1   12   11    7
H     1.092035  1   119.324692  1     1.648823  1   15   13   12
H     1.090317  1   120.603336  1  -179.896400  1   16   15   13
H     1.089938  1   119.974505  1     3.118122  1   17   14    8
H     1.090694  1   119.594753  1   178.057319  1   18   16   15
H     1.091782  1   117.640505  1  -177.863366  1   21   20   19
H     1.089924  1   119.294595  1   176.216009  1   22   10    9
H     1.089570  1   122.216203  1  -179.312893  1   24   23   19
H     1.092179  1   117.090394  1  -178.702654  1   25   24   23
H     1.090097  1   119.850342  1   177.058437  1   26   20   19
0     0.000000  0     0.000000  0     0.000000  0    0    0    0
```

References

1. Faraday, M. *Ann. Phys.* **1825**, *5*, 306.
2. Mitscherlich, E. *Ann. Chem.* **1834**, *9*, 39.
3. (a) Kekulé, A. *Ann. Chem.* **1857**, *54*, 9. (b) Kekulé, A. *Ann. Chem.* **1858**, *56*, 129.
4. For an account of historic developments and a critical evaluation of Kekulé's contribution to organic chemistry, see: Partington, J. R. *A History of Chemistry*; McMillan: London, 1964; Vol.4, pp 533 - 565.
5. Kekulé, A. *Bull. Soc. Chim. France* **1865**, *3*, 98. Interestingly, Kekulé used the term "châine fermée" rather than the expression "cycle".
6. Kekulé, A. *Ann. Chem.* **1872**, *162*, 77.
7. (a) Kermack, W. O.; Robinson, R. *J. Chem. Soc.* **1922**, *121*, 427. (b) Armit, J. W.; Robinson, R. *J. Chem. Soc.* **1925**, *127*, 1604. (c) Robinson, R. *Outline of an Electrochemical Theory of Organic Reactions*; Institute of Chemistry of Great Britain and Ireland: London, 1932.
8. (a) Ingold, C. K. *J. Chem. Soc.* **1922**, *121*, 1133. (b) Ingold, C. K.; Ingold, E. H. *J. Chem. Soc.* **1926**, *129*, 1310. (c) Ingold, C. K. *J. Chem. Soc.* **1933**, *136*, 1120. (d) Ingold, C. K. *Chem. Rev.* **1934**, *15*, 225.
9. (a) Pauling, L.; Wheland, G. W. *J. Chem. Phys.* **1933**, *1*, 362. (b) Wheland, G. W.; Pauling, L. *J. Am. Chem. Soc.* **1935**, *57*, 2086. (c) Pauling, L. *The Nature of the Chemical Bond*, 3rd ed.; University: Ithaca, 1960.
10. (a) Hückel, E. *Z. Physik* **1931**, *70*, 204 - 286. (b) Hückel, E. *Z. Physik* **1931**, *70*, 310. (c) Hückel, E. *Grundzüge und Theorie ungesättigter und aromatischer Verbindungen*; Chemie: Berlin, 1938.
11. (a) Angus, W. R.; Bailey, C. R.; Ingold, C. K., Wilson, C. L. *J. Chem. Soc.* **1936**, 912. (b) Angus, W. R.; Ingold, C. K. *J. Chem. Soc.* **1936**, 925. (c) Bailey, C. R.; Hale, J. B.; Ingold, C.K.; Thompson, J. W. *J. Chem. Soc.* **1936**, 931. (d) Ingold,

C. K.; Wilson, C. L *J. Chem. Soc.* **1936**, 941 - 966. (e) Angus, W. R.; Bailey, C. R.; Hale, J. B.; Ingold, C. K.; Leckie, A. H.; Raisin, C. G.; Thompson, J. W.; Wilson, C. L. *J. Chem. Soc.* **1936**, 966 - 987.

12. (a) X-ray structure of benzene: Cox, E. G.; Cruickshank, D. W. J.; Smith, J. A. S. *Proc. Roy. Soc.* **1958**, *A247*, 1. (b) Neutron diffraction of benzene: Bacon, G. E.; Curry, N. A.; Wilson, S. A. *Proc. Roy. Soc.* **1964**, *A279*, 98.

13. It was pointed out that because of underlying assumptions in the interpretation of X-ray and neutron diffraction data and/or insufficient resolution, these methods are unable to distinguish between Kekulé-type D_{3h} geometries and a regular D_{6h} form of benzene. See: Ermer, O. *Angew. Chem.* **1987**, *99*, 791. *Angew. Chem., Int. Ed. Engl.* **1987**, *26*, 782.

14. Haddon, R. C.; Raghavachari, K. *J. Am. Chem. Soc.* **1985**, *107*, 289 and references therein.

15. Coulson, C. A. *Valence*, 2nd ed.; Oxford: New York, 1961.

16. (a) Shaik, S. S.; Bar, R. *Nouv. J. Chim.* **1984**, *8*, 411. (b) Shaik, S. S.; Hiberty, P. C.; Ohanessian, G.; Lefour, J.-M. *Nouv. J. Chim.* **1985**, *9*, 385. (c) Hiberty, P. C.; Shaik, S. S.; Lefour, J.-M.; Ohanessian, G. *J. Org. Chem.* **1985**, *50*, 4657. (d) Shaik, S. S.; Hiberty, P. C. *J. Am. Chem. Soc.* **1985**, *107*, 3089. (e) Shaik, S. S.; Hiberty, P. C.; Lefour, J.-M.; Ohanessian, G. *J. Am. Chem. Soc.* **1987**, *109*, 363. (f) Shaik, S. S.; Hiberty, P. C.; Ohanessian, G.; Lefour, J.-M. *J. Chem. Phys.* **1988**, *92*, 5086. (g) Ohanessian, G.; Hiberty, P. C.; Lefour, J.-M.; Flament, J.-P.; Shaik, S. S. *Inorg. Chem.* **1988**, *27*, 2219. (h) Hiberty, P. C. In *Topics in Current Chemistry*; Gutman, I.; Cyvin, J. S., Eds.; Springer: New York, 1990; Vol. 153, p 27.

17. (a) Lloyd, D. *Non-Benzenoid Conjugated Cyclic Compounds*; Elsevier: New York, 1984. (b) Garratt, P. J. *Aromaticity*; Wiley: New York, 1986. (c) Lloyd, D. *The Chemistry of Conjugated Cyclic Compounds*; Wiley: New York, 1989.

18. (a) Watts, L.; Fitzpatrick, J. D.; Pettit, R. *J. Am. Chem. Soc.* **1965**, *87*, 3253. (b) Lin, C. Y.; Krantz, A. *J. Chem. Soc., Chem. Commun.* **1972**, 1111. (c) Chapman, O. L.; McIntosh, C. L.; Pacansky, J. *J. Am. Chem. Soc.* **1973**, *95*, 614. (d) Chapman, O. L.; De La Cruz, D.; Roth, R.; Pacansky, J. *J. Am. Chem. Soc.* **1973**, *95*, 1337. (e) Krantz, A.; Lin, C. Y.; Newton, M. *J. Am. Chem. Soc.* **1973**, *95*, 2744. (f) Cram, D. J.; Tamner, M. E.; Thomas, R. *Angew. Chem.* **1991**, *103*, 1048. *Angew. Chem., Int. Ed. Engl.* **1991**, *30*, 1024.19. For a review of biphenylene and its chemistry, see: (a) Cava, M. P.; Mitchell, M. J. *Cyclobutadiene and Related Compounds*; Academic: New York, 1967; pp 255 - 316. (b) Barton, J. W. L. In *Nonbenzenoid Aromatics*; Snyder, J. P., Ed.; Academic: New York, 1969; Vol. 1, pp 32 - 62. (c) Toda, F.; Garratt, P. *Chem. Rev.* **1992**, *92*, 1685.

20. (a) Berris, B. C.; Lai, Y.-H.; Vollhardt, K. P. C. *J. Chem. Soc., Chem. Commun.* **1982**, 953. (b) Berris, B. C.; Hovakeemian, G. H.; Vollhardt, K. P. C. *J. Chem. Soc., Chem. Commun.* **1983**, 502. (c) Hovakeemian, G. H.; Vollhardt, K. P. C. *Angew. Chem.* **1983**, *95*, 1001. *Angew. Chem., Int. Ed. Engl.* **1983**, *12*, 994. (d) Berris, B. C.; Hovakeemian, G. H.; Lai, Y.-H.; Mestdagh, H.; Vollhardt, K. P. C. *J. Am. Chem. Soc.* **1985**, *107*, 5670. (e) Hirthammer, M.; Vollhardt, K. P. C. *J. Am. Chem. Soc.* **1986**, *108*, 2481. (f) Bianco, L.; Helson, H. E.; Hirthammer, M.; Mestdagh, H.; Spyroudis, S.; Vollhardt, K. P. V. *Angew. Chem.* **1987**, *99*, 1276. *Angew. Chem., Int. Ed. Engl.* **1987**, *26*, 1246. For an alternative synthesis of linear [3]phenylene, see: (g) Barton, J. W.; Rowe, D. J. *Tetrahedron Lett.* **1983**, 299.

21. (a) Diercks, R.; Vollhardt, K. P. C. *Angew. Chem.* **1986**, *98*, 268. *Angew. Chem., Int. Ed. Engl.* **1986**, *25*, 266. (b) Schmidt-Radde, R. H.; Vollhardt, K. P. C. *J. Am. Chem. Soc.* **1992**, *114*, 9713. (c) Radde, R. H. Ph. D. Thesis, University of California, Berkeley, 1989. For an alternative synthesis of angular [3]phenylene, see: (d) Barton, J. W.; Walker, R. B. *Tetrahedron Lett.* **1978**, 1005.

22. (a) Diercks, R.; Vollhardt, K. P. C. *J. Am. Chem. Soc.* **1986**, *108*, 3150. The intermediacy of triangular [4]phenylene in the conversion of cinnolines to hexadehydrotribenzo[12]annulenes was suggested. See: (b) Barton, J. W.; Sheppard, M. K. *Tetrahedron Lett.* **1984**, 4967.

23. (a) Albright, T. A.; Hofman, P.; Hoffmann, R. *J. Am. Chem. Soc.* **1977**, *99*, 7546. (b) Albright, T. A.; *Acc. Chem. Res.* **1982**, *15*, 149.

24. Nambu, M.; Siegel, J. S. *J. Am. Chem. Soc.* **1988**, *110*, 3675. Also see ref 89.

25. Mohler, D. L. Ph. D. Thesis, University of California, Berkeley, 1992.

26. Mohler, D. L.; Vollhardt, K. P. C.; Wolff, S. *Angew. Chem.* **1990**, *102*, 1200. *Angew. Chem., Int. Ed. Engl.* **1990**, *29*, 1151.

27. Muetterties, E. L.; Bleeke, J. R. *Acc. Chem. Res.* **1979**, *12*, 324.

28. Krätschmer, W.; Lamb, L. D.; Fostiropoulos, K.; Huffman, D. R. *Nature* **1991**, *347*, 357.

29. (a) Scott, L. T.; Hashemi, M. M.; Meyer, D. T.; Warren, H. B. *J. Am. Chem. Soc.* **1991**, *113*, 7082. (b) Borchardt, A.; Fuchicello, A.; Kilway, K. V.; Baldridge, K. K.; Siegel, J. S. *J. Am. Chem. Soc.* **1992**, *114*, 1921.

30. Barth, W. E.; Lawton, R. G. *J. Am. Chem. Soc.* **1971**, *93*, 1730.

31. Hanson, J. C.; Nordman, C. E. *Acta Crystallogr., Sect. B* **1976**, *32*, 1147.

32. (a) Foster, J. P; Weinhold, F. *J. Am. Chem. Soc.* **1980**, *102*, 7211. (b) Reed, A. E.; Curtiss, L. A.; Weinhold, F. *Chem. Rev.* **1988**, *88*, 899. (c) Glendening, E. D.; Reed, A. E.; Carpenter, J. E.; Weinhold, F. *QCPE Bull.* **1990**, *10*, 58.

33. Glendening, E. D. Ph. D. Thesis, University of Wisconsin, Madison, 1991.

34. Robinson, R. In *Nonbenzenoid Aromatic Compounds*; Ginsberg, D., Ed.; Interscience: New York, 1959; p v.

35. See, for example: (a) Hammett, L. P. *Physical Organic Chemistry: Reaction Rates, Equilibria, and Mechanisms*, 2nd ed.; McGraw-Hill: New York, 1970; pp 101 - 145. Also (b) Eyring, H. *J. Chem. Phys.* **1935**, *3*, 107.

36. Breslow, R. *Acc. Chem. Res.* **1973**, *6*, 393.

37. (a) Jones, A. J. *Rev. Pure Appl. Chem.* **1968**, *18*, 253. (b) Bergman, E. D.; Pullman, B., Eds. *"Aromaticity, Pseudo-Aromaticity, Anti-Aromaticity"*; Israel Academy of Sciences and Humanities: Jerusalem, 1971.

38. The terms "resonance" and "delocalization" will be used interchangeably. See: (a) Peters, D. *J. Chem. Soc.* **1960**, 1274. (b) ref 39b, p 75. For alternative definitions of "delocalization energy", see: (c) Salem, L. *The Molecular Orbital Theory of Conjugated Systems*; Benjamin: New York, 1966; p 103. (d) Dewar, M. J. S.; Schmeising, H. W. *Tetrahedron* **1959**, *5*, 166.

39. (a) Wheland, G. W. *The Theory of Resonance and its Application to Organic Chemistry*; Wiley: New York, 1944. (b) Wheland, G. W. *Resonance in Organic Chemistry*; Wiley: New York, 1955.

40. Coulson, C. A.; Altman, S. L. *Trans. Faraday Soc.* **1952**, *48*, 293.

41. (a) Streitwieser, A., Jr. *Molecular Orbital Theory for Organic Chemists*; Wiley: New York, 1961. (b) Parmenter, C. S. *Adv. Chem. Phys.* **1972**, *22*, 365. For a compilation of experimentally derived values for β, see: (c) Karplus, M.; Porter, R. N. *Atoms and Molecules*; Benjamin/Cummings: Menlo Park, 1970; p 391.

42. (a) Longuett-Higgins, H. C. *J. Chem. Phys.* **1950**, *18*, 265. (b) Longuett-Higgins, H. C. *J. Chem. Phys.* **1950**, *18*, 275. (c) Longuett-Higgins, H. C. *J. Chem. Phys.* **1950**, *18*, 283. (d) Dewar, M. J. S. *The Molecular Orbital Theory of Organic Chemistry*; McGraw-Hill: New York, 1969; Chapter 6. (e) Dewar, M. J. S.; Dougherty, R. C. *The PMO Theory of Organic Chemistry*; Plenum: New York, 1975.

43. Aihara, J.; Ichikawa, H. *Bull. Chem. Soc. Jpn.* **1988**, *61*, 223 and references therein.

44. Dewar, M. J. S.; de Llano, C. *J. Am. Chem. Soc.* **1969**, *91*, 789.

45. Conant, J. B.; Kistiakowsky, G. B. *Chem. Rev.* **1937**, *20*, 181.

46. (a) Hess, B. A., Jr.; Schaad, L. J. *J. Am. Chem. Soc.* **1971**, *93*, 305. (b) Schaad, L. J.; Hess, B. A., Jr. *J. Am. Chem. Soc.* **1972**, *94*, 3068.

47. (a) Randic, M. *Chem. Phys. Lett.* **1976**, *38*, 68. (b) Randic, M. *J. Am. Chem. Soc.* **1977**, *99*, 444. (c) Randic, M. *Tetrahedron* **1977**, *31*, 1477. (d) Randic, M.; Nikolic, S.; Trinajstic, N. In *Graph Theory and Topology in Chemistry*; King, R. N.; Ronvray, D. H., Eds.; Elsevier: Amsterdam, 1987; pp 429 - 447. (e) Nikolic, S.; Randic, M.; Klein, D. J.; Plavsic, D.; Trinajstic, N. *J. Mol. Struct. (THEOCHEM)* **1989**, *198*, 223. For an application of the conjugated circuit model to selected [N]phenylenes, see: (f) Trinajstic, N.; Schmalz, T. G.; Zivkovic, T. P.; Nikolic, S.; Hite, G. E.; Klein, D. J.; Seitz, W. A. *New J. Chem.* **1991**, *15*, 27.

48. Hehre, W. J.; Radom, L.; Schleyer, P. v. R.; Pople, J. A. *Ab Initio Molecular Orbital Theory*; Wiley: New York, 1986.

49. Kollmar, H. *J. Am. Chem. Soc.* **1979**, *101*, 4832.

50. (a) Haddon, R. C. *Pure Appl. Chem.* **1982**, *54*, 1129. (b) Hess, B. A., Jr.; Schaad, L. J. *J. Am. Chem. Soc.* **1983**, *105*, 7500.

51. (a) George, P.; Trachtman, M; Bock, C. W.; Brett, A. M. *J. Chem. Soc., Perkin Trans. 2* **1976**, 1222. (b) George, P.; Trachtman, M; Bock, C. W.; Brett, A. M. *J. Chem. Soc., Perkin Trans. 2* **1977**, 1036.

52. (a) Cox, J. D.; Pilcher, G. *Thermochemistry of Organic and Organometallic Compounds*; Academic: New York, 1970. (b) Pedley, J.; Naylor, R. D.; Kirby, S. P. *Thermochemical Data of Organic Compounds*, 2nd ed.; Chapman and Hall: New York, 1986.

53. See, for example: (a) Klages, F. *Chem. Ber.* **1947**, *82*, 358. (b) Franklin, J. L. *Ind. Eng. Chem.* **1949**, *41*, 1070. (c) Benson, S. W. *Thermochemical Kinetics*; Wiley: New York, 1968.

54. For a review of techniques and a compilation of ΔH_H data see: Jensen, J. L. *Prog. Phys. Org. Chem.* **1976**, *12*, 189.

55. George, P. *Chem. Rev.* **1975**, *75*, 85.

56. (a) Sutton, L. E., Ed. *Interatomic Distances Supplement*; Special Publication No. 18; The Chemical Society: London, 1965. (b) Allen, F. H.; Kennard, O.; Watson, D. G.; Brammer, L.; Orpen, A. G.; Taylor, T. *J. Chem. Soc., Perkin Trans. 2* **1987**, S1 - S19.

57. (a) Irngartinger, H.; Nixdorf, M.; Riegler, N. H.; Krebs, A.; Kimling, H.; Pocklington, J.; Maier, G.; Malsch, K.-D.; Schneider, K.-A. *Chem. Ber.* **1988**, *121*, 673. (b) Irngartinger, H.; Nixdorf, M. *Chem. Ber.* **1988**, *121*, 679.

58. (a) Bordner, J.; Parker, R. G.; Stanford, R. H., Jr. *Acta Crystallogr., Sect. B* **1972**, *28*, 1069. For a structure determination of cyclooctatetraene by electron diffraction, see: (b) Bastiansen, O.; Hedberg, L.; Hedberg, K. *J. Chem. Phys.* **1957**, *27*, 1311.

59. (a) Nordik, J. H.; van den Hark, T. E. M.; Mooij, J. J.; Klaassen, A. A. K. *Acta Crystallogr., Sect. B* **1974**, *30*, 833. For an X-ray structure of 1,3,5,7-tetramethylcylooctatetraene dianion, see: (b) Goldberg, S. Z.; Raymond, K. N.; Harmon, C. A.; Templeton, D. H. *J. Am. Chem. Soc.* **1974**, *96*, 1348.

60. Bregman, J.; Hirshfeld, F. L.; Rabinovich, D.; Schmidt, G. M. J. *Acta Crystallogr.* **1965**, *19*, 227. (b) Hirshfeld, F. L.; Rabinovich, D. *Acta Crystallogr.* **1965**, *19*, 235.

61. Sondheimer, F. *Acc. Chem. Res.* **1972**, *5*, 81.

62. (a) Longuett-Higgins, H. C.; Salem, L. *Proc. Roy. Soc.* **1959**, *A251*, 172. (b) Longuett-Higgins, H. C.; Salem, L. *Proc. Roy. Soc.* **1960**, *A257*, 445.

63. Dewar, M. J. S.; Gleicher, G. J. *J. Am. Chem. Soc.* **1965**, *87*, 685.

64. Leznoff, C. C.; Sondheimer, F. *J. Am. Chem. Soc.* **1967**, *89*, 4247.

65. (a) Binsch, G.; Heilbronner, E. *Tetrahedron* **1968**, *24*, 1215. (b) Binsch, G.; Tamir, J.; Hill, R. D. *J. Am. Chem. Soc.* **1969**, *91*, 2446. (c) Binsch, G.; Tamir, J. *J. Am. Chem. Soc.* **1969**, *91*, 2450.

66. (a) Vogel, E.; Roth, H. D. *Angew. Chem.* **1964**, *76*, 145. *Angew. Chem., Int. Ed. Engl.* **1964**, *3*, 228. (b) Bianchi, R.; Pilati, T.; Simonetta, M. *Acta Crystallogr., Sect. B* **1980**, *36*, 3146.

67. (a) Fagan, P. J.; Calabrese, J. C.; Malone, B. *Acc. Chem. Res.* **1992**, *25*, 134. (b) Hawkins, J. M. *Acc. Chem. Res.* **1992**, *25*, 157. (c) Rubin, Y.; Khan, S.; Freedberg, D. I.; Yeretzian, C. *J. Am. Chem. Soc.* **1993**, *115*, 344.

68. (a) Pascal, P. *Ann. Chim. Phys.* **1910**, *19*, 5. (b) Selwood, P. W. *Magnetochemistry*, 2nd ed.; Wiley: New York, 1956.

69. (a) Pauling, L. *J. Chem. Phys.* **1936**, *4*, 673. (b) London, F. *J. Phys. Radium* **1937**, *8*, 397.

70. (a) Pople, J. A. *J. Chem. Phys.* **1964**, *41*, 2559. (b) Musher, J. I. *J. Chem. Phys.* **1965**, *43*, 4081. (c) Gaidis, J. M.; West, R. *J. Chem. Phys.* **1967**, *46*, 1218. (d) Musher, J. I. *J. Chem. Phys.* **1967**, *46*, 1219. (e) Musher, J. I. *Adv. Magn. Res.* **1967**, *2*, 177. (f) Abraham, R. J.; Thomas, W. A. *J. Chem. Soc. (B)* **1966**, 127. (g) Mallion, R. B. *Pure Appl. Chem.* **1980**, *52*, 1541.

71. (a) Dauben, H. J., Jr.; Wilson, J. D.; Laity, J. L. *J. Am. Chem. Soc.* **1968**, *90*, 811. (b) Dauben, H. J., Jr.; Wilson, J. D.; Laity, J. L. *J. Am. Chem. Soc.* **1969**, *91*, 1991. (c) Dauben, H. J., Jr.; Wilson, J. D.; Laity, J. L. In *Nonbenzenoid Aromatics*; Snyder, J. P., Ed.; Academic: New York, 1971; Vol. II, p 167.

72. Haberditzl, W. *Angew. Chem.* **1966**, *78*, 277. *Angew. Chem., Int. Ed. Engl.* **1966**, *5*, 288.

73. Units of Λ are 10^{-6} cm^3 mol^{-1}.

74. Memory, J. D.; Wilson, N. K. *NMR of Aromatic Compounds*; Wiley: New York, 1982.

75. (a) Pascal, R. A., Jr.; Winans, C. G.; Van Engen, D. *J. Am. Chem. Soc.* **1989**, *111*, 3007. For related structures involving other magnetically active nuclei, see:

(b) L'Esperance, P. L.; West, A. P., Jr.; Van Engen, D.; Pascal, R. A., Jr. *J. Am. Chem. Soc.* **1991**, *113*, 2672.

76. Sondheimer, F. *Proc. Roy. Soc.* **1967**, *A297*, 173.

77. Pople, J. A.; Untch, K. G. *J. Am. Chem. Soc.* **1966**, *88*, 4811.

78. Oth, J. F. M.; Gilles, J. M. *Tetrahedron Lett.* **1968**, 6259.

79. Elvidge, J. A.; Jackman, L. M. *J. Chem. Soc.* **1961**, 859.

80. (a) Fraenkel, G.; Asahi, Y.; Mitchell, M. J.; Cava, M. P. *Tetrahedron* **1964**, *20*, 1179. (b) Figeys, H. P. *J. Chem. Soc., Chem. Commun.* **1967**, 495. (c) Figeys, H. P.; Defay, N.; Martin, R. H.; McOmie, J. F. W.; Ayres, B. F.; Chadwick, J. B. *Tetrahedron*, **1976**, *32*, 2571. (d) Aihara, J. *J. Am. Chem. Soc.* **1979**, *101*, 5913. (e) Aihara, J. *Bull Chem. Soc. Jpn.* **1981**, *54*, 1245. (f) Aihara, J. *J. Am. Chem. Soc.* **1985**, *107*, 298.

81. (a) Mitchell, R. H.; Carruthers, R. J.; Mazuch, L.; Dingle, T. W. *J. Am. Chem. Soc.* **1982**, *104*, 2544. (b) Mitchell, R. H.; Williams, R. V.; Mahadevan, R.; Lai, Y. H.; Dingle, T. W. *J. Am. Chem. Soc.* **1982**, *104*, 2571. (c) Mitchell, R. H.; Slowey, P. D.; Kamada, T.; Williams, R. V.; Garratt, P. J. *J. Am. Chem. Soc.* **1984**, *106*, 2431. (d) Mitchell, R. H. *Adv. Theor. Interest. Mol.* **1989**, *1*, 135. (e) Mitchell, R.H.; Venugopalan, S.; Zhou, P.; Dingle, T. W. *Tetrahedron Lett.* **1990**, *37*, 5281. (f) Mitchell, R. H.; Zhou, P.; Venugopalan, S.; Dingle, T. W. *J. Am. Chem. Soc.* **1990**, *112*, 7812. (g) Mitchell, R. H.; Khalifa, N. A.; Dingle, T. W. *J. Am. Chem. Soc.* **1991**, *113*, 6696.

82. Clar, E. *The Aromatic Sextet*; Wiley: New York, 1972.

83. (a) Cooper, M. A.; Manatt, S. L. *J. Am. Chem. Soc.* **1969**, *91*, 6325. (b) Cremer, D.; Günther, H. *Liebigs Ann. Chem.* **1972**, *763*, 87. (c) Collins, M. J.; Halton, P. M.; Sternhell, S.; Tansey, C. W. *Magn. Res. Chem.* **1987**, *25*, 824. (d) Barfield, M.; Collins, M. J.; Gready, J. E.; Sternhell, S.; Tansey, C. W. *J. Am. Chem. Soc.* **1989**, *111*, 4285.

84. (a) Collman, J. P.; Hegedus, L. S.; Norton, J. R.; Finke, R. G. *Principles and Applications of Organotransition Metal Chemistry*; University Science Books: Mill Valley, CA, 1987. (b) Mann, B. E. In *Comprehensive Organometallic Chemistry*; Wilkinson, G.; Stone, F. G. A., Eds.; Pergamon: New York, 1982; Vol. 3, Chapter 20. (c) Uemura, M. *Adv. Met.-Org. Chem.* **1991**, *2*, 195 - 245.

85. (a) Chiu, N.-S.; Schäfer, L.; Seip, R. *J. Organomet. Chem.* **1975**, *101*, 331. (b) Jackson, W. R.; Pincombe, C. F.; Rae, I. D.; Thapebinkarn, S. *Aust. J. Chem.* **1975**, *28*, 1535.

86. (a) Fawcett, J. K.; Trotter, J. *Acta Crystallogr.* **1966**, *20*, 87. (b) Yokozeki, A.; Wilcox, C. E.; Bauer, S. H. *J. Am. Chem. Soc.* **1974**, *96*, 1026.

87. Rogers, R. D.; Atwood, J. L.; Albright, T. A.; Lee, W. A.; Rausch, M. D. *Organometallics* **1984**, *3*, 263.

88. Nambu, M. Ph. D. Thesis, University of California, San Diego, 1992.

89. The originally reported[24] barrier of 9.4 kcal mol^{-1} was found to be erroneous. The corrected value is 8.2 (± 0.5) kcal mol^{-1}: Siegel, J. S. Presented at the University of California, Berkeley, October 1991.

90. Mills, W. H.; Nixon, J. G. *J. Chem. Soc.* **1930**, 2510.

91. Badger, G. M. *Q. Rev. Chem. Soc.* **1951**, *5*, 147.

92. (a) Sutton, L. E.; Pauling, L. *Trans. Faraday Soc.* **1935**, 939. (b) Longuett-Higgins, H. C.; Coulson, C. A. *Trans. Faraday Soc.* **1946**, *42*, 756.

93. Meier, H.; Müller, E.; Suhr, H. *Tetrahedron* **1967**, *23*, 3713.

94. (a) Barfield, M.; Collins, M. J.; Gready, J. E.; Hatton, P. M.; Sternhell, S.; Tansey, C. W. *Pure Appl. Chem.* **1990**, *62*, 463. (b) Collins, M. J.; Gready, J. E.; Sternhell, S.; Tansey, C. W. *Aust. J. Chem.* **1990**, *43*, 1547.

95. Boyko, E. R.; Vaughan, P. A. *Acta Crystallogr.* **1964**, *17*, 152.

96. **41**: (a) Cava, M. P.; Napier, D. R. *J. Am. Chem. Soc.* **1958**, *80*, 2225. (b) Boese, R.; Bläser, D. *Angew. Chem.* **1988**, *100*, 293. *Angew. Chem., Int. Ed. Engl.* **1988**, *27*, 304.

42: (c) Thummel, R. P. *J. Am. Chem. Soc.* **1976**, *98*, 628. (d) Giovannini, E.; Vuilleumier, H. *Helv. Chim. Acta* **1978**, *60*, 1452.

8: (e) Nutakul, W.; Thummel, R. P.; Taggart, R. D. *J. Am. Chem. Soc.* **1979**, *101*, 770. (f) Thummel, R. P. *Acc. Chem. Res.* **1980**, *13*, 70. (g) Heilbronner, E.; Kovac, B.; Nutakul, W.; Taggart, A. D.; Thummel, R.P. *J. Org. Chem.* **1981**, *46*, 5279. (h) Doecke, C. W.; Garratt, P. J.; Shahriari-Zavereh, H.; Zahler, R. *J. Org. Chem.* **1984**, *49*, 1412.

97. (a) Cheung, C. S.; Cooper, M. A.; Manatt, S. L *Tetrahedron* **1971**, *27*, 701. (b) Halton, B.; Halton, M. P. *Tetrahedron*, **1973**, *29*, 1717. (c) Hiberty, P. C.; Ohanessian, G.; Delbecq, F. *J. Am. Chem. Soc.* **1985**, *107*, 3095. (d) Eckert-Maksic, M.; Kovacek, D.; Hodoscek, M.; Mitic, D.; Poljanek, K.; Maksic, Z. B. *J. Mol. Struct. (THEOCHEM)* **1990**, *206*, 89. (e) Maksic, Z. B.; Eckert-Maksic, M.; Kovacek, D.; Hodoscek, M.; Poljanek, K.; Kudnig, J. *J. Mol. Struct. (THEOCHEM)* **1991**, *234*, 201. (f) Stanger, A. *J. Am. Chem. Soc.* **1991**, *113*, 8277. (g) Baldridge, K. K.; Siegel, J. S. *J. Am. Chem. Soc.* **1992**, *114*, 9583.

98. Boese, R.; Bläser, D.; Haley, M. M.; Mohler, D. L.; Vollhardt, K. P. C., manuscript in preparation.

99. (a) Finnegan, R. A. *J. Org. Chem.* **1965**, *30*, 1333. (b) Streitwieser, A., Jr.; Ziegler, G. R.; Mowery, P. C.; Lewis, A.; Lawler, R. G. *J. Am. Chem. Soc.* **1968**, *90*, 1357.

100. (a) Billups, W. E.; Rodin, W. A.; Haley, M. M. *Tetrahedron* **1988**, *44*, 1305. (b) Haley, M. M. Ph. D. Thesis, Rice University, 1991. (c) Halton, B. *Chem. Rev.* **1989**, *89*, 1161.

101. Billups, W. E.; Chow, W. Y.; Leavell, K. H.; Lewis, E. S.; Margrave, J. C.; Sass, R. L.; Shieh, J. J.; Werness, P. G.; Wood, J. L. *J. Am. Chem. Soc.* **1973**, *95*, 7878.

102. Billups, W. E.; Arney, B. E., Jr.; Lin, L.-J. *J. Org. Chem.* **1984**, *49*, 3436.

103. (a) Neidlein, R.; Christen, D.; Poignée, V.; Boese, R.; Bläser, D.; Gieren, A.; Ruiz-Pérez, C.; Hübner, T. *Angew. Chem.* **1988**, *100*, 292. *Angew. Chem., Int. Ed. Engl.* **1988**, *27*, 294. (b) Bläser, D.; Boese, R.; Brett, W. A.; Rademacher, P.; Schwager, H.; Stanger, A.; Vollhardt, K. P. C. *Angew. Chem.* **1989**, *101*, 209. *Angew. Chem., Int. Ed. Engl.* **1989**, *28*, 206.

104. Neidlein, R.; Christen, D. *Helv. Chim. Acta* **1986**, *69*, 1623.

105. Apeloig, Y.; Arad, D. *J. Am. Chem. Soc.* **1986**, *108*, 3241.

106. (a) Greenberg, A.; Liebman, F. *Strained Organic Molecules*; Academic: New York, 1978. (b) Keehn, P. M.; Rosenfeld, S. M., Eds.; *Cyclophanes*; Academic: New York, 1983; Vols. 1 and 2. (c) Rossa, L.; Vögtle, F.; Boekelheide, V.; Tabushi, J.; Yamamura, K. *Top. Curr. Chem.* **1983**, *113*. (d) Vögtle, F., Ed. *Top. Curr. Chem.* **1983**, *115*. (e) Vögtle, F. *Cyclophan-Chemie*; Teubner: Stuttgart, 1990. (f) Diederich, F. *Cyclophanes*; Royal Society of Chemistry: Cambridge, 1991.

107. (a) van Straten, J. W.; de Wolf, W. H.; Bickelhaupt, F. *Rec. Trav. Chim. Pays-Bas* **1977**, *96*, 88. (b) Jenneskens, L. W.; de Kanter, F. J. J.; Kraakman, D. A.; Turkenburg, L. A. M.; Koolhaas, W. E.; de Wolf, W. H.; Bickelhaupt, F.; Tobe, Y.; Kakiuchi, K.; Odaira, Y. *J. Am. Chem. Soc.* **1985**, *107*, 3716.

108. (a) Kane, V. V.; Wolf, A. D.; Jones, M., Jr. *J. Am. Chem. Soc.* **1974**, *96*, 2643. (b) Kammula, S. L.; Iroff, L. D.; Jones, M., Jr.; van Straten, J. W.; de Wolf, W. H.; Bickelhaupt, F. *J. Am. Chem. Soc.* **1977**, *99*, 5815. (c) Tobe, Y.; Ueda, K.; Kakiuchi, K.; Odaira, Y. *Tetrahedron* **1986**, *42*, 1851.

109. Liebe, J.; Wolff, C.; Krieger, C.; Weiss, J.; Tochtermann, W. *Chem. Ber.* **1985**, *118*, 4144.

110. See, for example: (a) Cram, D. J.; Cram, J. M. *Acc. Chem. Res.* **1971**, *4*, 204. (b) Maier, G.; Schneider, K.-A. *Angew. Chem.* **1980**, *92*, 1056. *Angew. Chem., Int. Ed. Engl.* **1980**, *19*, 1022. (c) Maas, G.; Wingert, H.; Blatter, K.; Regitz, M. *Chem. Ber.* **1987**, *120*, 819. (d) Chance, J. M.; Kahr, B.; Buda, A. B.; Siegel, J. S. *J. Am. Chem. Soc.* **1989**, *111*, 5940. (e) Wolff, J. J.; Nelson, S. F.; Petillo, P. A.; Powell, D. R. *Chem. Ber.* **1991**, *124*, 1719.

111. (a) Couldwell, M. H.; Penfold, B. R. *J. Cryst. Mol. Struct.* **1976**, *6*, 59. (b) Weissensteiner, W.; Schuster, J. J.; Blount, J. F.; Mislow, K. *J. Am. Chem. Soc.* **1986**, *108*, 6664. (c) Sakurai, H.; Ebata, K.; Kabuto, C.; Sekiguchi, A. *J. Am. Chem. Soc.* **1990**, *112*, 1799.

112. (a) Martin, R. *Angew. Chem.* **1974**, *86*, 727. *Angew. Chem., Int. Ed. Engl.* **1974**, *13*, 649. (b) Meurer, K. P.; Vögtle, F. *Top. Curr. Chem.* **1985**, *127*, 1. (c) Vögtle, F. *Reizvolle Moleküle in der Organischen Chemie*; Teubner: Stuttgart, 1989; p 183 - 208.

113. Herndon, W. C.; Connor, D. A.; Lin, P. *Pure Appl. Chem.* **1990**, *62*, 435.

114. Pascal, R. A., Jr.; McMillan, W. D.; Van Engen, D.; Eason, R. G. *J. Am. Chem. Soc.* **1987**, *109*, 4660.

115. An entire issue of *Acc. Chem. Res.* has been devoted to the chemical and physical properties of the fullerenes: *Acc. Chem. Res.* **1992**, *25*, 98 - 175.

116. (a) Dixon, D. A.; Stevens, R. M.; Herschbach, D. R.; *Faraday Discuss. Chem. Soc.* **1977**, *62*, 110. (b) Ichikawa, H. *J. Am. Chem. Soc.* **1983**, *105*, 7467. (c) Haddon, R. C.; Raghavachari, K.; Whangbo, M. H. *J. Am. Chem. Soc.* **1984**, *106*, 5364. (d) Ichikawa, H. *J. Am. Chem. Soc.* **1984**, *106*, 6249.

117. (a) Plavsic, D.; Koutecky, J.; Pacchioni, G.; Bonacic-Koutecky, V. *J. Chem. Phys.* **1983**, *87*, 1096. (b) Pickup, B. T. *Proc. Roy. Soc.* **1973**, *A333*, 69.

118. (a) Vogler, A.; Wright, R. E.; Kunkely, H. *Angew. Chem.* **1980**, *92*, 745. *Angew. Chem., Int. Ed. Engl.* **1980**, *19*, 717. (b) Saxe, P; Schaefer, H. F., III. *J. Am.*

Chem. Soc. **1983**, *105*, 1760. (c) Lauderdale, W. J.; Stanton, J. F.; Bartlett, R. J. *J. Phys. Chem.* **1992**, *96*, 1173 and references therein.

119. Schleyer, P. v. R., private communication to F. Weinhold, University of Wisconsin, Madison.

120. (a) Baird, N. C. *J. Org. Chem.* **1986**, *51*, 3907. (b) Wiberg, K. B.; Nakaji, D.; Breneman, C. M. *J. Am. Chem. Soc.* **1989**, *111*, 4178. (c) Aihara, J. *Bull. Chem. Soc. Jpn.* **1990**, *63*, 1956. A rebuttal to Baird's criticism appears in (d) Hiberty, P. C.; Shaik, S. S.; Ohanessian, G.; Lefour, J.-M. *J. Org. Chem.* **1986**, *51*, 3908.

121. Jug, K.; Köster, A. M. *J. Am. Chem. Soc.* **1990**, *112*, 6772.

122. Stanger, A.; Vollhardt, K. P. C. *J. Org. Chem.* **1988**, *53*, 4889.

123. (a) Berry, R. S. *J. Chem. Phys.* **1961**, *35*, 29. (b) Berry, R. S. *J. Chem. Phys.* **1961**, *35*, 2253. (c) Epiotis, N. D. *Pure Appl. Chem.* **1983**, *55*, 229. (d) Epiotis, N. D. *Nouv. J. Chim.* **1984**, *8*, 11.

124. Mulliken, R. S.; Parr, R. G. *J. Chem. Phys.* **1951**, *19*, 1271.

125. GAUSSIAN 90, Rev. F: Frisch, M. J.; Head-Gordon, M; Trucks, G. W.; Foresman, J. B.; Schlegel, H. B.; Raghavachari, K.; Robb, M.; Binkley, J. S.; Gonzales, C.; Defrees, D. J.; Fox, D. J.; Whiteside, R. A.; Seeger, R.; Melius, C. F.; Baker, J.; Martin, R. L.; Kahn, L. R.; Stewart, J. J. P.; Topiol, S.; Pople, J. A. Gaussian, Inc. Pittsburgh, PA, 1990.

126. GAMESS: Schmidt, M. W.; Baldridge, K. K.; Boatz, J. A.; Jensen, J. H.; Koseki, S.; Gordon, M. S.; Nguyen, K. A.; Windus, T. L.; Elbert, S. T. *QCPE Bull.* **1990**, *10*, 52.

127. Hariharan, P. C.; Pople, J. A. *Chem. Phys. Lett.* **1972**, *66*, 217.

128. Szabo, A.; Ostlund, N. S. *Modern Quantum Chemistry*; McGraw-Hill: New York, 1982; pp 131 - 152.

129. Walsh, A. D. *J. Chem. Soc.* **1953**, 2266.

130. Due to crystal packing forces and steric repulsions between the ortho-trimethylsilyl groups, the molecular structure slightly deviates from D_{3h} symmetry (space group *I*2/a). The geometric effects of trimethylsilyl substitution can be assessed by comparing crystallographic data of 4,5-bis(trimethylsilyl)-1,2-dihydrocyclobutabenzene[131] to those of its parent.[96b]

131. Moder, K. P.; Duesler, E. N.; Leonard, N. J. *Acta Crystallogr., Sect. B.* **1981**, *37*, 289.

132. See, for example: (a) Kabuto, C.; Yagihara, M.; Asso, T.; Kitihara, Y. *Angew. Chem.* **1973**, *85*, 860. *Angew. Chem., Int. Ed. Engl.* **1973**, *12*, 1836. (b) Littke, W.; Drück, U. *Angew. Chem.* **1974**, *86*, 557. *Angew. Chem., Int. Ed. Engl.* **1974**, *13*, 539. (c) Krüger, C.; Roberts, P. J. *Cryst. Struct. Commun.* **1974**, *3*, 459. (d) Liu, L. K.; Davies, E. *Angew. Chem.* **1977**, *89*, 175. *Angew. Chem., Int. Ed. Engl.* **1977**, *16*, 169. (e) Schwesinger, R.; Piontek, K.; Littke, W.; Prinzbach, H. *Angew. Chem.* **1985**, *97*, 344. *Angew. Chem., Int. Ed. Engl.* **1985**, *24*, 318.

133. (a) Maas, M.; Lutterbeck, M.; Hunkler, D.; Prinzbach, H. *Tetrahedron Lett.* **1983**, *24*, 2143. (b) McMullen, G.; Lutterbeck, M.; Fritz, H.; Prinzbach, H. *Isr. J. Chem.* **1982**, *22*, 19.

134. A joint effort with Debra L. Mohler, Stefan Wolff, and Ajai Sahwaney.

135. (a) Collins, J.; Suschitzky, H. *J. Chem. Soc. (C)* **1969**, 2337. (b) Chen, C.-T.; Yan, S.-J.; Wang, C.-H. *Chem. Ind.* **1970**, 895. (c) Fink, W. *Helv. Chim. Acta* **1974**, *110*, 1010.

136. Alternate samples of known (cyclohexene) and unknown were hydrogenated in THF solution stirred over Pd/C. Completion and the absence of side reactions was ascertained by GLC analysis. Results in Table 3.3 are weighted arithmetic means of at least 25 runs and are given with uncertainties of 95% confidence limit. A detailed discussion of methodology and instrumentation employed can be found in: Rogers, D. W.; Dejroongruang, K. *J. Chem. Thermodynam.* **1988**, *20*, 675.

137. Roth, W. R.; Klärner, F.-G.; Siepert, G.; Lennartz, H.-W. *Chem. Ber.* **1992**, *125*, 217.

138. Baker, W. *Nature* **1942**, *150*, 210.

139. Roth, W. R.; Scholz, B. P. *Chem. Ber.* **1981**, *114*, 3741.

140. MMX data were obtained using PCMODEL distributed by Serena Software, P. O. Box 3076, Bloomington, IN 47402 - 3076. For a detailed discussion of molecular mechanics see: Burkert, U.; Allinger, N. L. *Molecular Mechanics*; American Chemical Society: Washington, 1982.

141. Semiempirical calculations were performed employing VAMP 4.30 a modified version of AMPAC 4.20, which was vectorized by Dr. T. Clark, Erlangen, Germany, and mounted on Stellar 2000 workstations. All geometries were optimized using "precise" as a keyword, and equilibrium structures were shown to be minima on their potential energy surfaces by frequency analyses. The PM3 parameter set is described in: (a) Stewart, J. J. P. *J. Comput. Chem.* **1989**, *10*, 209. (b) Stewart, J. J. P. *J. Comput. Chem.* **1989**, *10*, 221. For the MNDO method (chapter 5) see: (c) Dewar, M. J. S.; Thiel, W. *J. Am. Chem. Soc.* **1977**, *99*, 4899.

142. (a) Davis, M.; Hassel, O. *Acta Chem. Scand.* **1963**, *17*, 1181. (b) Giese, H. J.; Buijs, H. R.; Mijihoff, J. *J. Mol. Struct.* **1971**, *9*, 447.

143. (a) Beckhaus, H. D.; Rüchardt, C.; Smisek, M. *Thermochim. Acta* **1984**, *79*, 149. (b) Hubbard, W. N.; Scott, D. W.; Waddington, G. In *Experimental Chemistry*; Rossini, F. D., Ed.; Interscience: New York, 1956; Vol 1, chapter 6.

144. Reichardt, C. *Solvent and Solvent Effects in Organic Chemistry*, 2nd ed.; Chemie: New York, 1988; p 26.

145. Roth, W. R.; Biermann, M.; Dekker, H.; Jochems, R.; Mosselmann, C.; Hermann, H. *Chem. Ber.* **1978**, *111*, 3892.

146. Turner, R. B.; Goebel, P.; Mallon, B. J.; Doering, W. v. E.; Coburn, J. F., Jr.; Pomerantz, M. *J. Am. Chem. Soc.* **1968**, *90*, 4315.

147. Dixon, D. A.; Komornicki, A. *J. Phys. Chem.* **1990**, *94*, 5630 and references therein.

148. Squillacote, M.; Sheridan, R. S.; Chapman, O. L.; Anet, F. A. L *J. Am. Chem. Soc.* **1975**, *97*, 3244.

149. (a) Komornicki, A.; McIver, J. W., Jr. *J. Am. Chem. Soc.* **1973**, *95*, 4512. (b) Davis, T. D.; Frost, A. A. *J. Am. Chem. Soc.* **1975**, *97*, 7410.

150. Ab initio optimizations of **67** involving 6-31G* basis sets lead to alternating CC bond lengths of $R_{1\text{-}2}$ = 1.643 Å and $R_{1\text{-}6}$ = 1.519 Å (D_{3h} symmetry constraints imposed). The energy at the SCF level was found to be -234.085573 a.u., which compares to -234.208003 a.u. for the D_{3d} structure of **60** (R_{CC} = 1.534 Å).

151. (a) Class, R. C.; Springall, H. D.; Quincey, P. G. *J. Chem. Soc.* **1955**, 1188. (b) Bedford, A. E.; Carey, J. G.; Millar, I. T.; Mortimer, C. T.; Springall, H. D. *J. Chem. Soc.* **1962**, 3895.

152. Portions of this work have been published: Faust, R.; Glendening, E. D.; Streitwieser, A.; Vollhardt, K. P. C. *J. Am. Chem. Soc.* **1992**, *114*, 8263.

153. (a) Randic, M.; Maksic, Z. B. *Chem. Rev.* **1972**, *72*, 43. (b) Kovacevic, K.; Maksic, Z. B. *J. Org. Chem.* **1974**, *39*, 539. (c) Maksic, Z. B.; Rubcic, A. *J. Am. Chem. Soc.* **1977**, *99*, 4233.

154. (a) Wiberg K. B. In *The Chemistry of the Cyclopropyl Group*; Rappaport, Z., Ed.; Wiley: New York, 1987; p 1. (b) Wiberg, K. B. *Angew. Chem.* **1986**, *98*, 312. *Angew. Chem., Int. Ed. Engl.* **1986**, *25*, 312.

155. Pietro, W.; Francl, M. M.; Hehre, W. J.; Defrees, D. J.; Pople, J. A.; Binkley, J. S. *J. Am. Chem. Soc.* **1982**, *104*, 5039.

156. **68**: (a) Cava, M. P.; Deana, A. A.; Muth, K. *J. Am. Chem. Soc.* **1960**, *82*, 2524. (b) Thummel, R. P.; Nutakul, W. *J. Org. Chem.* **1977**, *42*, 300. (c) Gray, R.; Harruf, L. G.; Krymowsky, J.; Peterson, J.; Boekelheide, V. *J. Am. Chem. Soc.* **1978**, *100*, 2892. (d) Bradsher, C. K.; Hunt, D. A. *J. Org. Chem.* **1981**, *46*, 4608.

69: (e) Cava, M. P.; Mitchell, M. J. *J. Am. Chem. Soc.* **1963**, *85*, 2080.

72: (f) Chapman, O. L.; Chang, C. C.; Rosenquist, N. R. *J. Am. Chem. Soc.* **1976**, *98*, 261. (g) Koenig, T.; Imre, D.; Hoobler, J. A. *J. Am. Chem. Soc.* **1979**, *101*, 6446. (h) Trahanovsky, W. S.; Fischer, D. R. *J. Am. Chem. Soc.* **1990**, *112*, 4971.

157. The X-ray structures of some derivatives of **72** are known: (a) Winter, W.; Straub, H. *Angew. Chem.* **1978**, *90*, 142. *Angew. Chem., Int. Ed. Engl.* **1978**, *17*, 127. (b) Tsukada, H.; Shimanouchi, H.; Sasada, Y. *Acta Crystallogr., Sect. B* **1977**, *33*, 2951. (c) Tsukada, H.; Shimanouchi, H.; Sasada, Y. *Bull. Chem. Soc. Jpn.* **1978**, *51*, 985.

158. For recent applications of the hybridization model, see: Maksic, Z. B.; Orville-Thomas, W. J. *J. Mol. Struct. (THEOCHEM)* **1988**, *169*, 1 - 568.

159. (a) Huntsman, W. D.; Wristers, H. J. *J. Am. Chem. Soc.* **1963**, *85*, 3308. (b) Huntsman, W. D.; Wristers, H. J. *J. Am. Chem. Soc.* **1967**, *89*, 342.

160. (a) Skancke, A. in ref 37b, p 192. (b) Hess, B. A., Jr.; Schaad, L. J. *Aust. J. Chem.* **1972**, *25*, 2213 and references therein. (c) Leibovici, C. *J. Mol. Struct.* **1972**, *12*, 343. (d) Kent, J. E.; Harman, P. J.; O'Dwyer, M. F. *J. Phys. Chem.* **1981**, *85*, 2726. (e) Brown, R. D.; Godfrey, P. D.; Hart, B. T.; Ottrey, A. L.; Onda, M.; Woodruff, M. *Aust. J. Chem.* **1983**, *36*, 639.

161. (a) Bader, R. F. W. *Acc. Chem. Res.* **1985**, *18*, 9. (b) Bader, R. F. W. *Atoms in Molecules - A Quantum Theory*; Clarendon: Oxford, 1990.

162. Carsten-Oeser, E.; Müller, B.; Dürr, H. *Angew. Chem.* **1972**, *84*, 434. *Angew. Chem., Int. Ed. Engl.* **1972**, *11*, 422.

163. (a) Toda, F.; Ohi, M. *J. Chem. Soc., Chem. Commun.* **1975**, 506. (b) Toda, F.; Takahma, Y. *Bull. Chem. Soc. Jpn.* **1976**, *49*, 2515.

164. (a) Davis, R. E.; Pettit, R. *J. Am. Chem. Soc.* **1970**, *92*, 716. (b) Duclos, R. I.; Vollhardt, K. P. C.; Yee, L. S. *J. Organomet. Chem.* **1979**, *174*, 109. (c) Straub, H.; Doering, G.; Winter, W. *Z. Naturforsch., B* **1979**, *34*, 125. (d) Winter, W.;

Butters, T. *Acta Crystallogr., Sect. B* **1981**, *37*, 1528. (e) Butters, T.; Winter, W.; Toda, F. *Acta Crystallogr., Sect. B* **1981**, *37*, 1531. (f) Moreto, J.; Maruya, K.; Bailey, P. M.; Maitlis, P. M. *J. Chem. Soc., Dalton Trans.* **1982**, 1341.

165. For the construction of group orbitals, see: (a) Jorgensen, W. L.; Salem, L. *The Organic Chemist's Handbook of Orbitals*; Academic: New York, 1973. (b) Clark, T. *A Handbook of Computational Chemistry*; Wiley: New York, 1985; p 121-139.

166. (a) Brogli, F.; Giovannini, E.; Heilbronner, E.; Schurter, R. *Chem. Ber.* **1973**, *106*, 961. (b) Santiago, C.; Gandour, R. W.; Houk, K. N.; Nutakul, W.; Cravey, W. E.; Thummel, R. P. *J. Am. Chem. Soc.* **1978**, *100*, 3730.

167. Huzinaga, S.; Andzelm, J.; Klobukowski, M.; Radzio-Andzelm, E.; Sakai, Y.; Tatewaki, H. *Gaussian Basis Sets for Molecular Calculations*; Elsevier: Amsterdam; 1984. The MIDI basis set was used as implemented in GAMESS.

168. Williamson, R. L.; Hall, M. B. *Int. J. Quantum Chem. Symp.* **1987**, *21*, 503.

169. (a) Langhoff, S. R.; Bauschlicher, C. W., Jr. *Ann. Rev. Phys. Chem.* **1988**, *39*, 181. (b) Barnes, L. A.; Rosi, M.; Bauschlicher, C. W., Jr. *J. Chem. Phys.* **1991**, *94*, 2031.

170. Muetterties, E. L.; Bleeke, J. R.; Wucherer, E. J.; Albright, T. A. *Chem Rev.* **1982**, *82*, 499.

171. Proponents of a D_{3h} symmetry: (a) Jellinek, F. *Nature* **1960**, *187*, 871. (b) Jellinek, F. *J. Organomet. Chem.* **1963**, *1*, 43. (c) Keulen, E.; Jellinek, F. *J. Organomet. Chem.* **1966**, *5*, 490.

172. Views in favor of a D_{6h} symmetry: (a) Weiss, E.; Fischer, E. O. *Z. Anorg. Allg. Chem.* **1956**, *286*, 142. (b) Corradini, P.; Allegra, G. *J. Am. Chem. Soc.* **1959**, *81*, 2271. (c) den Broer, D. H. W.; den Broer, P. C.; Longuet-Higgins, H. C. *Mol. Phys.* **1962**, *5*, 387. (d) Cotton, F. A.; Dollase, W. A.; Wood, J. S. *J. Am. Chem. Soc.* **1963**, *85*, 1543. (e) Bailey, M. E.; Dahl, L. F. *Inorg. Chem.* **1965**, *4*, 1314.

173. (a) Rees, B.; Coppens, P. *J. Organomet. Chem.* **1972**, *42*, C102. (b) Rees, B.; Coppens, P. *Acta Crystallogr., Sect. B* **1973**, *29*, 2516. (c) Wang, Y.; Angermund, K.; Goddard, R.; Krüger, C. *J. Am. Chem. Soc.* **1987**, *109*, 587.

174. The alternative conformation of **34** has carbonyls residing above the benzenoid carbon centers and is 0.31 kcal mol^{-1} higher in energy with the following internuclear distances: $R_{1\text{-}2} = R_{1\text{-}6} = 1.399$ Å; $R_{Cr\text{-}Bz} = 1.832$ Å; $R_{Cr\text{-}CO} = 1.869$ Å; $R_{C\text{-}O} = 1.148$ Å.

175. Nambu, M.; Hardcastle, K.; Baldridge, K. K.; Siegel, J. S. *J. Am. Chem. Soc.* **1992**, *114*, 369.

176. Sandstrom, J. *Dynamic NMR Spectroscopy*; Academic: New York, 1982.

177. For an account of developments leading to the discovery of C_{60}, see: Kroto, H. *Angew. Chem.* **1992**, *104*, 113. *Angew. Chem., Int. Ed. Engl.* **1992**, *31*, 111.

178. Cioslowski, J. *J. Am. Chem. Soc.* **1991**, *113*, 4139.

179. McKee, M. L.; Herndon, W. C. *J. Mol. Struct.* ~~**1985**, *130*, 117~~ (Theochem). → No.! 187, 153 75.

180. Scott, L. T.; Hashemi, M. M.; Bratcher, M. S. *J. Am. Chem. Soc.* **1992**, *114*, 1920.

181. Schulman, J. M.; Peck, R. C.; Disch, R. L. *J. Am. Chem. Soc.* **1989**, *111*, 5675.

182. (a) Borden, W. T. *Chem. Rev.* **1989**, *89*, 1095. (b) Haddon, R. C. *J. Am. Chem. Soc.* **1990**, *112*, 3385.

183. Filippini, G. *J. Mol. Struct.* **1985**, *130*, 117.

184. Most endohedral complexes could only be detected mass spectroscopically: (a) McElvany, S. W.; Ross, M. M.; Callahan, J. H. *Acc. Chem. Res.* **1992**, *25*, 162. Recently, macroscopic amounts of La@C_{60} could be isolated: (b) Chai, Y.; Gno, N.; Jin, C.; Haufler, R. E.; Chibante, L. P. F.; Fure, J.; Wang, L.; Alford, J. M.; Smalley, R. E. *J. Chem. Phys.* **1991**, *95*, 7564. → Not the right one!

185. March, J. *Advanced Organic Chemistry*, 4th ed.; Wiley: New York, 1992; p 753.

186. Ayalon, A.; Rabinovitz, M.; Cheng, P.-C.; Scott, L. T. *Angew. Chem.* **1992**, *104*, 1691. *Angew. Chem., Int. Ed. Engl.* **1992**, *31*, 1636.

187. Laarhoven, W. H.; van Broekhoven, J. A. M. *Tetrahedron Lett.* **1970**, 73.

188. (a) Balaban, A. B.; Vanitzesku, C. D. In *Friedel Crafts and Related Reactions*; Olah, G. A., Ed.; Interscience: New York, 1964; Vol 2, part 2, p 9799. (b) Sato, T.; Nishiyama, K.; Murai, A. *J. Chem. Soc., Chem. Commun.* **1972**, 163. (c) Dopper, J. H.; Wynberg, H. *Tetrahedron Lett.* **1972**, 763. (d) Laarhoven, W. H. *J. Roy. Neth. Chem. Soc.* **1983**, *102*, 185. (e) Studt, P.; Win, T. *Liebigs Ann. Chem.* **1983**, 519. (f) Bunte, R.; Gundermann, K.-D.; Leitich, J.; Polansky, O. E.; Zander, M. *Chem. Ber.* **1987**, *120*, 247. (g) Michel, P.; Moradpour, A. *Synthesis* **1988**, 894.

189. For examples of Diels-Alder reactions involving the benzene nucleus, see: (a) Miller, R. G.; Stiles, M. *J. Am. Chem. Soc.* **1963**, *85*, 1798. (b) Liu, R. S. H. *J. Am. Chem. Soc.* **1968**, *90*, 215. (c) Ciganec, E. *Tetrahedron Lett.* **1967**, 3321. (d) Wagner-Jauregg, T. *Synthesis* **1980**, 165 and 769. (e) Grimme, W.; Grommes, T.; Roth, W. R.; Breuckmann, R. *Angew. Chem.* **1992**, *104*, 867. *Angew. Chem., Int. Ed. Engl.* **1992**, *31*, 872.

190. (a) Johnson, J. R. *Org. React.* **1942**, *1*, 210. (b) Amin, S.; Hecht, S. S.; LaVoie, E.; Hoffmann, D. *J. Med. Chem.* **1979**, *22*, 1336.

191. (a) Omura, K.; Swern, D. *Tetrahedron Lett.* **1978**, *34*, 1651. (b) Mancuso, J.; Swern, D. *Synthesis* **1981**, 165.

192. Winterfeldt, E. *Synthesis* **1975**, 617.

193. Maryanoff, B. E.; Reitz, A. B. *Chem. Rev.* **1989**, *89*, 863 and references therein.

194. Liu, L.; Yang, B.; Katz, T. J.; Poindexter, M. K. *J. Org. Chem.* **1991**, *56*, 3769.

195. McLafferty, F. W. *Interpretation of Mass Spectra*, 3rd ed.; University: Mill Valley, 1980.

196. (a) Vollhardt, K. P. C. *Pure Appl. Chem.* **1980**, *52*, 1645. (b) Thummel, R. P. *Isr. J. Chem.* **1982**, *22*, 11.

197. Moore, W. R.; Marcus, E.; Fenton, S. E.; Arnold, R. T. *Tetrahedron* **1959**, *5*, 179.

198. See, for example: (a) Blüm, G. P.; Gundermann, K.-D.; Zander, M. *Chem. Ber.* **1976**, *109*, 1991. (b) Lavit-Lamy, D.; Buu-Hoi, N. P. *J. Chem. Soc., Chem. Commun.* **1966**, 92. (c) Vingiello, F. A.; Yanez, J.; Greenwood, E. J. *J. Chem. Soc., Chem. Commun.* **1966**, 375. (d) Carruthers, W. *J. Chem. Soc., Chem. Commun.* **1966**,548.

199. Rabinovitz, M.; Cohen, Y. *Tetrahedron* **1988**, *44*, 6957.

200. Bastide, J.; Henri-Rousseau, O. In *The Chemistry of the Carbon-Carbon Triple Bond*; Patai, S., Ed.; Wiley: New York, 1978; p 447.

201. Brandsma, L.; Verkruijsse, H. *Preparative Polar Organometallic Chemistry*; Springer: New York, 1987; Vol 1, p 124.

202. Stille, J. K. *Angew. Chem.* **1986**, *98*, 504. *Angew. Chem., Int. Ed. Engl.* **1986**, *25*, 508.

203. Kelly, T. R.; Bridger, G. J.; Zhao, C. *J. Am. Chem. Soc.* **1990**, *112*, 8024.

204. Holmes, A. B.; Sporikou, C. N. *Org. Synth.* **1961**, *40*, 105.

205. Brandsma, L.; Verkruijsse, H. D. *Synthesis of Acetylenes, Allenes, and Cumulenes*; Elsevier: Amsterdam, 1981; p 56.

206. Heary, H.; Millar, I. T. *Org. Synth.* **1960**, *40*, 107.

207. Coulson, D. R. *Inorg. Synth.* **1972**, *13*, 121.

208. Rausch, M. D.; Tibbetts, F. E. *J. Organomet. Chem.* **1970**, *21*, 487.

209. (a) Piper, T. S.; Cotton, F. A.; Wilkinson, G. *J. Inorg. Nucl. Chem.* **1955**, *1*, 165. (b) Rausch, M. D.; Genetti, R. A. *J. Org. Chem.* **1970**, *35*, 3888.

210. Still, W. C.; Kahn, M.; Mitra, A. *J. Org. Chem.* **1978**, *43*, 2923.

DATE

FILMED

6/30/94

END